UNIVERSITAT DE BARCELONA

Geometric realizations using regular subdivisions:
Construction of many polytopes, sweep polytopes, *s*-permutahedra

Eva Philippe

Sorbonne Université
École doctorale 386 : Sciences mathématiques de Paris Centre
Institut de Mathématiques de Jussieu-Paris Rive Gauche
Universitat de Barcelona
Programa de Doctorat en Matemàtiques i Informàtica
Facultat de Matemàtiques i Informàtica

Geometric realizations using regular subdivisions:

Construction of many polytopes, sweep polytopes, s-permutahedra

Thèse de doctorat de mathématiques réalisée par
Eva Philippe

sous la direction de

Arnau Padrol	*Universitat de Barcelona*
Francisco Santos Leal	*Universidad de Cantabria*
Ilia Itenberg	*Sorbonne Université*

Soutenue le 7 juin 2024 devant le jury composé de :

Federico Ardila	San Fracisco State University	rapporteur
Jérémie Bouttier	Sorbonne Université	examinateur
Kolja Knauer	Universitat de Barcelona	examinateur
Viviane Pons	Université Paris-Saclay	rapportrice
Jorge Ramírez	Université de Montpellier	examinateur

Abstract

This thesis concerns three problems of geometric realizations of combinatorial structures via polytopes and polyhedral subdivisions. A polytope is the convex hull of a finite set of points in a Euclidean space $\mathbb{R}^d$. It is endowed with a combinatorial structure coming from its faces. A subdivision is a collection of polytopes whose faces intersect properly and such that their union is convex. It is regular if it can be obtained by taking the lower faces of a lifting of its vertices in one dimension higher.

We first present a new geometric construction of many combinatorially different polytopes of fixed dimension and number of vertices. This construction relies on showing that certain polytopes admit many regular triangulations. It allows us to improve the best known lower bound on the number of combinatorial types of polytopes.

We then study the projections of permutahedra, that we call *sweep polytopes* because they model the possible orderings of a fixed point configuration by hyperplanes that sweep the space in a constant direction. We also introduce and study a combinatorial abstraction of these structures: the *sweep oriented matroids*, that generalize Goodman and Pollack's theory of allowable sequences to dimensions higher than 2.

Finally, we provide geometric realizations of the s-weak order, a combinatorial structure that generalizes the weak order on permutations, parameterized by a vector $s \in (\mathbb{Z}_{>0})^n$. In particular, we answer Ceballos and Pons's conjecture that the s-weak order can be realized as the edge-graph of a polytopal complex that is moreover a subdivision of a permutahedron.

Keywords: polytopes, polyhedral combinatorics, regular subdivisions, geometric realizations, triangulations, permutahedra, oriented matroids, allowable sequences of permutations, sweep algorithms, monotone path polytopes, generalized Baues problem, flow polytopes, Cayley trick, tropical geometry, s-weak order, s-decreasing trees, Stirling s-permutations.

Résumé

Cette thèse concerne trois problèmes de réalisations géométriques de structures combinatoires par des polytopes et des subdivisions polyédrales. Un polytope est l'enveloppe convexe d'un ensemble fini de points dans un espace euclidien $\mathbb{R}^d$. Il est muni d'une structure combinatoire donnée par ses faces. Une subdivision est une collection de polytopes dont les faces s'intersectent correctement et dont l'union est convexe. Elle est régulière si elle peut être obtenue en prenant les faces inférieures d'un relèvement de ses sommets dans une dimension de plus.

Nous présentons d'abord une nouvelle construction géométrique d'un grand nombre de polytopes combinatoirement distincts, de dimension et nombre de sommets fixés. Cette construction consiste à montrer que certains polytopes admettent un grand nombre de triangulations régulières. Elle nous permet d'améliorer la meilleure borne inférieure connue sur le nombre de types combinatoires de polytopes.

Nous étudions ensuite les projections du permutoèdre, nommées polytopes de balayage (sweep polytopes) parce qu'elles modélisent les manières d'ordonner une configuration de points fixée en balayant l'espace par des hyperplans dans une direction constante. Nous introduisons également et étudions une abstraction combinatoire de ces structures : les matroïdes orientés de balayage, qui généralisent en dimension supérieure à 2 la théorie des suites admissibles de Goodman et Pollack.

Enfin, nous proposons des réalisations géométriques du s-ordre faible, une structure combinatoire qui généralise l'ordre faible sur les permutations, paramétrée par un vecteur $s \in (\mathbb{Z}_{>0})^n$. En particulier, nous résolvons une conjecture de Ceballos et Pons en montrant que le s-permutoèdre peut être réalisé comme le graphe d'un complexe polytopal qui est une subdivision du permutoèdre.

Mots-clés : polytopes, combinatoire polyédrale, subdivisions régulières, réalisations géométriques, triangulations, permutoèdres, matroïdes orientés, suites admissibles de permutations, algorithmes de balayage, polytopes des chemins monotones, problème de Baues généralisé, polytopes de flots, astuce de Cayley, géométrie tropicale, s-ordre faible, s-arbres décroissants, s-permutations de Stirling.

Resumen

Esta tesis se centra en tres problemas de realizaciones geométricas de estructuras combinatorias usando politopos y subdivisiones poliedrales. Un politopo es la envolvente convexa de un conjunto finito de puntos en un espacio Euclídeo $\mathbb{R}^d$. Tiene una estructura combinatoria dada por sus caras. Una subdivisión es una colección de politopos cuyas caras se intersecan correctamente y cuya unión es convexa. Es regular si se puede obtener con las caras inferiores de un levantamiento de sus vértices en una dimensión más.

Primero, presentamos una nueva construcción geométrica de un gran número de politopos combinatoriamente distintos, con dimensión y número de vértices fijados. Esta construcción consiste en mostrar que ciertos politopos admiten un gran número de triangulaciones regulares. Nos permite mejorar la mayor cota inferior conocida en el número de tipos combinatorios de politopos.

A continuación estudiamos las proyecciones del permutaedro, llamadas politopos de barrido (sweep polytopes) porque modelan las posibles ordenaciones de una configuración de puntos fijada inducidas por el barrido con hiperplanos que recorren el espacio en una dirección constante. Introducimos también y estudiamos una abstracción combinatoria de estas estructuras: las matroides orientadas de barrido, que generalizan en dimensión mayor que 2 la teoría de secuencias admisibles de Goodman y Pollack.

Por último, proporcionamos realizaciones geométricas del s-orden débil, una estructura combinatoria que generaliza el orden débil en permutaciones, parametrizada por un vector $\mathrm{s} \in (\mathbb{Z}_{>0})^n$. En particular, resolvemos una conjetura de Ceballos y Pons mostrando que se puede realizar el s-permutaedro como el grafo de aristas de un complejo politopal que es una subdivisión del permutaedro.

Palabras clave: politopos, combinatoria poliedral, subdivisiones regulares, realizaciones geométricas, triangulaciones, permutaedros, matroides orientadas, secuencias admisibles de permutaciones, algoritmos de barrido, politopos de caminos monotones, problema de Baues generalizado, politopos de flujos, truco de Cayley, geometría tropical, s-orden débil, s-árboles decrecientes, s-permutaciones de Stirling.

Acknowledgements - Remerciements

My heart is full of gratitude towards many people. My words are poor in comparison with what I would like to express.
Mon coeur est plein de gratitude envers de nombreuses personnes. Mes mots sont pauvres face à ce que je voudrais exprimer.

First, I am deeply grateful to my advisors, who were always present when I needed them, trusted me, supported me and taught me a lot. Dès notre première rencontre avant le M2 j'ai été gagnée par la passion communicative d'Arnau Padrol pour la combinatoire des polytopes. Tu as été un excellent guide pour mes premiers pas dans la recherche, motivant, bienveillant, inspirant, éclairant. Cette thèse te doit énormément. Tambien aprendí mucho con Paco Santos. Muchas gracias por tu acogida calurosa en Santander y la confianza que me demostraste. Merci beaucoup Ilia Itenberg d'avoir accepté de rejoindre l'équipe d'encadrement de cette thèse lorsque Arnau est parti à Barcelone.

I am honored and happy to have Federico Ardila and Viviane Pons as my thesis reviewers. I deeply admire both of you for your beautiful mathematics as well as for your constant commitment to diversity and social justice in the math community.

I am very grateful to Jérémie Bouttier, Kolja Knauer and Jorgé Ramírez Alfonsín for having accepted to be part of my thesis jury.

In addition to Arnau and Paco, I had the great luck to work with inspiring collaborators. Jean-Philippe Labbé and Federico Castillo introduced me very enthusiastically to quantum physics and its connection to polytopes. The adventures related to the s-permutahedron and flow polytopes in company of Rafael S. González D'León, Alejandro H. Morales, Daniel Tamayo Jiménez and Martha Yip were particularly instructive and enjoyable. It was very satisfactory to complete this subject lately with another perspective, thanks to Vincent Pilaud's impressive energy. I also benefited from fruitful discussions on related topics with Matias von Bell, Cesar Ceballos, Viviane Pons and Yannic Vargas.

Thanks to Germain Poullot and Daniel Tamayo Jiménez for many valuable comments on previous versions of this manuscript and for the authorization to use their LaTeX templates.

I am grateful to all professionals who contribute to provide good conditions for the research to be done. Je pense en particulier à Sitti Mchinda, Julienne Passave, Fenda Traoré, Gaëlle Callouard, Patricia Zizzo, Sakina Kawami, Evariste Ciret, Tarikakan Demirturk, Corentin Lacombe et aux personnes chargées du ménage des lieux que j'ai fréquentés.

I benefited from ideal material conditions and opportunities to travel thanks to École Normale Supérieure de Paris, Sorbonne Université, Institut de Mathématiques - Paris Rive Gauche, Universitat de Barcelona, ANR projects CAPPS and PAGCAP, additional ponctual fundings from Berlin Mathematical school, Mathematisches Forschungsinstitut Oberwolfach, IRN network, laboratoire IMAG, laboratoire LAMFA, FPSAC 2024.

Among all the many people that I was happy to meet during my PhD and with whom I shared passionate mathematical or non-mathematical discussions, I will start with the DGeCo crew. Ce séminaire des Doctorant·e·s en Géometrie Combinatoire a été une formidable expérience pour apprendre de jolies mathématiques, s'entraîner à donner des exposés dans un cadre bienveillant, se rencontrer et se motiver. Je garde de superbes souvenirs de nos voyages en Colombie, en Autriche, en Italie, à Bordeaux, à Massy. Germain Poullot, mon cher frère de thèse et co-bureau, merci pour ton soutien et ta constante disponibilité, notamment pour préparer des présentations ou gérer l'assistance technique de ma soutenance. Chiara Mantovani, j'ai apprécié tous nos moments partagés, notamment à Barcelone. Merci de m'avoir initiée aux arts du cirque, je te souhaite de trouver la voie dans laquelle tu pourras épanouir ta belle énergie. Daniel Tamayo-Jiménez, ta bonne humeur, ta créativité, ton habilité en programmation ont été très motivantes pour notre collaboration transcontinentale sur le s-permutaoèdre. C'est une chance de pouvoir compter sur un ami comme toi ! Merci aussi à ta maman pour l'accueil à Bogotá. Doriann Albertin, Noémie Cartier, Loïc Le Mogne, Balthazar Charles, Monica Garcia, Hugo Mlodecki, Clément Chenevière, Corentin Henriet merci pour tous les bons moments, vous êtes de chouettes personnes !

Merci à tou·e·s les collègues du couloir des doctorant·e·s, passé·e·s comme présent·e·s, pour les partages de repas, de pauses, de cafés, de discussions, de sourires (j'espère n'oublier personne, désolée si c'est le cas): Jacques Audibert, Perla Azzi, Mathieu Daylies, Arnaud Eteve, Xenia Flamm, Thomas Franzinetti, Christina Katsamaki, Christophe Levrat, Thibaut Mazuir, Mahya Mehrabdollahein, Thomas Le Fils, Raphaël Prunier, Adrien Rey, Maud Szusterman, Antoine Toussaint, Grace Younes, Haowen Zhang, Chenyu Bai, Tristan Bompard, Juan Felipe Cuastro Cardenas, Maxime Cazaux, Odylo Costa, Lucas Dauger, Yann Delaporte, Nastaran Einabadi, Mattias Ferreira-Filoramo, Antoine Galet, Pierre Godfard, Mathieu Helfter, Parian Khezerlou, Enrico Lampetti, Thiago Landim, Gaétan Leclerc, Joaquin Lejtreger, Haohao Liu, Tangi Pasquer, Pietro Piccione, Camille Pinto, Gabriel Ribeiro, Anna Roig Sanchis, Joao Ruiz, Nelson Schuback, Matteo Verni, Mingchen Xia. Mention spéciale à mes co-bureaux Thomas Guidoni, Francesco Morabito et Petra Flurin. J'étais aussi heureuse de retrouver pour un an Gabriel Pallier, sans doute la première personne qui m'ait parlé de polytopes ! Merci pour le prêt du livre de Coxeter à l'époque, et pour les superbes constructions en Zoom.

Gracias también a todos y todas las compañeras de doctorado en Barcelona, por vuestra acogida y todos los momentos agradables compartidos: Aina Ferrà, João Candeias, Jordi Daura Serrano, Enric Florit, Daniel Gil Muñoz, Javier Guillán Rial, Anna Jové Campabadal, Irene Macías Tarrío, David Martínez Carpena, Pedro Miguel Meneses Magalhaes, Ainoa Murillo López, Josu Pérez Zarraonandia, Ignasi Sanchez Rodríguez, Anna Sopena

Gilboy, Clara Torres Latorre.

Merci Jimmy Lamboley d'avoir été un directeur d'équipe toujours à l'écoute, merci Elias Tsigaridas et Fabrice Rouillier d'avoir assuré mon comité de suivi de thèse. Merci Frédéric Meunier pour les échanges enrichissants et l'opportunité de donner un TD en optimisation combinatoire à l'École des Ponts.

I am grateful to all the people who invited me to conferences or seminars (including online ones): Antonio Macchia, Federico Castillo, Raman Sanyal, Lorenzo Venturello, Arina Voorhaar, Ismaïl Razack, Thibaut Delcroix, Julien Boulanger, Alejandro H. Morales, Karim Adiprasito, Xavier Goaoc, Zuzana Patáková, Kolja Knauer, Georg Loho. These events were good opportunities to meet and gather with colleagues in a friendship atmosphere. I remember nice interactions with Bérénice Delcroix-Ogier, Jorge Ramírez Alfonsín, Lionel Pournin, Aenne Benjes, Sophie Rehberg, Marie Brandenburg, Evgenija Lagoda, Nikola Sadovek, Tatiana Levinson, William Dugan, Martin Winter, Justus Bruckamp, Martina Juhnke, Aram Dermenjian, Marta Pavelka, Georgy Scholten, Carolina Benedetti, Danai Deligeorgaki, Jesús De Loera, Guillaume Laplante-Anfossi. I have special gratitude to my elder academic sisters Giulia Codenotti and Monica Blanco, and to Georg Loho for his relevant recommendations.

Je souhaite profiter de cette thèse pour repenser à tous les professeurs qui m'ont marquée au cours de ma scolarité et dont les enseignements continuent de m'accompagner. Merci Annie, Jeanine, Ketty Milly, Françoise, M. Tara, M. Soussan, Mme Bourkaïb, Mme Corn, Mme Denis-Langlinay, M. Alarcon, Mme Lefeuvre, Julien Cubizolles, Roger Mansuy, Muriel Dunlop, Nicolas Tosel, Raphaël Cerf, Ariane Mézard, Ilia Itenberg, Omid Amini, Guillaume Chapuy, Arnau Padrol, Roxana Barbacaru, Michel Gross.

Mon goût pour les mathématiques s'est également développé en-dehors de l'école, grâce à de nombreuses activités portées par l'association Animath. Merci à tou·te·s les bénévoles qui permettent cela. Parmi celleux qui ont marqué mon chemin je pense en particulier à Martin Andler, Fabrice Rouillier, Matthieu Lequesne, Guillaume Conchon-Kerjan, Vincent Jugé, Thomas Budzinski, Margaret Bilu, Igor Kortchemski, Giancarlo Lucchini Arteche, Elsa Masson, Antoine Martin, Véronique Slovacek-Chauveau.

L'organisation d'événements spécifiquement destinés à des jeunes filles m'aura permis de rencontrer des mathématiciennes extrêmement inspirantes, qui m'ont donné beaucoup de motivation : Marie Albenque, Viviane Pons, Amandine Veber, Anna Song, Laura Monk, Azélie Picot, Elsa Maneval, Valentine Blanpain.

Je souhaite également rendre hommage aux ami·e·s, que j'ai rencontré·e·s bien avant la thèse et qui m'ont toujours soutenue, avec qui j'ai pu souffler et continuer à grandir. Merci Hugo Cui, Edwige Cyffers, Alain Delaët-Tixeuil, Clémence Elmira, Emmanuel Faure, Daria Fourgeot, Anne Fuster, Cécile Gachet, Louise Garrigou, Lucas Gierczak-Galle, Yohan Mandin-Hublé, Jane Marchand, Cécile Miteran, Marie-Lou Novène, Antoine Séré, Laura Soueidan, Lucas Vacossin, Anna Vayness, Katia Ziani, Philipp Ziani. (Vous méritez mieux qu'une liste classée par ordre alphabétique !)

Merci aussi à tou·te·s les ami·e·s dont j'ai croisé le chemin même si nous nous voyons moins maintenant.

À Barcelone, j'ai eu la chance de pouvoir compter sur ma coloc Clara Torres Latorre, mon amie d'enfance Hannah Bilsky et ses parents Carmen Gallego et Edgardo Bilsky pour me faire sentir chez moi. Moltes gràcies per tot!

Enfin, je pense à tou·te·s mes ami·e·s militant·e·s, qui me donnent de la force, de l'énergie et de l'espoir. Merci à toutes les personnes qui luttent pour la justice à travers le monde.

Côté famille, je pense d'abord aux disparus, dont le souvenir continue de m'accompagner et avec qui j'aurais aimé partagé la fierté d'accomplir cette thèse en mathématiques : Papi Ephrem, Papi Louis, Tonton Jean-Michel, Pascal Le Marthelot.

Merci à mes grand-mères, Manou et Danièle, à tous mes oncles et tantes et aux cousin·e·s pour la joie des retrouvailles et votre soutien.

Grâce à Mathieu, j'ai la chance de pouvoir élargir le spectre familial. Merci Pascale Pallard, Julien Barré, Christophe Barré et Maëlle Biotteau pour votre accueil et les exemples inspirants que vous me donnez. Merci Llewellyn, Tynawedd, Dwynwen, Hywel, Gwrvan, Aelwyd, Llawgad, Judwall, Arthvawr pour votre intensité de vie, je suis toujours contente de vous retrouver.

Paul, je suis contente que tu perpétues la flamme mathématique de la famille (tant que cela t'épanouit). Et je suis heureuse de nos autres centres d'intérêt communs, sur lesquels nous cheminons tous les deux. Zoé, quoi que t'apporte l'avenir je suis sûre que tu feras de grandes choses, et surtout, qui t'épanouissent. Ne perds jamais ta vivacité, ton audace, ta créativité ! Mes parents, mes chers parents, qui m'acompagnez dans toutes les étapes de la vie, sur qui je peux toujours compter, je ne sais comment vous témoigner tout l'amour et la reconnaissance que j'ai pour vous.

Mathieu Barré, merci d'être là, d'être toi, que nous soyons nous.

Contents

List of Figures

Introduction

Context

The present thesis finds its place at the crossroads between combinatorics and geometry. Roughly speaking, *combinatorics* is the science of studying (with the many senses this verb can take) mathematical discrete objects, that is, objects that we can count. Geometry, the science of shapes, spaces and measures, can have many different flavors. Here we consider *Euclidean geometry*, which looks like the geometry we do at elementary school but in a space $\mathbb{R}^d$ that can have any arbitrary (finite) dimension $d \in \mathbb{N}$.

Polytopes are the generalization in these higher dimensional spaces of the convex polygons of dimension 2 and convex polyhedra in dimension 3. Like them, their boundary is partitioned into faces of different dimensions: vertices of dimension 0, edges of dimension 1, faces of dimension 2, 3, $\dots$, $d-1$. The structure of these faces defines the *combinatorial type* of a polytope and raises many fascinating questions of a combinatorial nature. For example, in Chapter 2 of this thesis we will deal with the question of counting the number of possible combinatorial types of polytopes, which is already hard in dimensions higher than 3.

Besides studying the combinatorial properties of geometric structures, one can ask the reverse question: given a family of objects with a combinatorial structure, can we find a geometric object that reflects this structure? Indeed, having *geometric realizations* sheds new lights on the combinatorial objects we are studying. Two important examples of polytopes related to fundamental combinatorial structures are the *permutahedron*, whose vertices are related to permutations and whose edge-graph is related to the weak order, and the *associahedron*, whose vertices are related to Catalan objects (such as planar binary trees, parenthesized words, Dyck paths, triangulations of polygons, ...) and whose edge-graph is related to the Tamari lattice. We devote Section 1.4 of the preliminaries to present several ways to realize the permutahedron geometrically, that will be generalized with the realizations of the *sweep polytope* (Chapter 3) and the s-*permutahedron* (Chapter 4).

The constructions presented in this thesis are all related to *subdivisions*, and more precisely *regular subdivisions*. To put it roughly, a subdivision of a polytope $\boldsymbol{P}$ is a collection of subpolytopes whose union is $\boldsymbol{P}$ and such that they intersect nicely. A *triangulation* is a subdivision that is as fine as possible, i.e. all the subpolytopes are simplices. Similarly to polytopes, subdivisions (or more generally polytopal complexes) are geometric objects with an intrinsic combinatorial face structure, and we can ask for the realizability of combinatorial structures in terms of polytopal complexes. *Regular subdivisions* are a particular family of subdivisions, which enjoy special geometric properties that will be important for us: they can be obtained by *lifting* the polytope in one dimension higher, they can be *dualized*, and the set of all regular subdivisions of a polytope are encoded into the *secondary polytope*.

Outline of the thesis and contributions

This thesis is divided into four chapters. The first one provides preliminary background and the next three present three projects that I worked on during my PhD, in collaboration with several people. These three chapters can be read independently and each one starts with its own introduction. We give an outline of their content below.

Chapter 1: Preliminaries

We give an overview of the main mathematical notions involved in this thesis.

In Section 1.1 we provide some background definitions in discrete geometry, starting with the purely combinatorial notions of *partially ordered sets* and *lattices*, then turning to *polytopes*, *polyhedral complexes* and *subdivisions*. We end this section with the *Cayley trick*, a technique that gives a correspondence between two families of subdivisions of different polytopes.

In Section 1.2 we focus on *regular subdivisions* of point configurations and provide three geometric realizations associated to them. First, we define a regular subdivision as a polytopal complex obtained by *lifting* a point configuration to a polytope in one dimension higher. Secondly, we show that such a regular subdivision with a lifting function can be *dualized*, and a convenient language to express this dualization is given by *tropical geometry*. Finally, we present the *secondary polytope*, a polytope which encodes all regular subdivisions of a point configuration.

In Section 1.3 we look at subdivisions that arise from *projections*. Within this more general framework, we present the *fiber polytope*, which generalizes both the secondary polytope and the *monotone path polytope*. We also introduce the *generalized Baues problem*, which deals with the topology of refinement posets of subdivisions.

In Section 1.4, we present the *permutahedron*. We first describe the combinatorial structure of this polytope, which is related to the *weak order* and to *ordered partitions*. Then we provide several geometric constructions: explicit coordinates of the vertices, zonotope dual to the braid arrangement, monotone path polytope of the cube, and dual of a triangulation of the cube. We also give a few explanations on the associahedron and its connections to the permutahedron.

Chapter 2: Many polytopes and many regular triangulations

This chapter is based on the article [PPS23], written with my advisors Arnau Padrol and Francisco Santos.

We address the problem of estimating the number of combinatorial types of polytopes of fixed dimension and number of vertices. Except for dimension 2 and 3, precise numbers and estimations seem out of reach, but one can look for asymptotic bounds. It was known from previous works that the number of different labeled combinatorial types of d-polytopes with n vertices for fixed $d > 3$ and n growing to infinity is at most $(n!)^{d^2 \pm o(1)}$ and at least $(n!)^{\lfloor d/2 \rfloor \pm o(1)}$. Our main result is an improvement of this lower bound, to $(n!)^{d-2\pm o(1)}$.

We first show that certain polytopes, that can be built by adding vertices iteratively in a controlled way, admit many regular triangulations. This allows us to improve the best known lower bound on the maximal number of regular triangulations of a point configuration. For instance, we show that there are realizations of the cyclic d-polytope with n vertices that admit at least $(n!)^{\lfloor \frac{d-1}{2} \rfloor \pm o(1)}$ regular triangulations.

Then, we show that the *lexicographic lifting* construction previously used by Padrol to build many polytopes has the properties that ensure having many regular triangulations. By adding a vertex and a dimension to all these regular triangulations, we obtain the many combinatorially distinct polytopes that give the lower bound.

Chapter 3: Sweep polytopes and sweep oriented matroids

This chapter is based on the article [PP23], written with my advisor Arnau Padrol.

The motivation of this work was to provide combinatorial models for point configurations by means of their *sweeps*, and generalize in higher dimension Goodman and Pollack's theory of allowable sequences (2-dimensional case). A sweep of a point configuration is an ordered partition obtained by recording in which order the points are hit by a hyperplane that sweeps the space in a constant direction.

We first give geometric realizations of the poset of all sweeps of a point configuration in terms of its *sweep hyperplane arrangement* and its *sweep polytope*. We provide several constructions of the sweep polytope: zonotope dual to the sweep hyperplane arrangement, projection of a permutahedron, monotone path polytope of a zonotope.

Since we have a hyperplane arrangement, it is natural to associate to this structure an oriented matroid, that we call the *sweep oriented matroid* of the considered point configuration. Oriented matroids (also known as *order types* or *chirotopes*) are purely combinatorial structures that abstract some properties of point configurations over the reals, real hyperplane arrangements, linear programming and directed graphs. An oriented matroid consists of a set of vectors in $\{0, +, -\}^E$ that satisfies certain axioms, for a finite ground set E. The usual oriented matroid associated to a configuration $\boldsymbol{A}$ of n labeled points in $\mathbb{R}^d$, that we call the *little oriented matroid* of $\boldsymbol{A}$, has ground set $[n]$ and rank $d+1$. In comparison, the sweep oriented matroid of $\boldsymbol{A}$ has ground set $\binom{[n]}{2}$ (the set of pairs of elements in $[n]$) and rank d. We show that it is a finer invariant. We give a purely axiomatic description of sweep oriented matroids, beyond the realizable cases coming from point configurations. Any such sweep oriented matroid is still associated to a little oriented matroid, which is not necessarily realizable anymore.

We give a characterization of oriented matroids that are sweep oriented matroids in terms of the existence of a *tight modular hyperplane*. We provide an example of an oriented matroid that is not sweepable: it cannot be obtained as the little oriented matroid of a sweep oriented matroid. We relate sweep oriented matroids to the *Dilworth truncation* operation in (unoriented) matroid theory and this allows us to give an upper bound on the number of sweep permutations (the maximal covectors) of a sweep oriented matroid.

Then, we turn to the study of *pseudo-sweeps*: a generalization of sweeps in which the sweeping hyperplane is allowed to slightly change direction. This notion can be extended to arbitrary oriented matroids, in terms of cellular strings. We prove the strong Generalized Baues Problem for cellular strings of sweepable oriented matroids.

Finally, we introduce a second combinatorial abstraction of the posets of sweeps of point configurations: the *allowable graphs of permutations*. They are symmetric sets of permutations pairwise connected by allowable sequences. They have the structure of acycloids and include sweep oriented matroids but it is open whether they are exactly the same as sweep oriented matroids or contain more elements.

Let us mention here that our work on sweep polytopes also gave rise to a collaboration in quantum physics with mathematicians Federico Castillo and Jean-Philippe Labbé and physicists Julia Liebert and Christian Schilling [CLL+23]. To put it in a nutshell, it appeared that a special case of *lineup polytope* (a variant of sweep polytope) is exactly the set of spectra of the convex hull of 1-body reduced density matrices that come from a system of many particles with fixed energy levels. This result provided an effective way to compute constraints that generalize the famous Pauli's exclusion principle "No two fermions can occupy at the same time the same quantum state". We chose not to include more material on this subject in the present manuscript because it would require to introduce a heavy formalism on quantum physics.

Chapter 4: Geometric realizations of the s-weak order and its quotients

The first three sections of this chapter rely on the article [GDMP+23], written with Rafael S. González D'León, Alejandro H. Morales, Daniel Tamayo Jiménez and Martha Yip.

We provide three geometric realizations of the s-*weak order* for any $s \in (\mathbb{Z}_{>0})^n$. This lattice structure was introduced by Ceballos and Pons as a generalization of the usual weak order on permutations that mimicks the generalization of the Tamari lattice to the ν-Tamari lattice. The objects of this lattice structure can be defined in terms of s-*decreasing trees* or in terms of *Stirling* s-*permutations*. The usual weak order is recovered with $s = (1, \dots, 1)$. In our first realization, the Hasse diagram of the s-weak order is obtained as the dual graph of a *DKK triangulation* of the *flow polytope* of the *oruga graph*. Along the way, we prove a few new results about the structure of the oriented dual graphs of DKK triangulations for general flow polytopes. In particular we provide a *Lidskii-type decomposition* of these graphs.

The Cayley trick allows us to show that the Hasse diagram of the s-weak order is also the dual graph of a certain mixed subdivision of cubes. Finally, we apply tropical dualization to this mixed subdivision and obtain a realization of the s-permutahedron (a polytopal complex whose edge-graph is the Hasse diagram of the s-weak order) as a subdivision of the n-permutahedron. This third construction answers a first conjecture by Ceballos and Pons.

The last section of this chapter sketches lines of research that were recently being developed to provide geometric realizations of the *lattice quotients* of the s-weak order. Indeed, similarly to the Tamari lattice and the weak order, Ceballos and Pons showed that the s-Tamari lattice is a lattice quotient of the s-weak order and they conjectured that certain realizations of the s-associahedron could be obtained by removing facets from certain realizations of the s-permutahedron.

With Vincent Pilaud, we adapted in the article [PP24] the tools developed to realize the quotients of the weak order (*non-crossing arc diagrams*, *shards* and *shard polytopes*) to the s-weak order. This requires to deal with polytopal complexes instead of polytopes and answers Ceballos and Pons second conjecture.

With Rafael S. González D'León, Alejandro H. Morales, Daniel Tamayo Jiménez, Martha Yip, Matias von Bell and Yannic Vargas, we are working on a graph operation whose consequences on the DKK triangulation of the associated flow polytope model certain lattice congruences. Applied to the s-oruga graph, these operations should provide realizations of a family of lattice quotients of the s-weak order that generalizes *permutrees*.

Chapter 1

Preliminaries

References that we used extensively to write these preliminaries and that we warmly recommend are the books *Lectures on Polytopes*, by Ziegler [Zie95], and *Triangulations, Structures for Algorithms and Applications*, by De Loera, Rambau and Santos [DRS10].

In all this work we denote by $\mathbb{R}^d$ the standard Euclidean space of dimension d, equipped with the canonical basis $\boldsymbol{e}_1, \dots, \boldsymbol{e}_d$ and the standard orthogonal scalar product $\langle \cdot, \cdot \rangle$ (most of the time we will cheerfully identify $\mathbb{R}^d$ and its dual space $(\mathbb{R}^d)^*$).

We denote the all-zero vector $\mathbf{0}$ and the all-one vector $\mathbf{1} := \sum \boldsymbol{e}_i$.

For $n \in \mathbb{N}$ we denote by $[n]$ the set $\{1, \dots, n\}$. We denote by $|X|$ the number of elements of a finite set X.

1.1 Polytopes and subdivisions

1.1.1 Partially ordered sets and lattices

Before delving into geometry, we give a few definitions related to posets, since they appear in many places in this thesis.

A *poset* is a *partially ordered set*, that is, a set X equipped with a binary relation $\preceq$ which is reflexive ($x \preceq x$ for all $x \in X$), anti-symmetric (if $x \preceq y$ and $y \preceq x$, then $x = y$) and transitive (if $x \preceq y$ and $y \preceq z$, then $x \preceq z$). This relation is said to be *partial* because we do not ask that for any pair of elements $x, y \in X$ we have either $x \preceq y$ or $y \preceq x$, contrary to *total* orders (also called *linear* orders).

For an example of poset, one can think of the set of subsets of a given set S, ordered by inclusion. Such poset is called the *Boolean lattice* on S.

We use the notation $x \prec y$ to mean that $x \preceq y$ and $x \neq y$, and the notation $x \succeq y$ to mean that $y \preceq x$.

A *cover relation* of the poset is a pair $x, y \in X$ such that $x \prec y$ and no $z \in X$ satisfies $x \prec z \prec y$.

A *chain* of the poset is a set of elements of X of the form $\{x_1, \ldots, x_k\}$ such that $x_1 \prec \ldots \prec x_k$.

The *Hasse diagram* of the poset is the directed graph whose vertices are the elements of X and there is an oriented edge from x to y exactly when there is a cover relation $x \preceq y$.

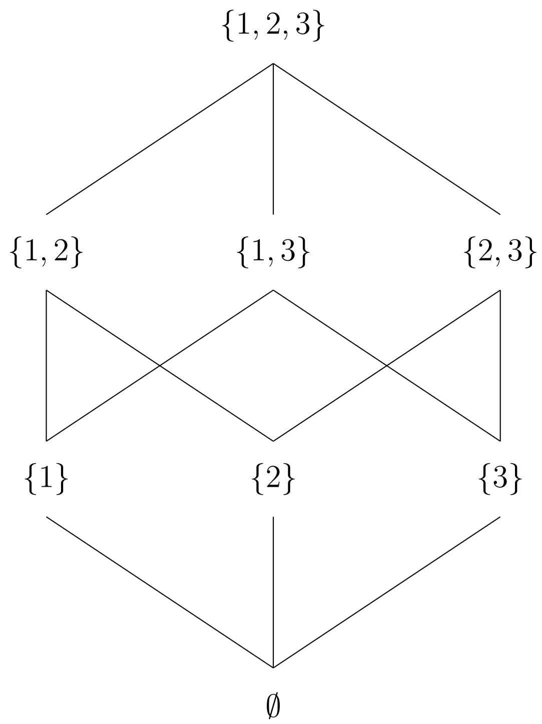

Figure 1.1: Hasse diagram of the Boolean lattice on [3] (set of subsets of [3] ordered by inclusion). The edges are oriented upward.

Figure 1.1 shows the Hasse diagram of the Boolean lattice on [3]. We will always represent Hasse diagrams with the edges oriented upward (and sometimes rightward for horizontal edges).

If $(X, \preceq)$ and $(X', \preceq')$ are two posets, a *poset isomorphism* between them is a bijection $\phi : X \to X'$ such that for any $x, y \in X$, $x \preceq y$ if and only if $\phi(x) \preceq' \phi(y)$.

If $(X, \preceq)$ is a poset, its *opposite poset* is the poset $(X, \succeq)$.

Much of the posets that we encounter in this thesis have the following stronger structure.

A poset $(X, \preceq)$ is a *lattice* if for any non-empty subset of elements $Y \subseteq X$, its set of upper bounds $\{z \in X \mid z \succeq y \text{ for all } y \in Y\}$ has a unique minimal element, called the *join* of Y and denoted by $\bigvee Y$, and its set of lower bounds $\{z \in X \mid z \preceq y \text{ for all } y \in Y\}$ has a unique maximal element, called the *meet* of Y and denoted by $\bigwedge Y$.

For example, in the Boolean lattice on a set S, the join corresponds to taking union and the meet to taking intersection.

1.1.2 Polytopes

The *convex hull* of a set $\boldsymbol{X} \subseteq \mathbb{R}^d$ is the convex set:

$$\operatorname{conv}(\boldsymbol{X}) := \left\{ \sum_{i\in[n]} \lambda_i \boldsymbol{x}_i \;\middle|\; n \in \mathbb{N},\ \boldsymbol{x}_i \in \boldsymbol{X} \text{ and } \lambda_i \in \mathbb{R}_{\geq 0} \text{ for all } i \in [n] \text{ and } \sum_{i\in[n]} \lambda_i = 1 \right\}.$$

The *affine hull* of a set $\boldsymbol{X} \subseteq \mathbb{R}^d$ is the affine subspace:

$$\operatorname{aff}(\boldsymbol{X}) := \left\{ \sum_{i\in[n]} \lambda_i \boldsymbol{x}_i \;\middle|\; n \in \mathbb{N},\ \boldsymbol{x}_i \in \boldsymbol{X} \text{ for all } i \in [n] \text{ and } \sum_{i\in[n]} \lambda_i = 1 \right\}.$$

The *relative interior* of a set $\boldsymbol{X} \subseteq \mathbb{R}^d$ is the convex relatively open (i.e. open in its affine hull) set:

$$\operatorname{relint}(\boldsymbol{X}) := \left\{ \sum_{i\in[n]} \lambda_i \boldsymbol{x}_i \;\middle|\; n \in \mathbb{N},\ \boldsymbol{x}_i \in \boldsymbol{X} \text{ and } \lambda_i \in \mathbb{R}_{> 0} \text{ for all } i \in [n] \text{ and } \sum_{i\in[n]} \lambda_i = 1 \right\}.$$

A *point configuration* is an ordered sequence $\boldsymbol{A} = (\boldsymbol{a}_1, \dots, \boldsymbol{a}_n) \in \mathbb{R}^{d\times[n]}$ of points in $\mathbb{R}^d$ indexed by $[n]$. We formally consider $\boldsymbol{A}$ a sequence rather than a set since the ordering of the points $\boldsymbol{a}_i$ is sometimes important, but we will slightly abuse notation and write things like $\boldsymbol{a}_i \in \boldsymbol{A}$, or call the points $\boldsymbol{a}_i$ the elements of $\boldsymbol{A}$. We do not require the points to be distinct.

A *polytope* $\boldsymbol{P}$ can be simply defined as the convex hull of a finite number of points in a Euclidean space.

The dimension of $\boldsymbol{P}$, denoted $\dim(\boldsymbol{P})$, is the dimension of its affine hull, and we take the convention $\dim(\emptyset) = -1$.

In spite of their very simple geometric definition, polytopes come with a rich combinatorial structure, given by their faces.

Definition 1.1.1. Let $\boldsymbol{P}$ be a polytope in $\mathbb{R}^d$. Let $\boldsymbol{u}$ be a point in $\mathbb{R}^d$, thought of as a direction. We say that the set of points of $\boldsymbol{P}$ that maximize the linear form $\langle \cdot, \boldsymbol{u} \rangle$ is a *face* of $\boldsymbol{P}$, that we denote

$$\boldsymbol{P}^{\boldsymbol{u}} := \left\{ \boldsymbol{x} \in \boldsymbol{P} \;\middle|\; \langle \boldsymbol{x}, \boldsymbol{u} \rangle = \max_{\boldsymbol{y}\in\boldsymbol{P}} \langle \boldsymbol{y}, \boldsymbol{u} \rangle \right\}.$$

Such a face is itself a polytope in $\mathbb{R}^d$.

By convention, we also consider that the empty set $\emptyset$ is a face of $\boldsymbol{P}$. Note that the whole polytope $\boldsymbol{P}$ is a face of itself, maximized by the direction $\boldsymbol{u} = \boldsymbol{0}$. Faces of $\boldsymbol{P}$ of dimension 0 are called *vertices*, faces of dimension 1 are called *edges* and faces of dimension $\dim(\boldsymbol{P}) - 1$ are called *facets*. Faces of dimension k are called *k-faces*. The set of faces of dimension at most k of $\boldsymbol{P}$ is called the *k-skeleton* of the polytope. The 1-skeleton is also called the *graph* of the polytope.

The set of faces of $\boldsymbol{P}$, endowed with the order relation of inclusion is called the *face poset* of $\boldsymbol{P}$, or its *face lattice* since it has the property of being a lattice ([Zie95, Theorem 2.7]).

The face poset of a polytope defines its *combinatorial type*: we say that two polytopes are *combinatorially equivalent* if their face posets are isomorphic (as posets).

Example 1.1.2 (Simplices). The simplest possible example of a d-polytope is called a *simplex* (*simplices* in the plural) and can be obtained by taking the convex hull of any set of $d+1$ points that are affinely independent (i.e. $(\boldsymbol{a}_1, \dots, \boldsymbol{a}_{d+1}) \in \mathbb{R}^{D\times[d+1]}$ such that there is no $(\lambda_1, \dots, \lambda_{d+1}) \in \mathbb{R}^{d+1}$ with $\sum_{i=1}^{d+1} \lambda_i = 1$ and $\sum_{i=1}^{d+1} \lambda_i \boldsymbol{a}_i = \boldsymbol{0}$). The *standard simplex* is obtained with the vectors of the canonical basis of $\mathbb{R}^{d+1}$:

$$\begin{aligned}\triangle_d &= \operatorname{conv}\left(\{\boldsymbol{e}_1, \dots, \boldsymbol{e}_{d+1}\}\right) \subset \mathbb{R}^{d+1} \\ &= \left\{ \boldsymbol{x} \in \mathbb{R}^{d+1} \;\middle|\; \sum_{i\in[d+1]} x_i = 1 \text{ and } x_i \geq 0 \text{ for all } i \in [d+1] \right\}.\end{aligned}$$

For any subset $I \subseteq [d+1]$, the vertices $\{\boldsymbol{e}_i \mid i \in I\}$ define a face of $\triangle_d$, that is maximized in the direction $\sum_{i\in I} \boldsymbol{e}_i$. Thus, the face poset of the simplex is isomorphic to the Boolean lattice on $[d+1]$.

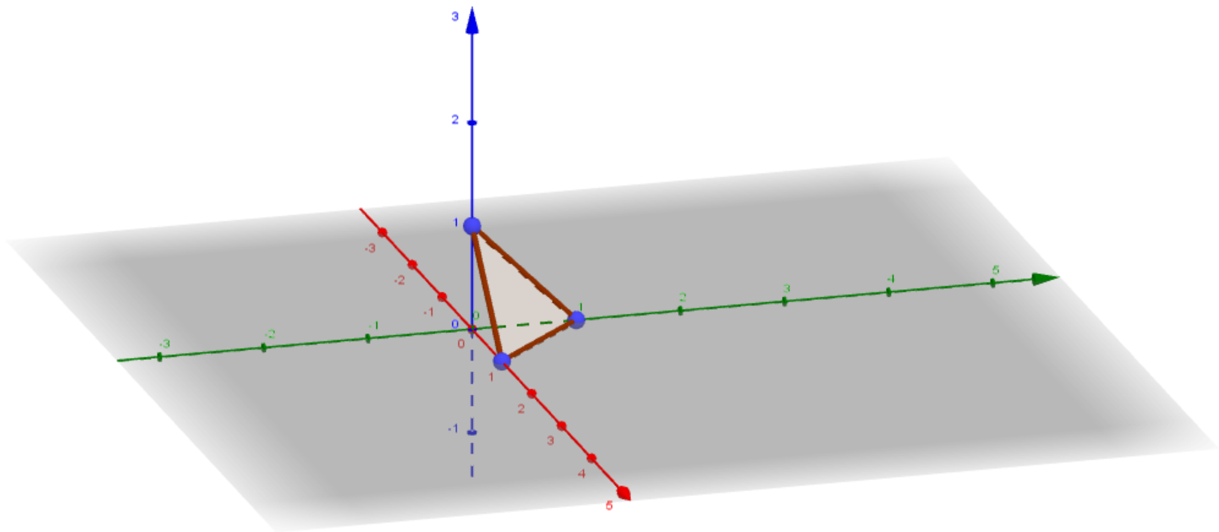

Figure 1.2: Standard simplex $\triangle_2$.

Figure 1.2 shows the standard simplex $\triangle_2$, embedded in $\mathbb{R}^3$. Its face lattice is isomorphic to the Boolean lattice on [3], which is depicted on Figure 1.1.

Example 1.1.3 (Cubes). Another kind of geometric realization of the Boolean lattice is given by the *cube*:

$$\begin{aligned}\square_d &= \operatorname{conv}\left(\left\{\sum_{i\in I}\boldsymbol{e}_i \,\middle|\, I\subseteq[d]\right\}\right)\subseteq\mathbb{R}^d\\ &= \left\{\boldsymbol{x}\in\mathbb{R}^d \,\middle|\, 0\le x_i\le 1 \text{ for all } i\in[d]\right\}.\end{aligned}$$

Here, the subsets of $[d]$ index the vertices of the polytope, and we recover the Boolean lattice on $[d]$ by orienting the edges of $\square_d$ along the direction $\mathbf{1}$.

The poset of non-empty faces of the cube is isomorphic to the poset of sequences in $\{+,-,0\}^d$ with the partial order relation $\preceq$ such that $(a_1,\dots,a_d)\preceq(b_1,\dots,b_d)$ if and only if for all $i\in[d]$, either $a_i=b_i$, or $b_i=0$. The face of $\square_d$ corresponding to the sequence $(a_1,\dots,a_d)\in\{+,-,0\}^d$ is maximized in the direction $\sum_{a_i=+}\boldsymbol{e}_i-\sum_{a_i=-}\boldsymbol{e}_i$.

Figure 1.3 shows the Hasse diagram of the face lattice of the cube $\square_3$, with non-empty faces indexed by sequences in $\{+,-,0\}^3$. One can also see that an orientation of the graph of the cube (on top) allows to recover the Hasse diagram of the Boolean lattice on [3] shown on Figure 1.1.

A polytope is *simplicial* if all its facets are simplices, or equivalently if its combinatorial type is stable under small perturbations of its vertices.

Even though face posets of polytopes are very structured (for example they are lattices, they are graded by the dimensions of faces, they are atomic and co-atomic, ..., see [Zie95, Theorem 2.7]), for dimensions higher than 3 there exists no combinatorial characterization for posets that are realizable as face posets of polytopes. Mnëv's Universality Theorem [Mnë88] and its extension by Richter-Gebert [RG96], imply that deciding whether a poset is the face lattice of a 4-dimensional polytope is computationally hard ($\exists\mathbb{R}$-complete). The problem remains hard even when restricting to the generic case of simplicial polytopes, see [AP17]. A consequence of this lack of combinatorial characterization is that the enumeration of combinatorial types of polytopes is also a hard problem, that we discuss in Chapter 2.

Definition 1.1.4. Let $\boldsymbol{P}$ be a polytope in $\mathbb{R}^d$ and $\boldsymbol{F}$ one of its nonempty faces. We call *normal cone of* $\boldsymbol{F}$ the closed cone of all directions that maximize $\boldsymbol{F}$ among faces of $\boldsymbol{P}$: $\left\{\boldsymbol{u}\in\mathbb{R}^d \,\middle|\, \boldsymbol{F}\subseteq\boldsymbol{P}^{\boldsymbol{u}}\right\}$. It is a *cone* because it is stable under addition and multiplication by a non-negative scalar.

The *normal fan* of $\boldsymbol{P}$, that we denote $\boldsymbol{\mathcal{N}}(\boldsymbol{P})$, is the collection of the normal cones of the nonempty faces of $\boldsymbol{P}$.

Two polytopes are *normally equivalent* if they have the same normal fan.

See Figures 1.4 and 1.5 for examples in dimension 2.

Normal equivalence implies combinatorial equivalence, since the cones of $\boldsymbol{\mathcal{N}}(\boldsymbol{P})$ ordered by reverse inclusion form a poset that is isomorphic to the poset of nonempty faces of $\boldsymbol{P}$. In other words, the combinatorial information of a polytope is contained in its normal fan.

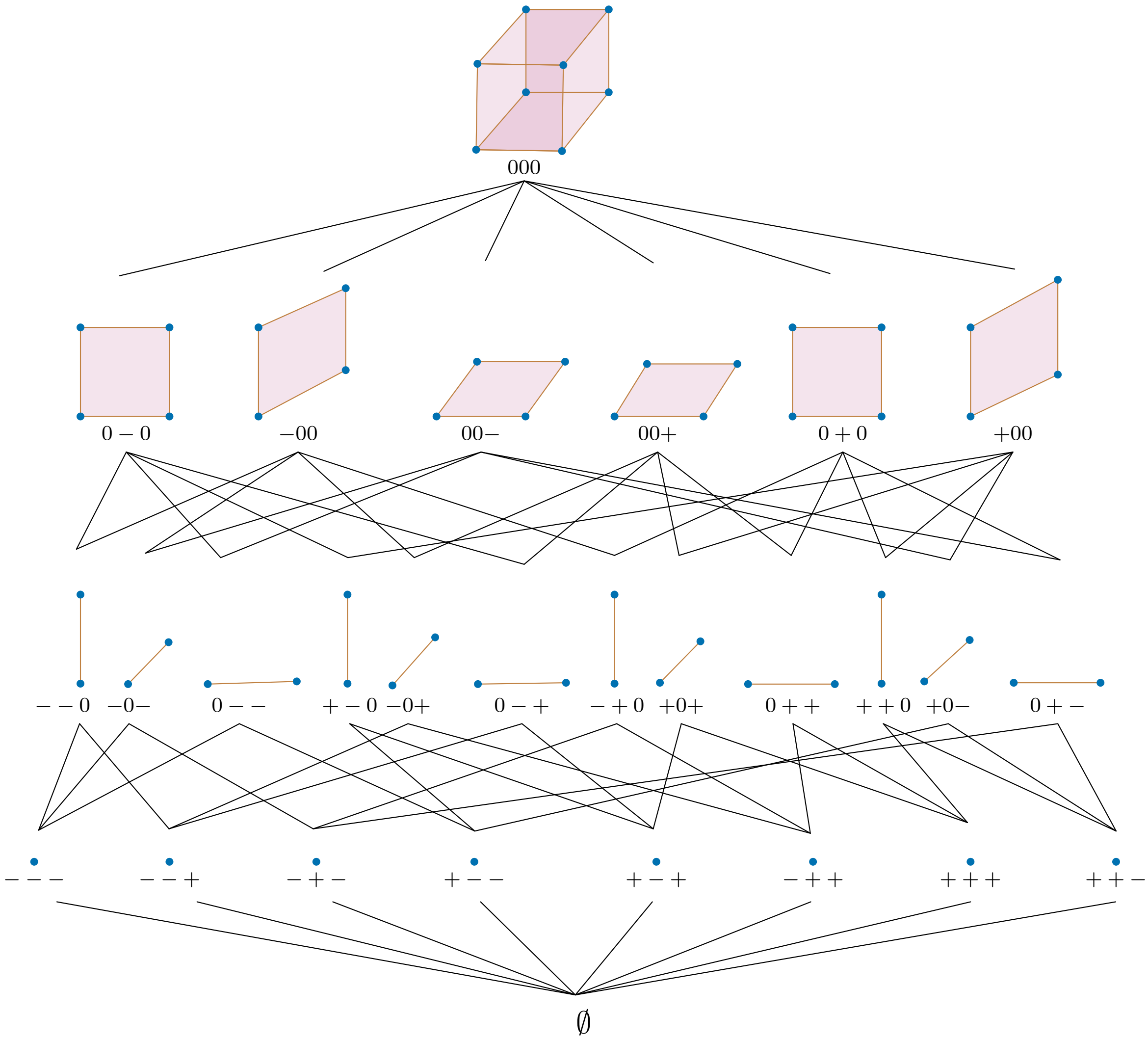

Figure 1.3: Face lattice of the cube $\square_3$. The non-empty faces are indexed with sequences in $\{+,-,0\}^3$ to show the isomorphism alluded to in Example 1.1.3.

As the example of Figure 1.5 shows, the converse is not true: there are polytopes that are combinatorially equivalent but not normally equivalent.

The following basic construction is at the heart of the Cayley trick and appears in several places in Chapters 3 and 4.

Definition 1.1.5. Let $\boldsymbol{A}_1, \ldots, \boldsymbol{A}_k$ be a collection of k point configurations in $\mathbb{R}^d$, with $\boldsymbol{A}_j = (\boldsymbol{a}_{j,1}, \ldots, \boldsymbol{a}_{j,m_j}) \in \mathbb{R}^{d \times [m_j]}$ for all $j \in [k]$. Their *Minkowski sum* is the point configu-

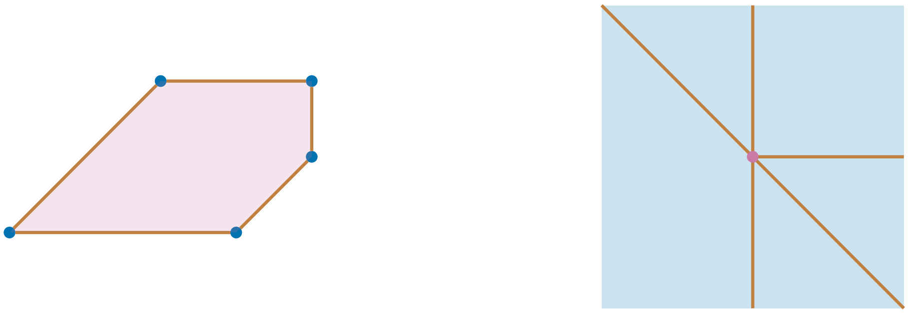

Figure 1.4: A polygon (left) and its normal fan (right).

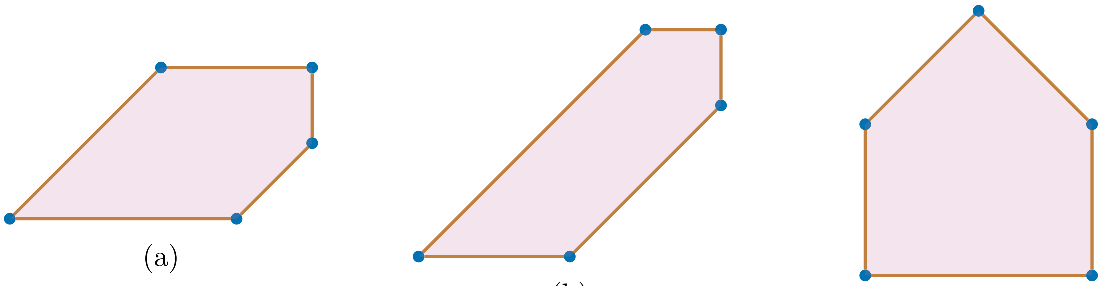

(a) (b) (c)

Figure 1.5: Example of three polygons that are combinatorially equivalent. The polygons (a) and (b) are moreover normally equivalent.

ration

$$\boldsymbol{A}_1 + \ldots + \boldsymbol{A}_k := \{\boldsymbol{a}_{1,i_1} + \cdots + \boldsymbol{a}_{k,i_k} \,|\, (i_1, \ldots, i_k) \in [m_1] \times \ldots \times [m_k]\} \in \mathbb{R}^{d \times ([m_1] \times \ldots \times [m_k])}.$$

The point configurations $\boldsymbol{A}_1, \ldots, \boldsymbol{A}_k$ are called the *summands* of the Minkowski sum.

For the Minkowski sum of k copies of a point configuration $\boldsymbol{A}$ we simply write $k\boldsymbol{A}$.

The Minkowski sum of k polytopes $\boldsymbol{P}_1, \ldots, \boldsymbol{P}_k$ in $\mathbb{R}^d$ is defined similarly as the polytope $\boldsymbol{P}_1 + \ldots + \boldsymbol{P}_k := \{\boldsymbol{x}_1 + \cdots + \boldsymbol{x}_k \,|\, \boldsymbol{x}_i \in \boldsymbol{P}_i\}$ in $\mathbb{R}^d$.

A Minkowski sum of segments (one-dimensional polytopes) is called a *zonotope*. For example, the standard cube $\square_n$ is a zonotope obtained by taking the Minkowski sum of segments $\operatorname{conv}(\boldsymbol{0}, \boldsymbol{e}_i)$ for $i \in [d]$.

See Figure 1.6 for an example of Minkowski sum in dimension 2.

We also introduce the following basic construction.

Definition 1.1.6. Let $\boldsymbol{P}_1 \subset \mathbb{R}^{d_1}, \ldots, \boldsymbol{P}_k \subset \mathbb{R}^{d_k}$ be a collection of k polytopes (or more general sets) in different Euclidean spaces.

Their *product* is the polytope $\boldsymbol{P}_1 \times \ldots \times \boldsymbol{P}_k := \{(\boldsymbol{x}_1, \ldots, \boldsymbol{x}_k) \,|\, \boldsymbol{x}_i \in \boldsymbol{P}_i\} \subset \mathbb{R}^{d_1 + \ldots + d_k}$, where $(\boldsymbol{x}_1, \ldots, \boldsymbol{x}_k)$ is an abuse of notation to denote the point of $\mathbb{R}^{d_1 + \ldots + d_k}$ whose sequence of coordinates is the concatenation of the coordinates of the $\boldsymbol{x}_i$.

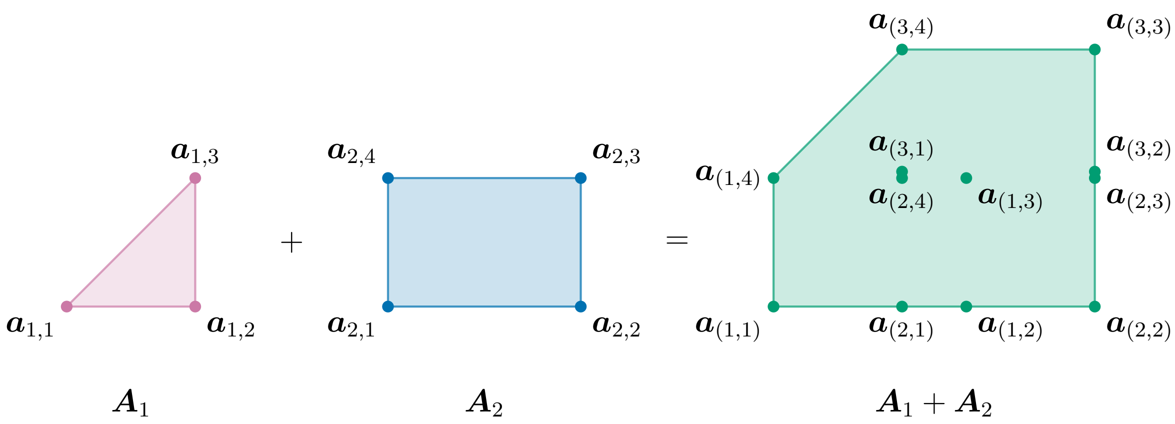

Figure 1.6: Minkowski sum of two point configurations $\boldsymbol{A}_1$ and $\boldsymbol{A}_2$ (represented with their convex hull). A point $\boldsymbol{a}_{1,i_1} + \boldsymbol{a}_{2,i_2}$ is labeled by $\boldsymbol{a}_{(i_1,i_2)}$.

1.1.3 Polyhedral complexes and subdivisions

A *hyperplane* in $\mathbb{R}^d$ is a set of points of the form $\{\boldsymbol{x} \in \mathbb{R}^d \mid \langle \boldsymbol{u}, \boldsymbol{x} \rangle = c\}$ for a certain vector $\boldsymbol{u} \in \mathbb{R}^d$ and a certain value $c \in \mathbb{R}$. If $c = 0$ we say that such hyperplane is *linear*.

A *halfspace* in $\mathbb{R}^d$ is a set of points of the form $\{\boldsymbol{x} \in \mathbb{R}^d \mid \langle \boldsymbol{u}, \boldsymbol{x} \rangle \leq c\}$ for a certain vector $\boldsymbol{u} \in \mathbb{R}^d$ and a certain value $c \in \mathbb{R}$.

A *polyhedron* is the intersection of a finite number of halfspaces. Its dimension is the dimension of its affine hull.

The next theorem allows us to give another description of a polytope, that amounts to define it with its facets rather than with its vertices. The proof relies on elementary geometric techniques but it is not trivial, and the computational problem of going efficiently from one description to the other is hard.

Theorem 1.1.7 (see [Zie95, Theorem 1.1])**.** *A set of points in $\mathbb{R}^d$ is a polytope if and only if it is a bounded polyhedron.*

The same definition of faces than Definition 1.1.1 applies to polyhedra.

Definition 1.1.8. A *polyhedral complex* in $\mathbb{R}^d$ is a finite collection $\boldsymbol{\mathcal{C}}$ of polyhedra in $\mathbb{R}^d$, called its *cells*, or *faces*, such that:

1. if $\boldsymbol{P} \in \boldsymbol{\mathcal{C}}$ and $\boldsymbol{F}$ is a face of $\boldsymbol{P}$, then $\boldsymbol{F} \in \boldsymbol{\mathcal{C}}$,
2. for all $\boldsymbol{P}, \boldsymbol{Q} \in \boldsymbol{\mathcal{C}}$, $\boldsymbol{P} \cap \boldsymbol{Q}$ is a common face of $\boldsymbol{P}$ and $\boldsymbol{Q}$.

The set of cells of $\boldsymbol{\mathcal{C}}$ ordered by containment gives the *face poset* of $\boldsymbol{\mathcal{C}}$. The dimension of $\boldsymbol{\mathcal{C}}$ is the maximum over the dimensions of its cells. A complex is *pure* if all its inclusion-maximal cells have the same dimension. Its *support* is the union of all its cells.

A *polytopal complex* is a polyhedral complex whose all cells are bounded (hence they are polytopes). A *polytopal simplicial complex* is a polyhedral complex whose all cells are simplices. Note that it is a geometric realization of a more abstract combinatorial object: a *simplicial complex* on a finite set X is a finite collection $\mathcal{C}$ of subsets of X such that if $A \in \mathcal{C}$ and $B \subseteq A$ then $B \in \mathcal{C}$ (for a polytopal simplicial complex the set X would be its set of vertices).

Definition 1.1.9. Let $\boldsymbol{\mathcal{C}}, \boldsymbol{\mathcal{C}}'$ be two polyhedral complexes. We say that $\boldsymbol{\mathcal{C}}'$ *refines* $\boldsymbol{\mathcal{C}}$, or $\boldsymbol{\mathcal{C}}$ *coarsens* $\boldsymbol{\mathcal{C}}'$ if they have the same support and any cell of $\boldsymbol{\mathcal{C}}'$ is included in a cell of $\boldsymbol{\mathcal{C}}$.

We have already seen examples of polyhedral complexes: the set of faces of a polytope, the normal fan of a polytope. Here is another example.

Definition 1.1.10. A *hyperplane arrangement* in $\mathbb{R}^d$ is a finite set of hyperplanes $\boldsymbol{H}_1, \dots, \boldsymbol{H}_k$ in $\mathbb{R}^d$. It defines a polyhedral complex whose cells are the closures of the connected components of $\mathbb{R}^d \setminus \{\boldsymbol{H}_1, \dots, \boldsymbol{H}_k\}$ and all their faces.

Proposition 1.1.11 ([Zie95, Proposition 7.12]). *Let $\boldsymbol{P}_1, \dots, \boldsymbol{P}_k$ be polytopes in $\mathbb{R}^d$. The normal fan of their Minkowski sum $\sum_i \boldsymbol{P}_i$ is the common refinement of all their normal fans $\boldsymbol{\mathcal{N}}(\boldsymbol{P}_i)$. In particular, any normal fan of a summand $\boldsymbol{\mathcal{N}}(\boldsymbol{P}_i)$ coarsens the normal fan of the sum $\boldsymbol{\mathcal{N}}(\sum_i \boldsymbol{P}_i)$.*

As a special case, we see that the normal fan of a zonotope whose edge directions are $\boldsymbol{u}_1, \dots, \boldsymbol{u}_k$ is the arrangement of linear hyperplanes orthogonal to the vectors $\boldsymbol{u}_i$.

At first approximation, a *subdivision* of a point configuration $\boldsymbol{A}$ could be defined as a polytopal complex $\boldsymbol{\mathcal{S}}$ with support $\mathrm{conv}(\boldsymbol{A})$ such that all the polytopes in $\boldsymbol{\mathcal{S}}$ have their vertices in $\boldsymbol{A}$. This definition is valid for a point configuration $\boldsymbol{A}$ which is in *convex position*, namely its points correspond exactly to the vertices of the polytope $\mathrm{conv}(\boldsymbol{A})$ (in particular they are not repeated). In this case we moreover have that any subdivision of $\boldsymbol{A}$ uses all its points. However, when $\boldsymbol{A}$ is not in convex position, we need a more subtle definition that takes into account the labels of the points in $\boldsymbol{A}$ and makes a difference between two sets of labels even if they induce the same convex hull.

We recall that the notation $\mathrm{relint}(\boldsymbol{X})$ denotes the relative interior of the set $\boldsymbol{X}$.

Definition 1.1.12. Let $\boldsymbol{A} = (\boldsymbol{a}_1, \dots, \boldsymbol{a}_n)$ be a point configuration in $\mathbb{R}^{d \times [n]}$. A *subdivision* of $\boldsymbol{A}$ is a collection $\boldsymbol{\mathcal{S}}$ of subsets of $\boldsymbol{A}$, called its cells, such that:

1. if $\boldsymbol{B} \in \boldsymbol{\mathcal{S}}$ and $\boldsymbol{C}$ is the intersection of $\boldsymbol{B}$ with a face of $\mathrm{conv}(\boldsymbol{B})$, then $\boldsymbol{C} \in \boldsymbol{\mathcal{S}}$,
2. for all $\boldsymbol{B}, \boldsymbol{C} \in \boldsymbol{\mathcal{S}}$ such that $\boldsymbol{B} \neq \boldsymbol{C}$, $\mathrm{relint}(\boldsymbol{B}) \cap \mathrm{relint}(\boldsymbol{C}) = \emptyset$,
3. $\cup_{\boldsymbol{B} \in \boldsymbol{\mathcal{S}}} \mathrm{conv}(\boldsymbol{B}) = \mathrm{conv}(\boldsymbol{A})$.

A *triangulation* of $\boldsymbol{A}$ is a subdivision of $\boldsymbol{A}$ whose all cells consist of affinely independent points (in particular their convex hull are simplices).

The *trivial subdivision* of $\boldsymbol{A}$ is the collection formed by $\boldsymbol{A}$ and all its subsets that are on faces of $\operatorname{conv}(\boldsymbol{A})$.

For two subdivisions $\boldsymbol{\mathcal{S}}$ and $\boldsymbol{\mathcal{S}}'$ of $\boldsymbol{A}$ we say that $\boldsymbol{\mathcal{S}}'$ refines $\boldsymbol{\mathcal{S}}$, or $\boldsymbol{\mathcal{S}}$ coarsens $\boldsymbol{\mathcal{S}}'$ if any cell of $\boldsymbol{\mathcal{S}}'$ is contained in an element of $\boldsymbol{\mathcal{S}}$.

Example 1.1.13. Figure 1.7a shows a configuration $\boldsymbol{M}$ of six points in $\mathbb{R}^2$ that form concentric equilateral triangles. This configuration is called *"the mother of all examples"* in [DRS10]. Figure 1.7b shows the trivial subdivision $\boldsymbol{\mathcal{S}}_{\text{triv}}$ of $\boldsymbol{M}$ whose cells are $\{\boldsymbol{a}_1, \boldsymbol{a}_2, \boldsymbol{a}_3, \boldsymbol{a}_4, \boldsymbol{a}_5, \boldsymbol{a}_6\}, \{\boldsymbol{a}_1, \boldsymbol{a}_2\}, \{\boldsymbol{a}_1, \boldsymbol{a}_3\}, \{\boldsymbol{a}_2, \boldsymbol{a}_3\}, \{\boldsymbol{a}_1\}, \{\boldsymbol{a}_2\}, \{\boldsymbol{a}_3\}, \emptyset$. Figure 1.7c shows a triangulation $\boldsymbol{\mathcal{T}}$ of $\boldsymbol{M}$, whose cells are $\{\boldsymbol{a}_1, \boldsymbol{a}_2, \boldsymbol{a}_3\}, \{\boldsymbol{a}_1, \boldsymbol{a}_2\}, \{\boldsymbol{a}_1, \boldsymbol{a}_3\}, \{\boldsymbol{a}_2, \boldsymbol{a}_3\}, \{\boldsymbol{a}_1\}, \{\boldsymbol{a}_2\}, \{\boldsymbol{a}_3\}, \emptyset$. Note that these two subdivisions are different, and $\boldsymbol{\mathcal{T}}$ refines $\boldsymbol{\mathcal{S}}_{\text{triv}}$.

Other examples of subdivisions and triangulations of $\boldsymbol{M}$ are provided on Figure 1.11. The triangulations of Figures 1.11c and 1.11d coarsen the subdivision of Figure 1.11b.

The set of all subdivisions of a point configuration can be ordered by refinement. Then the triangulations are the minimal elements of this poset and the trivial subdivision is the maximal one.

1.1.4 Cayley trick

The Cayley trick originally comes from elimination theory on polynomial systems and the study of resultants and discriminants ([GKZ94, Chapter 9, Proposition 1.7]). A polytopal version was first given by Sturmfels in [Stu94, Section 5] as a correspondence between two families of regular subdivisions of different polytopes. Humber, Rambau, and Santos showed in [HRS00] that there is the same correspondence for non-necessarily regular subdivisions. In this section, we start with this version of the Cayley trick, before introducing regular subdivisions in the next section, and revisit the Cayley trick in Proposition 1.2.4. We refer to [DRS10, Section 9.2] for a detailed presentation.

Definition 1.1.14. Let $\boldsymbol{A}_1 \in \mathbb{R}^{d \times [m_1]}, \dots, \boldsymbol{A}_k \in \mathbb{R}^{d \times [m_k]}$ be a collection of k point configurations in $\mathbb{R}^d$. We denote by $\sum \boldsymbol{A}_i$ their Minkowski sum. A *Minkowski cell* of $\sum \boldsymbol{A}_i$ is a Minkowski sum $\sum \boldsymbol{B}_i$ where for each i, $\boldsymbol{B}_i$ is a subset of $\boldsymbol{A}_i$. A *mixed subdivision* of $\sum \boldsymbol{A}_i$ is a subdivision of $\sum \boldsymbol{A}_i$ whose all cells are Minkowski cells (see [DRS10, Definition 9.2.5] or [San05, Definition 1.1]). A *fine mixed subdivision* is a minimal mixed subdivision via containment of its summands.

See Figures 1.8 and 1.9 for examples.

We recall that $\boldsymbol{e}_1, \dots, \boldsymbol{e}_k$ denotes the standard basis of $\mathbb{R}^k$. We call the point configuration

$$\mathbf{Cay}(\boldsymbol{A}_1, \dots, \boldsymbol{A}_k) := (\{\boldsymbol{e}_1\} \times \boldsymbol{A}_1, \dots, \{\boldsymbol{e}_k\} \times \boldsymbol{A}_k) \in \mathbb{R}^{(k+d) \times (\{1\} \times [m_1] \cup \ldots \cup \{k\} \times [m_k])}$$

the *Cayley embedding* of $\boldsymbol{A}_1, \dots, \boldsymbol{A}_k$.

Proposition 1.1.15 (The Cayley trick, special case of [HRS00, Theorem 3.1])**.** *Let* $\boldsymbol{A}_1, \dots, \boldsymbol{A}_k$ *be point configurations in* $\mathbb{R}^d$*. The polytopal subdivisions (respectively triangulations) of*

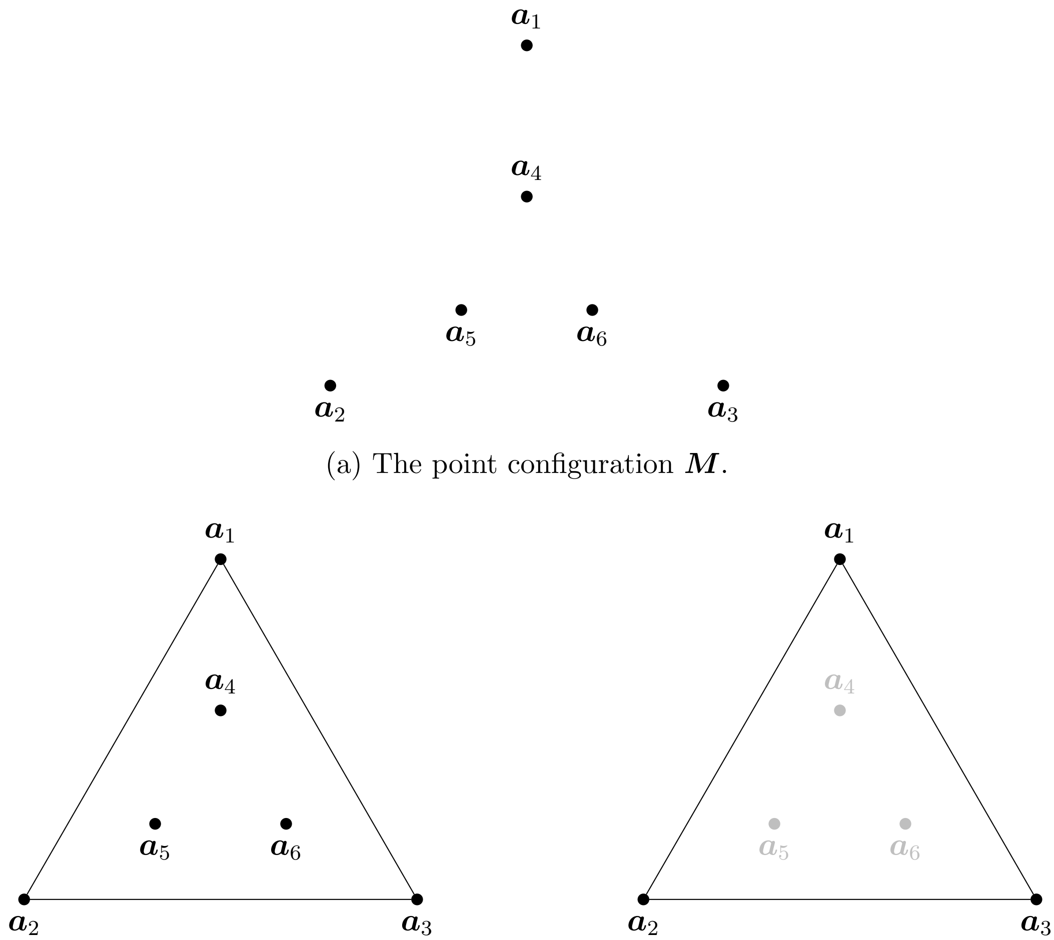

(a) The point configuration $\boldsymbol{M}$.

(b) The trivial subdivision of $\boldsymbol{M}$.

(c) A triangulation of $\boldsymbol{M}$.

Figure 1.7: Example of a point configuration with its trivial subdivision and an example of triangulation.

$\boldsymbol{Cay}(\boldsymbol{A}_1, \ldots, \boldsymbol{A}_k)$ *are in bijection with the mixed subdivisions (respectively fine mixed subdivisions) of* $\boldsymbol{A}_1 + \ldots + \boldsymbol{A}_k$.

A concrete way to have this bijection (see the "one-picture-proof" in [HRS00, Figure 1], or Figure 1.10 below) is to intersect a subdivision of $\mathbf{Cay}(\boldsymbol{A}_1, \ldots, \boldsymbol{A}_k)$ with the subspace $(\frac{1}{k}, \ldots, \frac{1}{k}) \times \mathbb{R}^d$ of $\mathbb{R}^k \times \mathbb{R}^d$. Up to dilation by the factor k we obtain a mixed subdivision of $\boldsymbol{A}_1 + \ldots + \boldsymbol{A}_k$.

Example 1.1.16. Let us make some comments about the examples of Figures 1.6, 1.8 and 1.9. The Minkowski sum $\boldsymbol{A}_1 + \boldsymbol{A}_2$ shown on Figure 1.6 has repeated points. For example, the points $\boldsymbol{a}_{(3,1)} := \boldsymbol{a}_{1,3} + \boldsymbol{a}_{2,1}$ and $\boldsymbol{a}_{(2,4)} := \boldsymbol{a}_{1,2} + \boldsymbol{a}_{2,4}$ have the same position. However, the labelings are important for the definition of a subdivision. Similarly, the

Minkowski cell depicted on Figure 1.8 would not be valid if $\boldsymbol{a}_{(3,1)}$ were replaced by $\boldsymbol{a}_{(2,4)}$, or if the points $\boldsymbol{a}_{(2,1)}$ and $\boldsymbol{a}_{(1,2)}$ were not included.

The careful reader can check that all the cells of the subdivisions depicted on Figure 1.9 are indeed Minkowski cells of $\boldsymbol{A}_1 + \boldsymbol{A}_2$.

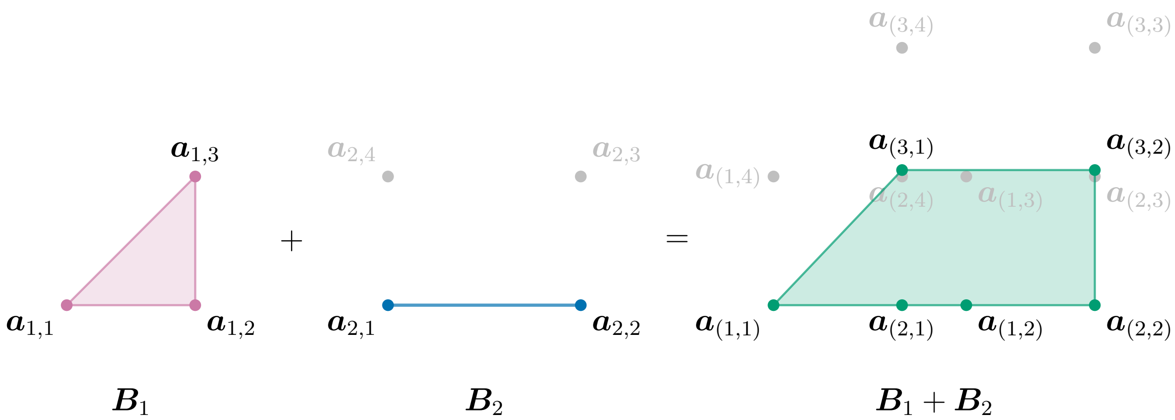

Figure 1.8: A Minkowski cell of the sum $\boldsymbol{A}_1 + \boldsymbol{A}_2$ from Figure 1.6.

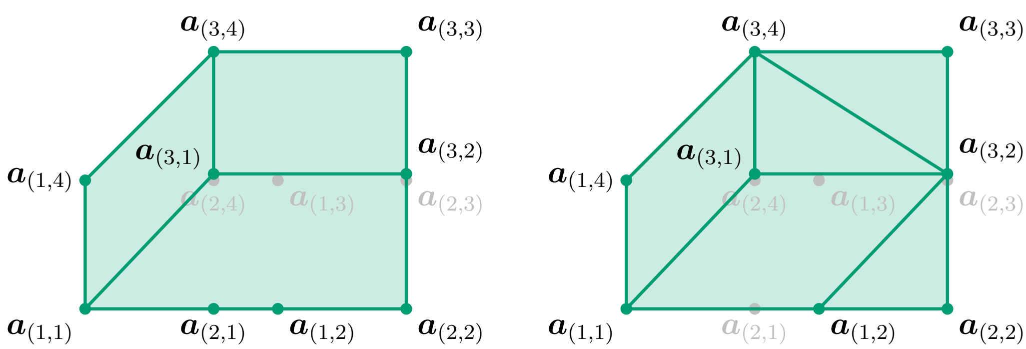

Figure 1.9: Two mixed subdivisions of the sum $\boldsymbol{A}_1 + \boldsymbol{A}_2$ from Figure 1.6. The one on the right is a fine mixed subdivision.

1.2 Regular subdivisions

It might not be obvious that all point configurations admit subdivisions, but we will show a geometric way to obtain some, consisting in lifting the points of the configuration in one dimension higher. The subdivisions that can be obtained this way are called regular subdivisions. In this section we review three polyhedral constructions associated to regular subdivisions that play a role in this thesis.

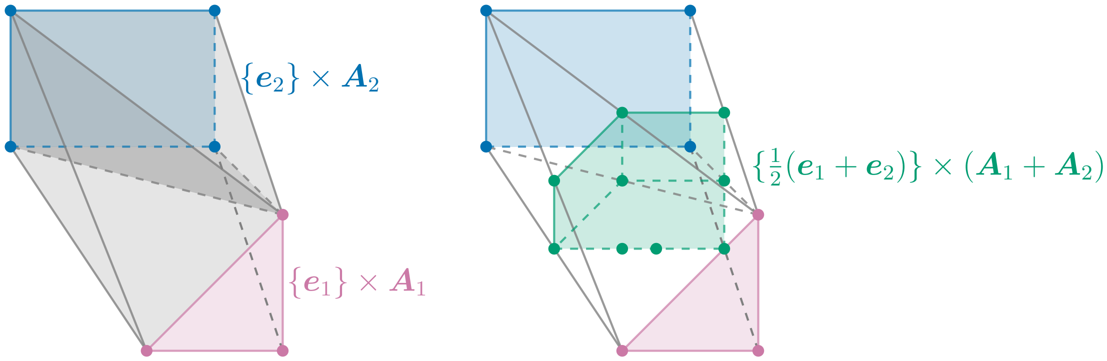

Figure 1.10: Illustration of the Cayley trick: a subdivision of the Cayley embedding of point configurations $\boldsymbol{A}_1$ and $\boldsymbol{A}_2$ from Figure 1.6 (left) is intersected so that we recover the mixed subdivision of $\boldsymbol{A}_1 + \boldsymbol{A}_2$ depicted on the left of Figure 1.9 (right).

1.2.1 Lifting and admissible lifting function

Liftings are at the heart of our construction to build many polytopes in Chapter 2.

Definition 1.2.1. Let $\boldsymbol{A} = (\boldsymbol{a}_1, \ldots, \boldsymbol{a}_n) \in \mathbb{R}^{d\times[n]}$ be a point configuration in $\mathbb{R}^d$. Let $\ell : [n] \to \mathbb{R}$ be a function that we call the *lifting function*. (We could also define it as a vector in $\mathbb{R}^{[n]}$.) Then the *lifting* of $\boldsymbol{A}$ according to ℓ is the point configuration $\widehat{\boldsymbol{A}} := ((\boldsymbol{a}_1, \ell(1)), \ldots, (\boldsymbol{a}_n, \ell(n)))$ in $\mathbb{R}^{d+1}$.

A face $\boldsymbol{F}$ of the corresponding lifted polytope $\mathrm{conv}(\widehat{\boldsymbol{A}})$ is called *lower* if its normal cone contains a vector with last coordinate negative, that is to say if there is a direction $\boldsymbol{u} \in \mathbb{R}^{d+1}$ with $u_{d+1} < 0$ that is maximized on $\boldsymbol{F}$.

We denote by $\pi : \begin{cases} \mathbb{R}^{d+1} & \to \mathbb{R}^d \\ (\boldsymbol{x}, x_{d+1}) & \mapsto \boldsymbol{x} \end{cases}$ the projection that forgets the last coordinate. Then, the collection $\boldsymbol{\mathcal{S}} := \left\{ \pi(\boldsymbol{F} \cap \widehat{\boldsymbol{A}}) \,\middle|\, \boldsymbol{F} \text{ is a lower face of } \mathrm{conv}(\widehat{\boldsymbol{A}}) \right\}$ is a subdivision of $\boldsymbol{A}$. A subdivision that can be obtained this way by a lifting is called *regular*, and we will say that ℓ is an *admissible lifting function* for $\boldsymbol{\mathcal{S}}$.

Example 1.2.2. Figure 1.11 shows again the configuration $\boldsymbol{M}$ of six points in $\mathbb{R}^2$ that form concentric equilateral triangles (1.11a), together with examples of a regular subdivision (1.11b), a regular triangulation (1.11c) and a non-regular triangulation (1.11d). The following argument should convince the reader that indeed there can be no admissible lifting function for the triangulation $\boldsymbol{\mathcal{T}}$ of Figure 1.11d. Suppose that there were such a lifting function ℓ. Then, the fact that the edge $[\boldsymbol{a}_1, \boldsymbol{a}_5]$ is in $\boldsymbol{\mathcal{T}}$ implies that $\epsilon\ell(1) + (1-\epsilon)\ell(5) < \epsilon\ell(2) + (1-\epsilon)\ell(4)$, where $\epsilon \in]0,1[$ is such that the segments $[\boldsymbol{a}_1, \boldsymbol{a}_5]$ and $[\boldsymbol{a}_2, \boldsymbol{a}_4]$ intersect at $\epsilon\boldsymbol{a}_1 + (1-\epsilon)\boldsymbol{a}_5 = \epsilon\boldsymbol{a}_2 + (1-\epsilon)\boldsymbol{a}_4$. Similarly, by looking at edges $[\boldsymbol{a}_2, \boldsymbol{a}_6]$ and $[\boldsymbol{a}_3, \boldsymbol{a}_4]$ we would have $\epsilon\ell(2) + (1-\epsilon)\ell(6) < \epsilon\ell(3) + (1-\epsilon)\ell(5)$ and $\epsilon\ell(3) + (1-\epsilon)\ell(4) < \epsilon\ell(1) + (1-\epsilon)\ell(6)$. Summing these inequalities would give

$\epsilon(\ell(1)+\ell(2)+\ell(3))+(1-\epsilon)(\ell(4)+\ell(5)+\ell(6)) < \epsilon(\ell(1)+\ell(2)+\ell(3))+(1-\epsilon)(\ell(4)+\ell(5)+\ell(6))$, which is not possible.

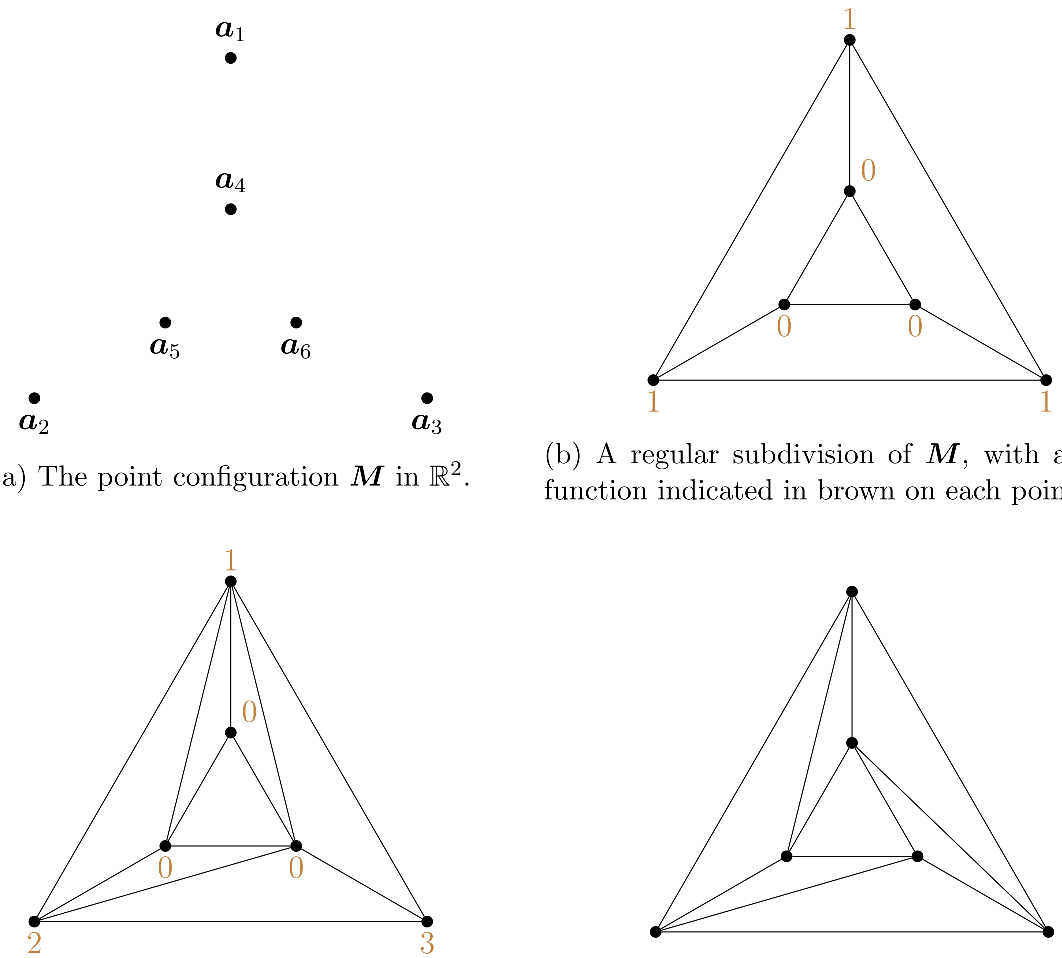

(a) The point configuration $\boldsymbol{M}$ in $\mathbb{R}^2$.

(b) A regular subdivision of $\boldsymbol{M}$, with a lifting function indicated in brown on each point.

(c) A regular triangulation of $\boldsymbol{M}$, with a lifting function indicated in brown on each point.

(d) A triangulation of $\boldsymbol{M}$ which is not regular.

Figure 1.11: Example of a point configuration with regular and non-regular subdivisions. See Example 1.2.2.

The next proposition is a variant of the Cayley trick (Proposition 1.1.15) restricted to regular subdivisions. Note that this was the first polytopal version of the Cayley trick, and it was initially stated in terms of fiber polytopes (which gives more information).

Definition 1.2.3. Let $\boldsymbol{A}_1 \in \mathbb{R}^{d\times[m_1]}, \ldots, \boldsymbol{A}_k \in \mathbb{R}^{d\times[m_k]}$ be a collection of k point configurations in $\mathbb{R}^d$. A mixed subdivision of the Minkowski sum $\sum \boldsymbol{A}_i \in \mathbb{R}^{d\times([m_1]\times\ldots\times[m_k])}$ is said to be *coherent* if it can be obtained from a lifting function $\ell : [m_1] \times \ldots \times [m_k] \to \mathbb{R}$ of the form $\ell(i_1, \ldots, i_k) = \sum \ell_j(i_j)$ for some lifting functions $\ell_j : [m_j] \to \mathbb{R}$ for $j \in [k]$.

This is a special case of coherent subdivisions for subdivisions coming from projections, see Remark 1.3.2.

For example, the mixed subdivisions of Figure 1.9 are coherent. For the one on the right, an admissible lifting function is shown on Figure 1.12.

Proposition 1.2.4 (The Cayley trick for regular subdivisions [Stu94, Section 5]). *Let $\boldsymbol{A}_1, \dots, \boldsymbol{A}_k$ be point configurations in $\mathbb{R}^d$. The regular subdivisions (respectively triangulations) of $\boldsymbol{Cay}(\boldsymbol{A}_1, \dots, \boldsymbol{A}_k)$ are in bijection with the coherent mixed subdivisions (respectively coherent fine mixed subdivisions) of $\boldsymbol{A}_1 + \dots + \boldsymbol{A}_k$.*

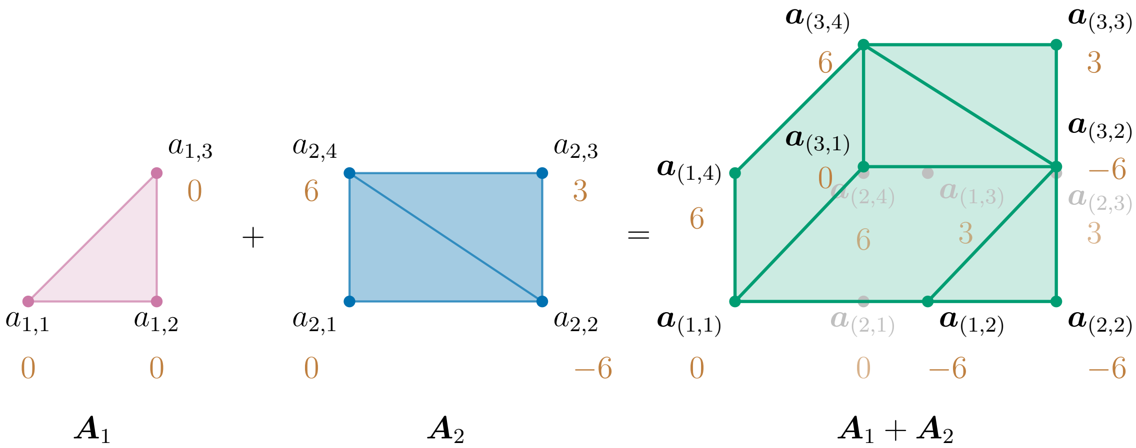

Figure 1.12: Minkowski sum of the two point configurations $\boldsymbol{A}_1$ and $\boldsymbol{A}_2$ with lifted functions indicated in brown, and the corresponding coherent mixed subdivision of $\boldsymbol{A}_1 + \boldsymbol{A}_2$.

1.2.2 Tropical dualization

In our search for geometrical realizations, it will prove useful (see Section 4.4.3) to be able to dualize certain polyhedral complexes. It happens that tropical geometry offers a convenient setting to do so, for the case of regular polyhedral subdivisions.

This section is based on the work of Joswig in [Jos21, Chapter 1] and [Jos17] for the case of the Cayley trick.

We stick to Joswig's choice to define the tropical addition with min rather than max.

The *tropical semiring* is the set $\mathbb{T} := \mathbb{R} \cup \{\infty\}$ equipped with

- the *tropical addition* $x \oplus y := \min(x, y)$,
- the *tropical multiplication* $x \odot y := x + y$.

We will call *tropical polynomial* on d variables any function $F : \mathbb{R}^d \to \mathbb{R}$ of the form:

$$F(\boldsymbol{x}) = \bigoplus_{i\in[n]} c_i \odot \boldsymbol{x}^{\boldsymbol{a}_i} = \min\left\{c_i + \langle \boldsymbol{a}_i, \boldsymbol{x}\rangle \mid i \in n\right\},$$

where $n \in \mathbb{N}$ and for all $i \in [n]$, $c_i \in \mathbb{T}$ and $\boldsymbol{a}_i \in \mathbb{R}^d$.

This is a concave piecewise affine function. Note that F is not uniquely determined by the exponents $\boldsymbol{a}_i$ and the coefficients c_i.

Remark 1.2.5. Here we go beyond the usual definition of a polynomial by allowing the exponents $\boldsymbol{a}_i$ to take non-integer values. However, there will be no harm for us to do so since our purposes are more geometric than algebraic.

The *tropical hypersurface* defined by the tropical polynomial F, or *vanishing locus* of F, is the set

$$\mathcal{T}(F) := \left\{\boldsymbol{x} \in \mathbb{R}^d \mid \text{the minimum of } F(\boldsymbol{x}) \text{ is attained at least twice}\right\}.$$

It is the image codimension-2-skeleton of the *dome*

$$\mathcal{D}(F) := \left\{(\boldsymbol{x}, y) \in \mathbb{R}^{d+1} \mid \boldsymbol{x} \in \mathbb{R}^d,\ y \in \mathbb{R},\ y \leq F(\boldsymbol{x})\right\}$$

under the orthogonal projection that omits the last coordinate [Jos21, Corollary 1.6].

See the right of Figures 1.13 and 1.14 for examples.

The *cells* of $\mathcal{T}(F)$ are the projections of the faces of $\mathcal{D}(F)$ (here we include the regions of $\mathbb{R}^d$ delimited by $\mathcal{T}(F)$ as its d-dimensional cells ; in fact we are considering the normal complex $NC(F)$ defined in [Jos21, after Example 1.7]).

Definition 1.2.6. Let $\boldsymbol{A} = \{\boldsymbol{a}_1, \dots, \boldsymbol{a}_n\}$ be a point configuration in $\mathbb{R}^d$, and $\boldsymbol{\mathcal{S}}$ a regular subdivision of $\boldsymbol{A}$ with admissible lifting function ℓ.

Such a point configuration together with its lifting function ℓ is associated to the *tropical polynomial*:

$$F(\boldsymbol{x}) = \bigoplus_{i\in[n]} \ell(i) \odot \boldsymbol{x}^{\boldsymbol{a}_i} = \min\left\{\ell(i) + \langle \boldsymbol{a}_i, \boldsymbol{x}\rangle \mid i \in [n]\right\},$$

where $\boldsymbol{x} \in \mathbb{R}^d$.

We say that $\mathcal{T}(F)$ is the *tropical dual* of the subdivision $\boldsymbol{\mathcal{S}}$ with admissible function ℓ, since we have the following theorem:

Theorem 1.2.7 ([Jos21, Theorem 1.13])**.** *There is a bijection between the k-dimensional cells of $\boldsymbol{\mathcal{S}}$ and the $(d-k)$-dimensional cells of $\mathcal{T}(F)$, that reverses the inclusion order.*

This bijection sends a vertex $\boldsymbol{a}_j$ to the region

$$\left\{\boldsymbol{x} \in \mathbb{R}^d \;\middle|\; \ell(j) + \langle \boldsymbol{a}_j, \boldsymbol{x}\rangle = \min_{i\in[n]}\{\ell(i) + \langle \boldsymbol{a}_i, \boldsymbol{x}\rangle\}\right\},$$

and a cell of $\boldsymbol{\mathcal{S}}$ to the intersection of the regions corresponding to its vertices.

See Figures 1.13 and 1.14 for examples.

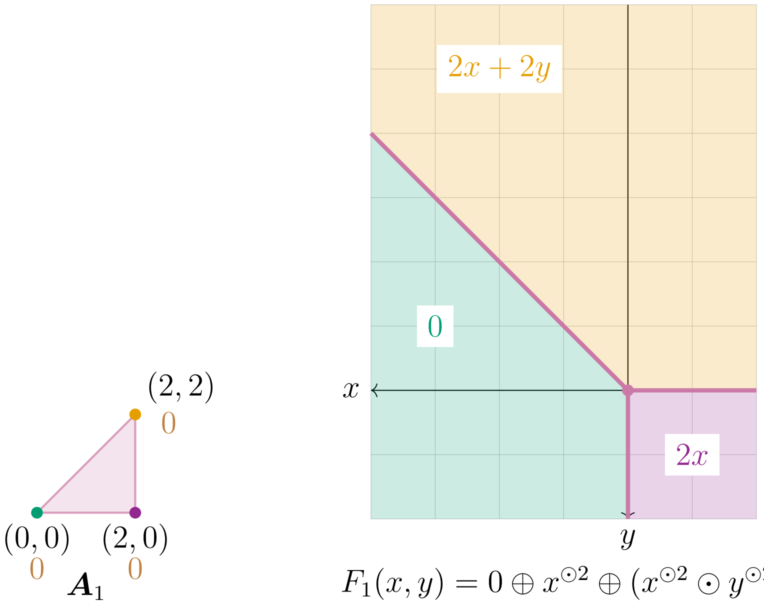

$F_1(x, y) = 0 \oplus x^{\odot 2} \oplus (x^{\odot 2} \odot y^{\odot 2})$

Figure 1.13: Left: Point configuration $\boldsymbol{A}_1$ with lifting indicated in brown. Right: The corresponding tropical hypersurface, associated to the tropical polynomial F_1. The regions are labeled by the evaluation of F_1 on them, and colored according to their associated vertex of $\boldsymbol{A}_1$. Coordinate axes are flipped with respect to the usual orientation.

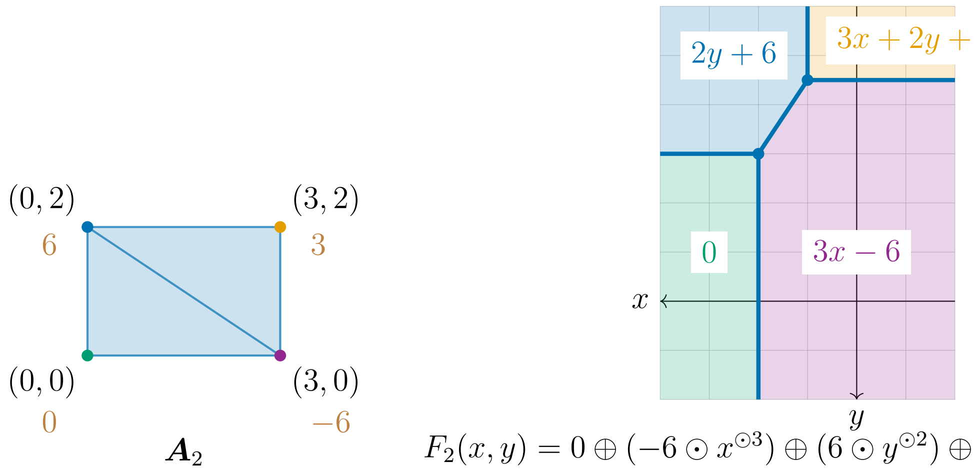

$F_2(x, y) = 0 \oplus (-6 \odot x^{\odot 3}) \oplus (6 \odot y^{\odot 2}) \oplus (3 \odot x^{\odot 3} \odot y^{\odot 2})$

Figure 1.14: Left: A subdivision of the point configuration $\boldsymbol{A}_2$ with lifting indicated in brown. Right: The corresponding tropical hypersurface, associated to the tropical polynomial F_2. The regions are labeled by the evaluation of F_2 on them, and colored according to their associated vertex of $\boldsymbol{A}_2$. Coordinate axes are flipped with respect to the usual orientation.

Example 1.2.8. If we take $\boldsymbol{A}$ to be the vertex configuration of a polytope $\boldsymbol{P}$ and consider the trivial subdivision, obtained with a constant lifting function, then for the tropical dual we obtain the image of the normal fan of $\boldsymbol{P}$ by the function $\boldsymbol{x} \mapsto -\boldsymbol{x}$ (since we defined the faces as maximizing sets but chose the min convention for the tropical dualization). An example can be seen on Figure 1.13.

In our work we need the following refinement of the previous theorem.

Lemma 1.2.9 ([GDMP+23, Lemma 5.2])**.** *The bijection of Theorem 1.2.7 restricts to a bijection between the interior cells of* $\boldsymbol{\mathcal{S}}$ *and the bounded cells of* $\mathcal{T}(F)$*.*

Proof. It is sufficient to show that the bijection restricts to a bijection between the interior facets ($(d-1)$-dimensional cells) of $\boldsymbol{\mathcal{S}}$ and the bounded edges of $\mathcal{T}(F)$. Indeed, suppose that it is the case. Any cell of $\boldsymbol{\mathcal{S}}$ is either maximal and associated to a vertex of $\mathcal{T}(F)$, or it is an intersection of facets of $\boldsymbol{\mathcal{S}}$. A non-maximal cell of $\boldsymbol{\mathcal{S}}$ is interior if and only if it is included only in interior facets of $\boldsymbol{\mathcal{S}}$. Thus it is sent via the bijection to a cell of $\mathcal{T}(F)$ that only contains bounded edges. Reciprocally, a non-bounded cell of $\mathcal{T}(F)$ contains a non-bounded edge, so it is sent to a boundary cell of $\boldsymbol{\mathcal{S}}$.

Let us show the statement about the interior facets of $\boldsymbol{\mathcal{S}}$ in a fashion similar to the proof of [Jos21, Theorem 1.13]. Let $\widetilde{\mathcal{N}}(F) := \operatorname{conv}\{(\boldsymbol{a}_i, r) \mid i \in [n], r \geq \ell(i)\} \subseteq \mathbb{R}^{d+1}$ be the extended Newton polyhedron of F, whose lower faces project bijectively onto the cells of $\boldsymbol{\mathcal{S}}$. Let $\boldsymbol{e}$ be an edge of $\mathcal{T}(F)$ and $\boldsymbol{H}$ its corresponding facet in $\boldsymbol{\mathcal{S}}$ via the bijection. Suppose that $\boldsymbol{e}$ is unbounded, of the form $\boldsymbol{e} = \boldsymbol{w} + \mathbb{R}_+\boldsymbol{v}$ for some $\boldsymbol{v}, \boldsymbol{w} \in \mathbb{R}^d$. Then, for any $\lambda \in \mathbb{R}_+$ the vector $-(\boldsymbol{w} + \lambda\boldsymbol{v}, 1)$ is in the normal cone of the lift of $\boldsymbol{H}$ in $\widetilde{\mathcal{N}}(F)$. Taking the limit of $\lambda \to 0$ of $-\left(\frac{1}{\lambda}\boldsymbol{w} + \boldsymbol{v}, \frac{1}{\lambda}\right)$, we obtain that $-(\boldsymbol{v}, 0)$ is in the normal cone of the lift of $\boldsymbol{H}$, hence $\boldsymbol{H}$ is in the boundary of $\boldsymbol{\mathcal{S}}$.

Reciprocally, if $\boldsymbol{H}$ is a boundary facet of $\boldsymbol{\mathcal{S}}$, it means that the normal cone of the lift of $\boldsymbol{H}$ in $\widetilde{\mathcal{N}}(F)$ is a two-dimensional cone whose extremal rays can be written $-\mathbb{R}_+(\boldsymbol{v}, 0)$ and $-\mathbb{R}_+(\boldsymbol{w}, 1)$, for some $\boldsymbol{v}, \boldsymbol{w} \in \mathbb{R}^d$. For any $\lambda \in \mathbb{R}_+$, the vector $-(\boldsymbol{w} + \lambda\boldsymbol{v}, 1) = -\lambda(\frac{1}{\lambda}\boldsymbol{w} + \boldsymbol{v}, \frac{1}{\lambda})$ is in this cone, so the point $\boldsymbol{w} + \lambda\boldsymbol{v}$ belongs to the edge $\boldsymbol{e}$ in $\mathcal{T}(F)$. Hence, this edge is unbounded. $\square$

In the case where $\boldsymbol{A}$ is a Cayley embedding, Joswig explains in [Jos21, Corollary 4.9] how the Cayley trick allows us to describe the tropical dual of a regular mixed subdivision with an arrangement of tropical hypersurfaces. This extends what was known for regular triangulations of a product of simplices $\triangle_{m-1} \times \triangle_{d-1}$ (which is the Cayley embedding of m copies of the standard simplex $\triangle_{d-1}$): these triangulations are dual to arrangements of tropical hyperplanes, see [DS04, Section 4], [FR15].

We consider $\boldsymbol{A}$ to be the Cayley embedding $\mathbf{Cay}(\boldsymbol{A}_1, \ldots, \boldsymbol{A}_k) \in \mathbb{R}^{(k+d)\times(\{1\}\times[m_1]\cup\ldots\cup\{k\}\times[m_k])}$, with $\boldsymbol{A}_j = (\boldsymbol{a}_{j,1}, \ldots, \boldsymbol{a}_{j,m_j}) \in \mathbb{R}^{d\times[m_j]}$, and consider a regular subdivision given by a lifting function $\ell : \{1\} \times [m_1] \cup \ldots \cup \{k\} \times [m_k] \to \mathbb{R}$.

After the Cayley trick we obtain the subdivision $\widetilde{\boldsymbol{\mathcal{S}}}$ of the point configuration $\widetilde{\boldsymbol{A}} := \sum \boldsymbol{A}_i \in \mathbb{R}^{d\times([m_1]\times\ldots\times[m_k])}$ with the lifting function $\tilde{\ell} : [m_1] \times \ldots \times [m_k] \to \mathbb{R}$ such that $\tilde{\ell}(i_1, \ldots, i_k) = \sum_{j=1}^{k} \ell(j, i_j)$.

The corresponding tropical polynomial is

$$\begin{aligned}\widetilde{F}(\boldsymbol{x}) &= \bigoplus_{(i_1,\ldots,i_k)\in[m_1]\times\ldots\times[m_k]} \widetilde{\ell}(i_1,\ldots,i_k)\odot \boldsymbol{x}^{\sum_{j=1}^k \boldsymbol{a}_{j,i_j}} \\ &= \bigoplus_{(i_1,\ldots,i_k)\in[m_1]\times\ldots\times[m_k]} \bigodot_{j=1}^{k} \ell(j,i_j)\odot \boldsymbol{x}^{\boldsymbol{a}_{j,i_j}} \\ &= \bigodot_{j=1}^{k} \bigoplus_{i_j\in[m_j]} \ell(j,i_j)\odot \boldsymbol{x}^{\boldsymbol{a}_{j,i_j}} \\ &= \bigodot_{j=1}^{k} F_j(\boldsymbol{x}),\end{aligned}$$

where F_j is the tropical polynomial $F_j(\boldsymbol{x}) = \bigoplus_{i_j\in[m_j]} \ell(j,i_j)\odot \boldsymbol{x}^{\boldsymbol{a}_{j,i_j}}$.

Then, the vanishing locus $\mathcal{T}(\widetilde{F})$ is obtained by taking the union of the vanishing loci $\mathcal{T}(F_j)$ for $j\in[k]$ and the cells of $\mathcal{T}(\widetilde{F})$ are the intersections of the cells of all $\mathcal{T}(F_j)$, $j\in[k]$. We say that these cells are *induced* by the arrangement of tropical hypersurfaces $\{\mathcal{T}(F_j)\mid j\in[k]\}$. We have the following theorem as a consequence of Theorem 1.2.7.

Theorem 1.2.10. *The tropical dual of the mixed subdivision $\widetilde{\boldsymbol{\mathcal{S}}}$ is the polyhedral complex of cells induced by the arrangement of tropical hypersurfaces $\{\mathcal{T}(F_j)\mid j\in[k]\}$.*

See Figure 1.15 for an example, related to Figures 1.12, 1.13 and 1.14.

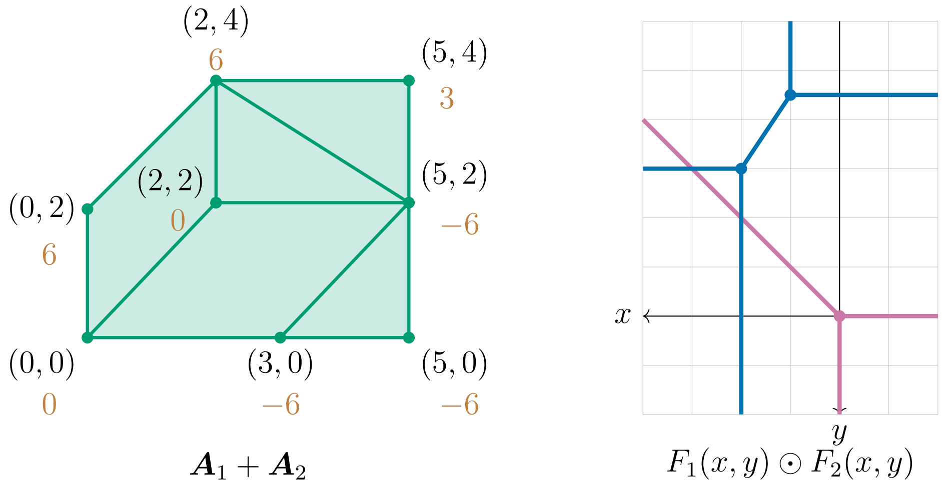

Figure 1.15: Illustration of the Cayley trick on tropical hypersurfaces. Left: A mixed subdivision $\widetilde{\boldsymbol{\mathcal{S}}}$ of the Minkowski sum $\widetilde{\boldsymbol{A}} = \boldsymbol{A}_1+\boldsymbol{A}_2$. Right: The corresponding arrangement of tropical hypersurfaces, associated to the tropical polynomial $\widetilde{F} = F_1\odot F_2$.

1.2.3 Secondary polytope

In this section, we describe a polytope whose structure encodes the set of all regular subdivisions of a given point configuration. The secondary polytope was first defined by Gef'fand, Kapranov and Zelevinsky in [GKZ94] in their study of discriminants and resultants of polynomial systems.

We give here their first definition, but we will see in Section 1.3.2 another definition, as a fiber polytope, in the more general framework of coherent subdivisions compatible with a projection. We recommend [DRS10, Section 5.1] for an in-depth presentation of the secondary polytope.

For a polytope $\boldsymbol{P}$ in $\mathbb{R}^d$ we denote by $\mathrm{vol}_{\mathrm{Eucl}}(\boldsymbol{P})$ its usual Euclidean volume (in particular, if $\boldsymbol{P}$ lives in an affine subspace of dimension smaller than d then $\mathrm{vol}_{\mathrm{Eucl}}(\boldsymbol{P}) = 0$).

Definition 1.2.11. Let $\boldsymbol{A} \in \mathbb{R}^{d\times[n]}$ be a point configuration that affinely spans $\mathbb{R}^d$.

To each triangulation $\boldsymbol{\mathcal{T}}$ of $\boldsymbol{A}$, we associate the following vector in $\mathbb{R}^n$, called the *GKZ-vector* of $\boldsymbol{\mathcal{T}}$ (named after Gef'fand, Kapranov, Zelevinsky):

$$\boldsymbol{gkz}(\boldsymbol{\mathcal{T}}) := \sum_{\boldsymbol{C}\in\boldsymbol{\mathcal{T}}} \mathrm{vol}_{\mathrm{Eucl}}(\boldsymbol{C}) \left(\sum_{\boldsymbol{a}_j \text{ vertex of } \boldsymbol{C}} \boldsymbol{e}_j \right).$$

The secondary polytope of $\boldsymbol{A}$ is:

$$\boldsymbol{\Sigma}(\boldsymbol{A}) := \mathrm{conv}(\{\boldsymbol{gkz}(\boldsymbol{\mathcal{T}}) \mid \boldsymbol{\mathcal{T}} \text{ triangulation of } \boldsymbol{A}\}).$$

Theorem 1.2.12 ([GKZ94, Chapter 7, Theorem 2.4])**.** *Let $\boldsymbol{A}$ be a point configuration. The poset of non-empty faces of $\boldsymbol{\Sigma}(\boldsymbol{A})$ is isomorphic to the refinement poset of the regular subdivisions of $\boldsymbol{A}$. In particular, the vertices of $\boldsymbol{\Sigma}(\boldsymbol{A})$ are in bijection with the regular triangulations of $\boldsymbol{A}$.*

A remarkable example of secondary polytope is the associahedron, which we will present briefly in Section 1.4.6. The associahedron of dimension $n-3$ can be realized as the secondary polytope of any 2-dimensional n-gon ([GKZ94, Section 7.3.B]).

1.3 Projections and compatible subdivisions

We now introduce the framework of subdivisions that are compatible with projections and two related topics: fiber polytopes, which generalize secondary polytopes, and the Generalized Baues Problem, which deals with the topology of refinement posets of subdivisions.

In this section we consider an affine projection $\pi : \mathbb{R}^D \to \mathbb{R}^d$, that maps the vertex configuration $(\boldsymbol{p}_1, \dots, \boldsymbol{p}_n)$ of a polytope $\boldsymbol{P} \subset \mathbb{R}^D$ to a point configuration $\boldsymbol{A} = (\boldsymbol{a}_1, \dots, \boldsymbol{a}_n) \in \mathbb{R}^{d\times[n]}$. We also denote $\boldsymbol{Q}$ the polytope $\mathrm{conv}(\boldsymbol{A}) = \pi(\boldsymbol{P})$.

1.3.1 Subdivisions compatible with a projection

A *π-compatible subdivision* of $\boldsymbol{A}$ is a subdivision of $\boldsymbol{A}$ all of whose cells label faces of $\boldsymbol{P}$.

Such a π-compatible subdivision is *π-coherent* if it is regular and admits a lifting function of the form $\ell : \begin{cases} [n] & \to \mathbb{R} \\ i & \mapsto \langle \boldsymbol{u}, \boldsymbol{p}_i \rangle \end{cases}$, for a certain direction $\boldsymbol{u} \in \mathbb{R}^D$.

See Figure 1.16 for an example.

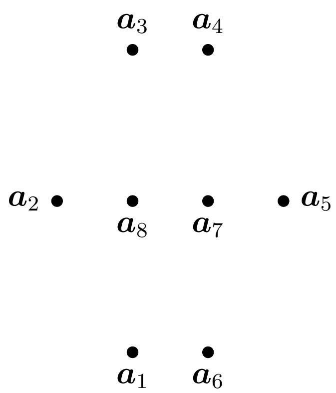

(a) A point configuration $\boldsymbol{A}$ in $\mathbb{R}^2$ that is the image of a 3-dimensional cube by a projection π.

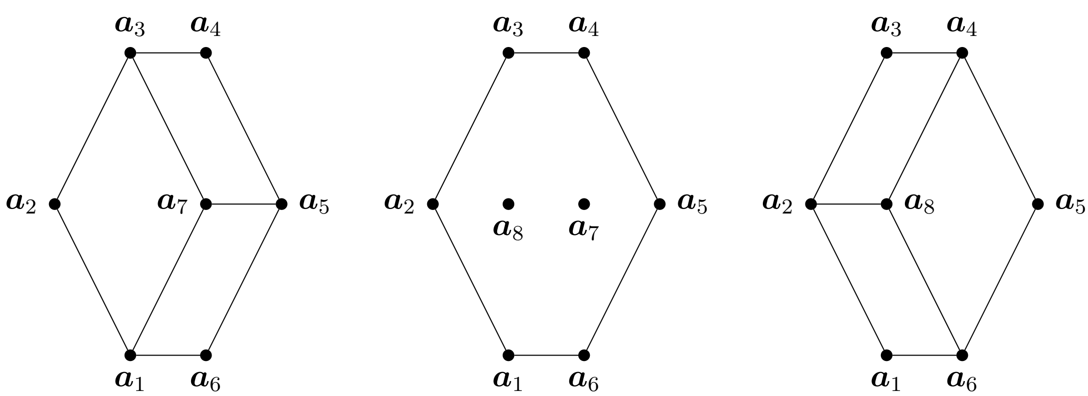

(b) The three π-compatible subdivisions of $\boldsymbol{A}$ (they are also π-coherent).

Figure 1.16: Example of a point configuration and compatible subdivisions.

Remark 1.3.1. Note that we can recover our previous definitions of subdivisions and regular subdivisions by taking the simplicial linear projection $\pi_\triangle : \begin{cases} \mathbb{R}^n & \to \mathbb{R}^d \\ \boldsymbol{e}_i & \mapsto \boldsymbol{a}_i \end{cases}$ from the simplex $\triangle_{n-1}$. Indeed, the subdivisions of $\boldsymbol{A}$ are then the $\pi_\triangle$-compatible subdivisions of $\boldsymbol{A}$ and the coherent subdivisions of $\boldsymbol{A}$ are the $\pi_\triangle$-coherent subdivisions of $\boldsymbol{A}$.

Remark 1.3.2. Note that the Cayley trick (Propositions 1.1.15 and 1.2.4) can be expressed in this setting.

Let $\boldsymbol{A}_1 = (\boldsymbol{a}_{1,1}, \dots, \boldsymbol{a}_{1,m_1})$, ..., $\boldsymbol{A}_k = (\boldsymbol{a}_{k,1}, \dots, \boldsymbol{a}_{k,m_k})$ be k point configurations in $\mathbb{R}^d$. We define the Minkowski linear projection

$$\pi_M : \begin{cases} \triangle_{m_1-1} \times \dots \times \triangle_{m_k-1} \subset \mathbb{R}^{m_1+\dots+m_k} & \to \boldsymbol{A}_1 + \dots + \boldsymbol{A}_k \subset \mathbb{R}^d \\ \boldsymbol{e}_{i_1} \times \dots \times \boldsymbol{e}_{i_k} & \mapsto \boldsymbol{a}_{1,i_1} + \dots + \boldsymbol{a}_{k,i_k} \end{cases}.$$

Then the (resp. coherent) mixed subdivisions of $\sum \boldsymbol{A}_i$ as defined in Definition 1.1.14 (resp. Definition 1.2.3) are exactly the (resp. π_M-coherent) π_M-compatible subdivisions of $\sum \boldsymbol{A}_i$.

1.3.2 Fiber polytopes

The construction of fiber polytopes was introduced by Billera and Sturmfels in [BS92], generalizing the theory of secondary polytopes in a unified way that encompasses concepts such as monotone path polytopes, zonotopal tiling polytopes and secondary polytopes. We refer to [Zie95, Lec. 9] and [DRS10, Sec. 9.1] for gentle introductions to the topic.

Recall that we are considering polytopes $\boldsymbol{P}$ and $\boldsymbol{Q}$ related by an affine surjection $\pi : \boldsymbol{P} \to \boldsymbol{Q}$. The fibers of π over $\boldsymbol{Q}$ form a *polytope bundle* $\boldsymbol{y} \in \boldsymbol{Q} \mapsto \pi^{-1}(\{\boldsymbol{y}\}) \cap \boldsymbol{P}$ whose *Minkowski integral*, after some normalization, is the *fiber polytope* $\boldsymbol{\Sigma}(\boldsymbol{P}, \pi)$:

$$\boldsymbol{\Sigma}(\boldsymbol{P}, \pi) = \frac{1}{\mathrm{vol}_{\mathrm{Eucl}}(\boldsymbol{Q})} \int_{\boldsymbol{Q}} (\pi^{-1}(\{\boldsymbol{y}\}) \cap \boldsymbol{P}) d\boldsymbol{y}.$$

This Minkowski integral is well-defined by the construction of Riemann integrals, as a limit of finite Minkowski sums of fibers over points of $\boldsymbol{Q}$.

The fiber polytope can also be described as a finite Minkowski sum. Namely,

$$\boldsymbol{\Sigma}(\boldsymbol{P}, \pi) = \frac{1}{\mathrm{vol}_{\mathrm{Eucl}}(\boldsymbol{Q})} \sum_{\boldsymbol{C} \in \Gamma(\boldsymbol{P}, \pi)} \mathrm{vol}_{\mathrm{Eucl}}(\boldsymbol{C})\ \pi^{-1}(\{\boldsymbol{b}_{\boldsymbol{C}}\}) \cap \boldsymbol{P},$$

where $\Gamma(\boldsymbol{P}, \pi)$ is the set of *chambers*: the subsets of $\boldsymbol{Q}$ of the form

$$\boldsymbol{C}_{\boldsymbol{y}} = \bigcap_{\substack{\boldsymbol{F} \text{ face of } \boldsymbol{P} \\ \boldsymbol{y} \in \pi(\boldsymbol{F})}} \pi(\boldsymbol{F})$$

for $\boldsymbol{y} \in \boldsymbol{Q}$; and $\boldsymbol{b}_{\boldsymbol{C}}$ is the barycenter of the chamber $\boldsymbol{C}$.

Note that $\boldsymbol{\Sigma}(\boldsymbol{P}, \pi)$ lies in the fiber over the barycenter of $\boldsymbol{Q}$, $\pi^{-1}\left(\frac{1}{\mathrm{vol}_{\mathrm{Eucl}}(\boldsymbol{Q})} \int_{\boldsymbol{Q}} \boldsymbol{y}\ d\boldsymbol{y}\right) \cap \boldsymbol{P}$, thus it is a polytope of dimension $\dim(\boldsymbol{P}) - \dim(\boldsymbol{Q})$.

Figure 1.17 shows an example of this construction. When $\boldsymbol{P}$ is the three dimensional cube $\square_3$ and π is the projection from $\mathbb{R}^3$ to $\mathbb{R}$ that sums the coordinates, we obtain that the fiber polytope $\boldsymbol{\Sigma}(\boldsymbol{P}, \pi)$ is a regular hexagon.

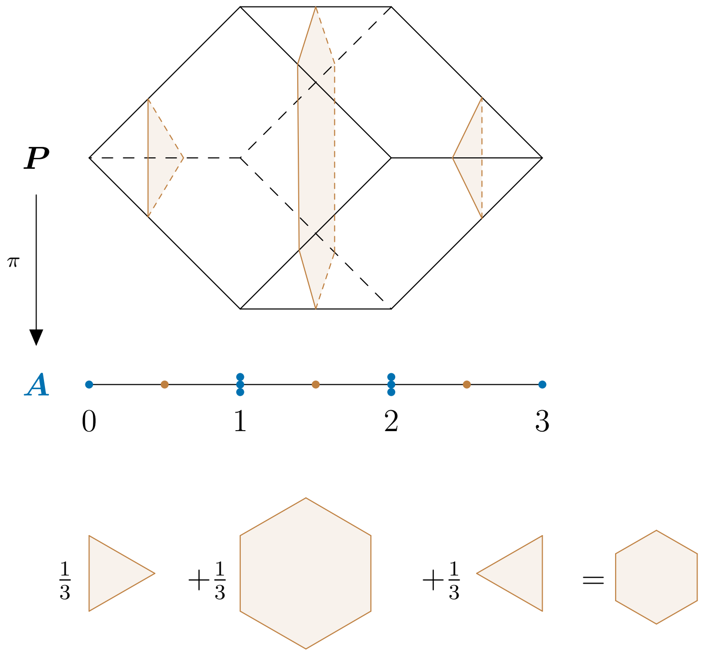

Figure 1.17: Construction of the fiber polytope $\boldsymbol{\Sigma}(\boldsymbol{P}, \pi)$, where $\boldsymbol{P} = \square_3$ and π is the projection from $\mathbb{R}^3$ to $\mathbb{R}$ that sums the coordinates.

Theorem 1.3.3 ([BS92, Theorem 2.1])**.** *The poset of non-empty faces of $\boldsymbol{\Sigma}(\boldsymbol{P}, \pi)$ is isomorphic to the refinement poset of the π-coherent subdivisions of $\boldsymbol{A}$.*

As Remark 1.3.1 suggests, the secondary polytope that we defined in Definition 1.2.11 is a special case of fiber polytope (up to dilation).

Theorem 1.3.4 ([BS92, Theorem 2.5])**.** *Let $\boldsymbol{A} = (\boldsymbol{a}_1, \dots, \boldsymbol{a}_n) \in \mathbb{R}^{d\times[n]}$ be a point configuration, $\boldsymbol{Q}$ its convex hull and $\pi_\triangle$ the linear projection from $\mathbb{R}^n$ to $\mathbb{R}^d$ that maps $\boldsymbol{e}_i$ to $\boldsymbol{a}_i$ for any $i \in [n]$. Then $\boldsymbol{\Sigma}(\boldsymbol{A}) = (d+1)\,\mathrm{vol}_{\mathrm{Eucl}}(\boldsymbol{Q})\boldsymbol{\Sigma}\left(\triangle_{n-1}, \pi_\triangle\right)$.*

Theorem 1.3.3 is remarkable, since it shows that the set of π-coherent subdivisions have a very special structure among all π-compatible subdivisions.

1.3.3 Monotone path polytopes

We now present an important class of fiber polytopes: the monotone path polytopes, which will reappear in Chapter 3 (Section 3.2.3, Section 3.6.1).

If $\boldsymbol{Q}$ is a one-dimensional polytope and $\boldsymbol{P} \subset \mathbb{R}^n$, then $\pi : \boldsymbol{P} \to \boldsymbol{Q}$ is a linear form defined by a vector $\boldsymbol{u} \in \mathbb{R}^n$ via $\pi(\boldsymbol{x}) = \langle \boldsymbol{u}, \boldsymbol{x} \rangle$. For simplicity, assume that π is generic in the sense that it is not constant along any edge of $\boldsymbol{P}$, and let $\boldsymbol{p}_m$ and $\boldsymbol{p}_M$ be the minimal and maximal vertices of $\boldsymbol{P}$ with respect to π. A *π-monotone path* is a path from $\boldsymbol{p}_m$ to $\boldsymbol{p}_M$ composed of edges of $\boldsymbol{P}$ along which π is always increasing. One way to obtain π-monotone

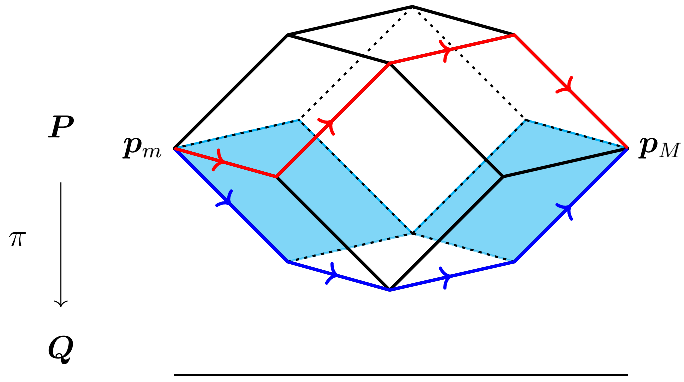

Figure 1.18: A projection $\pi : \boldsymbol{P} \to \boldsymbol{Q}$ with a parametric simplex path in blue at the bottom, a non-coherent π-monotone path in red and a coherent cellular string of 2-dimensional faces in cyan.

paths is to consider some generic vector $\boldsymbol{w}$ orthogonal to $\boldsymbol{u}$ and consider the sequence of vertices of $\boldsymbol{P}$ that are extremal in the direction $\boldsymbol{w} + \lambda\boldsymbol{u}$ as λ ranges from $-\infty$ to ∞. These paths induce the finest π-coherent subdivisions of $\boldsymbol{Q}$, and are known as *parametric simplex paths* in linear programming, where they play an important role as they are the paths followed by the shadow-vertex simplex method [Bor87, GS55].

More generally, a *cellular string* on $\boldsymbol{P}$ with respect to π is a sequence of faces $\boldsymbol{F}_1, \dots, \boldsymbol{F}_k$ of $\boldsymbol{P}$ of dimension at least 1 such that $\boldsymbol{p}_m \in \boldsymbol{F}_1$, $\boldsymbol{p}_M \in \boldsymbol{F}_k$, and every two adjacent faces $\boldsymbol{F}_i, \boldsymbol{F}_{i+1}$ meet at a vertex $\boldsymbol{p}_i$ such that $\pi(\boldsymbol{x}) \leq \pi(\boldsymbol{p}_i) \leq \pi(\boldsymbol{y})$ for each $\boldsymbol{x} \in \boldsymbol{F}_i$ and $\boldsymbol{y} \in \boldsymbol{F}_{i+1}$. Such a cellular string is π-coherent if there is some (not-necessarily generic) vector $\boldsymbol{w}$ orthogonal to $\boldsymbol{u}$ such that these are the maximal faces of $\boldsymbol{P}$ maximized in a direction of the form $\boldsymbol{w} + \lambda\boldsymbol{u}$.

See examples of π-monotone paths and cellular string on Figure 1.18

The fiber polytope $\boldsymbol{\Sigma}(\boldsymbol{P}, \pi)$ is called the *monotone path polytope* of $\boldsymbol{P}$ and π. Its vertices are in one-to-one correspondence with the parametric π-monotone paths of $\boldsymbol{P}$, and its faces are in correspondence with the π-coherent cellular strings.

The example of fiber polytope on Figure 1.17 is a monotone path polytope.

1.3.4 Generalized Baues problem

The generalized Baues problem, or GBP for short, deals with topological properties of the whole refinement poset of π-compatible subdivisions of a given point configuration. It will be at the center of Section 3.6.2, where we prove a particular case of the strong GBP in a more abstract setting related to oriented matroids.

In this section, we provide a quick overview of the GBP, based on Reiner's survey [Rei99]. We will not give much details about the topological concepts involved, and refer to [Bjö95] and [BLS⁺99, Section 4.7].

Definition 1.3.5. Let X be a poset. Its *order complex* $\Delta(X)$ is the simplicial complex formed by all its chains. The *topology* of X refers to the topological space that realizes the simplicial complex $\Delta(X)$.

Definition 1.3.6. For the projection $\pi : \boldsymbol{P} \to \boldsymbol{A}$, we denote $\omega(\boldsymbol{P}, \pi)$ the refinement poset of non-trivial π-compatible subdivisions of $\boldsymbol{A}$. We denote $\omega_{coh}(\boldsymbol{P}, \pi)$ the subposet of non-trivial π-coherent subdivisions of $\boldsymbol{A}$.

Note that it follows from Theorem 1.3.3 that $\omega_{\mathrm{coh}}(\boldsymbol{P}, \pi)$ has the topology of a $(\dim(\boldsymbol{P}) - \dim(\boldsymbol{A}) - 1)$-sphere. Indeed, the barycentric subdivision of the boundary of $\boldsymbol{\Sigma}(\boldsymbol{P}, \pi)$ is a geometric realization of $\Delta(\omega_{\mathrm{coh}}(\boldsymbol{P}, \pi))$.

Weak GBP. Is $\omega(\boldsymbol{P}, \pi)$ homotopy equivalent to a $(\dim(\boldsymbol{P}) - \dim(\boldsymbol{A}) - 1)$-sphere? It is the case if the inclusion $\omega_{\mathrm{coh}}(\boldsymbol{P}, \pi) \hookrightarrow \omega(\boldsymbol{P}, \pi)$ induces a homotopy equivalence.

Strong GBP. Is the inclusion $\omega_{\mathrm{coh}}(\boldsymbol{P}, \pi) \hookrightarrow \omega(\boldsymbol{P}, \pi)$ a strong deformation retraction?

The name of the problem comes from a conjecture stated by Baues in his study of iterated loop spaces ([Bau80]), that corresponds to the weak GBP for monotone paths of the permutahedron. The more general version of the weak GBP was asked by Billera and Sturmfels in [BS92, end of Section 5].

There are examples for which the answer to the GBP is negative, but to characterize the projections $\pi : \boldsymbol{P} \to \boldsymbol{A}$ that satisfy the conjecture remains an actively studied open problem. Here are some families for which the strong generalized Baues conjecture was proven to be true:

- $\dim(\boldsymbol{P}) - \dim(\boldsymbol{A}) \leq 2$ ([R94]),
- $\boldsymbol{A}$ is 1-dimensional ([BKS94a]): the π-compatible subdivisions are then the π-monotone paths. This answers positively Baues's initial conjecture.
- $\boldsymbol{P}$ is the hypersimplex $\triangle_{n,k} = \triangle_{n-1}^{(k)}$ and $\boldsymbol{A} = \boldsymbol{C}_n^{(k)}$, where $\boldsymbol{C}_n$ is a configuration of n points in convex position in $\mathbb{R}^2$, and for any point configuration (resp. polytope) $\boldsymbol{R}$ with n vertices $\boldsymbol{s}_1, \dots, \boldsymbol{s}_n$ and $k \in [n]$, $\boldsymbol{R}^{(k)}$ denotes (resp. the convex hull of) the configuration $\left\{\sum_{i \in I} \boldsymbol{s}_i \,\middle|\, I \subseteq [n], |I| = k\right\}$ ([OS22]). This family of subdivisions, called *hypersimplicial*, is related to the study of plabic graphs and the positive Grassmannian.

And here are a some examples were the generalized Baues conjecture was disproved:

- first particular counterexample: $\boldsymbol{P}$ is a simplicial 5-polytope with 10 vertices, projected onto a hexagon in $\mathbb{R}^2$ ([RZ96]),
- $\boldsymbol{P}$ is the simplex $\triangle_{16}$ and $\boldsymbol{A}$ a configuration of 17 points in general position in $\mathbb{R}^6$, whose graph of triangulations flips is not connected ([San06]),
- $\boldsymbol{P}$ is a cube and $\boldsymbol{Q}$ a zonotope of dimension 4 whose graph of zonotopal tilings is not connected ([Liu20]). This counter-example also disproves the conjecture that the extension space of realizable oriented matroids of rank d has the homotopy type of a $(d-1)$-sphere.

1.4 Several realizations of the permutahedron

In this section we present the permutahedron, a very well-known and important polytope that we will generalize in two different directions in Chapter 3 and Chapter 4. We first present the combinatorial structure encoded by the faces of the permutahedron and then give several constructions of the permutahedron, that are related to our generalizations.

1.4.1 Combinatorics of the permutahedron

The Weak order

Let $n \in \mathbb{N}$. A *permutation* of $[n]$ is a bijection from $[n]$ to $[n]$. We can visualize a permutation σ as a word $\sigma(1)\sigma(2)\ldots\sigma(n)$. We denote by $\mathfrak{S}_n$ the set of all permutations of $[n]$. Even though we will not use it in this work, let us mention that the composition law $\circ$ endows this set with a group structure called the *symmetric group*. This is a very central object in mathematics, that embraces combinatorial, algebraic and geometric aspects. In this thesis we will be more interested with the following poset structure on $\mathfrak{S}_n$.

The set of *inversions* of a permutation $\sigma \in \mathfrak{S}_n$ is:

$$\mathrm{inv}(\sigma) := \{(\sigma(i), \sigma(j)) \,|\, i < j \text{ and } \sigma(i) > \sigma(j)\}\,.$$

The *(right) weak order* on $\mathfrak{S}_n$ is the partial order $\preceq$ such that for two permutations $\sigma, \tau \in \mathfrak{S}_n$ we have $\sigma \preceq \tau$ if and only if $\mathrm{inv}(\sigma) \subseteq \mathrm{inv}(\tau)$.

See Figure 1.19 for examples with $n = 2, 3, 4$.

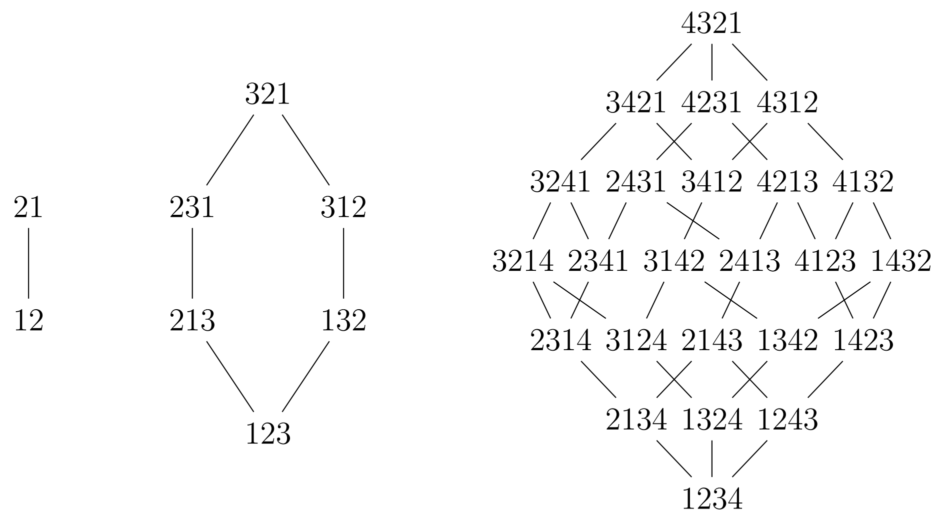

Figure 1.19: Hasse diagrams of the weak orders on $\mathfrak{S}_2, \mathfrak{S}_3$ and $\mathfrak{S}_4$. Figure adapted from Viviane Pons.

One of the first studies of this poset concerns the analysis of voting systems, and shows that this poset is a lattice [GR63]. The name “permutoèdre” (in French) appears in the same article.

Ordered partitions

An *ordered partition* of $[n]$ is an ordered collection of non-empty disjoint subsets $(I_1, \ldots, I_l)$ whose union is $[n]$. Ordered partitions where all parts are singletons are identified with permutations. They are the maximal elements in the *refinement order*: we say that $J = (J_1, \ldots, J_l)$ refines $I = (I_1, \ldots, I_k)$, denoted $J \succeq I$, if each I_i is the union of some consecutive J_j's.

Definition 1.4.1. We call *n-permutahedron* any polytope whose poset of non-empty faces is isomorphic to the opposite of the refinement poset of ordered partitions of $[n]$.

See Figure 1.20 for an example with $n = 3$.

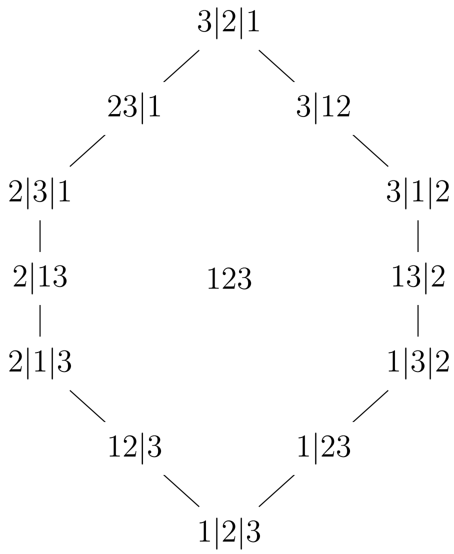

Figure 1.20: Ordered partitions of [3] indexing the faces of the 3-permutahedron. Figure adapted from Viviane Pons.

In particular, the vertices of such a polytope are indexed by permutations in $\mathfrak{S}_n$. There is an edge between two vertices indexed by σ and $\sigma' \in \mathfrak{S}_n$ if and only if σ' can be obtained from σ by exchanging two adjacent letters $\sigma(i)$ and $\sigma(i+1)$ of the permutation. Hence, this graph can be oriented to recover the Hasse diagram of the weak order on permutations (we orient the edge from σ to σ' if $\sigma(i) < \sigma(i+1)$).

1.4.2 Vertices and normal fan

Unlike its cousin the associahedron (Section 1.4.6), or its generalization the s-permutahedron (Chapter 4), it is very easy to give explicit coordinates for the permutahedron. It seems (according to [Zie95, Example 0.10]) that it was first studied by Schoute in 1911 in [Sch11].

Definition 1.4.2. We define the *standard n-permutahedron* to be the polytope:

$$\mathbf{Perm}_n := \operatorname{conv}\big(\big\{(\sigma^{-1}(1), \dots, \sigma^{-1}(n)) \,\big|\, \sigma \in \mathfrak{S}_n\big\}\big) \subset \mathbb{R}^n.$$

It lives in the $(n-1)$-dimensional affine subspace of the sum of coordinates constant equal to $\sum_{i\in[n]} i = \frac{n(n+1)}{2}$. See Figure 1.21 for an example with $n = 3$ and the left of Figure 1.24 or the right of Figure 3.3 for examples with $n = 4$.

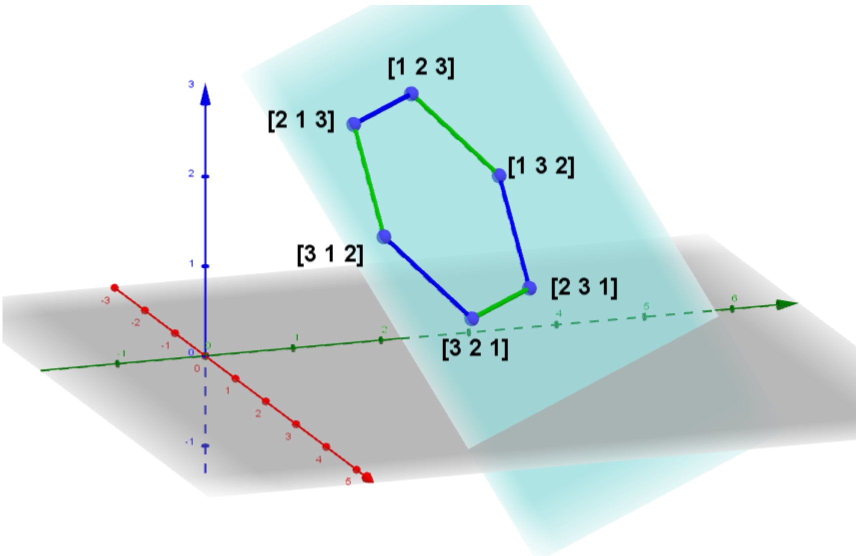

Figure 1.21: Standard 3-permutahedron (vertices indexed by their coordinates).

Lemma 1.4.3. *The standard n-permutahedron is indeed a permutahedron in the sense of Definition 1.4.1.*

Proof. Let $\boldsymbol{u} = (u_1, \dots, u_n)$ be a direction in $\mathbb{R}^n$. We associate to it the ordered partition $I = (I_1, \dots, I_l)$ of $[n]$ such that for any $1 \leq i < j \leq l$, $k_1 \in I_i$ and $k_2 \in I_j$ implies that $u_{k_1} < u_{k_2}$ and $k_1, k_2 \in I_i$ implies $u_{k_1} = u_{k_2}$. Then, we have that the vertices of the face $\mathbf{Perm}_n^{\boldsymbol{u}}$ are exactly the points $(\sigma^{-1}(1), \dots, \sigma^{-1}(n))$ for the permutations $\sigma \in \mathfrak{S}_n$ that refine the ordered partition I. $\square$

This proof also shows that the normal fan of $\mathbf{Perm}_n$ is the *braid arrangement* $\boldsymbol{\mathcal{B}}_n$: the arrangement of hyperplanes $\{\boldsymbol{u} \in \mathbb{R}^n \,|\, \langle \boldsymbol{u}, \boldsymbol{e}_i\rangle = \langle \boldsymbol{u}, \boldsymbol{e}_j\rangle\}$ for all $1 \leq i < j \leq n$.

We see that the facets of $\mathbf{Perm}_n$ correspond to ordered partitions with two parts. Its facet description is:

$$\mathbf{Perm}_n = \left\{ \boldsymbol{x} \in \mathbb{R}^{n+1} \;\middle|\; \sum_{i\in[n]} x_i = \tfrac{n(n+1)}{2} \text{ and } \sum_{i\in I} x_i \geq \tfrac{|I|(|I|+1)}{2}, \text{ for all } \emptyset \neq I \subsetneq [n] \right\}.$$

1.4.3 Zonotope

The fact that its normal fan is a hyperplane arrangement implies that $\mathbf{Perm}_n$ is normally equivalent to a zonotope, obtained by summing segments in the directions $\boldsymbol{e}_i - \boldsymbol{e}_j$ for all $1 \leq i < j \leq n$. In fact, we can recover exactly $\mathbf{Perm}_n$ as the zonotope:

$$\mathbf{Perm}_n = \tfrac{n+1}{2}\mathbf{1}_n + \sum_{1\leq i<j\leq n} \left[-\frac{\boldsymbol{e}_i - \boldsymbol{e}_j}{2}, \frac{\boldsymbol{e}_i - \boldsymbol{e}_j}{2} \right],$$

where $[\boldsymbol{p}, \boldsymbol{q}] \subset \mathbb{R}^n$ denotes the segment between the points $\boldsymbol{p}$ and $\boldsymbol{q}$ (see [Zie95, Ex. 7.15]).

1.4.4 Monotone path polytope of the cube

Let $\square_n = [0,1]^n$ be the n-dimensional cube, and let $\pi : \mathbb{R}^n \to \mathbb{R}$ be the linear form that sums the coordinates, i.e. the form $\pi = \langle \mathbf{1}_n, \cdot \rangle$ induced by the all-ones vector.

Then it is quite straightforward to see that the π-monotone paths are in bijection with the permutations in $\mathfrak{S}_n$, and that they are all π-coherent. More precisely, to a permutation $\sigma \in \mathfrak{S}_n$ we associate the monotone path that passes through the vertices of the cube of the form $\sum_{i=1}^{k} \boldsymbol{e}_{\sigma(i)}$ for $k = 0, 1, \dots, n$. It is π-coherent since it can be maximized by the direction $\boldsymbol{w} = \sum_{i=1}^{n} (n-i)\boldsymbol{e}_{\sigma(i)}$.

In fact we have:

Proposition 1.4.4 ([BS92, Ex. 5.4], see also [Zie95, Ex. 9.8])**.** *The monotone path polytope $\boldsymbol{\Sigma}(\square_n, \pi)$ is a permutahedron, and up to a translation and dilation it is the standard permutahedron: $\boldsymbol{\Sigma}(\square_n, \pi) = \frac{2}{n}\boldsymbol{Perm}_n - \frac{n+1}{n}\mathbf{1}_n$.*

See Figure 1.17 for an example with $n = 3$.

In Section 3.2.3 we will re-interpret this monotone path construction as a special example of a sweep polytope seen as a monotone path polytope of a zonotope.

1.4.5 Dual of a triangulation of the cube

It happens that the π-monotone paths of $\square_n$ that we just described also provide a triangulation of $\square_n$, that we denote $\boldsymbol{\mathcal{T}}_{\mathbf{Perm}_n}$, with maximal cells

$$\operatorname{conv}\left(\left\{ \sum_{i=1}^{k} \boldsymbol{e}_{\sigma(i)} \;\middle|\; k \in \{0, \dots, n\} \right\} \right) = \left\{ \boldsymbol{x} \in [0,1]^n \;\middle|\; x_{\sigma(1)} \geq \dots \geq x_{\sigma(n)} \right\}$$

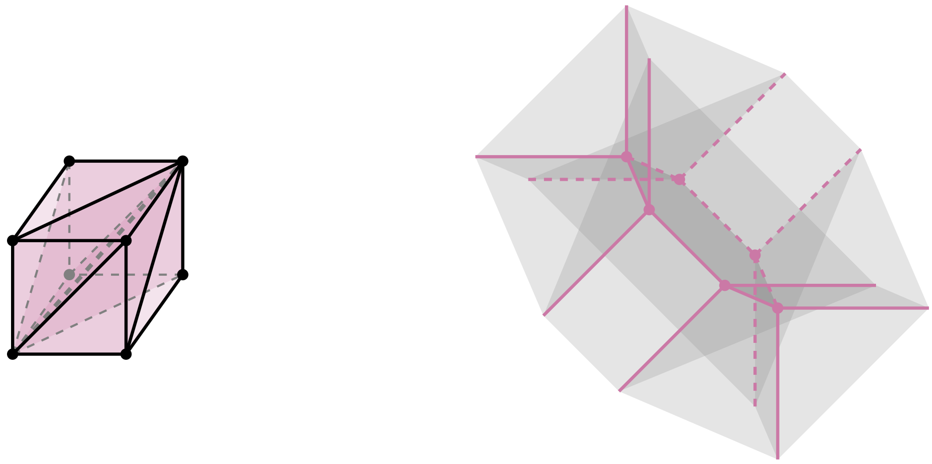

Figure 1.22: The triangulation $\boldsymbol{\mathcal{T}}_{\mathbf{Perm}_n}$ of the cube (left) and its corresponding tropical hypersurface (right).

for all $\sigma \in \mathfrak{S}_n$ ([DRS10, Proposition 6.3.4]). Note that this triangulation is obtained by intersecting the braid fan $\boldsymbol{\mathcal{B}}_n$ with the cube $[0,1]^n$.

This triangulation $\boldsymbol{\mathcal{T}}_{\mathbf{Perm}_n}$ is regular, an admissible lifting function is $\ell(I) = -\frac{|I|(|I|+1)}{2}$ if we index the vertices of $\square_n$ by the subsets $I \subseteq [n]$.

If we apply the tropical dualization process described in Section 1.2.2 we obtain the tropical polynomial $F_{\mathbf{Perm}_n}(\boldsymbol{x}) = \min\left\{\ell(I) + \sum_{i\in I} x_i \,\middle|\, I \subseteq [n]\right\}$.

Proposition 1.4.5. *The bounded cells of the tropical hypersurface $\mathcal{T}(F_{\mathbf{Perm}_n})$ are exactly the faces of the standard permutahedron $\boldsymbol{Perm}_n$.*

The example for $n = 3$ is depicted on Figure 1.22.

Proof. First, we can see that the inclusion poset of interior cells of $\boldsymbol{\mathcal{T}}_{\mathbf{Perm}_n}$ is isomorphic to the poset of ordered partitions. Indeed, an interior cell of $\boldsymbol{\mathcal{T}}_{\mathbf{Perm}_n}$ is of the form

$$\left\{\boldsymbol{x} \in [0,1]^n \,\middle|\, x_{i_1} = \ldots = x_{i_{k_1}} < x_{i_{k_1+1}} = \ldots = x_{i_{k_1+k_2}} < \ldots < x_{i_{k_1+\ldots+k_{l-1}+1}} = \ldots = x_{i_{k_1+\ldots+k_l}}\right\}$$

for a certain ordered partition $I = (\{i_1, \ldots, i_{k_1}\}, \ldots, \{i_{k_1+\ldots+k_{l-1}+1}, \ldots, i_{k_1+\ldots+k_l}\})$ of $[n]$.

Then, it follows from Theorem 1.2.7 that the bounded cells of $\mathcal{T}(F_{\mathbf{Perm}_n})$ are in bijection with the faces of $\mathbf{Perm}_n$. It only remains to show that for any $\sigma \in \mathfrak{S}_n$, the point $(\sigma(1), \ldots, \sigma(n))$ is indeed a vertex of $\boldsymbol{\mathcal{T}}_{\mathbf{Perm}_n}$. Let $\sigma \in \mathfrak{S}_n$ and $\boldsymbol{v} := (\sigma(1), \ldots, \sigma(n))$. Then for any $I \subseteq [n]$, $\ell(I) + \sum_{i\in I} v_i = -\frac{|I|(|I|+1)}{2} + \sum_{i \in I} \sigma(i) \geq 0$ with equality if and only if $I = \{\sigma^{-1}(1), \ldots, \sigma^{-1}(k)\}$ for a certain $k \in [n]$. Moreover, $\boldsymbol{v}$ is the only point in $\mathbb{R}^n$ that satisfies these equality cases for all $k \in [n]$, thus it is a vertex of $\mathcal{T}(F_{\mathbf{Perm}_n})$. $\square$

This realization can be seen as a special example of the tropical realization of the s-permutahedron that will be presented in Section 4.4.3. Indeed, for s $= (1, \ldots, 1)$ the flow polytope of the graph Oru_n is exactly the cube $\square_n$ and its DKK triangulation is the triangulation $\mathcal{T}_{\mathbf{Perm}_n}$.

1.4.6 Relation with the associahedron

Let us say a few words here about the associahedron and its connection to the permutahedron. Indeed, even though we will not allude much to the associahedron in the rest of this thesis, this *"mythical polytope"* is a very good example of nontrivial realizations of an omnipresent combinatorial structure. Moreover, its relation to the permutahedron motivated Ceballos and Pons Conjecture 4.1.2, to which we give elements of solution in Section 4.5.

Among the abundant literature on the topic, we refer to the surveys [MHPS12] and [PSZ23].

The combinatorial structure behind the associahedron was first defined by Tamari in 1951 ([Tam51]) and Stasheff in 1963 ([Sta63]) with motivation from associativity and loop spaces. In particular, the now called *Tamari lattice* can be defined on the *parenthesized words* of length $n+1$ such that the covering relations correspond to the rewriting rule of the form $(u_1u_2)u_3 \preceq u_1(u_2u_3)$. See the Hasse diagrams for $n = 2, 3, 4$ depicted on Figure 1.23.

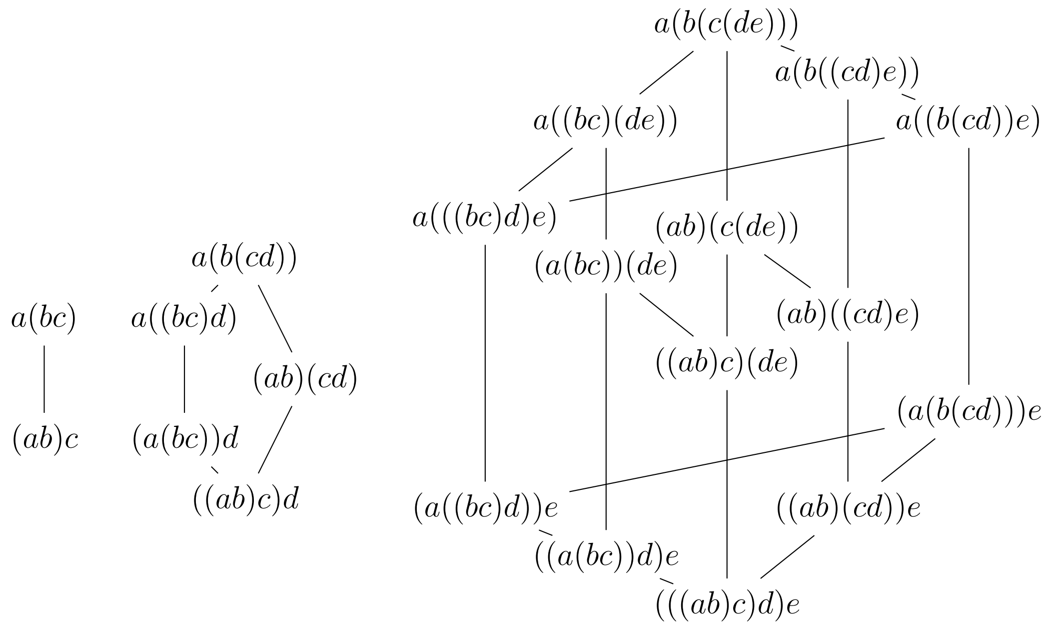

Figure 1.23: Hasse diagrams of the Tamari lattices on parenthesized words of length $3, 4, 5$. Figure adapted from Viviane Pons.

The same structure can be defined on other Catalan families, for example with rotations on planar rooted binary trees with $n+1$ leaves, flips on triangulations of a polygon with $n+2$ edges, Tamari rotations on Dyck paths of length $2n$.

We call *n-associahedron* any polytope of dimension $n-1$ whose graph can be oriented to recover the Tamari lattice on parenthesized words of size $n+1$. Then, the higher dimensional faces of such a polytope will be in bijection with partially parenthesized words of size $n+1$ (or Schröder trees with $n+1$ leaves, or subdivisions of a polygon with $n+2$ edges, ...)

A drawing of a polytopal realization of the associahedron in dimension 3 was already provided in Tamari's thesis. However, it is only in 1989 that an explicit realization valid for any dimension was first published by Lee ([Lee89]). Since then, several different families of realizations were found, with fruitful connections to other topics in mathematics and still mysteries and questions (see for example [CZ12]).

The weak order and the Tamari lattice are related in several ways, for example the Tamari lattice is a *lattice quotient* of the weak order (see Section 4.5.1). This combinatorial relationship can be translated geometrically: some realizations of the associahedron can be obtained by *deforming* realizations of the permutahedron. In particular, Loday's realization ([Lod04]) can be obtained by *removing facets* from the permutahedron, since its facet description is:

$$\mathbf{Ass}_n = \left\{ \boldsymbol{x} \in \mathbb{R}^n \;\middle|\; \sum_{i\in[n]} x_i = \tfrac{n(n+1)}{2} \text{ and } \sum_{a\le i\le b} x_i \ge \tfrac{(b-a+1)(b-a+2)}{2} \text{ for all } 1 \le a \le b \le n \right\}.$$

See Figure 1.24 for an example of this geometric phenomenon.

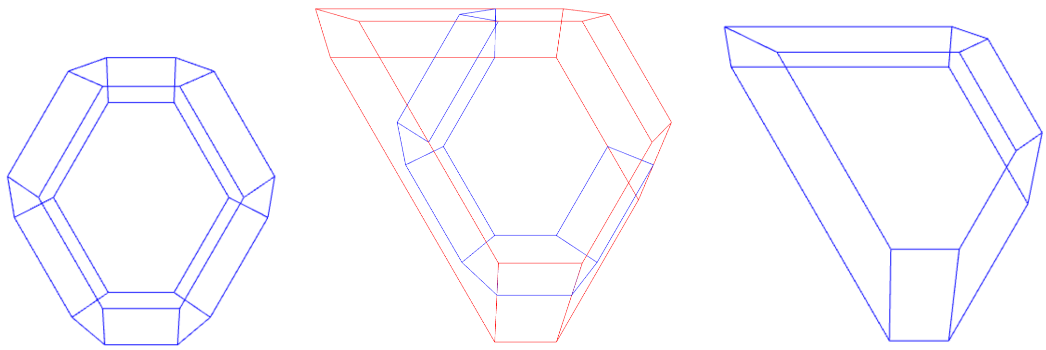

Figure 1.24: The standard 4-permutahedron (left), Loday's 4-associahedron (right), and the superposition of both (middle). Figures from Viviane Pons.

Chapter 2

Many polytopes and many regular triangulations

This chapter reproduces the article [PPS23], written with Arnau Padrol and Francisco Santos.

We show that for fixed $d > 3$ and n growing to infinity there are at least $(n!)^{d-2\pm o(1)}$ different labeled combinatorial types of d-polytopes with n vertices. This is about the square of the previous best lower bounds. As an intermediate step, we show that certain neighborly polytopes (such as particular realizations of cyclic polytopes) have at least $(n!)^{\lfloor (d-1)/2 \rfloor \pm o(1)}$ regular triangulations.

2.1 Introduction

In the preface of his classical book in polytope theory [Grü03], Grünbaum traces the problem of enumerating the number of combinatorial types of polytopes back to Euler, and cites its difficulty as one of the main reasons for the "*decline in the interest in convex polytopes*" at the beginning of the XXth century.

These efforts were concentrated in the case of 3-dimensional polytopes, starting with many contributions by Cayley and Kirkman, according to Grünbaum's historical remarks in [Grü03, Chapter 13.6]. Thanks to Steinitz's Theorem, which gives a correspondence between combinatorial types of 3-dimensional polytopes and 3-connected planar graphs, nowadays we have quite precise knowledge on the number of 3-polytopes with n vertices [BW88, RW82] and the distribution of many combinatorial parameters [BGR92].

In contrast, for higher-dimensional polytopes the problem is still very far from being solved. One of the main difficulties lies in the lack of a combinatorial characterization of face lattices of polytopes, as explained in Section 1.1.2.

However, the mere number of polytopes is relatively small. In 1986 Goodman and Pollack [GP86] showed that the number of (labeled) combinatorially different simplicial

d-polytopes with n vertices is bounded by $(n!)^{c_d}$ for some constant c_d depending solely on d, and Alon [Alo86] proved that this upper bound is valid for non-necessarily simplicial polytopes too. This contrasts with the number of combinatorially different simplicial $(d-1)$-spheres with n vertices, which grows at least as $e^{\Omega(n^{\lfloor d/2 \rfloor})}$ [Kal88, NSW16].

In 1982 Shemer [She82] had devised constructions producing about $(n!)^{\frac{1}{2}\pm o(1)}$ different simplicial polytopes. This matches the upper bound, except for the fact that the constant c_d in the upper bound of Goodman and Pollack and Alon is $d^2 \pm o(1)$, much bigger than the $1/2$ obtained by Shemer. The construction was greatly improved by Padrol [Pad13] (see also [GP16]) who showed that there are at least $(n!)^{\lfloor d/2 \rfloor \pm o(1)}$ (labeled) neighborly polytopes. There are alternative constructions that give these many different combinatorial types of polytopes, which led Nevo and Padrol to ask whether the number of d-dimensional polytopes with n vertices and m facets was bounded above by $m^{n+o(n)}$ (unpublished). As the maximal number of facets of a d-polytope with n vertices is $O(n^{\lfloor d/2 \rfloor})$ by the Upper Bound Theorem [McM70], this would imply that the bound of $(n!)^{\lfloor d/2 \rfloor \pm o(1)}$ is asymptotically tight.

The main result in this chapter gives a negative answer to this question, by essentially doubling the exponent of $n!$ in the construction of Padrol:

Theorem 2.1.1. *The number of different labeled combinatorial types of d-polytopes with n vertices for fixed $d > 3$ and n growing to infinity is at least $(n!)^{d-2\pm o(1)}$.*

All the polytopes that we construct are $\lfloor (d-1)/2 \rfloor$-neighborly. That is, they are neighborly for odd d, but only $\left(\frac{d}{2}-1\right)$-neighborly if d is even. In fact, for even d the number of neighborly polytopes in our family is at most the same as in the family constructed by Padrol. See Remark 2.4.12 for more details.

Enumerating polytopes is intimately tied to enumerating regular triangulations of point configurations. In fact, the number of (combinatorial types of) simplicial d-polytopes with n vertices coincides with that of $(d-1)$-dimensional regular triangulations with $n-1$ vertices. See the beginning of Section 2.4 for details on this relation. In the same vein, counting all triangulations, regular or not, is related to counting simplicial spheres.

In particular, the Goodman-Pollack bound implies the same upper bound of $(n!)^{d^2\pm o(1)}$ for the number of regular triangulations, while the construction of Kalai [Kal88] can be adapted to derive that the cyclic d-polytope with n vertices has at least $e^{\Omega(n^{\lfloor d/2 \rfloor})}$ triangulations in total [DRS10, Theorem 6.1.2].

Observe that the upper bound is for the total number of (combinatorially different) regular triangulations of *all* polytopes (for fixed parameters n and d), while the construction of Kalai counts triangulations of *a single polytope*. For regular triangulations of a single polytope, it is shown in [DRS10, Theorem 7.2.10] that the Cartesian product of a cyclic 3-polytope with n vertices and a segment has at least $(n/2)! = (n!)^{1/2\pm o(1)}$ regular triangulations. The second result in this chapter is a significant improvement of this lower bound, showing for example that:

Theorem 2.1.2. *For fixed $d \geq 3$ and n going to infinity, there are realizations of the cyclic d-polytope with n vertices having at least*

$$(n!)^{\left\lfloor \frac{d-1}{2} \right\rfloor \pm o(1)}$$

regular triangulations.

It has to be noted that the total number of triangulations of a polytope (or point configuration) depends only on its *oriented matroid* (another combinatorial invariant that is finer than the combinatorial type and that we will present in Section 3.3.1), while the number of regular triangulations varies for different realizations of the same oriented matroid.

Apart of its intrinsic interest, Theorem 2.1.2 is an intermediate step for Theorem 2.1.1; the proof of Theorem 2.1.1 consists in showing that *all* of the many polytopes constructed by Padrol [Pad13] admit realizations with the many regular triangulations stated in Theorem 2.1.2.

This makes our proof of Theorem 2.1.1 more geometric, as opposed to combinatorial, than previous constructions of "many" polytopes. In fact, the combinatorial types of polytopes obtained with our method may depend on choices made along the construction, for example via the particular realizations used for the Padrol polytopes, which affects what triangulations of them are regular, or via the particular lifting functions used for the regular triangulations.

2.2 Definitions and notation

In this chapter we will usually assume that the points in a point configuration $\boldsymbol{A} = (\boldsymbol{p}_1, \dots, \boldsymbol{p}_n) \in \mathbb{R}^{d\times[n]}$ are distinct and in convex position. We will allow ourselves to identify $\boldsymbol{p}_i$ and i in some notations that should not be ambiguous though.

We say that $\boldsymbol{A}$ is *k-neighborly* if any subset of k points is the vertex set of a face of $\operatorname{conv}(\boldsymbol{A})$, and just *neighborly* if it is $\lfloor \frac{d}{2} \rfloor$-neighborly; the latter makes sense since the simplex is the only d-polytope that is more than $\lfloor \frac{d}{2} \rfloor$-neighborly.

We denote *RegTriang*$(\boldsymbol{A})$ the set of regular triangulations of $\boldsymbol{A}$.

A point $\boldsymbol{q} \notin \boldsymbol{A}$ is said to be in *general position* with respect to $\boldsymbol{A}$ if no hyperplane spanned by points of $\boldsymbol{A}$ contains $\boldsymbol{q}$, and in *very general position* with respect to $\boldsymbol{A}$ if moreover no small perturbation of $\boldsymbol{q}$ changes *RegTriang*$(\boldsymbol{A} \cup \{\boldsymbol{q}\})$. An argument similar to that in [Ath99, Part 2] shows that configurations in very general position form a dense open subset of the space of all point configurations.

Two points $\boldsymbol{p}_i, \boldsymbol{p}_j \in \boldsymbol{A}$ are said to be *triangulation-inseparable* in $\boldsymbol{A}$ if we have that

(i) *RegTriang*$(\boldsymbol{A} \setminus \{\boldsymbol{p}_i\})$ = *RegTriang*$(\boldsymbol{A} \setminus \{\boldsymbol{p}_j\})$ up to relabeling j to i, and

(ii) for any $\boldsymbol{\mathcal{T}} \in$ *RegTriang*$(\boldsymbol{A} \setminus \{\boldsymbol{p}_i\})$ there is a lifting function $\ell : [n] \to \mathbb{R}$ which restricted to both $\boldsymbol{A} \setminus \{\boldsymbol{p}_i\}$ and $\boldsymbol{A} \setminus \{\boldsymbol{p}_j\}$ produces $\boldsymbol{\mathcal{T}}$ as a regular triangulation (up to relabeling j to i).

Let $\boldsymbol{p}$ be a vertex of $\operatorname{conv}(\boldsymbol{A})$. We define $\boldsymbol{A}/\boldsymbol{p}$ to be any point configuration obtained as the intersection of the half-lines positively spanned by $\{\boldsymbol{p}' - \boldsymbol{p} \mid \boldsymbol{p}' \in \boldsymbol{A} \setminus \{\boldsymbol{p}\}\}$ with an affine hyperplane that does not contain $\boldsymbol{p}$ and intersects all these half-lines. Following [DRS10, Definition 4.2.9] we call $\boldsymbol{A}/\boldsymbol{p}$ the *contraction* of $\boldsymbol{A}$ at the point $\boldsymbol{p}$. All the configurations that can be obtained as $\boldsymbol{A}/\boldsymbol{p}$ have the same triangulations and the same regular triangulations. In fact, regular triangulations of $\boldsymbol{A}/\boldsymbol{p}$ are exactly the links at $\boldsymbol{p}$ of regular triangulations of $\boldsymbol{A}$ [DRS10, Lemmas 4.2.20 and 4.2.22]. Here, the *link* of a triangulation $\mathcal{T}$ at a point $\boldsymbol{p}_i$, which we denote $\mathcal{T}/\boldsymbol{p}_i$, is defined as

$$\mathcal{T}/\boldsymbol{p}_i := \{F \subset [n] \setminus \{i\} \,|\, F \cup \{i\} \in \mathcal{T}\}\,.$$

2.3 Many regular triangulations

The main idea of our construction of configurations with a large number of regular triangulations is to split a point into two triangulation-inseparable points and to estimate the number of regular triangulations generated after this operation. This is inspired by the study of triangulations of cyclic polytopes done in [Ram97, RS00].

First, we show that we can indeed obtain triangulation-inseparable pairs by such a splitting.

Lemma 2.3.1. *Let $\boldsymbol{A}$ be a point configuration in $\mathbb{R}^d$ and $\boldsymbol{p} \in \boldsymbol{A}$ in very general position with respect to $\boldsymbol{A} \setminus \{\boldsymbol{p}\}$. Then there is an $\varepsilon > 0$ such that $\boldsymbol{p}$ and $\boldsymbol{p}'$ are triangulation-inseparable in $\boldsymbol{A} \cup \{\boldsymbol{p}'\}$ for any $\boldsymbol{p}' \in B(\boldsymbol{p}, \varepsilon)$ in very general position with respect to $\boldsymbol{A}$. Here $B(\boldsymbol{p}, \varepsilon)$ denotes the ball of radius ε centered at $\boldsymbol{p}$.*

Proof. Up to relabeling, we can assume that $\boldsymbol{A} = (\boldsymbol{p}_1, \ldots, \boldsymbol{p}_n)$ and $\boldsymbol{p} = \boldsymbol{p}_n$. By definition of being in very general position with respect to $\boldsymbol{A} \setminus \{\boldsymbol{p}_n\}$, there exists some $\eta > 0$ such that $\mathit{RegTriang}(\boldsymbol{A}) = \mathit{RegTriang}(\boldsymbol{A} \setminus \{\boldsymbol{p}_n\} \cup \{\boldsymbol{p}'\})$ for all $\boldsymbol{p}' \in B(\boldsymbol{p}_n, \eta)$. In particular, any such a $\boldsymbol{p}'$ fulfills the first condition for being triangulation-inseparable with $\boldsymbol{p}$.

For each regular triangulation $\mathcal{T} \in \mathit{RegTriang}(\boldsymbol{A})$ we can choose a specific lifting function $w_{\mathcal{T}} : [n] \to \mathbb{R}$ that induces $\mathcal{T}$, and choose it so that the point $(\boldsymbol{p}_n, w_{\mathcal{T}}(n))$ is still in general position with respect to the lifted configuration $\{(\boldsymbol{p}_i, w_{\mathcal{T}}(i)) \,|\, i \in [n-1]\}$. Hence there is some $0 < \varepsilon_T < \eta$ such that $\{(\boldsymbol{p}_i, w_{\mathcal{T}}(i)) \,|\, i \in [n]\}$ and $\{(\boldsymbol{p}_i, w_{\mathcal{T}}(i)) \,|\, i \in [n-1]\} \cup \{(\boldsymbol{p}', w_{\mathcal{T}}(n))\}$ have the same faces, for all $\boldsymbol{p}' \in B(\boldsymbol{p}_n, \varepsilon_{T},)$. This means that w_T induces T as a regular triangulation of $\boldsymbol{A} \setminus \{p_n\} \cup \{\boldsymbol{p}'\}$ for all $\boldsymbol{p}' \in B(\boldsymbol{p}_n, \varepsilon_{\mathcal{T}})$.

If we take $\varepsilon = \min\limits_{\mathcal{T} \in \mathit{RegTriang}(\boldsymbol{A})} \varepsilon_T$, we obtain that $\boldsymbol{p}$ and $\boldsymbol{p}'$ are triangulation-inseparable in $\boldsymbol{A} \cup \{\boldsymbol{p}'\}$ for all $\boldsymbol{p}' \in B(\boldsymbol{p}, \varepsilon)$. □

The following result is our main technical lemma, which provides lower bounds for the number of triangulations under the presence of triangulation-inseparable points. The main ideas are illustrated in Example 2.3.3.

Lemma 2.3.2. *Let $\boldsymbol{A}$ be a point configuration in $\mathbb{R}^d$ and let $\boldsymbol{p} \in \boldsymbol{A}$ be a vertex of $\operatorname{conv}(\boldsymbol{A})$ that is in very general position with respect to $\boldsymbol{A} \setminus \{\boldsymbol{p}\}$. We denote C the minimum number of cells in a regular triangulation of $\boldsymbol{A}/p$.*

Let $\boldsymbol{p}'$ be such that $\boldsymbol{p}$ and $\boldsymbol{p}'$ are triangulation-inseparable in $\boldsymbol{A} \cup \{\boldsymbol{p}'\}$, $\boldsymbol{p}'$ is in very general position with respect to $\boldsymbol{A}$, and $\boldsymbol{p}'$ is a vertex of $\operatorname{conv}(\boldsymbol{A} \cup \{\boldsymbol{p}'\})$. Then we have

$$|\mathit{RegTriang}(\boldsymbol{A} \cup \{\boldsymbol{p}'\})| \geq |\mathit{RegTriang}(\boldsymbol{A})| \times (C + 1).$$

Proof. We denote $\boldsymbol{A}'$ the point configuration $\boldsymbol{A} \setminus \{\boldsymbol{p}\} \cup \{\boldsymbol{p}'\}$.

Let us call a regular triangulation $\tilde{\mathcal{T}}$ of $\boldsymbol{A} \cup \boldsymbol{A}'$ *good* if there is a regular triangulation $\mathcal{T}$ of $\boldsymbol{A}$ such that $\mathcal{T}$ and $\tilde{\mathcal{T}}$ coincide when restricted to $\boldsymbol{A} \setminus \{\boldsymbol{p}\}$. Since a regular triangulation of $\boldsymbol{A}$ is determined by its restriction to $\boldsymbol{A} \setminus \{\boldsymbol{p}\}$, this definition implicitly gives a map

$$\phi : \{\text{good triangulations of } \boldsymbol{A} \cup \boldsymbol{A}'\} \to \mathit{RegTriang}(\boldsymbol{A}).$$

We claim that for every $\mathcal{T} \in \mathit{RegTriang}(P)$ we have

$$|\phi^{-1}(\mathcal{T})| \geq c(\mathcal{T}/\boldsymbol{p}) + 1 \geq C + 1,$$

where we denote by $c(L)$ (and call size of L) the number of cells of a pure polyhedral complex L. This formula implies the statement.

Let $\mathcal{T}$ be a regular triangulation of $\boldsymbol{A}$. To avoid confusion we denote by $\mathcal{T}'$ the triangulation $\mathcal{T}$ but considered as a triangulation of $\boldsymbol{A}'$. Let $w \in \mathbb{R}^{\boldsymbol{A} \cup \boldsymbol{A}'}$ be a lifting vector producing $\mathcal{T}$ and $\mathcal{T}'$ when restricted to $\boldsymbol{A}$ and $\boldsymbol{A}'$, which exists because $\boldsymbol{p}$ and $\boldsymbol{p}'$ are triangulation-inseparable. We will assume moreover a genericity condition on w that will be detailed later at item (8).

For each $t \in \mathbb{R}$ we consider the following lifting vector $w_t \in \mathbb{R}^{\boldsymbol{A} \cup \boldsymbol{A}'}$, which varies continuously with t:

- For $\boldsymbol{q} \in \boldsymbol{A} \setminus \{\boldsymbol{p}\}$, $w_t(\boldsymbol{q}) := w(\boldsymbol{q})$ is independent of t.
- If $t \leq 0$ then $w_t(\boldsymbol{p}) := w(\boldsymbol{p})$ and $w_t(\boldsymbol{p}') := w(\boldsymbol{p}') - t$.
- If $t \geq 0$ then $w_t(\boldsymbol{p}) := w(\boldsymbol{p}) + t$ and $w_t(\boldsymbol{p}') := w(\boldsymbol{p}')$.

Let $\mathcal{T}_t$ be the regular subdivision of $\boldsymbol{A} \cup \boldsymbol{A}'$ produced by w_t. We have that:

1. *The restriction of $\mathcal{T}_t$ to $\boldsymbol{A} \setminus \{\boldsymbol{p}\}$ coincides with the restriction of $\mathcal{T}$:* Indeed, if σ is a face of $\mathcal{T}$ contained in $\boldsymbol{A} \setminus \{\boldsymbol{p}\}$ then w, and hence any w_t, sends all of $\boldsymbol{A} \cup \boldsymbol{A}' \setminus \sigma$ above some supporting hyperplane of the lift of σ; hence, σ is a face in $\mathcal{T}_t$. Conversely, suppose σ is a cell in $\mathcal{T}_t$ for some t that is contained in $\boldsymbol{A} \setminus \{\boldsymbol{p}\}$. If $t \leq 0$ then w_t, and hence w, sends $\boldsymbol{A} \setminus \sigma$ above the hyperplane. Hence, σ is a cell of $\mathcal{T}$. If $t \geq 0$ then w_t, and hence w, sends $\boldsymbol{A}' \setminus \sigma$ above the hyperplane. Hence, σ is a cell of $\mathcal{T}'$, which restricted to $\boldsymbol{A} \setminus \{\boldsymbol{p}\}$ coincides with $\mathcal{T}$.

2. *If $t \leq 0$ then for every cell $\sigma \in \mathcal{T}_t$, $\sigma \setminus \{\boldsymbol{p}'\}$ is a face in $\mathcal{T}$:* This is because for $t \leq 0$ we have that w_t restricted to $\boldsymbol{A}$ equals w, which produces $\mathcal{T}$ as a regular triangulation of $\boldsymbol{A}$.

3. *If $t \geq 0$ then for every cell $\sigma \in \mathcal{T}_t$, $\sigma \setminus \{\boldsymbol{p}\}$ is a face in $\mathcal{T}'$:* Same proof.

4. *If $\mathcal{T}_t$ is not a triangulation for a certain t then every non-simplicial cell is of the form $\tau \cup \{\boldsymbol{p}, \boldsymbol{p}'\}$ where τ is a cell of $\mathcal{T}/\boldsymbol{p}$.* Let σ be a non-simplicial cell of $\mathcal{T}_t$. By claims (2) and (3), σ uses both of $\boldsymbol{p}$ and $\boldsymbol{p}'$ and either $\sigma \setminus \{\boldsymbol{p}'\}$ is in $\mathcal{T}$ or $\sigma \setminus \{\boldsymbol{p}\}$ is in $\mathcal{T}'$. Hence, $\sigma \setminus \{\boldsymbol{p}, \boldsymbol{p}'\}$ is in $\mathcal{T}/\boldsymbol{p} = \mathcal{T}'/\boldsymbol{p}'$.

5. *Each such $\tau \cup \{\boldsymbol{p}, \boldsymbol{p}'\}$ appears as a cell for at most one value of t:*

   If $t \leq 0$ then the value of t is fixed by the fact that $w_t(\boldsymbol{p}') = w(\boldsymbol{p}') - t$ equals the height at which the lifted hyperplane containing $\tau \cup \{\boldsymbol{p}\}$ meets the vertical line $\{\boldsymbol{p}'\} \times \mathbb{R}$; same, changing $\boldsymbol{p}$ and $\boldsymbol{p}'$, if $t \geq 0$. Thus, we at most have one value of t in $(-\infty, 0]$ and one in $[0, \infty)$. Moreover, there cannot be two values, one negative and one positive. Indeed, if $\tau \cup \{\boldsymbol{p}, \boldsymbol{p}'\}$ is a cell of $\boldsymbol{\mathcal{T}}_t$ for $t < 0$, then the point $(\boldsymbol{p}', w(\boldsymbol{p}'))$ is below the lifted hyperplane containing $\tau \cup \{\boldsymbol{p}\}$, so $(\boldsymbol{p}, w(\boldsymbol{p}))$ is above the lifted hyperplane containing $\tau \cup \{\boldsymbol{p}'\}$ and there is no $t' > 0$ such that $\tau \cup \{\boldsymbol{p}, \boldsymbol{p}'\}$ is a cell of $\boldsymbol{\mathcal{T}}_{t'}$.

6. *Assuming $\boldsymbol{\mathcal{T}}_t$ is a triangulation, let $L_t := \boldsymbol{\mathcal{T}}_t/\boldsymbol{p} \setminus \{\boldsymbol{p}'\}$ and $L'_t := \boldsymbol{\mathcal{T}}_t/\boldsymbol{p}' \setminus \{\boldsymbol{p}\}$. L_t and L'_t are contained in $\boldsymbol{\mathcal{T}}/\boldsymbol{p}$ and they are complementary in the sense that their union equals $\boldsymbol{\mathcal{T}}/\boldsymbol{p}$ and their intersection is lower dimensional.* L_t and L'_t are contained in $\boldsymbol{\mathcal{T}}/\boldsymbol{p} = \boldsymbol{\mathcal{T}}'/\boldsymbol{p}'$ by properties (2) and (3). They are complementary because every cell $\tau \in \boldsymbol{\mathcal{T}}/\boldsymbol{p}$ needs to be joined to one and only one of $\boldsymbol{p}$ and $\boldsymbol{p}'$ to give a cell of $\boldsymbol{\mathcal{T}}_t$.

7. *In the limit when $t \to -\infty$ we have that $L_t = \boldsymbol{\mathcal{T}}/\boldsymbol{p}$ (and hence L'_t is lower-dimensional) and in the limit $t \to +\infty$ we have that $L'_t = \boldsymbol{\mathcal{T}}/\boldsymbol{p}$ (and hence L_t is lower-dimensional).* In these limits, $\boldsymbol{\mathcal{T}}_t$ equals the triangulation obtained by *placing* point $\boldsymbol{p}'$ (respectively $\boldsymbol{p}$) in $\boldsymbol{\mathcal{T}}$ (respectively in $\boldsymbol{\mathcal{T}}'$). This implies $L_t = \boldsymbol{\mathcal{T}}/\boldsymbol{p}$ (respectively $L'_t = \boldsymbol{\mathcal{T}}/\boldsymbol{p}$).

8. *We can take w sufficiently generic so that no $\boldsymbol{\mathcal{T}}_t$ contains two different non-simplicial cells.* Suppose that (τ_1, τ_2) is a pair of cells in $\boldsymbol{\mathcal{T}}/\boldsymbol{p}$ such that $\tau_1 \cup \{\boldsymbol{p}, \boldsymbol{p}'\}$ and $\tau_2 \cup \{\boldsymbol{p}, \boldsymbol{p}'\}$ are in $\boldsymbol{\mathcal{T}}_t$ for the same value of t. Let $\boldsymbol{H}_1$ and $\boldsymbol{H}_2$ be the two hyperplanes in $\mathbb{R}^{d+1}$ spanned by the lifts of $\tau_1 \cup \{\boldsymbol{p}\}$ and $\tau_2 \cup \{\boldsymbol{p}\}$ for that t. Our hypothesis implies that $\boldsymbol{H}_1$ and $\boldsymbol{H}_2$ intersect the vertical line $\{\boldsymbol{p}'\} \times \mathbb{R}$ at the same height (namely, at height $w_t(\boldsymbol{p}')$). If this happens for a sufficiently generic choice of w then the intersection of $\boldsymbol{H}_1$ with $\{\boldsymbol{p}'\} \times \mathbb{R}$ does not change when slightly perturbing the heights of all points in $\tau_1 \setminus \tau_2$: This implies that this intersection point lies in the affine span of (the lifted) configuration $(\tau_1 \cap \tau_2) \cup \{\boldsymbol{p}\}$. Hence, $\boldsymbol{p}'$ lies in the affine span of (the original) $(\tau_1 \cap \tau_2) \cup \{\boldsymbol{p}\}$, and $\boldsymbol{p}'$ is not in general position.

9. *If $\boldsymbol{\mathcal{T}}_t$ is not a triangulation, and $\varepsilon > 0$ is small enough, then $c(L_{t+\varepsilon}) = c(L_{t-\varepsilon}) - 1$ and $c(L'_{t+\varepsilon}) = c(L'_{t-\varepsilon}) + 1$.* There is a single cell of $\boldsymbol{\mathcal{T}}_t$ of the form $\tau \cup \{\boldsymbol{p}, \boldsymbol{p}'\}$. If s is in the neighborhood of t, all the cells of $\boldsymbol{\mathcal{T}}_s$ not contained in $\tau \cup \{\boldsymbol{p}, \boldsymbol{p}'\}$ remain unchanged because they are defined by an open condition on s. For $s < t$, we have that $\tau \cup \{\boldsymbol{p}\}$ is a cell of $\boldsymbol{\mathcal{T}}_s$ but $\tau \cup \{\boldsymbol{p}'\}$ is not, because $\boldsymbol{p}'$ is above the hyperplane spanned by $\tau \cup \{\boldsymbol{p}\}$. Similarly, for $s > t$, we have that $\tau \cup \{\boldsymbol{p}\}$ is not a cell of $\boldsymbol{\mathcal{T}}_s$ but $\tau \cup \{\boldsymbol{p}'\}$ is.

Claim (1) says that whenever $\boldsymbol{\mathcal{T}}_t$ is a triangulation it is a good triangulation and it lies in the preimage of $\boldsymbol{\mathcal{T}}$. As we move t continuously from $-\infty$ to $+\infty$ there are finitely many values of t where $\boldsymbol{\mathcal{T}}_t$ is not a triangulation, by claims (4) and (5). Of course, outside those values the triangulation $\boldsymbol{\mathcal{T}}_t$ is constant, and claim (8) says that (if $\boldsymbol{p}'$ is in general position and w is generic) at those values the change in the triangulation is a geometric bistellar flip in a cell of the form $\tau \cup \{\boldsymbol{p}, \boldsymbol{p}'\}$. This flip changes the numbers of cells of $\boldsymbol{\mathcal{T}}/\boldsymbol{p}$ contained in L_t and in L'_t by one unit, increasing L'_t and decreasing L_t as t increases, by (9). By property (7) the size of L'_t grows from zero to $c(\boldsymbol{\mathcal{T}}/\boldsymbol{p})$ as t goes from $-\infty$ to $+\infty$, so we encounter at least $c(\boldsymbol{\mathcal{T}}/\boldsymbol{p}) + 1$ different good triangulations in the preimage of $\boldsymbol{\mathcal{T}}$ along the process. □

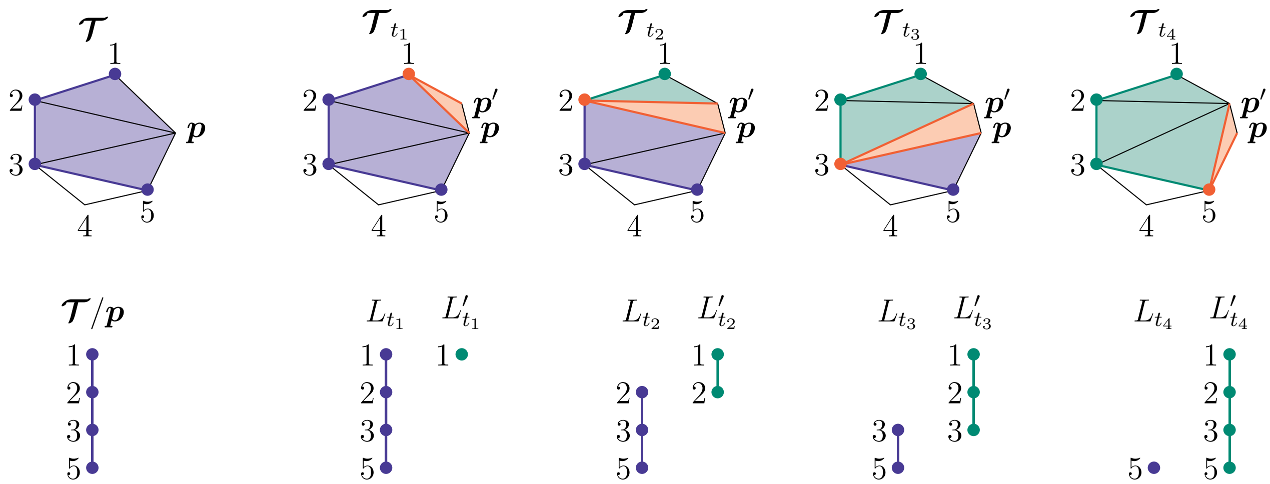

Figure 2.1: A two-dimensional illustration of the proof of Lemma 2.3.2. In the left picture, a triangulation of a hexagon. In the rest, the vertex $\boldsymbol{p}$ is split into $\{\boldsymbol{p}, \boldsymbol{p}'\}$, and increasing values of the parameter t induce different good triangulations of the heptagon $\boldsymbol{A} \cup \boldsymbol{A}'$.

Example 2.3.3. To illustrate Lemma 2.3.2, we use a two-dimensional example (reminiscent of some classical proofs of the recurrence relation for Catalan numbers). It has the advantage of clarity, as it can be easily depicted, see Figure 2.1.

When a point $\boldsymbol{p}$ is split into $\{\boldsymbol{p}, \boldsymbol{p}'\}$, the facets of the polytope that were incident to $\boldsymbol{p}$ are divided into two families, those that remain facets after the splitting, and those that replace $\boldsymbol{p}$ by $\boldsymbol{p}'$. Moreover, new facets containing both $\boldsymbol{p}$ and $\boldsymbol{p}'$ are created. Similarly, the cells incident to $\boldsymbol{p}$ in a triangulation are divided into two families, those containing $\boldsymbol{p}$ and those containing $\boldsymbol{p}'$, and new cells containing both $\boldsymbol{p}$ and $\boldsymbol{p}'$ are created. This can be read in the link $\boldsymbol{\mathcal{T}}/\boldsymbol{p}$, which is divided into two parts, L_t and L'_t, without full dimensional intersection: We have that $F \cup \{\boldsymbol{p}\} \in \boldsymbol{\mathcal{T}}_t$ whenever $F \in L_t$, $F \cup \{\boldsymbol{p}'\} \in \boldsymbol{\mathcal{T}}_t$ whenever $F \in L'_t$, and that $F \cup \{\boldsymbol{p}, \boldsymbol{p}'\} \in T_t$ whenever $F \in L_t \cap L'_t$.

When $t = -\infty$, we have that $L_t \cap L'_t = L'_t$, and it coincides with the boundary faces of $\boldsymbol{\mathcal{T}}/\boldsymbol{p}$ that are incident to $\boldsymbol{p}'$ in $\operatorname{conv}(\boldsymbol{A} \cup \{\boldsymbol{p}'\})$. As the values of t increase, $L_t \cap L'_t$ flips successively through each of the simplices of $\boldsymbol{\mathcal{T}}/\boldsymbol{p}$, giving rise to different triangulations. At the end, when $t = \infty$, we have that $L_t \cap L'_t = L_t$, and it coincides with the boundary faces of $\boldsymbol{\mathcal{T}}/\boldsymbol{p}$ that are incident to $\boldsymbol{p}$ in $\operatorname{conv}(\boldsymbol{A} \cup \{\boldsymbol{p}'\})$. The number of different triangulations thus created is therefore one more than the number of cells in the link $\boldsymbol{\mathcal{T}}/\boldsymbol{p}$.

There are some important differences that only appear in higher dimensions. First of all, all triangulations of a polygon are regular, while starting in dimension 3 there are polytopes with non-regular triangulations. Moreover, in dimension two there is only one way to go from $\boldsymbol{\mathcal{T}}_{-\infty}$ to $\boldsymbol{\mathcal{T}}_{\infty}$ since the link $\boldsymbol{\mathcal{T}}/\boldsymbol{p}$ is one-dimensional, while in higher dimensions there are usually several different paths between these two triangulations. The $c(\boldsymbol{\mathcal{T}}/\boldsymbol{p})+1$ triangulations $\boldsymbol{\mathcal{T}}_t$ that we see as t ranges from $-\infty$ to ∞ will depend on the relative position of $\boldsymbol{p}$ and $\boldsymbol{p}'$ and the choice of the lifting function w. Finally, in a polygon, the vertex figure is just a segment (with interior points) and the number C in the statement is always 1, so the lemma does not give an interesting bound in that case.

Without any further constraint this lemma is not very useful, as $\operatorname{conv}(\boldsymbol{A}/\boldsymbol{p})$ could be a simplex and $C=1$. However, a lower bound on C can be proved if we have knowledge on the neighborliness of $\boldsymbol{A}/\boldsymbol{p}$, thanks to the following lemma.

For a pure d-dimensional simplicial complex $\mathcal{C}$ and $0 \le j \le d+1$ we denote

$$h_j(\mathcal{C}) = \sum_{k=0}^{j} (-1)^{j-k} \binom{d+1-k}{d+1-j} f_{k-1}(\mathcal{C}),$$

where $f_k(\mathcal{C})$ is the number of faces of $\mathcal{C}$ of dimension k. The numbers $h_0(\mathcal{C}),\dots,h_{d+1}(\mathcal{C})$, collectively called the *h-vector* of $\mathcal{C}$, are known to be nonnegative in certain special cases, which include $\mathcal{C}$ being a topological sphere; see [Zie95, Chapter 8].

Lemma 2.3.4. *Let $d>2$ and $1 \le k \le d+1$. Let $\boldsymbol{Q}$ be a d-dimensional simplicial polytope on n vertices. Then the number of cells in any triangulation of $\boldsymbol{Q}$ is bounded from below by $h_k(\partial \boldsymbol{Q})$.*

In particular, if $\boldsymbol{Q}$ is k-neighborly for $1 \le k \le \left\lfloor \frac{d}{2} \right\rfloor$, then this number is bounded by:

$$h_k(\partial \boldsymbol{Q}) = \binom{n-d-1+k}{k}.$$

Proof. Let T be a triangulation of $\boldsymbol{Q}$. We want a bound on $f_d(T)$.

We use the following result from McMullen and Walkup [MW71, Thm. 2], cited in a modern version in [DRS10, Thm. 2.6.11]. For any $0 \le j \le d$,

$$h_j(\partial \boldsymbol{Q}) - h_{j-1}(\partial \boldsymbol{Q}) = h_j(T) - h_{d+1-j}(T),$$

where $\partial \boldsymbol{Q}$ is the boundary simplicial complex of $\boldsymbol{Q}$, of dimension $d-1$, and we take $h_{-1}(\partial \boldsymbol{Q}) = 0$.

Then we have:

$$\begin{aligned} f_d(T) &= \sum_{l=0}^{d+1} h_l(T) \\ &= h_k(\partial \boldsymbol{Q}) - h_{-1}(\partial \boldsymbol{Q}) + \sum_{j=0}^{k} h_{d+1-j}(T) + \sum_{l=k+1}^{d+1} h_l(T) \\ &\ge h_k(\partial \boldsymbol{Q}). \end{aligned}$$

The first h-coefficients of neighborly polytopes are well known, as they achieve the maximum allowed by the Upper Bound Theorem ([McM70, Lemma 2], see also [Zie95, Lemma 8.26]). In particular we have:

$$h_k(\partial \boldsymbol{Q}) = \binom{n-d-1+k}{k}.$$

$\square$

Remark 2.3.5. From the proof one derives that for $1 \leq k \leq \left\lfloor \frac{d}{2} \right\rfloor$, a triangulation T has exactly $h_k(\partial(\boldsymbol{Q}))$ cells if, and only if, $h_j(T) = 0$ for every $j \geq k+1$. This, in turn, is equivalent to all interior cells of T having dimension at least $d-k$.

As a consequence of the previous two lemmas we have:

Theorem 2.3.6. *Let $\boldsymbol{A} = (\boldsymbol{p}_1, \ldots, \boldsymbol{p}_{n-1}, \boldsymbol{q})$ be a configuration of n points in very general convex position in $\mathbb{R}^d$ such that:*

(i) for every $d+1 \leq i \leq n-1$, $\boldsymbol{p}_i$ and $\boldsymbol{q}$ are triangulation-inseparable in $\boldsymbol{A}_i := (\boldsymbol{p}_1, \ldots, \boldsymbol{p}_i, \boldsymbol{q})$, and

(ii) the point configuration $\boldsymbol{A}/\boldsymbol{q}$ is k-neighborly.

Then

$$|RegTriang(\boldsymbol{A})| \geq \prod_{m=d}^{n-1} \binom{m-d+k}{k},$$

which is of order $(n!)^{k \pm o(1)}$ for fixed k and d.

Proof. For $k = 0$ the statement is void, therefore we assume that $k \geq 1$. We proceed by induction on n. In the base case $n = d+1$ we have that $\boldsymbol{A} = \boldsymbol{A}_d$ is a simplex, with only one regular triangulation, so the result is trivial.

Assume that the theorem is true for $n = m-1$. Note that $\boldsymbol{A}_{m-1}$ satisfies the hypotheses of the theorem. Indeed, the first condition is automatic and the second follows because $\boldsymbol{A}_m/\boldsymbol{q}$ is a subset of $\boldsymbol{A}/\boldsymbol{q}$, and a subset of a k-neighborly point configuration is still k-neighborly.

Now, since $\boldsymbol{p}_m$ and $\boldsymbol{q}$ are triangulation-inseparable in $\boldsymbol{A}_m$ by the first hypothesis, we can apply Lemma 2.3.2 to deduce that

$$|RegTriang(\boldsymbol{A}_m)| \geq |RegTriang(\boldsymbol{A}_{m-1})| \times (C_m + 1),$$

where C_m is the minimum number of cells in a regular triangulation of $\boldsymbol{A}_m/\boldsymbol{q} = (\boldsymbol{A}/\boldsymbol{q}) \setminus \{\boldsymbol{p}_{m+1}, \ldots, \boldsymbol{p}_{n-1}\}$. And since $\boldsymbol{A}_m/\boldsymbol{q}$ is a k-neighborly $(d-1)$-dimensional simplicial polytope on m vertices (all points are vertices since it is at least 1-neighborly), Lemma 2.3.4 implies that $C_m \geq \binom{m-d+k}{k}$.

At the end, using the induction hypothesis we conclude that:

$$
\begin{aligned}
|RegTriang(\boldsymbol{A})| &\geq \prod_{m=d}^{n-1} \binom{m-d+k}{k} \\
&\geq \prod_{m=d}^{n-1} \left(\frac{m-d+k}{k}\right)^k \\
&= ((n-d-1+k)!)^k \times \frac{1}{\left((k-1)!k^{(n-d)}\right)^k} \\
&= \exp(kn\log n + o(n\log n)).
\end{aligned}
$$

□

The combination of these results provides Theorem 2.1.2: a lower bound of order $(n!)^{\lfloor\frac{d-1}{2}\rfloor \pm o(1)}$ for the number of regular triangulations of cyclic polytopes in certain realizations. The *cyclic d-polytope* with n vertices is a neighborly simplicial polytope that can be realized as the convex hull of n arbitrary points $\boldsymbol{p}_1, \ldots, \boldsymbol{p}_n$ along the moment curve $\left\{(t, t^2, \ldots, t^d) \in \mathbb{R}^d \,\middle|\, t \in \mathbb{R}\right\}$. See for example [Zie95, Example 0.6] for details.

Proof of Theorem 2.1.2. We first fix the last vertex $\boldsymbol{q} = \boldsymbol{p}_n$ on the moment curve and then define the points $\boldsymbol{p}_1, \ldots, \boldsymbol{p}_{n-1}$ consecutively. At step i, we slide the point $\boldsymbol{p}_i$ along the moment curve until it is close enough to $\boldsymbol{p}_n$ so that Lemma 2.3.1 implies them to be triangulation-inseparable, after a perturbation of $\boldsymbol{p}_i$ into very general position if needed. For $d \geq 3$, the contraction of the last vertex in a cyclic polytope with n vertices is a $(d-1)$-dimensional cyclic polytope with $n-1$ vertices, and in particular $\lfloor\frac{d-1}{2}\rfloor$-neighborly. Hence Theorem 2.3.6 gives the result. □

It is not clear to us whether cyclic polytopes (or neighborly polytopes in general) do indeed have more triangulations than "typical" simplicial polytopes of the same dimension and number of vertices. In fact, in dimension two quite the opposite is true: the convex n-gon minimizes the number of triangulations and of regular triangulations among point configurations of n points in general position [KVY23, GS21].

2.4 Many polytopes

Let us call *polytopal (simplicial) d-ball* any (labeled) simplicial complex that can be realized as a regular triangulation of a configuration of points in dimension d. By adding a point "at infinity" to a polytopal d-ball one obtains a polytopal d-sphere with one more vertex, and viceversa. Thus, the number of combinatorially different labeled polytopal d-balls with n vertices coincides with the number of combinatorially different labeled simplicial $(d+1)$-polytopes with $n+1$ vertices.

On the other hand, if two simplicial polytopes are combinatorially different then no triangulation of the first can be combinatorially equal to one of the second, because we can recover the boundary complex of a simplicial polytope from any of its triangulations. Hence:

Lemma 2.4.1. *If $\boldsymbol{A}_1, \dots, \boldsymbol{A}_N$ are configurations of dimension d and size n in convex and general position and with combinatorially different convex hulls, then there are at least*

$$\sum_{i=1}^{N} |\mathit{RegTriang}(\boldsymbol{A}_i)|$$

combinatorially different labeled simplicial $(d+1)$-polytopes with $n+1$ vertices.

In this section we show that not only cyclic polytopes but all the *Gale sewn* polytopes introduced in [Pad13] fulfill (in certain realizations) the conditions of Theorem 2.3.6. This provides us with a large family of polytopes with many regular triangulations, to which we can apply Lemma 2.4.1 and obtain even more polytopes.

In order to have a self-contained presentation, we give in Section 2.4.1 all the definitions and lemmas that are used in the proofs of the constructions in the Section 2.4.2. Most of the contents of the latter can be traced back to [Pad13, GP16], but observe that the presentation in [Pad13] is formulated in the Gale dual setting of extensions while ours, and the one in [GP16], is already formulated in a primal setting of liftings.

2.4.1 Lexicographic liftings

A central tool for our construction are lexicographic liftings, which are a way to derive $(d+1)$-dimensional point configurations from d-dimensional point configurations.

Definition 2.4.2. A *positive lexicographic lifting* of a point configuration $\boldsymbol{A} = (\boldsymbol{p}_1, \dots, \boldsymbol{p}_n) \subset \mathbb{R}^d$ (with respect to the order induced by the labels) is any configuration $\widehat{\boldsymbol{A}} = (\widehat{\boldsymbol{p}}_1, \dots, \widehat{\boldsymbol{p}}_n, \widehat{\boldsymbol{q}})$ of $n+1$ labeled points in $\mathbb{R}^{d+1}$ such that:

(i) $\widehat{\boldsymbol{q}}$ is a point in the halfspace $x_{d+1} > 0$,

(ii) for $1 \leq i \leq n$, the point $\widehat{\boldsymbol{p}}_i$ lies in the half-line from $\widehat{\boldsymbol{q}}$ through $(\boldsymbol{p}_i, 0)$,

(iii) for $d+2 \leq i \leq n$, and for every hyperplane $\boldsymbol{H}$ spanned by $d+1$ points taken among $\{\widehat{\boldsymbol{p}}_1, \dots, \widehat{\boldsymbol{p}}_{i-1}\}$, the points $\widehat{\boldsymbol{q}}$ and $\widehat{\boldsymbol{p}}_i$ lie on the same side of $\boldsymbol{H}$.

Remark 2.4.3. Positive lexicographic liftings exist for every point configuration, and are a special case of the lexicographic liftings produced with a sign vector in $\{+,-\}^n$, as defined e.g. in [GP16, Def. 4.1]. One way to construct a positive lexicographic lifting is to choose $\widehat{\boldsymbol{q}}$ arbitrarily with $x_{d+1} > 0$ and then take $\widehat{\boldsymbol{p}}_i := (1-\varepsilon_i)\widehat{\boldsymbol{q}} + \varepsilon_i(\boldsymbol{p}_i, 0)$ for constants $0 < \varepsilon_n \ll \varepsilon_{n-1} \ll \cdots \ll \varepsilon_1$. See Figure 2.2.

The faces of $\operatorname{conv}(\widehat{\boldsymbol{A}})$ that do not contain $\widehat{\boldsymbol{q}}$ give a particular subdivision of $\boldsymbol{A}$ that is called the *placing*, or *pushing*, triangulation. We refer the reader to Section 4.3.1 of [DRS10] for more details.

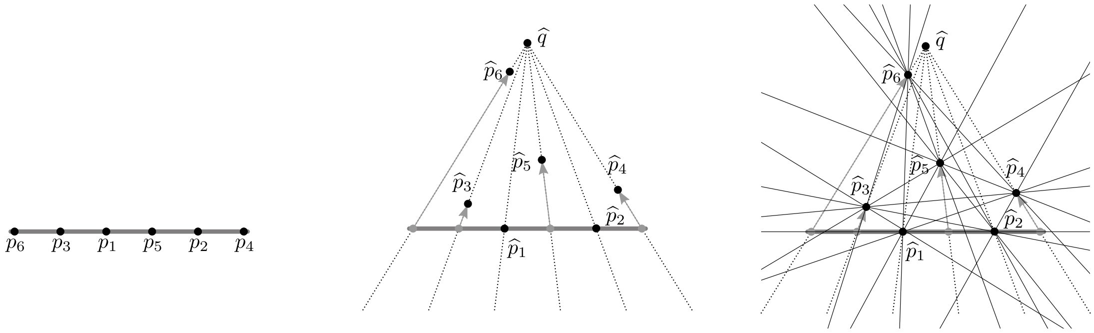

(a) $\boldsymbol{A}$ (b) $\widehat{\boldsymbol{A}}$ (c) Checking (iii)

Figure 2.2: A positive lexicographic lifting $\widehat{\boldsymbol{A}} \subset \mathbb{R}^2$ of a configuration $\boldsymbol{A} \subset \mathbb{R}^1$.

Definition 2.4.4. A face $\boldsymbol{F}$ of a polytope $\boldsymbol{P}$ is *visible* from a point $\boldsymbol{p} \in \mathbb{R}^d$ if there is an affine functional that is zero on $\boldsymbol{F}$, strictly positive on $\boldsymbol{p}$ and strictly negative on $\boldsymbol{P} \setminus \boldsymbol{F}$. $\boldsymbol{F}$ is *hidden* from $\boldsymbol{p}$ if there is an affine functional that is zero on $\boldsymbol{F}$ and strictly negative both on $\boldsymbol{p}$ and on $\boldsymbol{P} \setminus \boldsymbol{F}$. Note that a face that is not a facet can be both visible and hidden from $\boldsymbol{p}$, and if $\boldsymbol{p}$ is in general position with respect to $\boldsymbol{P}$ and $\boldsymbol{p} \notin \boldsymbol{P}$, then any face of $\boldsymbol{P}$ (even facets) is either visible or hidden from $\boldsymbol{p}$.

Let $\boldsymbol{A} = (\boldsymbol{p}_1, \ldots, \boldsymbol{p}_n)$ be a point configuration in general position in $\mathbb{R}^d$. We denote $\boldsymbol{A}_i := (\boldsymbol{p}_1, \ldots, \boldsymbol{p}_i)$. The *placing triangulation* $\boldsymbol{\mathcal{T}}_n$ of $\boldsymbol{A}_n$ is defined iteratively by taking for $\boldsymbol{\mathcal{T}}_1$ the singleton $\{1\}$ and for $\boldsymbol{\mathcal{T}}_i$ the union of the faces of $\boldsymbol{\mathcal{T}}_{i-1}$ with all simplices of the form $\boldsymbol{F} \cup \{i\}$ where $\boldsymbol{F}$ gives a face of $\operatorname{conv}(\boldsymbol{A}_{i-1})$ that is visible from $\boldsymbol{p}_i$. $\boldsymbol{\mathcal{T}}_i$ is the only triangulation of $\boldsymbol{A}_i$ that contains $\boldsymbol{\mathcal{T}}_{i-1}$. The *pulling* triangulation of $\boldsymbol{A}$ is the union of all simplices that give proper faces of $\operatorname{conv}(\boldsymbol{A})$ and all $\boldsymbol{F} \cup \{n\}$ where $\boldsymbol{F} \subseteq [n-1]$ gives a proper face of $\operatorname{conv}(\boldsymbol{A})$. (Proper faces are those different from the whole polytope).

Lemma 2.4.5. *Let $\widehat{\boldsymbol{A}} = (\widehat{\boldsymbol{p}}_1, \ldots, \widehat{\boldsymbol{p}}_n, \widehat{\boldsymbol{q}})$ be a positive lexicographic lifting of the point configuration $\boldsymbol{A} = (\boldsymbol{p}_1, \ldots, \boldsymbol{p}_n) \subset \mathbb{R}^d$ in convex position. For $i \in [n]$ we denote $\boldsymbol{A}_i := (\boldsymbol{p}_1, \ldots, \boldsymbol{p}_i)$ and $\widehat{\boldsymbol{A}}_i := (\widehat{\boldsymbol{p}}_1, \ldots, \widehat{\boldsymbol{p}}_i)$. Then:*

(i) The faces of $\operatorname{conv}(\widehat{\boldsymbol{A}}_n)$ that are hidden from $\widehat{\boldsymbol{q}}$ are exactly the liftings of faces of the placing triangulation of $\boldsymbol{A}_n$.

(ii) The faces of $\operatorname{conv}(\widehat{\boldsymbol{A}}_n)$ that are visible from $\widehat{\boldsymbol{q}}$ are exactly the liftings of faces of the pulling triangulation of $\boldsymbol{A}_n$.

(iii) For $i \in [n-1]$, the faces of $\operatorname{conv}(\widehat{\boldsymbol{A}}_i)$ that are hidden, resp. visible, from $\widehat{\boldsymbol{p}}_{i+1}$ coincide with the faces that are hidden, resp. visible, from $\widehat{\boldsymbol{q}}$.

(iv) The faces of $\operatorname{conv}(\widehat{\boldsymbol{A}})$ are exactly the faces of $\operatorname{conv}(\widehat{\boldsymbol{A}}_n)$ that are hidden from $\widehat{\boldsymbol{q}}$, which are the liftings of faces of the placing triangulation of $\boldsymbol{A}_n$, and all $\operatorname{conv}(\{\widehat{\boldsymbol{p}}_i \mid i \in \boldsymbol{F}\} \cup \{\widehat{\boldsymbol{q}}\})$ where $\boldsymbol{F}$ gives a face of $\operatorname{conv}(\boldsymbol{A}_n)$.

Proof. Items (i) and (ii) are reformulations of [DRS10, Lemma 4.3.4] and [DRS10, Lemma 4.3.6], which correspond to the case where the point $\widehat{\boldsymbol{q}}$ is "at infinity". In that case, the faces of $\operatorname{conv}(\widehat{\boldsymbol{A}}_n)$ hidden from $\widehat{\boldsymbol{q}}$ correspond to the lower faces of $\operatorname{conv}(\widehat{\boldsymbol{A}}_n)$, thus to faces of the corresponding induced regular subdivision of $\boldsymbol{A}_n$. The faces of $\operatorname{conv}(\boldsymbol{A}_n)$ visible from $\widehat{\boldsymbol{q}}$ correspond to the lower faces of the lifting of $\boldsymbol{A}_n$ induced by the opposite (negative) heights. Then, in both [DRS10, Lemma 4.3.4] and [DRS10, Lemma 4.3.6] where we take the opposite heights, the condition on the constant c_0 and the heights amounts to asking that the lifting is a positive lexicographic lifting.

Item (iii) follows from the definitions and the fact that a face of a polytope $\boldsymbol{P}$ is hidden, resp. visible, from a point $\boldsymbol{p}$ if and only if it is contained in a facet of $\boldsymbol{P}$ that is hidden, resp. visible from $\boldsymbol{p}$.

For (iv), notice that the faces of $\operatorname{conv}(\widehat{\boldsymbol{A}})$ that do not contain $\widehat{\boldsymbol{q}}$ are exactly the faces of $\operatorname{conv}(\widehat{\boldsymbol{A}}_n)$ hidden from $\widehat{\boldsymbol{q}}$. The same argument as before shows that they form the placing triangulation of $\widehat{\boldsymbol{A}}_n$. If $\boldsymbol{F} \subseteq [n]$ is such that $\boldsymbol{F} \cup \{\widehat{\boldsymbol{q}}\}$ gives a face of $\widehat{\boldsymbol{A}}$, let $\boldsymbol{H}$ be a supporting hyperplane of this face. Then the intersection of $\boldsymbol{H}$ with the hyperplane $x_{d+1} = 0$ is a supporting hyperplane of the face given by $\boldsymbol{F}$ for $\operatorname{conv}(\boldsymbol{A}_n)$ in $\mathbb{R}^d \times \{0\}$. □

Corollary 2.4.6. *Let $\boldsymbol{A} = (\boldsymbol{p}_1, \dots, \boldsymbol{p}_n) \subset \mathbb{R}^d$ be a point configuration in convex position. Let $\widehat{\boldsymbol{A}} = (\widehat{\boldsymbol{p}}_1, \dots, \widehat{\boldsymbol{p}}_n, \widehat{\boldsymbol{p}}_{n+1})$ be a positive lexicographic lifting of $\boldsymbol{A}$ and let $\widehat{\widehat{\boldsymbol{A}}} = (\widehat{\widehat{\boldsymbol{p}}}_1, \dots, \widehat{\widehat{\boldsymbol{p}}}_n, \widehat{\widehat{\boldsymbol{p}}}_{n+1}, \widehat{\widehat{\boldsymbol{p}}}_{n+2})$ be a positive lexicographic lifting of $\widehat{\boldsymbol{A}}$, with respect to the same order. Then the combinatorial type of $\operatorname{conv}(\widehat{\widehat{\boldsymbol{A}}})$ is completely determined by (the oriented matroid of) the point configuration $\boldsymbol{A}$.*

Proof. According to Lemma 2.4.5 (iv), the faces of $\operatorname{conv}(\widehat{\widehat{\boldsymbol{A}}})$ are the liftings of faces of the placing triangulation of $\widehat{\boldsymbol{A}}_{n+1}$ and all $\operatorname{conv}(\{\widehat{\widehat{\boldsymbol{p}}}_i \mid i \in \boldsymbol{F}\} \cup \{\widehat{\widehat{\boldsymbol{p}}}_{n+2}\})$ where $\boldsymbol{F}$ gives a face of $\operatorname{conv}(\widehat{\boldsymbol{A}}_{n+1})$. The definition of the placing triangulation and Lemma 2.4.5 (i), (ii), (iii) imply that the placing triangulation of $\widehat{\boldsymbol{A}}_{n+1}$ (and thus also the faces of $\operatorname{conv}(\widehat{\boldsymbol{A}}_{n+1})$) is determined by the placing and pulling triangulations of the P_i. □

If one starts with a 0-dimensional point configuration (that is a point repeated multiple times), and then perfoms a sequence of positive lexicographic liftings always with respect to the same order, then one obtains a cyclic polytope. If the order is altered at each step, then many combinatorial types of polytopes are obtained, but not necessarily neighborly. Moreover, different lifting orders might give rise to equivalent polytopes. However, if one restricts to changing the order of the lifting only every two dimensions, then neighborliness is preserved and the combinatorial type can be controlled. This is used in [Pad13] to construct many neighborly polytopes. The original presentation in [Pad13] is in terms of lexicographic extensions of the Gale dual, but we refer to the following primal version for liftings taken from [GP16]. We repeat the main ideas of that proof for the reader's convenience.

Theorem 2.4.7 ([GP16, Theorem 5.5(i)])**.** *Let $\boldsymbol{A} = (\boldsymbol{p}_1, \dots, \boldsymbol{p}_n) \subset \mathbb{R}^d$ be a k-neighborly point configuration in general position. Let $\widehat{\boldsymbol{A}} = (\widehat{\boldsymbol{p}}_1, \dots, \widehat{\boldsymbol{p}}_n, \widehat{\boldsymbol{p}}_{n+1})$ be a positive lexico-*

graphic lifting of $\boldsymbol{A}$ and let $\widehat{\widehat{\boldsymbol{A}}} = (\widehat{\widehat{\boldsymbol{p}}}_1, \dots, \widehat{\widehat{\boldsymbol{p}}}_n, \widehat{\widehat{\boldsymbol{p}}}_{n+1}, \widehat{\widehat{\boldsymbol{p}}}_{n+2})$ be a positive lexicographic lifting of $\widehat{\boldsymbol{A}}$, with respect to the same order. Then $\widehat{\widehat{\boldsymbol{A}}}$ is $(k+1)$-neighborly.

Proof. Let S be a subset of $[n]$ of size k or $k-1$. Then $\{\boldsymbol{p}_i \mid i \in S\}$ is the vertex set of a face of $\operatorname{conv}(\boldsymbol{A})$. Hence, it follows from Lemma 2.4.5 (iv) that $\{\widehat{\boldsymbol{p}}_i \mid i \in S\} \cup \{\widehat{\boldsymbol{p}}_{n+1}\}$ is the vertex set of a face of $\operatorname{conv}(\widehat{\boldsymbol{A}})$. The same reasoning shows that any subset of $\widehat{\widehat{\boldsymbol{A}}}$ of size $k+1$ that contains $\widehat{\widehat{\boldsymbol{p}}}_{n+2}$ or $\widehat{\widehat{\boldsymbol{p}}}_{n+1}$ is the vertex set of a face of $\widehat{\widehat{\boldsymbol{A}}}$.

For the remaining cases, let S be a subset of $[n]$ of size $k+1$. We want to show that $\{\widehat{\widehat{\boldsymbol{p}}}_i \mid i \in S\}$ is the vertex set of a face of $\operatorname{conv}(\widehat{\widehat{\boldsymbol{A}}})$. Let $m \le n$ be the largest element of S. Denote $\boldsymbol{A}_m = (\boldsymbol{p}_1, \dots, \boldsymbol{p}_m)$ and $\widehat{\boldsymbol{A}}_m = (\widehat{\boldsymbol{p}}_1, \dots, \widehat{\boldsymbol{p}}_m)$. We have that $S \setminus \{m\}$ gives a face of $\operatorname{conv}(\boldsymbol{A}_{m-1})$ by neighborliness, thus $S \setminus \{m\}$ gives a face of the pulling triangulation of $\boldsymbol{A}_{m-1}$, thus $S \setminus \{m\}$ gives a face of $\widehat{\boldsymbol{A}}_{m-1}$ visible from $\widehat{\boldsymbol{p}}_m$ by Lemma 2.4.5 (ii), thus S gives a face of the placing triangulation of $\widehat{\boldsymbol{A}}_m$, and thus S gives a face of the placing triangulation of $\widehat{\boldsymbol{A}}$. It follows from Lemma 2.4.5 (iv) that S gives a face of $\widehat{\widehat{\boldsymbol{A}}}$. □

The following lemma allows us to prove that the combinatorial type can be controlled without explicitly using the rigidity of neighborly oriented matroids of odd rank as it was originally done in [Pad13, Proposition 6.7].

Lemma 2.4.8. *Let $\boldsymbol{A} = (\boldsymbol{p}_1, \dots, \boldsymbol{p}_n)$ be an r-neighborly point configuration in even dimension $d = 2r$ such that $n > d+2$. Let $\widehat{\boldsymbol{A}} = (\widehat{\boldsymbol{p}}_1, \dots, \widehat{\boldsymbol{p}}_n, \widehat{\boldsymbol{p}}_{n+1})$ be a lexicographic lifting of $\boldsymbol{A}$ and let $\widehat{\widehat{\boldsymbol{A}}} = (\widehat{\widehat{\boldsymbol{p}}}_1, \dots, \widehat{\widehat{\boldsymbol{p}}}_n, \widehat{\widehat{\boldsymbol{p}}}_{n+1}, \widehat{\widehat{\boldsymbol{p}}}_{n+2})$ be a positive lexicographic lifting of $\widehat{\boldsymbol{A}}$, with respect to the same order. Then n is the only index $k \in [n]$ such that the double contraction $\widehat{\widehat{\boldsymbol{A}}}/\{\widehat{\widehat{\boldsymbol{p}}}_{n+1}, \widehat{\widehat{\boldsymbol{p}}}_k\}$ is r-neighborly.*

Proof. For $r \ge 1$, we know that $\widehat{\widehat{\boldsymbol{A}}}$ is 2-neighborly, so all pairs $\{n+1, k\}$ for $k \in [n]$ give edges of $\widehat{\widehat{\boldsymbol{A}}}$, and all points of the configuration $\widehat{\widehat{\boldsymbol{A}}}/\{\widehat{\widehat{\boldsymbol{p}}}_{n+1}\}$ are vertices. This justifies that the double contraction $\widehat{\widehat{\boldsymbol{A}}}/\{\widehat{\widehat{\boldsymbol{p}}}_{n+1}, \widehat{\widehat{\boldsymbol{p}}}_k\}$ is well-defined. If $d = r = 0$, $\widehat{\widehat{\boldsymbol{A}}}/\{\widehat{\widehat{\boldsymbol{p}}}_{n+1}\}$ is a 1-dimensional configuration of points ordered linearly $n, n-1, \dots, 2, 1, n+2$. Thus, the double contraction is well-defind only for $k = n+2$ and $k = n$ and we already have the result of the lemma.

Note that $\boldsymbol{A}$ is a realization of $\widehat{\widehat{\boldsymbol{A}}}/\{\widehat{\widehat{\boldsymbol{p}}}_{n+2}, \widehat{\widehat{\boldsymbol{p}}}_{n+1}\}$. It follows from the definition of contraction that a set $S \subseteq [n] \setminus \{k\}$ gives a face of $\operatorname{conv}(\widehat{\widehat{\boldsymbol{A}}}/\{\widehat{\widehat{\boldsymbol{p}}}_{n+1}, \widehat{\widehat{\boldsymbol{p}}}_k\})$ if and only if $S \cup \{n+1, k\}$ gives a face of $\operatorname{conv}(\widehat{\widehat{\boldsymbol{A}}})$.

We denote $\widehat{\boldsymbol{A}}_i := (\widehat{\boldsymbol{p}}_1, \dots, \widehat{\boldsymbol{p}}_i)$ for $i \in [n]$.

We first show that $\widehat{\widehat{\boldsymbol{A}}}/\{\widehat{\widehat{\boldsymbol{p}}}_{n+1}, \widehat{\widehat{\boldsymbol{p}}}_n\}$ is r-neighborly. Let $S \subseteq [n+2] \setminus \{n+1, n\}$ be a subset of cardinality r. If S contains $n+2$, we define $S' := S \cup \{n\} \setminus \{n+2\}$. S' is a subset of $[n]$ of cardinality r, hence it defines a face of $\operatorname{conv}(\boldsymbol{A})$ and $S \cup \{n+1, n\} = S' \cup \{n+1, n+2\}$ indeed defines a face of $\operatorname{conv}(\widehat{\widehat{\boldsymbol{A}}})$. If S does not contain $n+2$, then it is a subset of $[n]$ of cardinality r and hence it gives a face of $\operatorname{conv}(\boldsymbol{A})$. Thus, $S \cup \{n\}$ gives a face of the pulling triangulation of $\boldsymbol{A}$, and by Lemma 2.4.5(ii) a face of $\operatorname{conv}(\widehat{\boldsymbol{A}}_n)$ that is visible from $\widehat{\boldsymbol{p}}_{n+1}$. Therefore, $S \cup \{n, n+1\}$ gives a face of the placing triangulation of $\operatorname{conv}(\widehat{\boldsymbol{A}})$, thus a face of $\operatorname{conv}(\widehat{\widehat{\boldsymbol{A}}})$.

Now, let k be an element of $[n-1]$. To show that $\widehat{\widehat{\boldsymbol{A}}}/\{\widehat{\widehat{\boldsymbol{p}}}_{n+1}, \widehat{\widehat{\boldsymbol{p}}}_k\}$ is not r-neighborly, we will exhibit a subset $S \subseteq [n] \setminus \{n+1, k\}$ of cardinality r such that $S \cup \{n+1, k\}$ does not give a face of $\operatorname{conv}(\widehat{\widehat{\boldsymbol{A}}})$. Since $n > d+2$, we can find a subset W of $[n]$ of cardinality $d+2 = 2(r+1)$ that contains k but not n. Radon's theorem implies that there is a partition of W into two subsets W_1 and W_2 such that $\operatorname{conv}(\{\boldsymbol{p}_i \mid i \in W_1\}) \cap \operatorname{conv}(\{\boldsymbol{p}_j \mid j \in W_2\}) \neq \emptyset$. In particular, W_1 and W_2 do not give faces of $\operatorname{conv}(\boldsymbol{A})$. Since $\boldsymbol{A}$ is r-neighborly, W_1 and W_2 necessarily have at least $r+1$ elements, so they are both exactly of cardinality $r+1$. (This is where the assumption of even dimension is used). We define T to be the W_i that contains k, and $S := T \setminus \{k\}$. Since T does not give a face of $\operatorname{conv}(\boldsymbol{A})$ and does not contain n, it does not give a face of $\widehat{\boldsymbol{A}}_n$ that is visible from $\widehat{\boldsymbol{p}}_{n+1}$. Hence, $T \cup \{n+1\} = S \cup \{n+1, k\}$ does not give a face of the placing triangulation of $\widehat{\boldsymbol{A}}$. However, all faces of $\widehat{\widehat{\boldsymbol{A}}}$ not containing $n+2$ must be faces of the placing triangulation of $\widehat{\boldsymbol{A}}$ by Lemma 2.4.5(iv). Thus, $S \cup \{n+1, k\}$ does not give a face of $\widehat{\widehat{\boldsymbol{A}}}$. □

Corollary 2.4.9 ([Pad13, Proposition 6.1] and [GP16, Lemma 6.1])**.** *Let $\boldsymbol{A} = (\boldsymbol{p}_1, \dots, \boldsymbol{p}_n)$ be an r-neighborly point configuration in even dimension $d = 2r$. Then there are at least $\frac{n!}{(d+2)!}$ distinct labeled combinatorial types of $(d+2)$-polytopes with $n+2$ vertices obtained by the following construction:*

- *Choose a permutation σ of n.*
- *Define the point configuration $\boldsymbol{A}^\sigma = (\boldsymbol{p}_{\sigma(1)}, \dots, \boldsymbol{p}_{\sigma(n)})$.*
- *Let $\widehat{\boldsymbol{A}}^\sigma$ be a positive lexicographic lifting of $\boldsymbol{A}^\sigma$ and let $\widehat{\widehat{\boldsymbol{A}}}^\sigma = (\widehat{\widehat{\boldsymbol{p}}}_{\sigma(1)}, \dots, \widehat{\widehat{\boldsymbol{p}}}_{\sigma(n)}, \widehat{\widehat{\boldsymbol{p}}}_{n+1}, \widehat{\widehat{\boldsymbol{p}}}_{n+2})$ be a positive lexicographic lifting of $\widehat{\boldsymbol{A}}^\sigma$.*
- *Define $\widehat{\widehat{\boldsymbol{A}}} = (\widehat{\widehat{\boldsymbol{p}}}_1, \dots, \widehat{\widehat{\boldsymbol{p}}}_n, \widehat{\widehat{\boldsymbol{p}}}_{n+1}, \widehat{\widehat{\boldsymbol{p}}}_{n+2})$.*
- *Take the convex hull $\operatorname{conv}(\widehat{\widehat{\boldsymbol{A}}})$.*

Remark 2.4.10. In fact, [GP16, Lemma 6.1] gives a bound improved by a factor $n+1$, but this does not change the asymptotics of the bound on the total number of polytopes.

Proof. Let $\widehat{\widehat{\boldsymbol{A}}} = (\widehat{\widehat{\boldsymbol{p}}}_1, \dots, \widehat{\widehat{\boldsymbol{p}}}_n, \widehat{\widehat{\boldsymbol{p}}}_{n+1}, \widehat{\widehat{\boldsymbol{p}}}_{n+2})$ be a point configuration in $\mathbb{R}^{d+2}$ obtained as in the statement, with a permutation σ that we do not know. We will show that we can recover $\sigma(n), \sigma(n-1), \dots, \sigma(d+3)$ from $\boldsymbol{A}$ and the face lattice of $\operatorname{conv}(\widehat{\widehat{\boldsymbol{A}}})$. This implies that distinct choices for $\sigma(n), \sigma(n-1), \dots, \sigma(d+3)$ give distinct labeled combinatorial types $\operatorname{conv}(\widehat{\widehat{\boldsymbol{A}}})$, and there are $\frac{n!}{(d+2)!}$ such choices.

We will consecutively recover the values of $\sigma(m)$ starting from $m = n$ until $m = d+3$. Suppose that we have already recovered $\sigma(n), \sigma(n-1), \dots, \sigma(m+1)$ for some $d+3 \leq m \leq n$.

We consider the point configuration $\widehat{\widehat{\boldsymbol{A}}}_m := \widehat{\widehat{\boldsymbol{A}}} \setminus \{\widehat{\widehat{\boldsymbol{p}}}_{\sigma(n)}, \dots, \widehat{\widehat{\boldsymbol{p}}}_{\sigma(m+1)}\}$ (where we abuse notation for the labels but the only important thing is to record the last two points). It follows from Corollary 2.4.6 that its combinatorial type is well defined, because it is obtained as the relabeling of the double lifting of the point configuration $(\boldsymbol{p}_{\sigma(1)}, \dots, \boldsymbol{p}_{\sigma(m)})$ (with the two additional points $\widehat{\widehat{\boldsymbol{p}}}_{n+1}$ and $\widehat{\widehat{\boldsymbol{p}}}_{n+2}$). Moreover, since the point configuration $(\boldsymbol{p}_{\sigma(1)}, \dots, \boldsymbol{p}_{\sigma(m)})$ is r-neighborly, it follows from Lemma 2.4.8 that we can recover $\sigma(m)$ as the only index $k \in [m]$ such that $\widehat{\widehat{\boldsymbol{A}}}_m / \{\widehat{\widehat{\boldsymbol{p}}}_{n+1}, \widehat{\widehat{\boldsymbol{p}}}_k\}$ is r-neighborly. □

2.4.2 Construction of many polytopes

We will use the following slight variation of the construction used in [Pad13] to give a lower bound for the number of polytopes.

Theorem 2.4.11 ([Pad13, Theorem 6.8])**.** *The number of labeled combinatorial types of neighborly d-polytopes with $n > d$ vertices obtained from a 0-dimensional point configuration by a sequence of positive lexicographic liftings (with orders that might change along each step of the sequence) is at least*

$$(n!)^{\lfloor \frac{d}{2} \rfloor \pm o(1)}.$$

Proof. We build iteratively sets $\mathcal{P}_{2k}$ that contain realizations of distinct labeled combinatorial types of neighborly polytopes of dimension $2k$ with $n-d+2k$ vertices.

We define $\mathcal{P}_0$ to be the singleton with the degenerate configuration of $n-d$ labeled points in the 0- dimensional space.

Suppose that we have constructed $\mathcal{P}_{2k}$ for some $0 \le k < \lfloor \frac{d}{2} \rfloor$. Let $\mathcal{P}_{2k+2}$ be the union over all configurations $\boldsymbol{A} \in \mathcal{P}_{2k}$ of the distinct labeled point configurations obtained from $\boldsymbol{A}$ by relabelings and two positive lexicographic liftings in the same order, as in Corollary 2.4.9. This union is disjoint because if $\widehat{\widehat{\boldsymbol{A}}}$ is a double lifting of $\boldsymbol{A}$, we can recover the combinatorial type of $\boldsymbol{A}$ by taking $\widehat{\widehat{\boldsymbol{A}}} / \{\widehat{\widehat{\boldsymbol{p}}}_{n-d+2k+2}, \widehat{\widehat{\boldsymbol{p}}}_{n-d+2k+1}\}$. Hence, Corollary 2.4.9 gives that $|\mathcal{P}_{2k+2}| \ge |\mathcal{P}_{2k}| \times \frac{(n-d+2k)!}{(2k+2)!}$. Theorem 2.4.7 ensures that the point configurations in $\mathcal{P}_{2k+2}$ are neighborly.

For $k = \lfloor \frac{d}{2} \rfloor$ we obtain that:

$$\begin{aligned}
|\mathcal{P}_{2\lfloor \frac{d}{2} \rfloor}| &\ge \prod_{k=0}^{\lfloor \frac{d}{2} \rfloor - 1} \frac{(n-d+2k)!}{(2k+2)!} \\
&\ge \frac{((n-d)!)^{\lfloor \frac{d}{2} \rfloor}}{\prod_{k=1}^{\lfloor \frac{d}{2} \rfloor} (2k)!} \\
&= (n!)^{\lfloor \frac{d}{2} \rfloor + o(1)}.
\end{aligned}$$

If d is odd, instead of taking a pyramid as in [Pad13, Corollary 6.10], we do one last positive lexicographic lifting on all the elements of $\mathcal{P}_{2\lfloor \frac{d}{2} \rfloor}$ to obtain $(n!)^{\lfloor \frac{d}{2} \rfloor + o(1)}$ realizations of distinct labeled combinatorial types of d-polytopes with n vertices. This variant still conserves the number of distinct combinatorial types since we recover the polytopes in $\mathcal{P}_{2\lfloor \frac{d}{2} \rfloor}$ by taking the contractions of the last labeled point. $\square$

The combination of these constructions allows us to prove Theorem 2.1.1: The number of different labeled combinatorial types of d-polytopes with n vertices for fixed $d > 3$ and n growing to infinity is at least $(n!)^{d-2\pm o(1)}$.

Proof of Theorem 2.1.1. We start by applying Theorem 2.4.11 in dimension $d-1$. The last step of the construction of the many $(d-1)$-polytopes in that theorem is a positive lexicographic lifting $\widehat{\boldsymbol{A}} = (\widehat{\boldsymbol{p}}_1, \dots, \widehat{\boldsymbol{p}}_{n-1}, \widehat{\boldsymbol{q}})$ from a $\lfloor \frac{d-2}{2} \rfloor$-neighborly $(d-2)$-polytope $\boldsymbol{A}$.

Lemma 2.3.1 ensures that we can do this lifting step by step so that for every i from d to $n-1$, $\widehat{\boldsymbol{p}}_i$ and $\widehat{\boldsymbol{q}}$ are triangulation-inseparable in $(\widehat{\boldsymbol{p}}_1, \dots, \widehat{\boldsymbol{p}}_i, \widehat{\boldsymbol{q}})$. Indeed, the value of ε_i in Remark 2.4.3 can be taken arbitrarily small. While very general position is not guaranteed by the construction, note that these configurations are in general position, and hence we can do a small perturbation into very general position if needed without changing the combinatorial type.

Moreover, note that by construction $\boldsymbol{A}$ is the contraction $\widehat{\boldsymbol{A}}/\widehat{\boldsymbol{q}}$, and that similarly $(\boldsymbol{p}_1, \dots, \boldsymbol{p}_i) = (\widehat{\boldsymbol{p}}_1, \dots, \widehat{\boldsymbol{p}}_i, \widehat{\boldsymbol{q}})/\widehat{\boldsymbol{q}}$. These contractions are thus $\lfloor \frac{d-2}{2} \rfloor$-neighborly.

Hence Theorem 2.3.6 applies: each of these polytopes has at least $(n!)^{\lfloor \frac{d-2}{2} \rfloor n \pm o(1)}$ regular triangulations. Then Lemma 2.4.1 gives us a lower bound of $(n!)^{d-2\pm o(1)}$ labeled simplicial types of d-polytopes with n vertices. $\square$

Remark 2.4.12. It follows from the construction that all these many d-polytopes are $\lfloor \frac{d-1}{2} \rfloor$-neighborly, because they come from regular triangulations of Padrol's neighborly $(d-1)$-polytopes.

Hence, for odd d our polytopes are neighborly, since in this case $\lfloor \frac{d}{2} \rfloor = \lfloor \frac{d-1}{2} \rfloor$.

On the other hand, if d is even then the following lemma shows that we do not improve Padrol's bound on the number of neighborly polytopes, because each of the Padrol polytopes that we use has at most one neighborly triangulation.

Lemma 2.4.13. *A polytope in odd dimension $2k+1$ has at most one triangulation that is $(k+1)$-neighborly.*

Proof. This is a direct consequence of the observation after [Dey93, Lemma 3.1], see also [DRS10, Lemma 8.4.1]: a triangulation of a d-polytope is completely determined by its $\lfloor \frac{d}{2} \rfloor$-skeleton. For a triangulation of a $(2k+1)$-polytope, being $(k+1)$-neighborly exactly means that its k-skeleton is complete. $\square$

Chapter 3

Sweep polytopes and sweep oriented matroids

This chapter is based on the article *Sweeps, polytopes, oriented matroids, and allowable graphs of permutations* [PP23], written with my advisor Arnau Padrol.

A sweep of a point configuration is any ordered partition induced by a linear functional. Posets of sweeps of planar point configurations were formalized and abstracted by Goodman and Pollack under the theory of allowable sequences of permutations. We introduce two generalizations that model posets of sweeps of higher dimensional configurations.

Sweeps of a point configuration are in bijection with faces of an associated sweep polytope. Mimicking the fact that sweep polytopes are projections of permutahedra, we define sweep oriented matroids as strong maps of the braid oriented matroid. Allowable sequences are then the sweep oriented matroids of rank 2, and many of their properties extend to higher rank. We show strong ties between sweep oriented matroids and Dilworth truncations from (unoriented) matroid theory. Pseudo-sweeps are a generalization of sweeps in which the sweeping hyperplane is allowed to slightly change direction, and that can be extended to arbitrary oriented matroids in terms of cellular strings. We prove that for sweepable oriented matroids, sweep oriented matroids provide a sphere that is a deformation retract of the poset of pseudo-sweeps. This generalizes a property of sweep polytopes (which can be interpreted as monotone path polytopes of zonotopes), and solves a special case of the strong Generalized Baues Problem for cellular strings.

A second generalization are allowable graphs of permutations: symmetric sets of permutations pairwise connected by allowable sequences. They have the structure of acycloids and include sweep oriented matroids.

3.1 Introduction

It is very natural to order a point configuration by the values of a linear functional, and it is not surprising that applications abound in discrete and combinatorial geometry. For example, this is the core of sweep algorithms, a central paradigm in computational geometry (see [dBCvKO08, Section 2.1]). The simplex methods for linear programming visit vertices of a convex polytope in such a linear order (see for example [MG06]). Moreover, these orderings are precisely those inducing the Bruggesser-Mani line shellings in the polar polytope [BM71] (see [Zie95, Lec. 8]).

The set of all linear orderings of a planar point configuration was already studied by Perrin in 1882 [Per82]. This was a precursor to the theory of *allowable sequences*, introduced and developed by Goodman and Pollack [GP80a, GP80b, GP82, GP84, GP93]. The idea is the following. Given a configuration $\boldsymbol{A}$ of n points in the plane, for each generic vector $\boldsymbol{u} \in \mathbb{R}^2$, we sweep the plane with a line orthogonal to $\boldsymbol{u}$. The order in which the points are hit by the line gives rise to a permutation $\sigma \in \mathfrak{S}_n$ (see Figure 3.1). As $\boldsymbol{u}$ rotates 180° clockwise, we obtain a sequence of permutations in which:

(i) the move from a permutation to the next one consists of reversing one or more disjoint substrings;

(ii) each pair i, j with $1 \leq i < j \leq n$ is reversed in exactly one move along the sequence.

An *allowable sequence* is a sequence of permutations from the identity to its reverse ($\sigma, \overline{\sigma} \in \mathfrak{S}_n$ are *reverse* if $\sigma(t) = \overline{\sigma}(n - t + 1)$ for all t) fulfilling these two conditions. Contrary to Perrin's claim, Goodman and Pollack showed that there are unrealizable allowable sequences [GP80a, Fig. 3 and Thm. 3.1], that is, that do not arise from a point configuration with this construction (c.f. Figure 3.10).

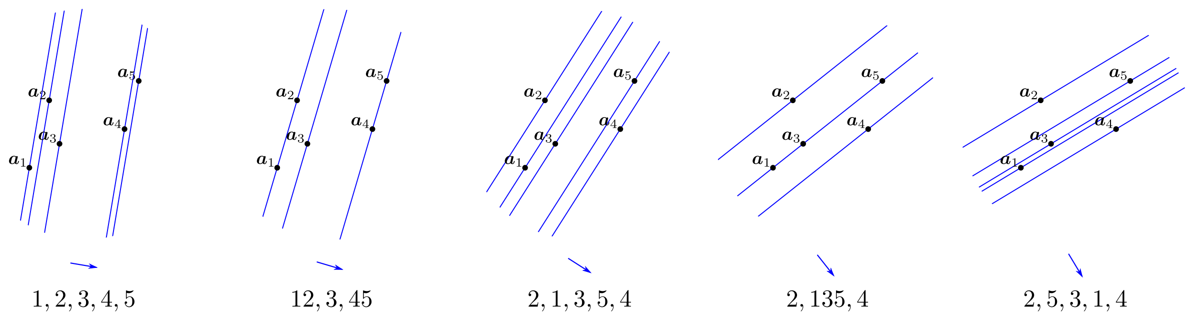

Figure 3.1: A segment of an allowable sequence. The sweeps between two consecutive permutations in the sequence correspond to ordered partitions.

Allowable sequences are hence purely combinatorial objects abstracting geometric properties of planar point configurations. They are closely related to pseudoline arrangements and oriented matroids (see [BLS+99, Sects. 1.10 & 6.4]), although their combinatorial structure is in some senses easier to grasp and manipulate. In particular, in the *simple* case (where consecutive permutations differ by a transposition), allowable sequences are in correspondence with reduced decompositions of the reverse of the identity and maximal chains in the weak order of $\mathfrak{S}_n$, see [BLS+99, Sec. 6.4], as well as with (minimal primitive) sorting networks [Knu98, Sec. 5.3.4]. This has allowed for their complete enumeration [Sta84, EG87], as well as the study of uniform random instances [AHRV07, ADHV19, Dau19].

They turned out to be a very effective tool to study problems of geometric combinatorics in the plane, used for example to prove Ungar's theorem (a configuration of $2n$ points not all on a same line determines at least $2n$ slopes) [Ung82], to decide the stretchability of arrangements of at most eight pseudolines [GP80b], or to estimate the number of k-sets and $(\leq k)$-sets [AG86, LVWW04, Wel86]. See [GP93, Ch. V] and [Fel04, Ch. 6] for some of their applications.

The construction detailed above extends naturally to any higher dimensional point configuration $\boldsymbol{A} \in \mathbb{R}^{d\times[n]}$. Every vector $\boldsymbol{u} \in \mathbb{R}^d$ defines a *sweep*, which is the ordered partition of $[n]$ in which the points of $\boldsymbol{A}$ are met when sweeping with a hyperplane in direction $\boldsymbol{u}$. Goodman and Pollack already observed that sweeps induce a complex on the unit sphere $\mathbb{S}^{d-1}$, *"which has not yet been fully investigated"* ([GP93, after Def. 2.3]). This was further explored by Edelman [Ede00] and Stanley [Sta15] who, in particular, presented a tight upper bound for the number of sweeping orders of a d-dimensional configuration of n points.

Ordered by refinement, the *poset of sweeps* $\overline{\Pi}(\boldsymbol{A})$ is isomorphic to the face poset of a polyhedral fan generated by a hyperplane arrangement $\boldsymbol{\mathcal{SH}}(\boldsymbol{A})$, called the *valid order arrangement* by Stanley in a polar formulation [Sta15]. As we discuss in Section 3.2.3, this is the normal fan of a zonotope: the *sweep polytope* $\boldsymbol{SP}(\boldsymbol{A})$ (mentionned under the name of *shellotope* by Gritzmann and Sturmfels in [GS93]).

Posets of sweeps of point configurations are the high-dimensional analogue of realizable allowable sequences. However, there is no purely combinatorial description of these objects. Indeed, Hoffmann and Merckx recently adapted the classical Universality Theorem for oriented matroids by Mnëv [Mnë88] to give a Universality Theorem for allowable sequences [HM18]. This shows that already in the plane the problem of deciding whether an allowable sequence arises from a point configuration is very hard (equivalent to the "existential theory of the reals", and in particular NP-hard).

Our main goal is to give a purely combinatorial high-dimensional generalization of allowable sequences that abstracts and encompasses the posets of sweeps of point configurations. We present two strongly related approaches with two levels of generality (*sweep oriented matroids* and *sweep acycloids*). As we will see, the objects that we introduce fill a gap connecting several topics studied by different communities, providing a new and unified point of view. We also hope that, beside their intrinsic interest, having a purely combinatorial framework without the rigid constraints of realizability will open the door to new approaches to problems on discrete and combinatorial geometry, as happened in the two-dimensional case.

Our starting point are sweep polytopes. We report alternative constructions that highlight different points of view. On the one hand, sweep polytopes are affine projections of permutahedra. Up to translation, every affine projection of a permutahedron is a sweep polytope, which gives a natural combinatorial interpretation of permutahedral shadows. Moreover, sweep polytopes can be realized as fiber polytopes, and in particular as monotone path polytopes of zonotopes [Ede00, Sec. 5]. These are polytopes whose vertices encode the parametric simplex paths induced by a linear functional [BS92, BKS94b]. Conversely, every monotone path polytope of a zonotope is a sweep polytope (under mild technical conditions, see Proposition 3.2.10). This interpretation of sweep polytopes appears in the study of pivot rules in linear programming [BDLLS22].

Moreover, this construction naturally reveals a decomposition of sweep polytopes as Minkowski sums of *k-set polytopes* [AW03, EVW97] (see Remark 3.2.9). After the appearance of the first version of this work, most of these constructions have been generalized to *lineup polytopes*, which encode prefixes of sweeps and are relevant for the 1-body N-representability problem in quantum physics, see [CLL⁺23] and references therein.

Inspired by the characterization of sweep polytopes as permutahedral shadows, in Section 3.3 we define *sweep oriented matroids* as strong maps of the oriented matroid of the braid arrangement. The strong link between allowable sequences, oriented matroids of rank 3, and arrangements of pseudolines is well documented in [BLS⁺99, Sects. 1.10 & 6.4] and explained in terms of *big* and *little oriented matroids*. These concepts extend to high dimensions too: each sweep oriented matroid of rank r determines a little and a big oriented matroid of rank $r + 1$ (Theorem 3.4.1 and Lemma 3.4.4). For sweep oriented matroids of rank 2, which are equivalent to allowable sequences, we recover the original definitions. In particular, in the realizable case, the little oriented matroid is the standard oriented matroid associated to the point configuration.

We show that, up to isomorphism, big oriented matroids are characterized by having a *tight modular hyperplane* (Theorem 3.4.9). Modular flats of matroids were introduced by Stanley [Sta71] and play a structural role for matroid constructions [Bry75]. We call a modular hyperplane *tight* if it is no longer modular after the deletion of one of its elements. The operation that determines the big oriented matroid from its sweep oriented matroid extends to all oriented matroids equipped with certain decorations (Corollary 3.4.10), and can be seen as an oriented matroid version of [Bon06, Thm. 2.1].

We extend the bounds from [Ede00] and [Sta15] to the non-realizable case (Theorem 3.5.6). For this, we show in Section 3.5 that, at the level of the underlying unoriented matroids, the lattice of flats of a sweep oriented matroid is (a weak map of) the first Dilworth truncation of the lattice of flats of the little oriented matroid (Theorem 3.5.2). When one removes all the atoms from a geometric lattice, the resulting poset is no longer a geometric lattice. The first Dilworth truncation is a lattice obtained by adding the necessary joins in the most generic way to obtain a geometric lattice [Bry86, Dil44]. We can therefore view sufficiently generic sweep oriented matroids as an oriented version of the first Dilworth truncation of the associated little oriented matroid. Unfortunately, in contrast to rank 3, not every (little) oriented matroid can be extended to a big oriented matroid (Theorem 3.4.13). The question of characterizing oriented matroids admitting such an extension is open.

In Section 3.6, we discuss *pseudo-sweeps*, which correspond to sweeps in which the sweeping hyperplane is allowed to change direction (in a controlled monotonous way). Whereas sweeps of a point configuration correspond to the parametric (coherent) monotone paths on an associated zonotope, pseudo-sweeps take into account all monotone paths. They admit a polar formulation in terms of galleries and cellular strings of pseudo-hyperplane arrangements, which extends to oriented matroids [Bjö92]. This way, for every (little) oriented matroid, even those that cannot be extended to a big oriented matroid, one can define a poset of pseudo-sweeps. In general, an oriented matroid $\mathcal{M}$ can be the little oriented matroid of several sweep oriented matroids; each with a different associated poset of sweeps. They are all subposets of the poset of pseudo-sweeps of $\mathcal{M}$. A classification of the cases when all pseudo-sweeps are actual sweeps is given in [EJLM21].

There is a lot of literature concerning the graphs of pseudo-sweep permutations of oriented matroids. Cordovil and Moreira had shown that they are connected [CM93], extending to oriented matroids results that went back to Tits [Tit69] (for reflection arrangements), Deligne [Del72] (for simplicial arrangements), and Salvetti [Sal87] (for realizable oriented matroids). More results concerning graphs of pseudo-sweeps can be found in [AS01, RR13].

The topology of the posets of pseudo-sweeps has been extensively studied as a special case of the *generalized Baues problem* [BS92, Rei99]. Without the trivial sweep, their order complexes have the homotopy type of, but in general are not homeomorphic to, a sphere. In the realizable case, Billera, Kapranov, and Sturmfels proved that the poset of sweeps is a strong deformation retract of the poset of pseudo-sweeps [BKS94b]. Their proof uses strongly the geometry of the fiber polytope construction. Björner [Bjö92] and Athanasiadis, Edelman, and Reiner [AER00] found combinatorial proofs that extend to general oriented matroids, but only give the homotopy type. Nevertheless, Björner claims that it is *"undoubtedly true"* that even for unrealizable oriented matroids there must be a sphere to which the poset of pseudo-sweeps retracts [Bjö92, below Thm. 2]. However, there were no explicit candidates for these spheres. For oriented matroids that are little oriented matroids, we show in Theorem 3.6.6 that any of the associated sweep oriented matroids can play this role. That is, that the poset of non-trivial sweeps (which is a sphere) is a strong deformation retract of the poset of non-trivial pseudo-sweeps of the little oriented matroid. This highlights the fact that sweep oriented matroids should be seen as combinatorial analogues of monotone path polytopes of zonotopes; that is, sweep polytopes. Unfortunately, the existence of oriented matroids that are not little oriented matroids leaves some cases where Björner's observation remains open.

In Section 3.7 we present a further generalization of sweep oriented matroids in terms of *allowable graphs of permutations*, which are closer to the original formulation of allowable sequences. Allowable graphs of permutations are graphs whose vertex sets are sets of permutations closed under taking reverses in which every pair of permutations is connected through a sequence of permutations fulfilling conditions (i) and (ii) above (plus some technical conditions when the moves are not simple). In the simple case, these are antipodal isometric subgraphs of the permutahedron. Translating back to sign-vectors, we obtain *sweep acycloids* (Theorem 3.7.12), which have the structure of acycloids [Han90], also known as antipodal partial cubes [FH93]. Again, sweep acycloids (and thus allowable graphs of permutations) of rank 2 are equivalent to allowable sequences. Not every acycloid is an oriented matroid [Han93, Sec. 7], but there are characterizations of those that are [Han93, dS95, KM20]. Since sweep acycloids that are oriented matroids are sweep oriented matroids (Corollary 3.7.18), these give alternative characterizations of sweep oriented matroids in terms of allowable graphs of permutations (Corollary 3.7.20). So far we could not find any example of a sweep acycloid that is not a sweep oriented matroid, and we leave this question as an open problem.

A note concerning the terminology

The terms *sweep* and *sweeping* had already been used in the oriented matroids literature in the context of *topological sweepings* of affine oriented matroids and pseudo-hyperplane arrangements. These concepts should not be confused with the notions that we introduce in this chapter.

The two colliding terminologies arise from the two classical dual geometric representations of realizable oriented matroids; namely, point configurations and hyperplane arrangements. Both give rise to a natural definition of *sweep* that generalizes to non-realizable matroids.

On the one hand, our definition of *sweep* is meant to model sweeps of point configurations by parallel hyperplanes. Such a sweep induces an ordering of the points, which are the elements of the underlying oriented matroid. When this picture is polarized, the point configuration gives rise to a hyperplane arrangement, but the collection of sweeping hyperplanes becomes a point that travels in a linear direction (the associated sweep permutation records the order in which the point crosses the hyperplanes). This is the formulation studied by Edelman [Ede00] and Stanley [Sta15].

On the other hand, one can consider sweeps of hyperplane arrangements by parallel hyperplanes. Such a sweep induces an ordering of the vertices of the arrangement, which are the cocircuits of the underlying oriented matroid. This is the point of view of the literature on *topological sweepings* of pseudo-hyperplane arrangements and oriented matroids (see, for example, [BLS+99, p.172], [EG89], [EOS86], [Hoc16] and [FW01]), which concerns mostly the rank 3 case (pseudoline arrangements).

In rank 3, the two notions are strongly related. Indeed, the allowable sequence of a planar point configuration (which is a collection of sweeps in our terminology), can be interpreted as a topological sweep of the dual arrangement of lines. This correspondence exists in rank 3 but completely fails in higher rank, as it only works because in an oriented matroid of rank 3 the lines (flats of rank 2) coincide with the hyperplanes (flats of corank 1).

It is worth to note that in this second setup there exist other approaches to generalize allowable sequences to higher dimensions. For example, the *signotopes* described in [FW01] (see also [Fel04]). These are strongly related to higher Bruhat orders [MS89] and single-element extensions of cyclic hyperplane arrangements [FZ01, Zie93]. However, as these generalizations are meant to model (topological) sweeps of hyperplane arrangements with a (pseudo) hyperplane, they do not cover the spherical complexes that Goodman and Pollack alluded to in [GP93] as the natural way to generalize allowable sequences to higher dimensions.

Structure of this chapter

This chapter gravitates around the concept of sweep oriented matroid, which lies in the intersection of the theories of allowable sequences, valid order arrangements, and the generalized Baues problem for cellular strings. Our hope is to provide a unified reference that reflects all these connections. To this end, we give a broad overview of the topic, as we expect readers with diverse backgrounds and motivations to be interested in different aspects. In particular, most of the sections can be read independently.

Section 3.2 serves as an introduction and focuses in the realizable case. We present polytopal constructions that serve as motivation for the upcoming definitions. Sweep oriented matroids are defined in Section 3.3. In Section 3.4 we show how the structural results on allowable sequences from [BLS+99] generalize to sweep oriented matroids of arbitrary rank. Section 3.5 demonstrates that the results in [Ede00, Sta15] do not require realizability. Section 3.6 depicts sweep oriented matroids as highlighted spheres inside the poset of cellular strings of oriented matroids whose existence was conjectured by [Bjö92]. A presentation in terms of permutations, akin to Goodman and Pollack's original formulation of allowable sequences [GP93], is given in Section 3.7 under the name of allowable graphs of permutations.

We end by discussing some open problems and further directions of research in Section 3.8.

3.2 Sweeps and sweep polytopes

3.2.1 Sweeps of point configurations

For any integer n, we use $\binom{[n]}{2} = \{(i,j) \mid 1 \le i < j \le n\}$ to denote the set of non-repeating sorted pairs of elements of $[n]$. We recall that an *ordered partition* of $[n]$ is an ordered collection of non-empty disjoint subsets $(I_1,\dots,I_l)$ whose union is $[n]$. In some proofs, it will be more comfortable to think of an ordered partition $I = (I_1,\dots,I_l)$ as the surjection p_I from $[n]$ to $[l]$ such that $I_k = p_I^{-1}(\{k\})$ for all $1 \le k \le l$. Note that for a permutation σ, the ordered partition $I = (\{\sigma(1)\},\dots,\{\sigma(n)\})$ corresponds to the bijection $p_I = \sigma^{-1}$.

Let $\boldsymbol{A} = (\boldsymbol{a}_1,\dots,\boldsymbol{a}_n) \in \mathbb{R}^{d\times[n]}$ be a point configuration in $\mathbb{R}^d$. For $\boldsymbol{u} \in \mathbb{R}^d$, consider the linear form $\langle \boldsymbol{u}, \cdot\, \rangle : \mathbb{R}^d \to \mathbb{R}$ sending $\boldsymbol{x}$ to $\langle \boldsymbol{u}, \boldsymbol{x}\rangle$. The *sweep* of $\boldsymbol{A}$ associated to $\boldsymbol{u}$ is the ordered partition $I^{\boldsymbol{u}} = (I_1,\dots,I_l)$ of $[n]$ that verifies $\langle \boldsymbol{u}, \boldsymbol{a}_i\rangle = \langle \boldsymbol{u}, \boldsymbol{a}_j\rangle$ for all i,j in a same part I_k, and $\langle \boldsymbol{u}, \boldsymbol{a}_i\rangle < \langle \boldsymbol{u}, \boldsymbol{a}_j\rangle$ if $i \in I_r$, $j \in I_s$ with $r < s$. In particular, $\langle \boldsymbol{u}, \boldsymbol{a}_i\rangle \le \langle \boldsymbol{u}, \boldsymbol{a}_j\rangle$ if and only if $p_{I^{\boldsymbol{u}}}(i) \le p_{I^{\boldsymbol{u}}}(j)$. Note that the partition associated to the linear form $\boldsymbol{0}$ is the *trivial sweep* $([n])$.

The *poset of sweeps* of $\boldsymbol{A}$, denoted $\overline{\Pi}(\boldsymbol{A})$, is the set of all sweeps ordered by refinement. Its maximal elements are permutations whenever $\boldsymbol{A}$ does not contain repeated points. We will often assume that this is the case, as we can always identify repeated points. Under this assumption, we denote by $\Pi(\boldsymbol{A}) \subseteq \mathfrak{S}_n$ the set of its maximal elements, the *sweep permutations* of $\boldsymbol{A}$. If there are repeated points, we will still call the maximal elements *sweep permutations* for brevity.

Sweeps induce an equivalence relation on $\mathbb{R}^d$, where $\boldsymbol{u} \sim \boldsymbol{v}$ if they give the same sweep. Its equivalence classes are the cells of the polyhedral fan induced by the *sweep hyperplane arrangement* $\boldsymbol{\mathcal{SH}}(\boldsymbol{A})$; the arrangement of the linear hyperplanes $\left\{\boldsymbol{u} \in \mathbb{R}^d \,\middle|\, \langle \boldsymbol{u}, \boldsymbol{a}_i\rangle = \langle \boldsymbol{u}, \boldsymbol{a}_j\rangle\right\}$

for all $(i,j) \in \binom{[n]}{2}$. Note that the face poset of $\boldsymbol{\mathcal{SH}}(\boldsymbol{A})$ is isomorphic to the poset $\overline{\Pi}(\boldsymbol{A})$, with a bijection that sends each cell $\mathcal{C}$ of $\boldsymbol{\mathcal{SH}}(\boldsymbol{A})$ to the sweep I in $\overline{\Pi}(\boldsymbol{A})$ that verifies that the relative interior of $\mathcal{C}$ is $\left\{\boldsymbol{u} \in \mathbb{R}^d \,\middle|\, I^{\boldsymbol{u}} = I\right\}$. In particular, the cones of dimension d of $\boldsymbol{\mathcal{SH}}(\boldsymbol{A})$ are indexed by the sweep permutations in $\Pi(\boldsymbol{A})$.

We will see in Section 3.2.3 that $\boldsymbol{\mathcal{SH}}(\boldsymbol{A})$ is the normal fan of a polytope: the *sweep polytope* of $\boldsymbol{A}$, denoted by $\boldsymbol{SP}(\boldsymbol{A})$. Thus, the poset of sweeps $\overline{\Pi}(\boldsymbol{A})$ enlarged with a top element is isomorphic to the poset opposite to the face lattice of $\boldsymbol{SP}(\boldsymbol{A})$, and is in particular a lattice. This provides a natural labeling of the faces of $\boldsymbol{SP}(\boldsymbol{A})$ by sweeps. In particular, the vertices of $\boldsymbol{SP}(\boldsymbol{A})$ are labeled by the sweep permutations in $\Pi(\boldsymbol{A})$.

The identification of sweeps with faces of $\boldsymbol{SP}(\boldsymbol{A})$ reflects the inherent topological structure of the poset of sweeps. This can be made precise in terms of its order complex. In our case, the order complex of $\overline{\Pi}(\boldsymbol{A}) \setminus ([n])$, the poset of sweeps without the trivial sweep, is just the barycentric subdivision of the boundary of $\boldsymbol{SP}(\boldsymbol{A})$. We will implicitly identify $\overline{\Pi}(\boldsymbol{A})$ with $\Delta\left(\overline{\Pi}(\boldsymbol{A}) \setminus ([n])\right)$ whenever we make topological statements about posets of sweeps.

3.2.2 Examples

Before providing constructions for this polytope, we will present two particular examples.

The simplex and the permutahedron

If $\boldsymbol{A}_n$ is the set of vertices of a standard $(n-1)$-simplex $\triangle_{n-1}$, i.e. the points $\boldsymbol{a}_i$ are the canonical basis vectors $\boldsymbol{e}_i$ in $\mathbb{R}^n$, then $\boldsymbol{\mathcal{SH}}(\boldsymbol{A}_n)$ is the *braid arrangement* $\boldsymbol{\mathcal{B}}_n$ consisting of the hyperplanes $\{\boldsymbol{u} \,|\, \boldsymbol{u}_j - \boldsymbol{u}_i = 0\}$ for all $1 \le i < j \le n$, the set of sweep permutations is the whole symmetric group $\Pi(\boldsymbol{A}_n) = \mathfrak{S}_n$, and the poset of sweeps $\overline{\Pi}(\boldsymbol{A}_n)$ is the poset of all ordered partitions of $[n]$. Likewise for any set $\boldsymbol{A}$ of affinely independent points, up to affine transformation of the braid arrangement. We have seen in Section 1.4.2 that $\boldsymbol{\mathcal{B}}_n$ is the normal fan of the standard n-permutahedron $\mathbf{Perm}_n$.

The sweep polytope $\boldsymbol{SP}(\boldsymbol{A})$ associated to the standard simplex is the translation of $\mathbf{Perm}_n$ centered at the origin. We will denote this translated permutahedron by $\boldsymbol{P}'_n$

$$\boldsymbol{P}'_n = \sum_{1 \le i < j \le n} \left[-\frac{\boldsymbol{e}_i - \boldsymbol{e}_j}{2}, \frac{\boldsymbol{e}_i - \boldsymbol{e}_j}{2} \right] \tag{3.1}$$

to distinguish it from the standard realization. See Figures 3.2 and 3.3 for the cases $n = 3, 4$.

The cross-polytope and the permutahedron of type B

Let $\boldsymbol{B}_n$ be the set of vertices of the cross-polytope $\lozenge_n$, that is, the set of standard basis vectors of $\mathbb{R}^n$ and their opposites. It is convenient to index the points by $[\pm n] = \{-n, \dots, -1, 1, \dots, n\}$: $\boldsymbol{B}_n = \{\boldsymbol{b}_{-n} = -\boldsymbol{e}_n, \dots, \boldsymbol{b}_{-1} = -\boldsymbol{e}_1, \boldsymbol{b}_1 = \boldsymbol{e}_1, \dots, \boldsymbol{b}_n = \boldsymbol{e}_n\}$. Then the sweep permutations of $\boldsymbol{B}_n$ are the centrally symmetric permutations of $\mathfrak{S}_{[\pm n]}$, which

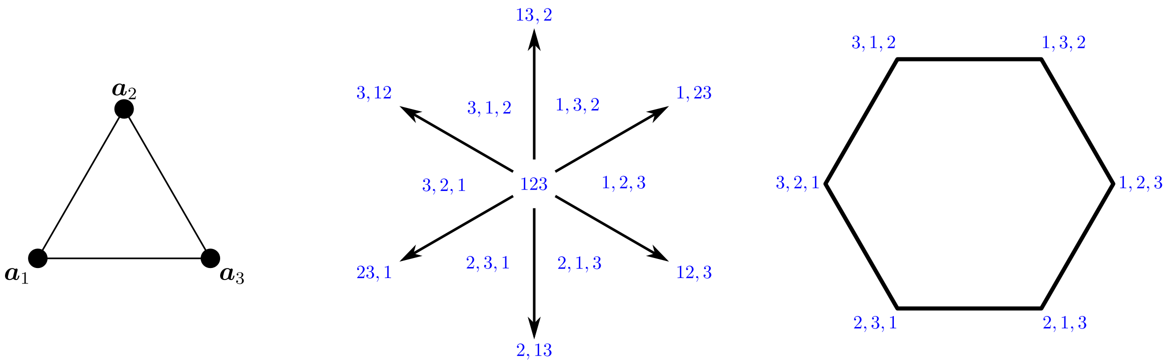

Figure 3.2: $\boldsymbol{A}_3$, its sweep hyperplane arrangement $\boldsymbol{\mathcal{SH}}(\boldsymbol{A}_3) = \boldsymbol{\mathcal{B}}_3$ (modulo linearity), and its sweep polytope $\boldsymbol{SP}(\boldsymbol{A}_3) = \boldsymbol{P}_3'$, the 3-permutahedron, where each vertex is labeled by the corresponding sweep permutation of $\boldsymbol{A}_3$.

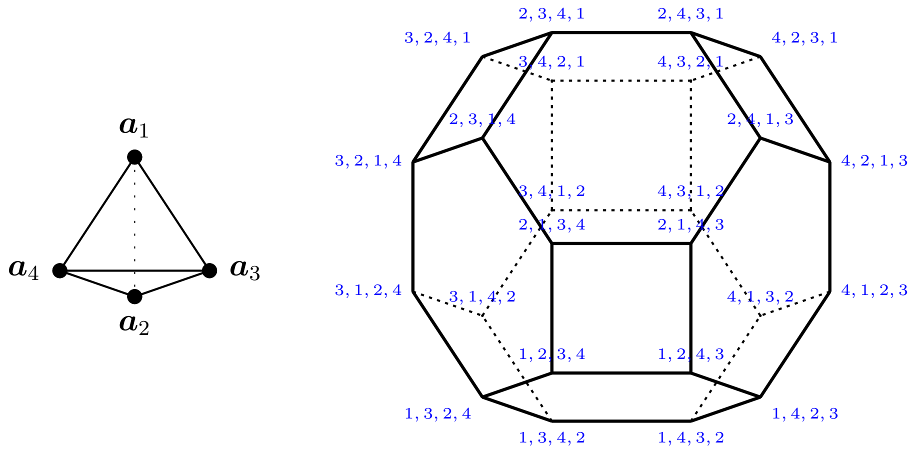

Figure 3.3: $\boldsymbol{A}_4$ and its sweep polytope $\boldsymbol{SP}(\boldsymbol{A}_4) = \boldsymbol{P}_4'$, the 4-permutahedron.

satisfy $\sigma(-i) = -\sigma(i)$ for all $i \in [\pm n]$. By symmetry, the first half determines the whole permutation. This way, they can be represented by signed permutations of $[n]$, where $-k$ is denoted by $\overline{k}$. We use this notation in Figures 3.4 and 3.5.

They are the elements of the Coxeter group of type B, also called hyperoctahedral group. See [BB05, Section 8.1] for more details on the combinatorics of this group. The sweep hyperplane arrangement $\boldsymbol{\mathcal{SH}}(\boldsymbol{B}_n)$ is the Coxeter arrangement of type B, which consists of the hyperplanes $\{\boldsymbol{u} \in \mathbb{R}^n \mid \boldsymbol{u}_i \pm \boldsymbol{u}_j = 0\}$ for all $1 \leq i < j \leq n$ and $\{\boldsymbol{u} \in \mathbb{R}^n \mid \boldsymbol{u}_i = 0\}$ for all $1 \leq i \leq n$. The sweeps are the centrally symmetric ordered partitions of $[\pm n]$. This complex is known as the Coxeter complex of type B, see [BLS+99, Sec. 2.3(c)]. See Figure 3.4 for an example.

The associated sweep polytope is the Coxeter permutahedron of type B, also known as the Coxeterhedron of type B [R94]. See Figures 3.4 and 3.5 for pictures in dimensions 2 and 3.

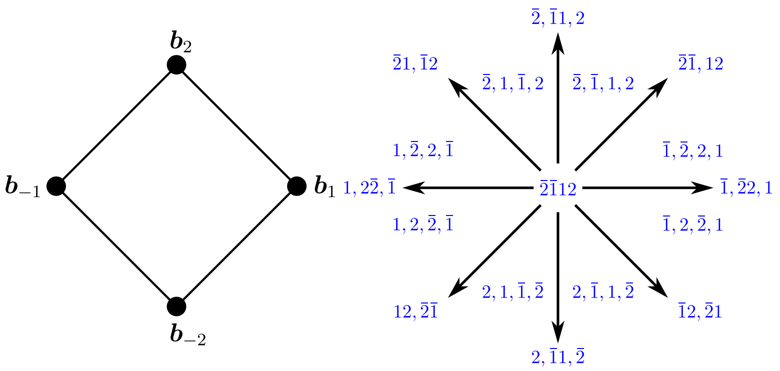

Figure 3.4: $\boldsymbol{B}_2$, its sweep hyperplane arrangement $\boldsymbol{\mathcal{SH}}(\boldsymbol{B}_2)$, and its sweep polytope $\boldsymbol{SP}(\boldsymbol{B}_2)$.

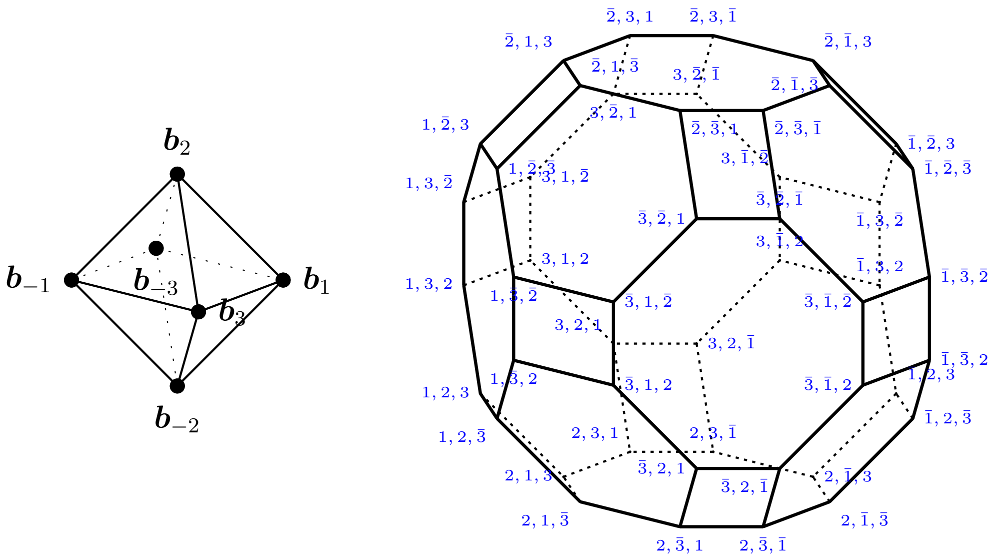

Figure 3.5: $\boldsymbol{B}_3$ and its sweep polytope $\boldsymbol{SP}(\boldsymbol{B}_3)$, the 3-permutahedron of type B.

Sweeping with polynomial functions

Sweep polytopes can also be used to model sweeps of a point configuration $\boldsymbol{A} = (\boldsymbol{a}_1, \ldots, \boldsymbol{a}_n) \in \mathbb{R}^{d\times[n]}$ by polynomial functions $p \in \mathbb{R}[x_1, \ldots, x_d]$ of bounded degree. The *polynomial sweep* of $\boldsymbol{A}$ associated to p is the ordered partition of $[n]$ induced by the ordered level sets of p on $\boldsymbol{A}$.

Let $\mathcal{M}$ be the set of monomials of degree at most D on variables $x_1, \ldots, x_d$. There are $|\mathcal{M}| = \binom{D+d}{D}$ elements in $\mathcal{M}$. For a point $\boldsymbol{v} = (v_1, \ldots, v_d) \in \mathbb{R}^d$ and a monomial $M \in \mathcal{M}$, denote by $M(\boldsymbol{v}) \in \mathbb{R}$ the evaluation of M on the values $x_1 = v_1, \dots, x_d = v_d$. The *Veronese mapping* is defined by the map

$$\chi : \begin{cases} \mathbb{R}^d & \to \mathbb{R}^{\mathcal{M}} \\ \boldsymbol{v} & \mapsto (M(\boldsymbol{v}))_{M \in \mathcal{M}} . \end{cases}$$

Then, the polynomial sweep of $\boldsymbol{A}$ induced by the polynomial $p = \sum_{M \in \mathcal{M}} c_M M$ exactly corresponds to the sweep of $\chi(\boldsymbol{A})$ induced by the linear functional $\langle \boldsymbol{c}, \cdot \rangle$ for $\boldsymbol{c} = (c_M)_{M \in \mathcal{M}} \in \mathbb{R}^{\mathcal{M}}$. In particular, the poset of sweeps of $\chi(\boldsymbol{A})$ coincides with the poset of polynomial sweeps of $\boldsymbol{A}$ induced by polynomials of degree at most D. Note that if $d = 1$, the image $\chi(\boldsymbol{A})$ is a standard cyclic polytope of dimension D with n vertices.

Variants of the Veronese mapping can be used for particular families of polynomial sweeps. For example, the embedding

$$(v_1, \dots, v_d) \mapsto (v_1, \dots, v_d, v_1^2 + \cdots + v_d^2)$$

onto the paraboloid models sweeps by families of concentric spheres.

3.2.3 Constructions for sweep polytopes

In what follows, we describe three approaches to construct the sweep polytope $\boldsymbol{SP}(\boldsymbol{A})$. Recall that $\boldsymbol{SP}(\boldsymbol{A})$ is a polytope whose normal fan coincides with the sweep hyperplane arrangement $\boldsymbol{\mathcal{SH}}(\boldsymbol{A})$, and whose face poset is opposite to the poset of sweeps $\overline{\Pi}(\boldsymbol{A})$.

As a zonotope

The most direct realization is as the Minkowski sum of the segments with directions the differences between the points of the configuration, which is (a translation of) the presentation of sweep polytopes given in [GS93] (under the name of *shellotopes*).

Definition 3.2.1. The *sweep polytope* $\boldsymbol{SP}(\boldsymbol{A})$ associated to the configuration $\boldsymbol{A} = (\boldsymbol{a}_1, \dots, \boldsymbol{a}_n) \in \mathbb{R}^{d \times [n]}$ is the zonotope:

$$\boldsymbol{SP}(\boldsymbol{A}) = \sum_{1 \le i < j \le n} \left[-\frac{\boldsymbol{a}_i - \boldsymbol{a}_j}{2}, \frac{\boldsymbol{a}_i - \boldsymbol{a}_j}{2} \right] \subset \mathbb{R}^d.$$

We saw as a consequence of Proposition 1.1.11 that the normal fan of a zonotope is the arrangement of the hyperplanes orthogonal to its generators. Applied to sweep polytopes, we directly get:

Proposition 3.2.2. *The normal fan of $\boldsymbol{SP}(\boldsymbol{A})$ is the hyperplane arrangement $\boldsymbol{\mathcal{SH}}(\boldsymbol{A})$.*

As a projection of the permutahedron

Our second incarnation is as a projection of the (centered) permutahedron $\boldsymbol{P}'_n$. For a configuration $\boldsymbol{A}$ of n points $\boldsymbol{a}_1, \dots, \boldsymbol{a}_n$ in $\mathbb{R}^d$, let $M_{\boldsymbol{A}}$ be the linear map

$$\begin{aligned} M_{\boldsymbol{A}} : \mathbb{R}^n &\to \mathbb{R}^d \\ \boldsymbol{e}_i &\mapsto \boldsymbol{a}_i. \end{aligned} \tag{3.2}$$

Then it follows from Definition 3.2.1 and the description of $\boldsymbol{P}'_n$ in (3.1) that:

Proposition 3.2.3. $\boldsymbol{SP}(\boldsymbol{A}) = M_{\boldsymbol{A}}(\boldsymbol{P}'_n)$.

Conversely, all affine images of permutahedra are sweep polytopes, up to translation. This provides a combinatorial interpretation, in terms of sweeps, of the face lattice of any affine projection of a permutahedron (a *permutahedral shadow*).

Corollary 3.2.4. *Let $M : \mathbb{R}^n \to \mathbb{R}^d$ be a linear map, then $M(\boldsymbol{P}'_n)$ is the sweep polytope of the point configuration $M(\boldsymbol{e}_1), \dots, M(\boldsymbol{e}_n)$.*

Note that, given a linear map from $\boldsymbol{P}'_n$ to $\mathbb{R}^d$, there is a d-dimensional family of ways to extend it to a linear map from $\mathbb{R}^n$ to $\mathbb{R}^d$. This amounts to the fact that point configurations related by a translation give rise to the same sweep polytope.

Remark 3.2.5. Proposition 3.2.3 follows from the fact that Minkowski sums and linear projections commute. This can be exploited also with other decompositions of the permutahedron. For example, the permutahedron $\mathbf{Perm}_n$ can be written as the Minkowski sum of the hypersimplices $\triangle_{n,k} = \{\boldsymbol{x} \in [0,1]^n \mid \sum \boldsymbol{x}_i = k\}$ with k ranging from 1 to $n-1$ (see for example [Pos09]). Therefore, any sweep polytope can be expressed as a Minkowski sum of projections of hypersimplices. Projections of hypersimplices are studied under the name of *k-set polytopes* [AW03, EVW97], which (up to homothety) can be described as the convex hull of the barycenters of all k-subsets of $\boldsymbol{A}$, see [MSP21]. The sweep polytope of $\boldsymbol{A}$ is thus the Minkowski sum of its k-set polytopes, up to translation and homothety. In particular, because $\mathrm{conv}(\boldsymbol{A}) = M_{\boldsymbol{A}}(\triangle_{n,1})$, this shows that $\mathrm{conv}(\boldsymbol{A})$ is a Minkowski summand of $\boldsymbol{SP}(\boldsymbol{A})$. See Figure 3.6 for an example. Another point of view on this Minkowski decomposition will be discussed in Remark 3.2.9.

As a monotone path polytope

Monotone path polytopes, that we presented in Section 1.3.3, give a new interpretation of sweep polytopes and provide motivation for the definition of pseudo-sweeps, that will be further explored in Section 3.6.

Example 3.2.6. We rephrase Proposition 1.4.4 in a translated setting that matches the conventions of this chapter to take centered zonotopes.

Let $\square'_n = [-1,1]^n$ be the n-dimensional centered ± 1-cube, and let $s : \mathbb{R}^n \to \mathbb{R}$ be the linear form that sums the coordinates, i.e. the form $s = \langle \mathbf{1}_n, \cdot \rangle$ induced by the all-ones vector. Then the fiber polytope $\boldsymbol{\Sigma}\left(\square'_n, s\right)$ is homothetic to the centered permutahedron $\boldsymbol{P}'_n$: $\boldsymbol{\Sigma}\left(\square'_n, s\right) = \frac{2}{n}\boldsymbol{P}'_n$.

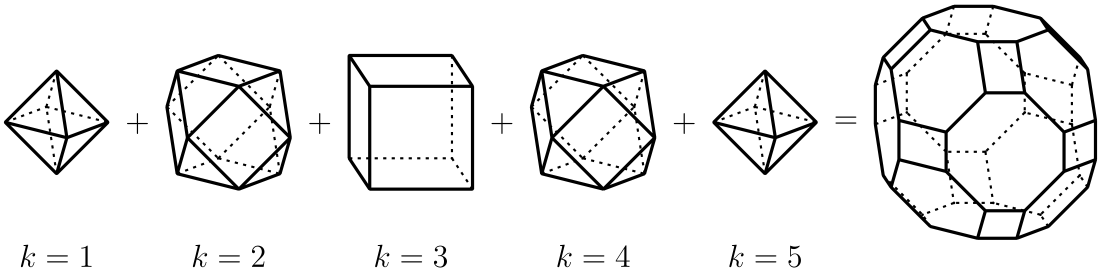

Figure 3.6: The sweep polytope $\boldsymbol{SP}(\boldsymbol{B}_3) = \boldsymbol{P}'_3$ as a Minkowski sum of the k-set polytopes of $\boldsymbol{B}_3$ for $k = 1, \ldots, 5$.

The following central property of fiber polytopes will be key for our purposes.

Lemma 3.2.7 ([BS92, Lem. 2.3])**.** *Let $\mathbb{R}^n \xrightarrow{\theta} \mathbb{R}^m \xrightarrow{\pi} \mathbb{R}^d$ be linear maps, and $\boldsymbol{P} \subset \mathbb{R}^n$ a polytope. Then $\boldsymbol{\Sigma}(\theta(\boldsymbol{P}), \pi) = \theta(\boldsymbol{\Sigma}(\boldsymbol{P}, \pi \circ \theta))$.*

We need some extra notation. Let $\boldsymbol{A} = (\boldsymbol{a}_1, \ldots, \boldsymbol{a}_n) \in \mathbb{R}^{d \times [n]}$ be a point configuration, and consider its *homogenization* $\bar{\boldsymbol{A}} = (\bar{\boldsymbol{a}}_1, \ldots, \bar{\boldsymbol{a}}_n) \in \mathbb{R}^{(d+1) \times [n]}$ consisting of the vectors $\bar{\boldsymbol{a}}_i = (\boldsymbol{a}_i, 1)$. We define the zonotope $\boldsymbol{Z}(\bar{\boldsymbol{A}})$ associated to $\boldsymbol{A}$ as the following Minkowski sum of centrally symmetric segments:

$$\boldsymbol{Z}(\bar{\boldsymbol{A}}) = \sum_{i=1}^{n} [-\bar{\boldsymbol{a}}_i, \bar{\boldsymbol{a}}_i].$$

Let $h : \mathbb{R}^{d+1} \to \mathbb{R}$ denote the map that returns the last coordinate of a point, that we call its *height*.

This gives us another point of view on sweep polytopes.

Proposition 3.2.8. *For any point configuration $\boldsymbol{A}$ we have*

$$\boldsymbol{\Sigma}\left(\tfrac{n}{2}\boldsymbol{Z}(\bar{\boldsymbol{A}}), h\right) = \boldsymbol{SP}(\boldsymbol{A}) \times \{0\},$$

and hence $\boldsymbol{SP}(\boldsymbol{A})$ is affinely isomorphic to the monotone path polytope $\boldsymbol{\Sigma}\big(\boldsymbol{Z}(\bar{\boldsymbol{A}}), h\big)$.

Proof. The projection $M_{\bar{\boldsymbol{A}}} : \mathbb{R}^n \to \mathbb{R}^{d+1}$ that maps $\boldsymbol{e}_i$ to $\bar{\boldsymbol{a}}_i = (\boldsymbol{a}_i, 1)$ is such that $\boldsymbol{Z}(\bar{\boldsymbol{A}}) = M_{\bar{\boldsymbol{A}}}(\square'_n)$ and $s = h \circ M_{\bar{\boldsymbol{A}}}$, where s is the linear form that sums the coordinates and $\square'_n$ is the cube $[-1, 1]^n$. Hence, by Lemma 3.2.7 and Example 3.2.6 we have $\boldsymbol{\Sigma}\big(\boldsymbol{Z}(\bar{\boldsymbol{A}}), h\big) = M_{\bar{\boldsymbol{A}}}(\boldsymbol{\Sigma}(\square'_n, s)) = M_{\bar{\boldsymbol{A}}}(\frac{2}{n}\boldsymbol{P}'_n)$. Now, $\boldsymbol{P}'_n$ lies in $s^{-1}\left(\frac{1}{\mathrm{vol}_{\mathrm{Eucl}}(\square'_n)} \int_{\square'_n} \boldsymbol{y} d\boldsymbol{y}\right) = s^{-1}(\boldsymbol{0}_n)$, and thus $M_{\bar{\boldsymbol{A}}}(\frac{2}{n}\boldsymbol{P}'_n)$ lies in the kernel of h, which means that $\boldsymbol{\Sigma}\big(\boldsymbol{Z}(\bar{\boldsymbol{A}}), h\big) = \frac{2}{n} M_{\boldsymbol{A}}(\boldsymbol{P}'_n) \times \{0\}$. Finally, by Proposition 3.2.3, we have $M_{\boldsymbol{A}}(\boldsymbol{P}'_n) = \boldsymbol{SP}(\boldsymbol{A})$, and therefore $\boldsymbol{\Sigma}\big(\boldsymbol{Z}(\bar{\boldsymbol{A}}), h\big) = \frac{2}{n}\boldsymbol{SP}(\boldsymbol{A}) \times \{0\}$. $\square$

Remark 3.2.9. If we intersect $\boldsymbol{Z}(\bar{\boldsymbol{A}})$ with the hyperplane of height equal to $-n+2$, we obtain

$$\operatorname{conv}(-\sum_{i=1}^{n} \bar{\boldsymbol{a}}_i + 2\bar{\boldsymbol{a}}_j, j \in [n]) = \operatorname{conv}(-\sum_{i=1}^{n} \boldsymbol{a}_i + 2\boldsymbol{A}) \times \{-n+2\},$$

which is an embedding of a dilation of the convex hull of $\boldsymbol{A}$ in $\mathbb{R}^{d+1}$. Similarly, for any $k \in [n]$ the slice at height $-n+2k$ is an embedding of a dilation of the projection of the hypersimplex $\triangle_{n,k}$ under the map $M_{\boldsymbol{A}}$. This is the k-set polytope of $\boldsymbol{A}$, see Remark 3.2.5. The fiber polytope realization reflects the decomposition of the sweep polytope as a sum of k-set polytopes.

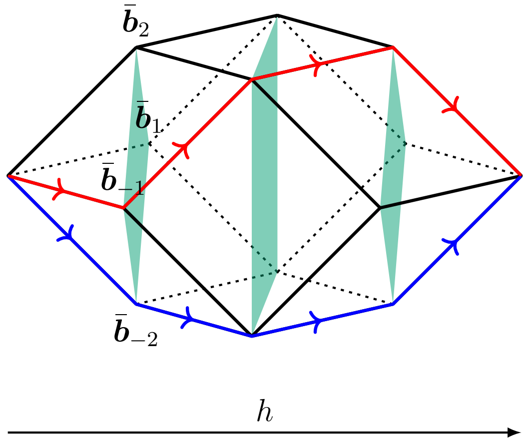

Figure 3.7: The zonotope $\boldsymbol{Z}(\bar{\boldsymbol{B}}_2)$. Three fibers of the height function h are highlighted, representing a copy of the convex hull of $\boldsymbol{B}_2$, and of its 2-set and 3-set polytopes. The lower (blue) path represents the coherent monotone path associated to the permutation $(\bar{2}, \bar{1}, 1, 2)$ (which can be read off the directions of the steps in the path). The upper (red) path is a monotone path that is not coherent. It is associated to the permutation $(\bar{1}, 2, 1, \bar{2})$, which is not a sweep permutation, but a pseudo-sweep permutation, see Section 3.6.

Conversely, monotone path polytopes of zonotopes for nondegenerate functionals are sweep polytopes, up to normal equivalence.

Proposition 3.2.10. *Let $\boldsymbol{Z} \subset \mathbb{R}^d$ be a zonotope, $\pi : \mathbb{R}^d \to \mathbb{R}$ a linear map, and $\boldsymbol{Z}^{\downarrow\pi}$ the face of $\boldsymbol{Z}$ minimizing π. Then the monotone path polytope $\Sigma(\boldsymbol{Z}, \pi)$ is normally equivalent to the Minkowski sum of $\boldsymbol{Z}^{\downarrow\pi}$ with the sweep polytope $\boldsymbol{SP}(\boldsymbol{A})$, where $\boldsymbol{A}$ consists of the points $\frac{1}{\pi(\boldsymbol{z}_i)}\boldsymbol{z}_i$ for the generators $\boldsymbol{z}_i$ of $\boldsymbol{Z}$ such that $\pi(\boldsymbol{z}_i) \neq 0$.*

Proof. Let $\boldsymbol{c}, \boldsymbol{z}_1 \ldots, \boldsymbol{z}_m \in \mathbb{R}^d$ be such that

$$\boldsymbol{Z} = \boldsymbol{c} + \sum_{i=1}^{m} [-\boldsymbol{z}_i, \boldsymbol{z}_i] \subset \mathbb{R}^d.$$

Then $\boldsymbol{Z}$ is normally equivalent to any zonotope $\boldsymbol{Z}' = \boldsymbol{c}' + \sum_{i=1}^{m} [-\lambda_i \boldsymbol{z}_i, \lambda_i \boldsymbol{z}_i]$, where $\boldsymbol{c}'$ is a vector in $\mathbb{R}^d$ and the λ_i are non-zero scalars.

Up to relabeling the $\boldsymbol{z}_i$, one can suppose that $\{i \mid \pi(\boldsymbol{z}_i) = 0\} = \{n+1, \dots, m\}$ for a certain $n \in \{0, \dots, m\}$. Let $\boldsymbol{Z}_1$ and $\boldsymbol{Z}_2$ be the zonotopes:

$$\boldsymbol{Z}_1 = \sum_{i=1}^{n} \left[-\frac{1}{\pi(\boldsymbol{z}_i)} \boldsymbol{z}_i, \frac{1}{\pi(\boldsymbol{z}_i)} \boldsymbol{z}_i \right], \qquad \boldsymbol{Z}_2 = \sum_{i=n+1}^{m} [-\boldsymbol{z}_i, \boldsymbol{z}_i].$$

Note that the face $\boldsymbol{Z}^{\downarrow\pi}$ is a translation of $\boldsymbol{Z}_2$.

Since $\boldsymbol{Z}$ is normally equivalent to the Minkowski sum $\boldsymbol{Z}_1 + \boldsymbol{Z}_2$, we have that its monotone path polytope $\boldsymbol{\Sigma}(\boldsymbol{Z}, \pi)$ is normally equivalent to the monotone path polytope $\boldsymbol{\Sigma}(\boldsymbol{Z}_1 + \boldsymbol{Z}_2, \pi)$ by [McM03, Cor. 4.4].

Moreover, $\boldsymbol{\Sigma}(\boldsymbol{Z}_1 + \boldsymbol{Z}_2, \pi) = \boldsymbol{\Sigma}(\boldsymbol{Z}_1, \pi) + \boldsymbol{Z}_2$ because $\pi(\boldsymbol{Z}_2) = \{0\}$, thus $(\boldsymbol{Z}_1 + \boldsymbol{Z}_2) \cap \pi^{-1}(\{y\}) = \boldsymbol{Z}_1 \cap \pi^{-1}(\{y\}) + \boldsymbol{Z}_2$ for any $y \in \mathbb{R}$. If we denote the configuration of points $\boldsymbol{a}_1 = \frac{1}{\pi(\boldsymbol{z}_1)} \boldsymbol{z}_1, \dots, \boldsymbol{a}_n = \frac{1}{\pi(\boldsymbol{z}_n)} \boldsymbol{z}_n$ in $\mathbb{R}^d$ by $\boldsymbol{A}$, we have exactly $s = \pi \circ M_{\boldsymbol{A}}$ and $\boldsymbol{Z}_1 = M_{\boldsymbol{A}}(\square'_n)$, with the same notations as in Proposition 3.2.3 and Example 3.2.6. Hence, Lemma 3.2.7 and Example 3.2.6 give $\boldsymbol{\Sigma}(\boldsymbol{Z}_1, \pi) = M_{\boldsymbol{A}}(\boldsymbol{\Sigma}(\square'_n, s)) = M_{\boldsymbol{A}}(\frac{2}{n}\boldsymbol{P}'_n) = \frac{2}{n}\boldsymbol{SP}(\boldsymbol{A})$.

Hence $\boldsymbol{\Sigma}(\boldsymbol{Z}, \pi)$ is normally equivalent to the Minkowski sum $\boldsymbol{SP}(\boldsymbol{A}) + \boldsymbol{Z}^{\downarrow\pi}$. $\square$

3.3 Sweep oriented matroids

The goal of this section is to provide a purely combinatorial definition of posets of sweeps generalizing allowable sequences to higher dimensions. Since already in the plane not all allowable sequences arise from point configurations, it is clear that our definition has to go beyond the realizable case. We will do it in terms of oriented matroids, which do have enough expressive power to completely describe allowable sequences. However, to motivate our definition, we will start by discussing some oriented matroids associated to point configurations, inspired by [BLS+99, Sects. 1.10 & 6.4]. While we will introduce the basic definitions in oriented matroid theory, we refer the reader not familiar with the topic to the introduction in [Zie95, Lec. 6], and to the classical book [BLS+99] for a comprehensive source.

3.3.1 Basic notions and notation on oriented matroids

There are several cryptomorphic approaches to oriented matroids. We will use the presentation in terms of the *covector axioms*, which describe oriented matroids in terms of collections of sign-vectors $\mathcal{M} \subseteq \{+, -, 0\}^E$, called *covectors*, labeled by a finite ground set E.

For $X \in \mathcal{M}$ and $e \in E$, X_e denotes the value of X at the coordinate e. The *opposite* $-X$ of $X \in \mathcal{M}$ is the sign-vector obtained by switching $+$ and $-$ in X; that is, $(-X)_e = -(X_e)$. For $X, Y \in \mathcal{M}$, the *composition* of X and Y is the sign-vector $X \circ Y \in \{+, -, 0\}^E$ such that $(X \circ Y)_e = X_e$ if $X_e \neq 0$; and $(X \circ Y)_e = Y_e$ otherwise. The *separation set* of X and Y, denoted $S(X,Y)$, is the set of elements $e \in E$ such that $(X_e, Y_e) \in \{(+,-),(-,+)\}$.

Definition 3.3.1 (cf. [BLS+99, Def. 4.1.1])**.** A collection of sign-vectors $\mathcal{M} \subseteq \{+,-,0\}^E$ is the set of covectors of an *oriented matroid* if it satisfies the following axioms:

(V0) $\mathbf{0} \in \mathcal{M}$,

(V1) $X \in \mathcal{M}$ implies $-X \in \mathcal{M}$,

(V2) $X, Y \in \mathcal{M}$ implies $X \circ Y \in \mathcal{M}$,

(V3) if $X, Y \in \mathcal{M}$ and $e \in S(X,Y)$ then there exists $Z \in \mathcal{M}$ such that $Z_e = 0$ and $Z_f = (X \circ Y)_f$ for all $f \notin S(X,Y)$.

The set of covectors of an oriented matroid, with the product partial order induced by $0 \prec +, -$ componentwise, forms a poset. It has the structure of a lattice, called the *big face lattice* of the oriented matroid, if a top element $\hat{\mathbf{1}}$ is adjoined. The *rank* of the oriented matroid is the length of the maximal chains in the poset of covectors. The minimal non-zero covectors are called *cocircuits*, and they determine the oriented matroid as every non-zero covector is a composition of cocircuits. The maximal covectors for this partial order are called the *topes* of the oriented matroid. They also determine the oriented matroid, as X is a covector of $\mathcal{M}$ if and only if $X \circ T$ is a tope for every tope T. In fact, the *tope-graph* of $\mathcal{M}$, whose vertices are the topes and whose edges are given by the covectors covered by exactly two topes, already determines the oriented matroid up to FL-isomorphism, see [BEZ90, Theorem 6.14] and [BLS+99, Theorem 4.2.14].

There are several standard notions of oriented matroid isomorphism. By *FL-isomorphism*, we mean the coarsest, induced by isomorphism of the big face lattices. FL-isomorphism, called just isomorphism in [FF02], is the equivalence relation induced by reorientation, relabeling, and introduction/deletion of loops and parallel elements.

To understand the concepts used in the definition of FL-isomorphism, we need some extra notation. For $X \in \{+,-,0\}^E$ and $F \subseteq E$, we denote by ${}_{-F}X$ the signed vector Z such that: $Z_f = -X_f$ for $f \in F$ and $Z_e = X_e$ for $e \in E \setminus F$, which we call the *reorientation* of X on F. If $\mathcal{M}$ is an oriented matroid on the ground set E, its *reorientation* on F is the oriented matroid ${}_{-F}\mathcal{M}$ with covectors ${}_{-F}X$ for $X \in \mathcal{M}$. The *support* of a sign-vector X is $\underline{X} = \{e \in E \,|\, X_e \neq 0\}$. A *loop* is an element $e \in E$ that does not belong to the support of any covector. Two elements $e, f \in E$ are said to be *parallel* if $X_f = X_e$ for all $X \in \mathcal{M}$ or $X_f = -X_e$ for all $X \in \mathcal{M}$. This defines an equivalence relation on E, whose equivalence classes are called *parallelism classes*. The parallelism class of $e \in E$ is denoted $\bar{\bar{e}}$. An oriented matroid is called *simple* if it does not contain loops or distinct parallel elements.

For $X \in \{+,-,0\}^E$ and $F \subseteq E$, *the restriction of X to F*, denoted $X\big|_F$ is the covector $Z \in \{+,-,0\}^F$ such that $Z_f = X_f$ for all $f \in F$. If $\mathcal{M}$ is an oriented matroid on the ground set E, the set $\{X\big|_F \,\big|\, X \in \mathcal{M}\}$ forms an oriented matroid, denoted $\mathcal{M}\big|_F$ and called the *restriction of $\mathcal{M}$ to F*. The set $\left\{X\big|_{E\setminus F} \,\middle|\, X \in \mathcal{M}, X_f = 0\, \forall f \in F\right\}$ also forms an oriented matroid, denoted $\mathcal{M}/_F$ and called the *contraction of $\mathcal{M}$ along F*.

An oriented matroid is called *acyclic* if the all-positive sign-vector $+_n$ is a tope.

The standard way to associate an oriented matroid to a real vector configuration $V = (\boldsymbol{v}_1, \dots, \boldsymbol{v}_n) \in \mathbb{R}^{d\times[n]}$ is to consider the set of covectors on the ground set $[n]$ induced by the signs of the evaluations of linear functionals on the elements of V:

$$\mathcal{M}(V) = \{(\mathrm{sign}(\langle \boldsymbol{u}, \boldsymbol{v}_1\rangle, \dots, \mathrm{sign}(\langle \boldsymbol{u}, \boldsymbol{v}_n\rangle) \mid \boldsymbol{u} \in \mathbb{R}^n\} \subseteq \{+, -, 0\}^n, \tag{3.3}$$

where $\mathrm{sign}(x) = \begin{cases} + & \text{if } x > 0 \\ - & \text{if } x < 0 \\ 0 & \text{if } x = 0. \end{cases}$

That is, to each linear oriented hyperplane, we record which vectors of the configuration lie on the hyperplane, and which lie at the positive and negative sides, respectively. The covectors $\mathcal{M}(V)$ label the regions of the hyperplane arrangement $\boldsymbol{\mathcal{H}}_V$ consisting of the hyperplanes orthogonal to the vectors of V. Under this labeling, the big face lattice is consistent with the inclusion order of the regions, the topes labeling the maximal cells of the arrangement. Thus, the big face lattice on $\mathcal{M}(V)$ is isomorphic to (the opposite of) the face lattice of the zonotope $\sum_{i\in[n]}[\boldsymbol{0}, \boldsymbol{v}_i]$. The rank of $\mathcal{M}(V)$ coincides with the dimension of the linear hull of V. We will call this oriented matroid the *oriented matroid associated to V*. Oriented matroids that arise this way are called *realizable*. Note that even non-realizable oriented matroids can be geometrically realized by *arrangements of pseudo-spheres*, see [BLS+99, Sec. 1.4.1 & 5.2].

3.3.2 Three realizable oriented matroids associated to a point configuration

The construction above extends directly to affine point configurations, by considering evaluations of affine functionals instead. (Or, equivalently, linear functionals on the homogenization $\bar{\boldsymbol{A}}$.) Although this is the standard way to associate an oriented matroid to a point configuration $\boldsymbol{A}$, we will call it the *little oriented matroid* of $\boldsymbol{A}$, which is consistent with the notation in [BLS+99, Sect. 1.10] for planar configurations. This is to avoid confusion with the other alternative notions of oriented matroid associated to a point configuration that we will introduce. The *big oriented matroid*, which contains more information than the little oriented matroid, is also inspired by [BLS+99, Sect. 1.10]. We will prefer a more compact presentation, the *sweep oriented matroid*, which was not explicitly introduced there.

Definition 3.3.2. Let $\boldsymbol{A} = (\boldsymbol{a}_1, \dots, \boldsymbol{a}_n) \in \mathbb{R}^{d\times[n]}$ be a full-dimensional point configuration (i.e. its affine span is the whole space $\mathbb{R}^d$):

(i) The *little oriented matroid* of $\boldsymbol{A}$, denoted $\mathcal{M}^{lit}(\bar{\boldsymbol{A}})$, is the oriented matroid of rank $d+1$ with ground set $[n]$ associated to the $(d+1)$-dimensional homogenized vector configuration $\bar{\boldsymbol{A}} = (\bar{\boldsymbol{a}}_1, \dots, \bar{\boldsymbol{a}}_n) \in \mathbb{R}^{(d+1)\times[n]}$, where $\bar{\boldsymbol{a}}_i = (\boldsymbol{a}_i, 1) \in \mathbb{R}^{d+1}$. This is always an acyclic oriented matroid.

(ii) The *sweep oriented matroid* of $\boldsymbol{A}$, denoted $\mathcal{M}^{sw}(\bar{\boldsymbol{A}})$, is the oriented matroid of rank d with ground set $\binom{[n]}{2} = \{(i,j) \mid 1 \le i < j \le n\}$ associated to the d-dimensional vector configuration

$$\left\{ \boldsymbol{a}_{(i,j)} = \boldsymbol{a}_j - \boldsymbol{a}_i \;\middle|\; (i,j) \in \binom{[n]}{2} \right\} \in \mathbb{R}^{d \times \binom{[n]}{2}}.$$

(iii) The *big oriented matroid*[1] of $\boldsymbol{A}$, denoted $\mathcal{M}^{big}(\bar{\boldsymbol{A}})$, is the oriented matroid of rank $d+1$ on the ground set $[n] \cup \binom{[n]}{2}$ associated to the $(d+1)$-dimensional vector configuration

$$\bar{\boldsymbol{A}} \cup \left\{ (\boldsymbol{a}_{(i,j)}, 0) \;\middle|\; (i,j) \in \binom{[n]}{2} \right\} \in \mathbb{R}^{(d+1) \times \left([n] \cup \binom{[n]}{2}\right)}.$$

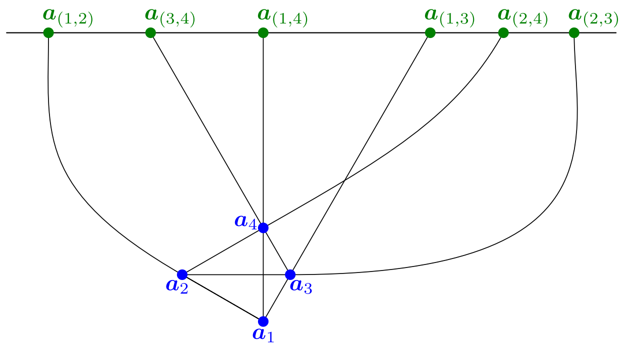

Figure 3.8: A big oriented matroid (with collinearities indicated). The points in the upper line, which represents the line at infinity, give rise to a sweep oriented matroid, whereas the points below give rise to the associated little oriented matroid.

Little, sweep and big oriented matroids obtained this way from a point configuration will be called *realizable*. In Sections 3.3.3 and 3.4.1, we give definitions for abstract sweep, little and big oriented matroids not necessarily arising from point configurations. We explain below how these structures are related to each other and to the poset of sweeps and the set of sweep permutations.

For a sweep $I = (I_1, \dots, I_l) \in \overline{\Pi}(\boldsymbol{A})$, corresponding to the surjection $p_I : [n] \to [l]$, we define the sign-vector $X^I \in \{+, -, 0\}^{\binom{[n]}{2}}$ such that

$$X^I_{(i,j)} = \begin{cases} + & \text{if } p_I(i) < p_I(j), \\ - & \text{if } p_I(i) > p_I(j), \\ 0 & \text{if } p_I(i) = p_I(j); \end{cases} \tag{3.4}$$

for $(i,j) \in \binom{[n]}{2}$.

[1] Our definition differs slightly from that in [BLS+99, Sect. 1.10]. We admit parallel vectors when the configuration is not generic, whereas in [BLS+99, Sect. 1.10] all parallel vectors of the form $\boldsymbol{a}_j - \boldsymbol{a}_i$ are merged into a single element of the oriented matroid.

For example, if I is the sweep $(\{1,3\},\{2\})$, we have $p_I(1) = p_I(3) = 1$, $p_I(2) = 2$, and the corresponding covector on the ground set $\{(1,2),(1,3),(2,3)\}$ is $X^I = (+,0,-)$. Compare Figures 3.2 and 3.9 to see other examples. As the figures illustrate, this map induces an isomorphism at the level of posets.

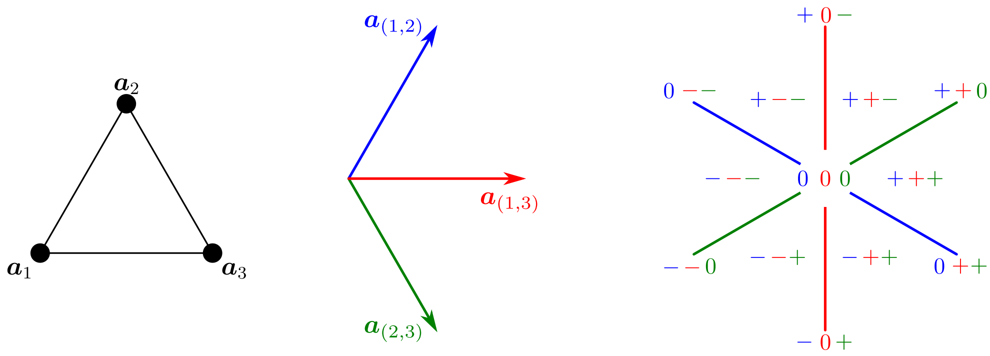

Figure 3.9: The vector configuration $\{\boldsymbol{a}_{(1,2)}, \boldsymbol{a}_{(1,3)}, \boldsymbol{a}_{(2,3)}\}$ associated to the point configuration $\boldsymbol{A}_3$ from Figure 3.2. The covectors associated to the regions of the sweep hyperplane are indicated by sign-vectors of length 3 containing the sign of the scalar product of a vector in the region with $\boldsymbol{a}_{(1,2)}$, $\boldsymbol{a}_{(1,3)}$, and $\boldsymbol{a}_{(2,3)}$, respectively. This should be compared with the labeling of the regions of the sweep hyperplane arrangement in terms of partitions in Figure 3.2.

Lemma 3.3.3. *The map $I \mapsto X^I$ induces a poset isomorphism between the poset of sweeps $\overline{\Pi}(\boldsymbol{A})$ and the poset of covectors of the sweep oriented matroid $\mathcal{M}^{\mathsf{sw}}(\bar{\boldsymbol{A}})$.*

In particular, $\overline{\Pi}(\boldsymbol{A}) \cup \hat{\mathbf{1}}$, where $\hat{\mathbf{1}}$ is an additional top element, is isomorphic to the big face lattice of $\mathcal{M}^{\mathsf{sw}}(\bar{\boldsymbol{A}})$, which is the opposite of the face lattice of the zonotope $\boldsymbol{SP}(\boldsymbol{A})$ (cf. [Zie95, Cor. 7.17.]).

Proof. Let I be an ordered partition in $\overline{\Pi}(\boldsymbol{A})$, with corresponding surjection p_I, and associated to the linear form $u \in \mathbb{R}^d$. This linear form u is also associated to a covector X of $\mathcal{M}^{\mathsf{sw}}(\bar{\boldsymbol{A}})$ that is exactly the image of I by the above bijection:

$$\begin{aligned} X_{(i,j)} = 0 \quad &\Leftrightarrow \langle u, a_j - a_i \rangle = 0 \quad \Leftrightarrow p_I(i) = p_I(j), \\ X_{(i,j)} = + \quad &\Leftrightarrow \langle u, a_j - a_i \rangle > 0 \quad \Leftrightarrow p_I(i) < p_I(j), \\ X_{(i,j)} = - \quad &\Leftrightarrow \langle u, a_j - a_i \rangle < 0 \quad \Leftrightarrow p_I(i) > p_I(j). \end{aligned}$$

Hence both the sweeps of $\overline{\Pi}(\boldsymbol{A})$ and the covectors of $\mathcal{M}^{\mathsf{sw}}(\bar{\boldsymbol{A}})$ are in bijection with the cells of the hyperplane arrangement $\boldsymbol{\mathcal{SH}}(\boldsymbol{A})$ and the bijections induce poset isomorphisms. $\square$

It follows from the previous lemma that the set of sweep permutations $\Pi(\boldsymbol{A})$ is in bijection with the topes of the sweep oriented matroid $\mathcal{M}^{\mathsf{sw}}(\bar{\boldsymbol{A}})$. Since the topes of an oriented matroid completely determine it (cf. [BLS+99, Proposition 3.8.2]), this implies:

Corollary 3.3.4. *The set of sweep permutations* $\Pi(\boldsymbol{A})$ *determines the whole poset of sweeps* $\overline{\Pi}(\boldsymbol{A})$*.*

The structures we have introduced are related by the following hierarchy (whose proof depends on the upcoming Proposition 3.4.3):

Theorem 3.3.5. *Let* $\boldsymbol{A} \in \mathbb{R}^{d\times[n]}$ *be a point configuration. Then the set of sweep permutations* $\Pi(\boldsymbol{A})$*, the poset of sweeps* $\overline{\Pi}(\boldsymbol{A})$*, the sweep oriented matroid* $\mathcal{M}^{\mathsf{sw}}(\bar{\boldsymbol{A}})$ *and the big oriented matroid* $\mathcal{M}^{\mathsf{big}}(\bar{\boldsymbol{A}})$ *(cryptomorphically) determine each other. They determine the little oriented matroid* $\mathcal{M}^{\mathsf{lit}}(\bar{\boldsymbol{A}})$*, which does not always determine them.*

In particular, the sweep oriented matroid is a combinatorial invariant of a point configuration that is finer than the order type (given by the little oriented matroid).

Proof. The fact that $\Pi(\boldsymbol{A})$ and $\overline{\Pi}(\boldsymbol{A})$ determine each other follows from Corollary 3.3.4. The equivalence between $\overline{\Pi}(\boldsymbol{A})$ and $\mathcal{M}^{\mathsf{sw}}(\bar{\boldsymbol{A}})$ follows from Lemma 3.3.3. The equivalence between $\mathcal{M}^{\mathsf{sw}}(\bar{\boldsymbol{A}})$ and $\mathcal{M}^{\mathsf{big}}(\bar{\boldsymbol{A}})$ will be proved later, as a consequence of Definition 3.4.2 and Proposition 3.4.3.

Finally, $\mathcal{M}^{\mathsf{big}}(\bar{\boldsymbol{A}})$ determines $\mathcal{M}^{\mathsf{lit}}(\bar{\boldsymbol{A}})$ by restriction to the ground set $[n]$ but this operation is not injective. Examples of planar configurations with different sets of sweep permutations but the same little oriented matroid can be found in [BLS+99, Section 1.10]. □

3.3.3 Sweep oriented matroids

The main insight for expanding the notion of sweep oriented matroids from Definition 3.3.2 beyond the realizable case is to note that a configuration of vectors of the form $\boldsymbol{a}_j - \boldsymbol{a}_i$ for $(i,j) \in \binom{[n]}{2}$ is just the projection of the *braid configuration* $\{\boldsymbol{e}_j - \boldsymbol{e}_i \mid (i,j) \in \binom{[n]}{2}\} \in \mathbb{R}^{n\times\binom{[n]}{2}}$ (the set of positive roots of the Coxeter root system A_{n-1}) under the linear map $M_{\boldsymbol{A}}$ defined in (3.2).

Consider the oriented matroid $\boldsymbol{\mathcal{B}}_n$ associated to the braid configuration, that is, the graphic oriented matroid of the complete graph K_n with the acyclic orientation induced by the usual order on $[n]$. We will use the same notation $\boldsymbol{\mathcal{B}}_n$ as with the hyperplane arrangement, as it will be always clear from the context whether we are considering the hyperplane arrangement or the associated oriented matroid. Note that, since the configuration of the $\boldsymbol{a}_j - \boldsymbol{a}_i$ is a linear projection of the braid configuration, every covector of $\mathcal{M}^{\mathsf{sw}}(\bar{\boldsymbol{A}})$ is a covector of the braid oriented matroid, as we can pull back linear forms with $M_{\boldsymbol{A}}^*$.

The oriented matroid analogues of linear projections are *strong maps*. For two oriented matroids $\mathcal{M}_1$ and $\mathcal{M}_2$ on the same ground set, we say that there is a *strong map* from $\mathcal{M}_1$ to $\mathcal{M}_2$, denoted $\mathcal{M}_1 \to \mathcal{M}_2$, if every covector of $\mathcal{M}_2$ is a covector of $\mathcal{M}_1$ (see [BLS+99, Sec. 7.7]). This will be the starting point for our definition.

Definition 3.3.6. An oriented matroid $\mathcal{M}$ on the ground set $\binom{[n]}{2}$ is a *sweep oriented matroid* if there is a strong map $\boldsymbol{\mathcal{B}}_n \to \mathcal{M}$ from $\boldsymbol{\mathcal{B}}_n$ to $\mathcal{M}$, i.e. if all covectors of $\mathcal{M}$ are covectors of $\boldsymbol{\mathcal{B}}_n$.

Remark 3.3.7. Note that, if $\mathcal{M}$ is a sweep oriented matroid, then we can interpret its covectors as covectors of the braid arrangement, and hence each covector can be uniquely identified with an ordered partition via the bijection inverse to (3.4). For a covector $X \in \mathcal{M}$ of a sweep oriented matroid, we will denote by I_X the associated ordered partition.

Our next result characterizes sweep oriented matroids via a 3-term orthogonality condition on covectors (c.f. [BLS⁺99, Sec. 3.4]) that provides an explicit test for deciding whether an oriented matroid is a sweep oriented matroid. It will be relevant later in the context of sweep acycloids in Section 3.7.

Recall that the *support* of a sign-vector $X \in \{+,-,0\}^E$ is $\underline{X} = \{e \in E \,|\, X_e \neq 0\}$. Two sign-vectors $X, Y \in \{+,-,0\}^E$ are said to be *orthogonal* if either $\underline{X} \cap \underline{Y} = \emptyset$, or the restrictions of X and Y to $\underline{X} \cap \underline{Y}$ are neither equal nor opposite (i.e., there are i, j with $X_i = Y_i \neq 0$ and $X_j = -Y_j \neq 0$).

Lemma 3.3.8. *An oriented matroid $\mathcal{M}$ on $\binom{[n]}{2}$ is a sweep oriented matroid if and only if for every covector X and every choice of $1 \leq i < j < k \leq n$, the triple $(X_{(i,j)}, X_{(j,k)}, X_{(i,k)})$ is orthogonal to the sign vector $(+,+,-)$.*

Equivalently, $\mathcal{M}$ is a sweep oriented matroid if and only if for any covector X, and for $1 \leq i < j < k \leq n$, the triple $(X_{(i,j)}, X_{(j,k)}, X_{(i,k)})$ does not belong to the following list of forbidden patterns:

$$\left\{ \begin{array}{ccccccc} (+,+,-), & (-,-,+), & (0,+,-), & (0,-,+), & (+,0,-), & (-,0,+), & (+,+,0), \\ (-,-,0), & (0,0,-), & (0,0,+), & (0,+,0), & (0,-,0), & (+,0,0), & (-,0,0) \end{array} \right\}.$$

Proof. There is a strong map $\boldsymbol{\mathcal{B}}_n \to \mathcal{M}$ if and only if all the covectors of $\mathcal{M}$ are covectors of $\boldsymbol{\mathcal{B}}_n$, which is equivalent to the condition that all the covectors of $\mathcal{M}$ are orthogonal to all circuits of $\boldsymbol{\mathcal{B}}_n$ (see [BLS⁺99, Prop. 7.7.1]).

The circuits of $\boldsymbol{\mathcal{B}}_n$ are induced by cycles of K_n. They are of the form $C^{i_1,\dots,i_r}$ for any collection $i_1, \dots, i_r$ of at least 3 distinct elements of $[n]$, with $C^{i_1,\dots,i_r}_{(i_k,i_{k+1})} = +$ if $i_k < i_{k+1}$ and $C^{i_1,\dots,i_r}_{(i_{k+1},i_k)} = -$ if $i_k > i_{k+1}$ for all $1 \leq k \leq r$ (with the convention $i_{r+1} = i_1$), and $C^{i_1,\dots,i_r}_{(h,l)} = 0$ for any other pair.

An easy induction shows that the orthogonality to the circuit $C^{i_1,\dots,i_r}$ is implied by the orthogonality to all circuits $C^{i_1,i_k,i_{k+1}}$ for $2 \leq k \leq r-1$, which is equivalent to our statement. □

This condition is actually a reformulation of the transitivity of the partial order induced by an ordered partition I (namely $i \preceq j$ if and only if $p_I(i) \leq p_I(j)$). For example, forbidding the patterns $(+,+,-)$ and $(+,+,0)$ is equivalent to stating that $i \prec j \prec k$ implies $i \prec k$, and so on. This is why we refer to it as the *transitivity condition* on sweep oriented matroids.

The *poset of sweeps* of a sweep oriented matroid $\mathcal{M}$ is the partially ordered set $\overline{\Pi}(\mathcal{M})$ of the ordered partitions I_X for the covectors $X \in \mathcal{M}$, ordered by refinement. Enlarged with a top element $\hat{\mathbf{1}}$, this poset is isomorphic to the big face lattice of $\mathcal{M}$. The topology of such complexes is well known [BLS+99, Thm. 4.3.3]. We describe it in the following proposition. Note that there is some ambiguity in the literature concerning the definition of the poset of faces of cell complexes, in particular whether it should be augmented by a bottom element or not (compare [Bjö84, Fig. 2] and [Bjö95, Fig. 2]). We follow [Bjö95] and [BLS+99] and do not include an additional bottom element in the definition of the *face poset* of a cell complex.

Proposition 3.3.9 ([BLS+99, Thm. 4.3.3])**.** *The poset of sweeps $\overline{\Pi}(\mathcal{M}) \smallsetminus ([n])$ of a sweep oriented matroid $\mathcal{M}$ of rank r without the trivial sweep is isomorphic to the face poset of a shellable regular cell decomposition of the $(r-1)$-sphere. In particular, the order complex $\Delta\left(\overline{\Pi}(\mathcal{M}) \smallsetminus ([n])\right)$ triangulates the $(r-1)$-sphere.*

3.4 Big and little oriented matroids

In this section we show how the big and little oriented matroids of a point configuration (Definition 3.3.2) are completely determined by its sweep oriented matroid. Actually, the construction of these matroids can be extended to any abstract sweep oriented matroid, providing definitions beyond the realizable case. This generalizes the results for rank 3 proved in [BLS+99, Sec. 1.10].

3.4.1 Big and little oriented matroids associated to sweep oriented matroids

First, we will show how to extend any sweep oriented matroid to what will be called a big oriented matroid. For a covector X of a sweep oriented matroid, let $p_X : [n] \to [l_X]$ be the surjection associated to the corresponding ordered partition. For each $1 \leq k \leq 2l_X + 1$, let $X^k \in \{+, -, 0\}^{[n] \cup \binom{[n]}{2}}$ be the sign-vector:

$$X_i^k = \begin{cases} - & \text{if } p_X(i) \leq \lfloor \frac{k-1}{2} \rfloor, \\ + & \text{if } p_X(i) > \lfloor \frac{k}{2} \rfloor, \\ 0 & \text{if } k \text{ is even and } p_X(i) = \frac{k}{2}. \end{cases} \qquad \text{for } 1 \leq i \leq n;$$

$$X_{(i,j)}^k = X_{(i,j)} \qquad \text{for all } 1 \leq i < j \leq n.$$

Theorem 3.4.1. *If $\mathcal{M}$ is the set of covectors of a sweep oriented matroid, then*

$$\mathcal{M}^{\mathit{big}} = \left\{ X^k \,\middle|\, X \in \mathcal{M},\ 1 \leq k \leq 2l_X + 1 \right\}$$

is the set of covectors of an oriented matroid.

Proof. We have to check that $\mathcal{M}$ satisfies the axioms of Definition 3.3.1, namely:

(V0) $\mathbf{0} \in \mathcal{M}^{\mathsf{big}}$,

(V1) $X \in \mathcal{M}^{\mathsf{big}}$ implies $-X \in \mathcal{M}^{\mathsf{big}}$,

(V2) $X, Y \in \mathcal{M}^{\mathsf{big}}$ implies $X \circ Y \in \mathcal{M}^{\mathsf{big}}$,

(V3) if $X, Y \in \mathcal{M}^{\mathsf{big}}$ and $e \in S(X, Y)$ then there exists $Z \in \mathcal{M}^{\mathsf{big}}$ such that $Z_e = 0$ and $Z_f = (X \circ Y)_f$ for all $f \notin S(X, Y)$.

$(V0)$ $\mathbf{0}_n \in \mathcal{M}$, associated to the one part ordered partition $(\{1, 2, \ldots, n\})$. Then $(\mathbf{0}_n)^2$ is the zero vector and it is in $\mathcal{M}^{\mathsf{big}}$.

$(V1)$ Let X^k be an element of $\mathcal{M}^{\mathsf{big}}$. Then, $-X^k = (-X)^{2l_X+2-k}$, so it is still in $\mathcal{M}^{\mathsf{big}}$.

$(V2)$ Let X^k, Y^h be two elements of $\mathcal{M}^{\mathsf{big}}$. Then $X^k \circ Y^h = (X \circ Y)^t$, where $t = 2(r_1 + \ldots + r_{\frac{k-1}{2}-1}) + 1$ if k is odd (with the same notations as in the definition of the composition between two ordered partitions), $t = 2(r_1 + \ldots + r_{\frac{k}{2}-1}) + j$ if k is even and j is the index corresponding to h when the elements of I_k are ordered according to Y (that is to say, for all $i \in I_k$, $p_{X \circ Y}(i) \le \lfloor \frac{t-1}{2} \rfloor \Leftrightarrow p_Y(i) \le \lfloor \frac{h-1}{2} \rfloor$ and $p_{X \circ Y}(i) > \lfloor \frac{t}{2} \rfloor \Leftrightarrow \lfloor p_Y(i) \rfloor > \lfloor \frac{h}{2} \rfloor$).

$(V3)$ Let X^k, Y^h be two elements of $\mathcal{M}^{\mathsf{big}}$, and $e \in S(X^k, Y^h)$. It remains to find $Z \in \mathcal{M}$ and $r \in \{1, \ldots, 2l_Z + 1\}$ such that $(Z^r)_e = 0$ and $(Z^r)_f = (X^k \circ Y^h)_f$ for any $f \notin S(X^k, Y^h)$. e can be of two types: $e = (i, j)$ or $e = i$.

In both cases, it will be convenient to define

$$\begin{aligned}
E_- &= \Big\{p \mid 1 \le p \le n \text{ and } \{(X^k)_p, (Y^h)_p\} \in \{\{-, -\}, \{0, -\}\}\Big\} \\
&= \Big\{p \in \{1, \ldots, n\} \setminus S(X^k, Y^h) \mid (X^k \circ Y^h)_p = -\Big\}, \\
E_+ &= \Big\{p \mid 1 \le p \le n \text{ and } \{(X^k)_p, (Y^h)_p\} \in \{\{+, +\}, \{0, +\}\Big\}, \\
E_0 &= \Big\{p \mid 1 \le p \le n \text{ and } \{(X^k)_p, (Y^h)_p\} = \{0, 0\}\Big\}.
\end{aligned}$$

Then $E_- \cup E_+ \cup E_0 = \{1, \ldots, n\} \setminus S(X^k, Y^h)$ and part of the condition is that $(Z^r)_p = \varepsilon$ for all $p \in E_\varepsilon$, $\varepsilon \in \{-, +, 0\}$.

1) If $e = (i, j)$, up to exchanging X^k and Y^h, one can suppose that $X_{(i,j)} = -$ and $Y_{(i,j)} = +$. Let $Z \in \mathcal{M}$ be given by $(V3)$ on $\mathcal{M}$. For any r we will have that $(Z^r)_e = 0$ and $(Z^r)_f = (X^k \circ Y^h)_f$ for any $f \notin S(X^k, Y^h)$ of the form $f = (p, q)$, because in that case, f is an index for X and Y that is not in $S(X, Y)$. Can we find r such that $(Z^r)_p = (X^k \circ Y^h)_p$ for any $1 \le p \le n$ such that $p \notin S(X^k, Y^h)$? It is sufficient to check that $p_Z(p) < p_Z(q)$ for all $(p, q) \in E_- \times E_+ \cup E_- \times E_0 \cup E_0 \times E_+$ and $p_Z(p) = p_Z(q)$ for all $(p, q) \in E_0 \times E_0$. $(p, q) \in E_0 \times E_0$ and $p < q$ implies that $X_{(p,q)} = Y_{(p,q)} = 0$, hence $Z_{(p,q)} = 0$ and $p_Z(p) = p_Z(q)$.

If $E_0 \neq \emptyset$, we take $r = 2p_Z(q)$ for any $q \in E_0$. Then, we treat the case $(p, q) \in E_- \times E_0$, since the case $(p, q) \in E_0 \times E_+$ is similar. If $p < q$, then $\{(X^k)_{(p,q)}, (Y^h)_{(p,q)}\} \in$

$\{\{+,+\},\{+,0\}\}$ and $Z_{(p,q)} = +$. If $p > q$, then $\{(X^k)_{(q,p)}, (Y^h)_{(q,p)}\} \in \{\{-,-\},\{-,0\}\}$ and $Z_{(q,p)} = -$. In any case, $p_Z(p) < p_Z(q)$, thus $(Z^r)_p = -$.

If $E_0 = \emptyset$, there may be several possibilities for r. The same reasoning as precedently shows that for any $(p,q) \in E_- \times E_+$, $p_Z(p) < p_Z(q)$. Hence there is at least one appropriate r which separates the parts that contain elements in E_- from parts that contain elements in E_+.

2) If $e = i$ for some $1 \leq i \leq n$, up to exchanging X^k and Y^h, one can suppose that $(X^k)_i = -$ and $(Y^h)_i = +$.

First, we consider the case where $E_0 = \emptyset$. We take $Z = X \circ Y$ and $r = 2p_{X\circ Y}(i)$ (corresponding to the part of i in Z). It only remains to check that if $p \in E_-$ (resp. E_+), than $(Z^r)_p = -$ (resp. $+$).

$p \in E_- \Rightarrow p_Y(p) < p_Y(i) \Rightarrow p_Z(p) < p_Z(i) \Rightarrow (Z^r)_p = -$,

$p \in E_+ \Rightarrow p_X(p) > p_X(i) \Rightarrow p_Z(p) > p_Z(i) \Rightarrow (Z^r)_p = +$.

If $E_0 \neq \emptyset$, let j be the smallest element of E_0. Than $p_X(i) < p_X(j)$ and $p_Y(i) > p_Y(j)$, thus $(i,j) \in S(X,Y)$. Let $Z \in \mathcal{M}$ be given by axiom $(V3)$ applied to $\mathcal{M}$ with X, Y and (i,j). Than, for any $k \in E_0$ other than j, $Z_{(j,k)} = 0$ because $X_{(j,k)} = 0$ and $Y_{(j,k)} = 0$ (resp. $Z_{(k,j)} = 0$ because $X_{(k,j)} = 0$ and $Y_{(k,j)} = 0$), and thus $Z_{(i,k)} = 0$ (resp. $Z_{(k,i)} = 0$), because $Z_{(i,j)} = 0$ and $\mathcal{M}$ satisfies the transitivity condition from Lemma 3.3.8. We choose $r = 2p_Z(i)$ (corresponding to the part of Z that contains i and all $k \in E_0$). Then:

$$p \in E_- \quad\Rightarrow\quad \begin{cases} p_X(p) < p_X(j) \\ p_Y(p) \leq p_Y(j) \end{cases} \text{or} \quad \begin{cases} p_X(p) = p_X(j) \\ p_Y(p) < p_Y(j) \end{cases} \quad\Rightarrow\quad p_Z(p) < p_Z(j) \quad\Rightarrow\quad (Z^r)_p = -,$$

$$p \in E_+ \quad\Rightarrow\quad \begin{cases} p_X(p) > p_X(i) \\ p_Y(p) \geq p_Y(j) \end{cases} \text{or} \quad \begin{cases} p_X(p) = p_X(i) \\ p_Y(p) > p_Y(j) \end{cases} \quad\Rightarrow\quad p_Z(p) > p_Z(j) \quad\Rightarrow\quad (Z^r)_p = +.$$

$\square$

Definition 3.4.2. Let $\mathcal{M}$ be a sweep oriented matroid. The oriented matroid $\mathcal{M}^{big}$ is the *big oriented matroid* of $\mathcal{M}$; and the oriented matroid $\mathcal{M}^{lit}$ obtained by deleting all pairs (i,j) from $\mathcal{M}^{\mathsf{big}}$ is the *little oriented matroid* of $\mathcal{M}$.

These definitions are indeed coherent with the realizable case, as the following proposition shows. This proves that the sweep oriented matroid of a point configuration determines its big and little oriented matroids, concluding the proof of Theorem 3.3.5.

Proposition 3.4.3. *The big and little oriented matroids of a point configuration are the big and little oriented matroids associated to its sweep oriented matroid.*

Proof. Let $\boldsymbol{A} = (\boldsymbol{a}_1, \ldots, \boldsymbol{a}_n) \in \mathbb{R}^{d\times[n]}$ be a d-dimensional point configuration. Every vector $\boldsymbol{u} \in \mathbb{R}^d$ induces an ordering of $\boldsymbol{A}$, which is encoded in a covector X of $\mathcal{M}^{\mathsf{sw}}(\bar{\boldsymbol{A}})$. For $c \in \mathbb{R}$, the partition

$$\{i \,|\, \langle \boldsymbol{u}, \boldsymbol{a}_i\rangle < c\}\,, \{i \,|\, \langle \boldsymbol{u}, \boldsymbol{a}_i\rangle = c\}\,, \{i \,|\, \langle \boldsymbol{u}, \boldsymbol{a}_i\rangle > c\}$$

only depends on which, or between which pair, of the l_X values attained by $\langle \boldsymbol{p}u, \cdot\, \rangle$ on $\boldsymbol{A}$ does c lie. These $2l_X + 1$ distinct partitions are precisely those encoded by the covectors X^k defining the big oriented matroid of $\mathcal{M}^{\mathsf{sw}}(\bar{\boldsymbol{A}})$. $\square$

Note that, by the definition of the big oriented matroid of $\mathcal{M}$, the zero covector $\mathbf{0}$ of $\mathcal{M}$ induces the all-positive tope $+_n$ in $\mathcal{M}^{\mathsf{lit}}$, which is hence an acyclic oriented matroid.

The following lemma concerning the ranks of the big and little oriented matroids will be needed later.

Lemma 3.4.4. *If the sweep oriented matroid $\mathcal{M}$ is of rank r, then $\mathcal{M}^{\mathsf{big}}$ and $\mathcal{M}^{\mathsf{lit}}$ are of rank $r+1$.*

Proof. To justify that $\mathcal{M}^{\mathsf{big}}$ has rank $r+1$, it is sufficient to notice that if $\mathbf{0}_{\binom{[n]}{2}} = Y^0 \prec Y^1 \prec \cdots \prec Y^r$ is a maximal chain of covectors of $\mathcal{M}$, then $\mathbf{0}_{[n]\cup\binom{[n]}{2}} = Z^{-1} \prec Z^0 \prec Z^1 \prec \cdots \prec Z^r$ is a maximal chain of covectors of $\mathcal{M}^{\mathsf{big}}$, where for any $k \in \{0, \dots, r\}$, we define Z^k by $Z^k\big|_{\binom{[n]}{2}} = Y^k$ and $Z^k\big|_{[n]} = +_n$. Indeed, we cannot add a covector Z in the big oriented matroid between Z^{-1} and Z^0 because if $Z_i = 0$ and $Z_j = +$ we necessarily have $Z_{(i,j)} \neq 0$ since i and j are not in the same part of the ordered partition l_Z. We cannot add a covector strictly between Z^k and Z^{k+1} either because its restriction to $\binom{[n]}{2}$ would give a covector of $\mathcal{M}$ strictly between Y^k and Y^{k+1}.

We prove that $\mathcal{M}^{\mathsf{lit}}$ also has rank $r+1$ by induction on r. If $\mathcal{M}$ is of rank $r = 0$, then $\mathbf{0}_{\binom{[n]}{2}}$ is its only covector. It induces the little oriented matroid of rank 1 consisting of the covectors $-_n$, $\mathbf{0}_n$, and $+_n$.

Now, suppose that $\mathcal{M}$ is a sweep oriented matroid on ground set $\binom{[n]}{2}$ that has rank $r \geq 1$. Up to relabelling, we can suppose that $(n-1, n)$ is not a loop. Then the contraction of $\mathcal{M}$ along $\{(n-1, n)\}$ has rank $r-1$. Under the bijection (3.4), the covectors of this contraction $\mathcal{M}/_{\{(n-1,n)\}}$ correspond to the partitions associated to covectors of $\mathcal{M}$ such that $n-1$ and n are in the same part. This implies that for all $i \leq n-2$, the pairs $(i, n-1)$ and (i, n) are parallel. By deleting all the pairs (i, n) we obtain an oriented matroid $\mathcal{M}'$ on $\binom{[n-1]}{2}$ isomorphic to $\mathcal{M}/_{\{(n-1,n)\}}$. The transitivity condition from Lemma 3.3.8 is preserved, and hence $\mathcal{M}'$ is a sweep oriented matroid of rank $r-1$ and $\mathcal{M}'^{\mathsf{lit}}$ has rank r, by induction. A maximal chain of the contraction $\mathcal{M}'^{\mathsf{lit}}/(n-1)$ induces a chain $\mathbf{0}_n = X^0 \prec \cdots \prec X^{r-1}$ of $\mathcal{M}^{\mathsf{lit}}$ in which $(X^i)_{n-1} = (X^i)_n = 0$ for all $0 \leq i \leq r-1$ and that is maximal with this property. Since $n-1$ and n are not parallel (because $(n-1, n)$ is not a loop), there is a covector Y of $\mathcal{M}^{\mathsf{lit}}$ such that $Y_{n-1} = +$ and $Y_n = 0$. Setting $X^r = X^{r-1} \circ Y$, and $X^{r+1} = X^r \circ +_n$, we obtain a chain

$$\mathbf{0}_n = X^0 \prec \cdots \prec X^{r-1} \prec X^r \prec X^{r+1}$$

of lenght $r+1$ of covectors of $\mathcal{M}^{\mathsf{lit}}$. Moreover, the restriction operation on oriented matroids cannot increase the rank, thus the rank of $\mathcal{M}^{\mathsf{lit}}$ cannot be bigger than the rank of $\mathcal{M}^{\mathsf{big}}$. Hence $\mathcal{M}^{\mathsf{lit}}$ also has rank $r+1$. $\square$

Example 3.4.5 (The braid oriented matroids in types A and B). The study of big oriented matroids of Coxeter hyperplane arrangements in types A and B unveils a recursive decomposition that, in view of the upcoming Section 3.4.2, explains the existence of a maximal chain of modular flats. This important property was first studied by Stanley under the name of *supersolvability* [Sta72].

Type A. The big oriented matroid of the braid oriented matroid $\boldsymbol{\mathcal{B}}_n$ is the braid oriented matroid $\boldsymbol{\mathcal{B}}_{n+1}$. More precisely, if we relabel the elements $i \in [n]$ by $(1, i+1)$ and the elements $(i,j) \in \binom{[n]}{2}$ by $(i+1, j+1)$, then we recover the braid oriented matroid $\boldsymbol{\mathcal{B}}_{n+1}$. Indeed, the topes of $\boldsymbol{\mathcal{B}}_n{}^{\mathsf{big}}$ are of the form X^{2k+1} where X is a tope of $\boldsymbol{\mathcal{B}}_n$ and $0 \leq k \leq n$. If X corresponds to the permutation $(\sigma(1), \dots, \sigma(n)) \in \mathfrak{S}_n$, then X^{2k+1} corresponds to the permutation in $\mathfrak{S}_{n+1}$:

$$(\sigma(1)+1, \dots, \sigma(k)+1, 1, \sigma(k+1)+1, \dots, \sigma(n)+1).$$

Type B. Consider the type B braid oriented matroid $\boldsymbol{\mathcal{B}}_n^B$ from Section 3.2.2, indexed by the elements in $\binom{[\pm n]}{2}$. That is, $\boldsymbol{\mathcal{B}}_n^B$ is the sweep oriented matroid of the vertex set of the cross-polytope. Then its big oriented matroid $(\boldsymbol{\mathcal{B}}_n^B)^{\mathsf{big}}$ is FL-isomorphic to $\boldsymbol{\mathcal{B}}_{n+1}^B$ without one element (of those of the form $(-i, i)$).

To see it, it is easier to consider first an enlarged version, with base elements

$$[-n, n] = \{-n, \dots, -1, 0, 1, \dots, n\}$$

corresponding to the point configuration

$$\widetilde{\boldsymbol{B}}_n = (-\boldsymbol{e}_n, \dots, -\boldsymbol{e}_1, \boldsymbol{0}, \boldsymbol{e}_1, \dots, \boldsymbol{e}_n)$$

that contains the vertices of the cross-polytope together with the origin. The FL-isomorphism class of the sweep oriented matroid does not change, but we get some new parallel elements. Namely, the elements labeled $(-i, i)$, $(-i, 0)$, and $(0, i)$ become parallel (with the same orientation) in the enlarged sweep oriented matroid $\widetilde{\boldsymbol{\mathcal{B}}}_n^B = \mathcal{M}^{\mathsf{sw}}(\widetilde{\boldsymbol{B}}_n)$. Now, relabel the elements $[-n, n] \cup \binom{[-n,n]}{2}$ to $\binom{[-n-1,n+1]}{2}$ by sending each $i \in [\pm n]$ to the pair of parallel elements $(-n-1, -i), (i, n+1)$; 0 to the triple of parallel elements $(-n-1, n+1), (-n-1, 0), (0, n+1)$; and leaving the pairs in $\binom{[-n,n]}{2}$ unchanged. Each tope X of the sweep oriented matroid $\widetilde{\boldsymbol{\mathcal{B}}}_n^B$ is represented by a centrally symmetric permutation σ of $[-n, n]$:

$$(-\sigma(n), \dots, -\sigma(1), 0, \sigma(1), \dots, \sigma(n)).$$

Under the relabeling we can read the topes X^{2k+1} of the big oriented matroid $(\widetilde{\boldsymbol{\mathcal{B}}}_n^B)^{\mathsf{big}}$ as centrally symmetric permutations of $[-n-1, n+1]$ representing topes of $\widetilde{\boldsymbol{\mathcal{B}}}_{n+1}^B$. Namely, for $0 \leq k \leq n+1$, the tope X^{2k+1} corresponds to the centrally symmetric permutation:

$$(-\sigma(n), \dots, -\sigma(n-k+1), -n-1, -\sigma(n-k), \dots, \sigma(n-k), n+1, \sigma(n+1-k), \dots \sigma(n)).$$

whereas for $n+2 \leq k \leq 2n+2$ it corresponds to:

$$(-\sigma(n), \dots, -\sigma(n-k+1), n+1, -\sigma(n-k), \dots, \sigma(n-k), -n-1, \sigma(n+1-k), \dots \sigma(n)).$$

This shows that $(\widetilde{\boldsymbol{\mathcal{B}}}_n^B)^{\mathsf{big}}$ is FL-isomorphic to $\widetilde{\boldsymbol{\mathcal{B}}}_{n+1}^B$, and hence to $\boldsymbol{\mathcal{B}}_{n+1}^B$.

If we want to consider the original configuration without the origin, we simply need to remove all the elements of the big oriented matroid that involve a label using 0. Every parallelism class conserves at least one representative except for the singleton 0, which was sent to the triple $(-n-1, n+1), (-n-1, 0), (0, n+1)$ with our relabeling. This shows that $(\boldsymbol{\mathcal{B}}_n^B)^{\mathsf{big}}$ is FL-isomorphic to $\boldsymbol{\mathcal{B}}_{n+1}^B \setminus (-n-1, n+1)$. □

Remark 3.4.6 (On labeling and isomorphism). The labeling plays an important role in the definition of a sweep oriented matroid and in Theorem 3.3.5. Indeed, non-isomorphic big oriented matroids might arise from isomorphic sweep oriented matroids. (Here, we mean FL-isomorphism, but the statement is also true for the other standard notions of oriented matroid isomorphism.) For example, all sufficiently generic planar n-point configurations give rise to FL-isomorphic sweep oriented matroids but their big oriented matroids are not FL-isomorphic.

Remark 3.4.7 (On realizability). Note that, for a big oriented matroid $\mathcal{M}$, realizability as an oriented matroid (i.e. in the sense of (3.3)) is equivalent to realizability as a big oriented matroid (i.e. in the sense of Definition 3.3.2). Indeed, any point configuration $\boldsymbol{A}$ such that $\mathcal{M}^{\mathsf{big}}(\bar{\boldsymbol{A}}) = \mathcal{M}$ can be extended (with the corresponding points at infinity) to an oriented matroid realization of $\mathcal{M}$. And reciprocally, the restriction of any oriented matroid realization of $\mathcal{M}$ to the elements indexed by $[n]$ can be sent, after a suitable projective transformation and dehomogenization, to a point configuration $\boldsymbol{A}$ such that $\mathcal{M}^{\mathsf{big}}(\bar{\boldsymbol{A}}) = \mathcal{M}$.

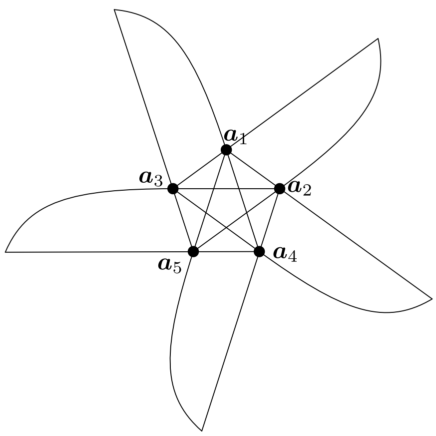

Figure 3.10: The allowable sequence $(1,2,3,4,5) \to (1,2,4,3,5) \to (2,1,4,3,5) \to (2,1,4,5,3) \to (2,4,1,5,3) \to (2,4,5,1,3) \to (4,2,5,1,3) \to (4,5,2,1,3) \to (4,5,2,3,1) \to (4,5,3,2,1) \to (5,4,3,2,1)$ cannot be realized by a point configuration, because it would necessarily be a pentagon whose sides and "parallel diagonals" meet as in the above picture, which is geometrically impossible [GP80a].

In contrast, there are sweep oriented matroids that are realizable as an oriented matroid but that are not of the form $\mathcal{M}^{\mathsf{sw}}(\bar{\boldsymbol{A}})$ for any point configuration $\boldsymbol{A}$. Indeed, the non-realizable pentagon of [GP80a] (see Figure 3.10) gives rise to a non-realizable allowable sequence; that is, to a non-realizable big oriented matroid of rank 3. The associated sweep oriented matroid is an oriented matroid of rank 2, and thus realizable (as an oriented matroid) [BLS+99, Cor. 8.2.3]. However, it is not the sweep oriented matroid of a point configuration, because the corresponding big oriented matroid is not realizable.

We end this remark by noting that the Universality Theorem for allowable sequences of Hoffmann and Merckx [HM18] implies that it is $(\exists\mathbb{R})$-hard to decide whether a big oriented matroid is realizable.

3.4.2 Big oriented matroids and tight modular hyperplanes

In this section we provide an alternative characterization of the FL-isomorphism classes of big oriented matroids, and hence of sweep oriented matroids. It is purely structural, without relying on the labeling of the elements. We show that they are closely related to the concept of modular hyperplanes.

According to our definition, every big oriented matroid $\mathcal{M}^{\mathsf{big}}$ on $[n] \cup \binom{[n]}{2}$ contains the cocircuit $Z = (+_n, \mathbf{0}_{\binom{n}{2}})$. Moreover, $X_{(i,j)} = 0$ for any covector X such that $X_i = X_j = 0$; which is equivalent to the fact that for any i, j not in the same parallelism class, the restriction of $\mathcal{M}^{\mathsf{big}}$ to the set $\{i, j, (i,j)\} \subset E$ has rank 2. These two properties show that the set of indices $\binom{[n]}{2}$ form a *modular hyperplane*.

The *flats* of an oriented matroid $\mathcal{M}$ of rank r on E are the flats of its underlying (unoriented) matroid $\underline{\mathcal{M}}$; that is, the zero-sets of its covectors. The poset of flats ordered by inclusion forms a geometric lattice [BLS+99, 4.1.13]. The *hyperplanes* are the flats of rank $r-1$, and they arise as zero-sets of cocircuits. A flat F is called *modular* if $\mathrm{rk}(F) + \mathrm{rk}(G) = \mathrm{rk}(F \wedge G) + \mathrm{rk}(F \vee G)$ for any other flat G, where $\mathrm{rk}(\cdot)$ is the rank function of the geometric lattice (for a flat F, $\mathrm{rk}(F)$ coincides with the rank of the oriented matroid $\mathcal{M}\big|_F$). Modular flats have many interesting properties, and play an important role in the theory of matroids, see [Sta71] and [Bry75].

Hence, a *modular hyperplane* is a hyperplane $F \subset E$ such that $\mathrm{rk}(F \wedge G) = \mathrm{rk}(F \cap G) = \mathrm{rk}(G) - 1$ for any flat G not contained in F. Said differently, $F \cap G$ is a hyperplane in $\mathcal{M}\big|_F$. In [Bry75, Cor. 3.4] it is shown that a hyperplane is modular if and only if it intersects every line (flat G with $\mathrm{rk}(G) = 2$). Equivalently, if for every pair of elements $x, y \in E \setminus F$ that are not parallel nor a loop, there is some element $z \in F$ such that for every covector X with $X_x = X_y = 0$ we have $X_z = 0$. We will say that a modular hyperplane F is *tight* if there is no $z \in F$ such that $F \setminus z$ is a modular hyperplane of $\mathcal{M}\big|_{E \setminus z}$.

The following result gives a characterization of big oriented matroids similar to the one given in [BLS+99, Sect. 6.4] for the rank 3 case.

Proposition 3.4.8. *Let $\mathcal{M}$ be an oriented matroid on ground set $E = [n] \cup \binom{[n]}{2}$ such that:*

1. *there exists a cocircuit Z of $\mathcal{M}$ such that $\{e \in E \mid Z_e = 0\} = \binom{[n]}{2}$ (i.e. $\underline{Z} = [n]$),*
2. *for any $(i,j) \in \binom{[n]}{2}$, for any covector X of $\mathcal{M}$, if two coordinates among X_i, X_j, $X_{(i,j)}$ are zero, then the third one is zero too.*

Then, up to reorientation, $\mathcal{M}$ is the big oriented matroid of the sweep oriented matroid $\mathcal{M}|_{\binom{[n]}{2}}$.

In a realizable setting, and without parallel elements and loops, the conditions on $\mathcal{M}$ amount to asking that the real vector representing (i, j) is in the intersection of the 2-plane spanned by the real vectors representing i and j and the hyperplane given by the cocircuit Z (which contains all the vectors corresponding to elements in $\binom{[n]}{2}$). One can check that the example depicted in Figure 3.8 satisfies this condition.

Proof. We need to prove that, after the reorientation of some elements of the ground set, the restriction $\mathcal{M}|_{\binom{[n]}{2}}$ is a sweep oriented matroid, i.e. it satisfies Lemma 3.3.8, and the covectors of $\mathcal{M}$ are exactly those obtained from the covectors of $\mathcal{M}|_{\binom{[n]}{2}}$ as in Theorem 3.4.1.

We can assume that, after a suitable reorientation of $\mathcal{M}$ we have that $Z = (+_n, \mathbf{0}_{\binom{[n]}{2}})$. Note that $\mathcal{M}|_{[n]}$ cannot have loops, as witnessed by Z; and that if i and j are parallel, then (i, j) must be a loop. We will from now on assume that $\mathcal{M}$ does not have parallel elements, as it simplifies the exposition.

Let us show that for any two covectors $X, Y \in \mathcal{M}$ such that $X_i = Y_i = -$, $X_j = Y_j = +$ we have $X_{(i,j)} = Y_{(i,j)} \neq 0$. Assume the contrary. Then the axiom 3.3.1 on oriented matroids would imply the existence of a covector $T \in \mathcal{M}$ such that $T_i = -$, $T_j = +$ and $T_{(i,j)} = 0$. A second application of the axiom 3.3.1 between T and Z would give the existence of a covector $T' \in \mathcal{M}$ such that $T'_i = T'_{(i,j)} = 0$ and $T'_j = +$, which contradicts the second assumption on $\mathcal{M}$. Hence, we can reorient (i, j) so that for any covector X of $\mathcal{M}$ with $X_i = -$ and $X_j = +$, we have $X_{(i,j)} = +$.

To check that $\mathcal{M}|_{\binom{[n]}{2}}$ is a sweep oriented matroid, it suffices to look at all restrictions of the form

$$\mathcal{M}|_{\{i,j,k,(i,j),(j,k),(i,k)\}}$$

for $1 \leq i < j < k \leq n$. This gives an oriented matroid of rank at most 3. One can easily check that with our conditions there are only three possible configurations, none of which violates the condition from Lemma 3.3.8.

Moreover, it is clear that any covector X of $\mathcal{M}$ can be obtained from the covector $X|_{\binom{[n]}{2}}$ of $\mathcal{M}|_{\binom{[n]}{2}}$ by the method described at the beginning of Section 3.4.1. Indeed, our reorientation on $\binom{[n]}{2}$ implies that the ordered partition of $[n]$ given by $(I_- = \{i \,|\, X_i = -\}, I_0 = \{i \,|\, X_i = 0\}, I_+ = \{i \,|\, X_i = +\})$ is refined by the ordered partition J induced by $X|_{\binom{[n]}{2}}$, in such a way that either $I_0 = \emptyset$ or I_0 is an entire part of J. Thus X is of the form $(X|_{\binom{[n]}{2}})^k$ for some k.

It remains to check that, for every covector $Y \in \mathcal{M}|_{\binom{[n]}{2}}$, all covectors Y^k obtained by the method described in Section 3.4.1 are indeed covectors of $\mathcal{M}$. We do it by induction on k. Observe first that $Y^1 = Z \circ \tilde{Y}$, where $\tilde{Y}$ is any covector in $\mathcal{M}$ whose restriction to $\binom{[n]}{2}$ gives Y. Thus, we have $Y^1 \in \mathcal{M}$.

Now, for an odd $k_0 \in [2l_Y]$, we apply the Elimination Axiom 3.3.1 to the covectors Y^{k_0} and $(-Z)\circ Y^{k_0}$, and the smallest element $i_0 \in p_Y^{-1}(\{\frac{k_0+1}{2}\})$ to obtain a covector T. We claim that $T = Y^{k_0+1}$. Indeed, for all i where $p_Y(i) < \frac{k_0+1}{2}$ we have $T_i = Y_i^{k_0} = (-Z)_i = -$. For all $i \in p_Y^{-1}(\{\frac{k_0+1}{2}\})$, we have $T_{i_0} = 0$ and $T_{(i_0,i)} = Y^{k_0}_{(i_0,i)} = (-Z)_{(i_0,i)} = 0$, so the second hypothesis on $\mathcal{M}$ implies that $T_i = 0$. Let i where $p_Y(i) > \frac{k_0+1}{2}$. We assume that $i > i_0$, the other case is analogous. We have that $T_{(i_0,i)} = Y^{k_0}_{(i_0,i)} \neq 0$ and $T_{i_0} = 0$, so $T_i \neq 0$ by the second hypothesis. This forces that $T_i = +$ as otherwise $T \circ Z$ would satisfy $(T\circ Z)_{i_0} = -(T\circ Z)_i = (T\circ Z)_{(i_0,i)}$, which contradicts our assumption on the reorientation.

To conclude, if k_0 is even, then $Y^{k_0+1} = Y^{k_0} \circ (-Z)$.

□

We get the following characterization as a direct corollary.

Theorem 3.4.9. *A simple oriented matroid $\mathcal{M}$ is FL-isomorphic to a big oriented matroid if and only if it has a tight modular hyperplane.*

Proof. It is straightforward to check that in a big oriented matroid the elements indexed by $\binom{[n]}{2}$ form a modular hyperplane that is tight up to the simplification of parallel elements.

For the converse, let E be the ground set of $\mathcal{M}$, and $F \subseteq E$ a tight modular hyperplane. We will relabel the elements of $E \smallsetminus F$ by $[n]$, where $n = |E \smallsetminus F|$. Now, for each $(i,j) \in \binom{[n]}{2}$ there is an element $z \in F$ in the line spanned by i and j by the modularity of F. We add to $\mathcal{M}$ an element parallel to z labeled by $(i,j) \in \binom{[n]}{2}$. We obtain this way an isomorphic oriented matroid $\mathcal{M}'$. Note that, since the modular hyperplane $F \subseteq E$ is tight, for each $z \in F$ there are some $i,j \in E \smallsetminus F$ such that i,j,z are collinear. Hence, z is parallel to (i,j) and $\mathcal{M}' \smallsetminus z$ is isomorphic to $\mathcal{M}$. We conclude that $\mathcal{M}'\big|_{[n]\cup\binom{[n]}{2}}$ is isomorphic to $\mathcal{M}$. It satisfies the conditions of Proposition 3.4.8 and is hence isomorphic to a big oriented matroid.

□

A consequence of this observation is that we can extend the process to determine the big oriented matroid from the sweep oriented matroid to any oriented matroid with a modular hyperplane (not necessarily tight). For sweep oriented matroids, this relies on the labeling of the elements (see Remark 3.4.6). Arbitrary modular hyperplanes also need a similar extra information. Let $\mathcal{M}$ be an oriented matroid on a ground set E with a modular hyperplane F. To simplify the exposition, we will assume that $\mathcal{M}$ is simple (no loops or parallel elements), that $E \smallsetminus F = [n]$, that $F \cap \binom{[n]}{2} = \emptyset$, and that all the elements of $E \smallsetminus F$ lie in a common halfspace defined by F. (We could omit this simplification by adding information to the decoration, but it unnecessarily complicates the notation.)

We will *decorate* the elements in F by constructing maps $\delta : F \to 2^{\binom{[n]}{2}}$ and $\epsilon : \binom{[n]}{2} \to \{+,-\}$ that associate a subset of elements of $\binom{[n]}{2}$ to each $f \in F$ and a sign to each pair in $\binom{[n]}{2}$. This is done with the following algorithm. We start decorating each element in F with an empty set. For every $(i,j) \in \binom{[n]}{2}$, let $f \in F$ be the element of F in the flat spanned by i and j. We add to the decoration $\delta(f)$ of f the ordered pair (i,j); and we set

$\epsilon(i,j) = +$ if there is a covector $X \in \mathcal{M}$ such that $X_i = 0$ and $X_j = X_f \neq 0$, or $\epsilon(i,j) = -$ otherwise. We will call this information the *decoration of F induced by $\mathcal{M}$*.

We will show that we can recover $\mathcal{M}$ from $\mathcal{M}' = \mathcal{M}\big|_F$, its restriction to F, and the decoration. To state our result, we introduce *valid decorations*, which are those that can be obtained with the procedure above. For any simple oriented matroid $\mathcal{M}'$ on the ground set F, we call a *valid decoration* a couple of maps $\delta : F \to 2^{\binom{[n]}{2}}$ and $\epsilon : \binom{[n]}{2} \to \{+,-\}$ for a certain n, such that:

- the decorations form a partition of $\binom{[n]}{2}$, with empty parts accepted: $\binom{[n]}{2} = \bigcup_{f \in F} \delta(f)$ with $\delta(f) \cap \delta(f') = \emptyset$ whenever $f \neq f'$; and
- the covectors $X \in \mathcal{M}$, seen as elements of $\{+,-,0\}^{\binom{[n]}{2}}$ by considering $X_{(i,j)} = \epsilon(i,j)X_f$ if $(i,j) \in \delta(f)$, satisfy the transitivity condition from Lemma 3.3.8.

The following result should be seen as the oriented version of [Bon06, Thm. 2.1], which similarly characterizes when an (unoriented) matroid can be extended so that its ground set is a modular hyperplane of the larger matroid.

Corollary 3.4.10. *If $\mathcal{M}'$ is a simple oriented matroid on F with a valid decoration (δ,ϵ), then $\mathcal{M}'$ can be extended to a unique oriented matroid $\mathcal{M}$ for which F is a modular hyperplane and (δ,ϵ) is the decoration of F induced by $\mathcal{M}$.*

In particular, an oriented matroid $\mathcal{M}$ with a modular hyperplane F is completely determined by $\mathcal{M}\big|_F$ together with the decoration of F induced by $\mathcal{M}$.

Proof. The proof is very simple, as it relies entirely on Theorem 3.4.1, but it involves some auxiliary oriented matroids and some cumbersome notation to identify them.

With the help of the decoration, we will first add to $\mathcal{M}'$ the elements of $\binom{[n]}{2}$ to get a new oriented matroid $\tilde{\mathcal{M}}'$ on $F \cup \binom{[n]}{2}$. We do this by adding for each $f \in F$ the parallel elements $(i,j) = \epsilon(i,j)f$ for $(i,j) \in \delta(f)$. The restriction of $\tilde{\mathcal{M}}'$ to $\binom{[n]}{2}$ is a sweep oriented matroid, as it fulfills the transitivity condition from Lemma 3.3.8 by hypothesis. We want to apply Theorem 3.4.1 to find the associated big oriented matroid. While Theorem 3.4.1 is only stated to extend a matroid from $\binom{[n]}{2}$ to $[n] \cup \binom{[n]}{2}$, the same proof carries on almost verbatim to extend a matroid from $F \cup \binom{[n]}{2}$ to $F \cup [n] \cup \binom{[n]}{2}$. We associate a family of covectors X^k on $F \cup [n] \cup \binom{[n]}{2}$ to every covector X of $\tilde{\mathcal{M}}'$ in the very same way, just ignoring the entries in F when generating the values for $[n]$ in X^k. These are the covectors of an oriented matroid $\tilde{\mathcal{M}}$ (by the same argument as in Theorem 3.4.1), and its restriction to $[n] \cup F$ is the desired oriented matroid $\mathcal{M}$. □

3.4.3 Not every oriented matroid is a little oriented matroid

Little oriented matroids are always acyclic, meaning that $+_n$ is a tope. A first guess could be that all acyclic oriented matroids can be extended to a big oriented matroid. After all, this is trivially the case for realizable oriented matroids. Moreover, it is also true for rank 3 oriented matroids. Although stated in a different language, this follows directly from [BLS+99, Thm. 6.3.3] and [FW01, Lemma 1][2], which was first proved in the uniform case in [SH91]. (Actually, their result is stronger, as the sweep oriented matroid they construct is Dilworth in the sense of the upcoming Section 3.5.1.)

Theorem 3.4.11 ([BLS+99, Thm. 6.3.3])**.** *Every loopless acyclic oriented matroid $\mathcal{M}$ of rank 3 is the little oriented matroid of a sweep oriented matroid.*

However, contrary to the rank 3 case, starting at rank 4 there exist acyclic oriented matroids that cannot be extended to big oriented matroids. The proof of Theorem 3.4.11 in [BLS+99] uses Levi's extension lemma, that states that every arrangement of pseudolines can be extended with an extra pseudoline through two given points. We use a famous counterexample to the analogous statement in rank 4 by Richter-Gebert [RG93] to present an acyclic oriented matroid that cannot be extended to a big oriented matroid.

Theorem 3.4.12 ([RG93, Cor. 3.4])**.** *There is an oriented matroid $\mathcal{RG}$ of rank 4 with ground set $[12]$ with two topes U and T such that no extending pseudoplane intersects U and T simultaneously.*

This means that if $\mathcal{RG}'$ is an oriented matroid on $[12] \cup \{f\}$ such that $\mathcal{RG}'\big|_{[12]} = \mathcal{RG}$, then it cannot contain covectors $U', T' \in \mathcal{RG}'$ such that $U'\big|_{[12]} \preceq U$ and $T'\big|_{[12]} \preceq T$ but $U'_f = T'_f = 0$.

Theorem 3.4.13. *The reorientation of $\mathcal{RG}$ sending U to $+_{12}$ is acyclic, but it is not the little oriented matroid of any sweep oriented matroid.*

Proof. After a suitable reorientation, assume that $U = +_{12}$. Suppose that there is a big oriented matroid $\mathcal{M}$ on $[12] \cup \binom{[12]}{2}$ such that $\mathcal{M}\big|_{[12]} = \mathcal{RG}$. It contains a cocircuit $U' \in \mathcal{M}$ with $U'_i = U_i = +$ for all $i \in [12]$ and $U'_{(i,j)} = 0$ for all $(i,j) \in \binom{[12]}{2}$.

Let X be a covector in $\mathcal{RG}$ such that $[X, T]$ forms an interval of length 2 in the face lattice of $\mathcal{RG}$.

This means that there are $1 \leq i_0 < j_0 \leq 12$ such that $X_{i_0} = X_{j_0} = 0$ and $X_i \preceq T_i$ for all $i \in [12] \setminus \{i_0, j_0\}$. Let X' be a covector in $\mathcal{M}$ such that $X'\big|_{[12]} = X$. Hence, we have $X'_{(i_0,j_0)} = 0$ and $X'\big|_{[12]} \preceq T$. Hence $\mathcal{RG}' = \mathcal{M}\big|_{[12]\cup\{(i_0,j_0)\}}$ is an extension of $\mathcal{RG}$ whose covectors $U'\big|_{[12]\cup\{(i_0,j_0)\}}$ and $X'\big|_{[12]\cup\{(i_0,j_0)\}}$ contradict the special property of $\mathcal{RG}$.

□

[2]This is usually presented in the context of "topological sweepings" of arrangements of pseudolines, for example in [FW01, Fel04]. Note that the notation in these references collides slightly with ours, see Section 3.1.

3.5 Lattices of flats of sweep oriented matroids

3.5.1 Dilworth sweep oriented matroids

It is also interesting to understand the underlying (unoriented) matroid $\underline{\mathcal{M}}^{\mathsf{sw}}$ associated to a sweep oriented matroid $\mathcal{M}^{\mathsf{sw}}$. In particular, because it plays an essential role in the enumeration of sweeps [BLS+99, Sec. 4.6]. In the realizable case, this was done by Edelman [Ede00] and Stanley [Sta15], who showed that, under certain genericity constraint, $\underline{\mathcal{M}}^{\mathsf{sw}}$ can be obtained from $\underline{\mathcal{M}}^{\mathsf{lit}}$ via the operation of *Dilworth truncation*.

We will work directly with the axiomatic of (unoriented) matroids in terms of *geometric lattices* of flats, which was already mentioned in Section 3.4.2. We refer to [Whi86] for a comprehensive reference on (unoriented) matroids.

If $\mathcal{M}$ is an oriented matroid on ground set E, a *flat* of $\mathcal{M}$ is a subset $F \subseteq E$ that is the zero-set of a covector of $\mathcal{M}$ (there is $X \in \mathcal{M}$ such that $F = \{e \in E \,|\, X_e = 0\}$). The set $\mathcal{F}_{\mathcal{M}}$ of all flats of $\mathcal{M}$, ordered by inclusion, has the special structure of a *geometric lattice*; that is, a finite atomistic semimodular lattice. If $\mathcal{M}$ has no loop, its minimal element is $\emptyset$. (Note that this order is reversed from the order on the covectors in the face lattice of $\mathcal{M}$.) Conversely, any geometric lattice can be seen as the lattice of flats of a matroid. Let $S \subseteq E$. There is only one minimal flat F that contains S. The *rank* of S is the length of any maximal chain from $\emptyset$ to F in $\mathcal{F}_{\mathcal{M}}$. It is denoted $\mathrm{rk}_{\mathcal{M}}(S)$, or $\mathrm{rk}_{\underline{\mathcal{M}}}(S)$. The rank function satisfies the *submodular inequality*:

$$\mathrm{rk}_{\mathcal{M}}(A) + \mathrm{rk}_{\mathcal{M}}(B) \geq \mathrm{rk}_{\mathcal{M}}(A \cap B) + \mathrm{rk}_{\mathcal{M}}(A \cup B).$$

The flats and the rank function give two cryptomorphic ways to define the underlying (unoriented) matroid $\underline{\mathcal{M}}$ of the oriented matroid $\mathcal{M}$. If $\underline{\mathcal{M}}(V)$ is the matroid associated to a real vector configuration $V = (\boldsymbol{v}_1, \ldots, \boldsymbol{v}_n)$, the flats correspond to the sets of vectors in a same linear subspace and the rank of $S \subseteq E$ is the dimension of the linear subspace generated by $\{\boldsymbol{v}_i \,|\, i \in S\}$.

The flats of the braid arrangement $\boldsymbol{\mathcal{B}}_n$ are in correspondence with the (unordered) partitions of $[n]$, and the lattice of flats of $\boldsymbol{\mathcal{B}}_n$ is just the lattice of partitions of $[n]$. Similarly, each flat of a sweep oriented matroid can be associated to a partition, and the sweeps corresponding to orderings of this partition correspond to the covectors with this zero-pattern.

We will need the oriented and unoriented notions of weak maps, which are the matroidal version of perturbing a configuration to a more special position. If $\mathcal{M}$ and $\mathcal{M}'$ are two oriented matroids on the same ground set E, we say that there is a *weak map* from $\mathcal{M}$ to $\mathcal{M}'$ if for every covector $X \in \mathcal{M}'$, there is a covector $Y \in \mathcal{M}$ such that $X \preceq Y$. Note that every strong map is also a weak map, but not the other way round (the definition of strong maps is given in Section 3.3.3). If $\underline{\mathcal{M}}$ and $\underline{\mathcal{M}}'$ are two unoriented matroids on the same ground set E, we say that there is a *weak map* from $\underline{\mathcal{M}}$ to $\underline{\mathcal{M}}'$ if for any subset $F \subseteq E$ we have $\mathrm{rk}_{\underline{\mathcal{M}}'}(F) \leq \mathrm{rk}_{\underline{\mathcal{M}}}(F)$. Note that a weak map between oriented matroids induces a weak map on the underlying unoriented matroids (cf. [BLS+99, Cor. 7.7.7]).

The idea behind the Dilworth truncation is the following: if $\mathcal{F}$ is a geometric lattice and we remove the elements of rank 1, we obtain a poset $\mathcal{F}'$ that is not necessarily a geometric lattice. The most generic way to augment it with all the joins needed to fulfill the semimodularity condition gives rise to a matroid called the *first Dilworth truncation* of $\mathcal{F}$. The construction works in more generality when the elements of rank $\leq k$ are removed, giving rise to the kth Dilworth truncation, but we will not need it in such generality ([Dil44], see also [Bry86]).

Definition 3.5.1 ([Bry86, Prop. 7.7.5])**.** Let $\underline{\mathcal{M}}$ be a matroid on ground set E. The *first Dilworth truncation* of $\underline{\mathcal{M}}$, denoted $D_1(\underline{\mathcal{M}})$, is defined on the ground set $\binom{E}{2}$ and its rank function is given by:

$$\begin{aligned} &\mathrm{rk}_{D_1(\underline{\mathcal{M}})}(\emptyset) = 0, \\ &\mathrm{rk}_{D_1(\underline{\mathcal{M}})}(F) = \min_{S \in \mathcal{S}(F)} r_S(F) \qquad\qquad \text{for } \emptyset \neq F \subseteq \binom{E}{2}, \end{aligned}$$

where $\mathcal{S}(F)$ is the set of (unordered) partitions $S = \{F_1, \ldots, F_l\}$ of F ($F = F_1 \cup \cdots \cup F_l$, $F_k \neq \emptyset$ for all $k \in [l]$, and $F_k \cap F_h = \emptyset$ for all $k \neq h$) and $r_S(F) = \big(\sum_{k=1}^{l} \mathrm{rk}_{\underline{\mathcal{M}}}(\bigcup\{i, j \mid (i, j) \in F_k\})\big) - l$.

The flats of rank 1 of $D_1(\underline{\mathcal{M}})$ are exactly the flats of rank 2 (i.e. the lines) of $\underline{\mathcal{M}}$. As noted by Brylawski [Bry86] and Mason [Mas77, Sec. 2.1], in the realizable case the Dilworth truncation can be geometrically realized by intersecting all the lines of $\underline{\mathcal{M}}$ with a generic affine hyperplane. If $\boldsymbol{A}$ is generic enough (in the sense that incomparable flats spanned by its subsets are never parallel), then the hyperplane at infinity fulfills this genericity condition and $\underline{\mathcal{M}^{\mathsf{sw}}}(\bar{\boldsymbol{A}})$ is the first Dilworth truncation of $\underline{\mathcal{M}^{\mathsf{lit}}}(\bar{\boldsymbol{A}})$. Otherwise, we only get a weak map of $D_1(\underline{\mathcal{M}^{\mathsf{lit}}}(\bar{\boldsymbol{A}}))$, as $\underline{\mathcal{M}^{\mathsf{sw}}}(\bar{\boldsymbol{A}})$ will be in less general position. This result extends to (not necessary realizable) sweep oriented matroids.

Theorem 3.5.2. *Let $\mathcal{M}$ be a sweep oriented matroid on $\binom{[n]}{2}$. Then there is a weak map from $D_1(\underline{\mathcal{M}^{\mathsf{lit}}})$ to $\underline{\mathcal{M}}$.*

The proof needs an auxiliary lemma.

Lemma 3.5.3. *Let $\mathcal{M}^{\mathsf{lit}}$ be the little oriented matroid of the sweep oriented matroid $\mathcal{M}$. If I is a flat of $\mathcal{M}^{\mathsf{lit}}$ of rank at least two, and J is the minimal flat in $\mathcal{M}$ that contains $\{(i, j) \mid i, j \in I\}$, then $\mathrm{rk}_{\mathcal{M}}(J) = \mathrm{rk}_{\mathcal{M}^{\mathsf{lit}}}(I) - 1$.*

Proof. Let $I' = \{(i, j) \in \binom{[n]}{2} \mid i, j \in I\}$. Then $\mathcal{M}\big|_{I'}$ is a sweep oriented matroid with little oriented matroid $\mathcal{M}^{\mathsf{lit}}\big|_{I}$, and their respective ranks are $\mathrm{rk}_{\mathcal{M}^{\mathsf{lit}}}(I) - 1$ and $\mathrm{rk}_{\mathcal{M}^{\mathsf{lit}}}(I)$ by Lemma 3.4.4. Therefore, $\mathrm{rk}_{\mathcal{M}}(J) = \mathrm{rk}_{\mathcal{M}^{\mathsf{lit}}}(I) - 1$, because the rank function of a restriction is just the restriction of the rank function, see [Bry86, Prop 7.3.1]. $\square$

Proof of Theorem 3.5.2. We want to show that $\mathrm{rk}_{\mathcal{M}}(G) \leq \mathrm{rk}_{D_1(\underline{\mathcal{M}^{\mathsf{lit}}})}(G)$ for every $G \subseteq \binom{[n]}{2}$. Let F be a minimal flat of $D_1(\underline{\mathcal{M}^{\mathsf{lit}}})$ that contains G, so that $\mathrm{rk}_{D_1(\underline{\mathcal{M}^{\mathsf{lit}}})}(F) =$

$\mathrm{rk}_{D_1(\underline{\mathcal{M}^{\mathsf{lit}}})}(G)$. Then there exists an unordered partition $\{I_1, \ldots, I_l\}$ of a subset of $[n]$ into flats of $\mathcal{M}^{\mathsf{lit}}$ of rank at least two such that $F = \bigsqcup_{k=1}^{l} \{(i,j) \,|\, i,j \in I_k\}$ and $\mathrm{rk}_{D_1(\underline{\mathcal{M}^{\mathsf{lit}}})}(F) = \sum_{k=1}^{l}(\mathrm{rk}_{\mathcal{M}^{\mathsf{lit}}}(I_k) - 1)$.

Indeed, let $S = \{F_1, \ldots, F_l\}$ be a partition of F that minimizes $r_S(F)$, and let $I_k = \bigcup\{i,j \,|\, (i,j) \in F_k\}$. The submodular inequality shows that $\mathrm{rk}_{\mathcal{M}^{\mathsf{lit}}}(I_1 \cup I_2) - 1 \leq \mathrm{rk}_{\mathcal{M}^{\mathsf{lit}}}(I_1) + \mathrm{rk}_{\mathcal{M}^{\mathsf{lit}}}(I_1) - 2$ whenever $I_1 \cap I_2 \neq \emptyset$. We can therefore assume that the I_k's are disjoint. Moreover, these parts I_k have to be flats of $\mathcal{M}^{\mathsf{lit}}$. Otherwise, if there was some $e \notin I_k$ such that $\mathrm{rk}_{\mathcal{M}^{\mathsf{lit}}}(I_k) = \mathrm{rk}_{\mathcal{M}^{\mathsf{lit}}}(I_k \cup \{e\})$, then we could add to F all the pairs (i,e) and (e,i) with $i \in I_k$ without augmenting its rank, but F was taken to be a flat.

Let J_k be the minimal flat in $\mathcal{M}$ that contains $\{(i,j) \,|\, i,j \in I_k\}$; and let J be the join of all the J_k in the lattice of flats of $\mathcal{M}$. The submodularity of geometric lattices implies that $\mathrm{rk}_{\mathcal{M}}(J) \leq \sum_{k=1}^{l} \mathrm{rk}_{\mathcal{M}}(J_k)$. Moreover, such a J contains all the J_k, hence it contains F, which contains G; and therefore $\mathrm{rk}_{\mathcal{M}}(G) \leq \mathrm{rk}_{\mathcal{M}}(J)$. We conclude by Lemma 3.5.3, that implies that for any k, $\mathrm{rk}_{\mathcal{M}}(J_k) = \mathrm{rk}_{\mathcal{M}^{\mathsf{lit}}}(I_k) - 1$. □

In view of this result, we will say that a sweep oriented matroid $\mathcal{M}$ is *Dilworth* if the weak map predicted by Theorem 3.5.2 is actually an equality and we have $\underline{\mathcal{M}} = D_1(\underline{\mathcal{M}^{\mathsf{lit}}})$.

This is the case if for any flat F of $\mathcal{M}$ associated to a partition $I = (I_1, \ldots, I_l)$ we have

$$\mathrm{rk}_{\mathcal{M}}(F) = \left(\sum_{k=1}^{l} \mathrm{rk}_{\mathcal{M}^{\mathsf{lit}}}(I_k) \right) - l. \tag{3.5}$$

In other words, coplanarities in $\mathcal{M}$ are induced by coplanarities in $\mathcal{M}^{\mathsf{lit}}$. For sweep oriented matroids that come from a point configuration, it prevents the case where some subspaces spanned by disjoint subsets of points are parallel.

Note that Dilworth sweep oriented matroids provide an oriented version of the matroid operation of Dilworth truncation. However, contrary to the unoriented case, such a truncation is often not unique and may even not exist, as shown by Theorem 3.4.13.

Even if Theorem 3.5.2 only works at the level of unoriented matroids, we expect that a stronger statement holds at the level of oriented matroids. The following conjecture is true for sweep oriented matroids of rank 2 (by [BLS+99, Thm. 6.3.3]), and for sweep oriented matroids arising from point configurations (it suffices to make a generic projective perturbation that removes unwanted parallelisms).

Conjecture 3.5.4. *For any sweep oriented matroid $\mathcal{M}$ there is a Dilworth sweep oriented matroid $\mathcal{M}'$ such that there is a weak map from $\mathcal{M}'$ to $\mathcal{M}$, and $\mathcal{M}$ and $\mathcal{M}'$ have the same little oriented matroid.*

3.5.2 Bounds on the number of sweep permutations

One motivation for studying the lattice of flats of an oriented matroid is that it completely determines its f-vector, as shown by the celebrated Las Vergnas-Zaslavsky Theorem [BLS+99, Thm 4.6.4].

Theorem 3.5.5. *The number of topes of an oriented matroid $\mathcal{M}$ only depends on its lattice of flats $\mathcal{F}$. More precisely, this number is:*

$$(-1)^r \chi_{\mathcal{F}}(-1),$$

where r is the rank of $\mathcal{M}$, and $\chi_{\mathcal{F}}$ is the characteristic polynomial of $\mathcal{F}$.

We can therefore adapt [Ede00, Thm. 3.4][3] and [Sta15, Thm. 7] to oriented matroids. As noted by Stanley in [Sta15], for fixed r the bound is a polynomial in n of degree $2(r-1)$.

Theorem 3.5.6. *Let $\mathcal{M}$ be a sweep oriented matroid on $\binom{[n]}{2}$ of rank r. Then its number of sweep permutations is bounded from above by:*

$$|\Pi(\mathcal{M})| \leq \sum_{i=0}^{\lfloor \frac{r-1}{2} \rfloor} 2c(n, n-r+1+2i),$$

where the $c(n, n-i)$ are the unsigned Stirling numbers of the first kind.

The equality is obtained for example for realizable sweep oriented matroids that come from generic configurations of n points in $\mathbb{R}^{r-1}$.

Proof. We demonstrate how the proof of [Ede00, Thm. 3.4] and [Sta15, Thm. 7] extends to our set-up. We repeat the main ideas for the reader's convenience and refer to these references for more details. We denote by $\mathcal{G}_n^r$ the geometric lattice obtained by removing all elements of rank greater than r from the Boolean lattice on $[n]$ and adding a top element. This is the lattice of flats of any generic point configuration of n points in $\mathbb{R}^{r-1}$. The computation and evaluation of the characteristic polynomial of $D_1(\mathcal{G}_n^r)$ gives the right hand side of the inequality (see [Ede00, Co. 3.2]), which is the number of topes of any oriented matroid whose lattice of flats is $D_1(\mathcal{G}_n^r)$ via Theorem 3.5.5. This is the case for the sweep oriented matroids arising from generic configurations.

By [KN86, Cor. 9.3.7], it suffices to show that there is a weak map from $D_1(\mathcal{G}_n^r)$ to $\underline{\mathcal{M}}$, because this implies that the coefficients of the characteristic polynomial of $\underline{\mathcal{M}}$ are bounded by those of the characteristic polynomial of $D_1(\mathcal{G}_n^r)$. Note that for any subset $F \subseteq [n]$, we have $\mathrm{rk}_{\mathcal{G}_n^r}(F) = \min(|F|, r)$. Like in any matroid, $\underline{\mathcal{M}^{\mathsf{lit}}}$ satisfies $\mathrm{rk}_{\underline{\mathcal{M}^{\mathsf{lit}}}}(F) \leq |F|$, and hence there is a weak map from $\mathcal{G}_n^r$ to $\underline{\mathcal{M}^{\mathsf{lit}}}$. It follows from Definition 3.5.1 of the Dilworth truncation by its rank function that this induces a weak map from $D_1(\mathcal{G}_n^r)$ to $D_1(\underline{\mathcal{M}^{\mathsf{lit}}})$. It follows from Theorem 3.5.2 that there is a weak map from $D_1(\mathcal{G}_n^r)$ to $\underline{\mathcal{M}}$. $\square$

3.6 Pseudo-sweeps

Even if the little oriented matroid does not change, the poset of sweeps of a point configuration is not invariant under admissible projective transformations (in the sense of [Zie95,

[3] There is a small typo in the statement of [Ede00, Thm. 3.4], but the correct statement can be recovered from [Ede00, Cor. 3.2] with $d = n - k - 1$.

App. 2.6]). In this section we describe a larger poset, the *poset of pseudo-sweeps*, that contains the sweeps with respect to all possible choices of "hyperplane at infinity". It is a poset of cellular strings, and as such it can be defined at the level of oriented matroids. Thus it exists even for those oriented matroids that are not little oriented matroids of any sweep oriented matroid.

3.6.1 Pseudo-sweeps

With the presentation of $\boldsymbol{SP}(\boldsymbol{A})$ as a monotone path polytope introduced in Section 3.2.3, we know that sweep permutations of a point configuration $\boldsymbol{A}$ can be interpreted as coherent monotone paths of the zonotope $\boldsymbol{Z}(\bar{\boldsymbol{A}})$ with respect to a linear form (which we called the height). Non-coherent monotone paths also give rise to permutations of the elements of $\boldsymbol{A}$, which we will call *pseudo-sweep permutations*. They can be read in terms of k-sets. A *k-set* of $\boldsymbol{A}$ is a k-element subset $\boldsymbol{S} \subseteq \boldsymbol{A}$ for which there is an affine hyperplane strictly separating $\boldsymbol{S}$ from $\boldsymbol{A} \setminus \boldsymbol{S}$. See [Mat02, Ch. 11] for background.

For simplicity, assume that $\boldsymbol{A} = (\boldsymbol{a}_1, \dots, \boldsymbol{a}_n) \in \mathbb{R}^{d \times [n]}$ does not contain repeated points. A *pseudo-sweep permutation* of $\boldsymbol{A}$ is a permutation $\sigma \in \mathfrak{S}_n$ such that $\left\{\boldsymbol{a}_{\sigma(i)} \,\middle|\, 1 \le i \le k\right\}$ is a k-set for all $1 \le k \le n$. Note that we are still sweeping with a hyperplane, although we are allowed to slightly change its direction every time the hyperplane hits a point, as long as the new hyperplane does not cross one of the already visited points.

This point of view can be extended to obtain ordered partitions (and lift the constraint of not having repeated points). Consider a sequence of affine functionals $\gamma_r(\boldsymbol{x}) = \langle \boldsymbol{u}_r, \boldsymbol{x}\rangle - c_r$ for $1 \le r \le m$ such that for each point $\boldsymbol{a}_i \in \boldsymbol{A}$ there is an r with $\gamma_r(\boldsymbol{a}_i) = 0$, $\gamma_s(\boldsymbol{a}_i) > 0$ for all $s < r$, and $\gamma_s(\boldsymbol{a}_i) < 0$ for all $r < s$; and such that for each $1 \le r \le m$ there is some i such that $\gamma_r(\boldsymbol{a}_i) = 0$. The sets $I_r = \{i \,|\, \gamma_r(\boldsymbol{a}_i) = 0\}$ with $1 \le r \le m$ form an ordered partition of $[n]$, which we call a *pseudo-sweep* of $\boldsymbol{A}$.

There is another way to interpret pseudo-sweeps of $\boldsymbol{A}$ and monotone paths/cellular strings of $\boldsymbol{Z}(\bar{\boldsymbol{A}})$ in terms of hyperplane arrangements, which extends to oriented matroids.

A *gallery* of a hyperplane arrangement (without parallels) is a sequence of chambers (topes) such that adjacent chambers are separated by exactly one hyperplane. More generally, a *gallery* of an oriented matroid is a collection of topes $T^0, \dots, T^{m+1}$ such that $S(T^i, T^{i+1})$ is a parallelism class for all i. A gallery is *minimal* if no parallelism class is crossed twice. We will work with acyclic oriented matroids and we will be interested in their minimal galleries from $+_n$ to its opposite $-_n$.

This definition can be relaxed to accept paths that go accross some covectors (other than subtopes). A *cellular string* of $\mathcal{M}$ with respect to $+_n$ is a sequence of non-tope covectors $(X^1, \dots, X^m)$ that are such that $X^1 \circ +_n = +_n$, $X^m \circ -_n = -_n$, and $X^i \circ -_n = X^{i+1} \circ +_n$ for all i. This notation is consistent with the notion of cellular string for a polytope with respect to a linear functional given in Section 3.2.3. Indeed, for a hyperplane arrangement which is the normal fan of a zonotope $\boldsymbol{Z}$, its cellular strings are equivalent to the cellular strings of $\boldsymbol{Z}$ with respect to a linear functional that is minimized at the vertex corresponding to $+_n$. (Minimal galleries are in correspondence with monotone paths.)

Note that an allowable sequence is just a cellular string on the braid arrangement based at the tope indexed by the permutation $\mathrm{id} = (1, 2, \dots, n)$, and that its galleries correspond to simple allowable sequences.

The following lemma sums up the relations between these objects in the realizable case. It is illustrated in Figure 3.11, where the example of $\boldsymbol{B}_2$ from Figures 3.4 and 3.7 is revisited.

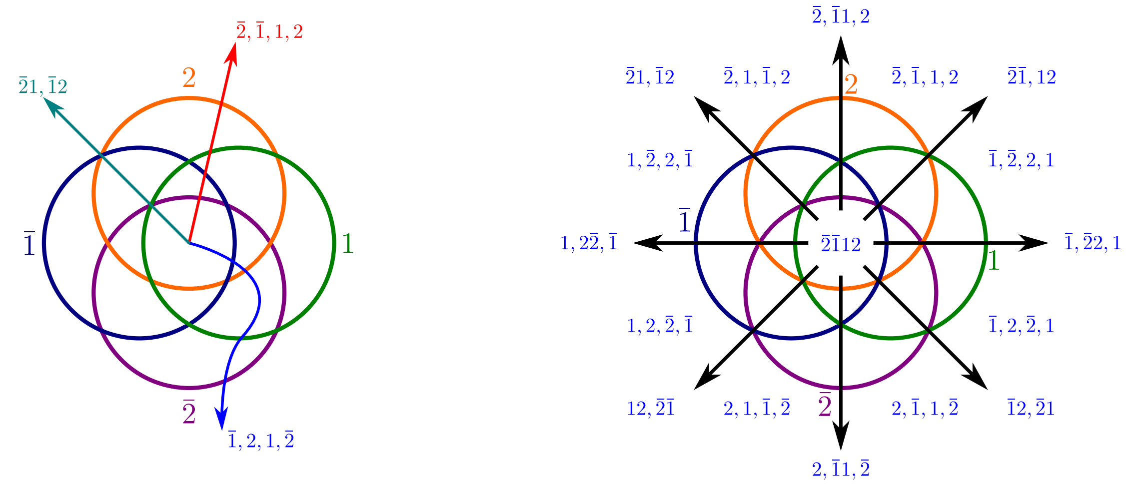

Figure 3.11: The hyperplane arrangement $\boldsymbol{\mathcal{H}}_{\bar{\boldsymbol{B}}_2}$. To depict the arrangement, it is intersected with the unit sphere and stereographically projected from the south pole $(0, 0, -1)$. We obtain an arrangement of circles, oriented so that the positive side is the interior. Two sweeps, corresponding to the permutation $\bar{2}, \bar{1}, 1, 2$ and the ordered partition $\bar{2}1, \bar{1}2$ are depicted; and also the pseudo-sweep that is not a sweep corresponding to the permutation $\bar{1}, 2, 1, \bar{2}$. (This resumes the example of Figure 3.7, where the monotone paths corresponding to these two permutations were depicted.) To represent these pseudo-sweeps, an oriented ray from the all-positive tope (containing the origin) to its opposite (at infinity) is depicted. The order in which the circles are crossed gives the corresponding permutation. If the ray meets more than one circle at the same time, then one recovers an ordered partition. Note that this gives an alternative method to construct the sweep hyperplane arrangement $\boldsymbol{\mathcal{SH}}(\boldsymbol{B}_2)$. Indeed, it is not hard to see that when one does this procedure (intersection of $\boldsymbol{\mathcal{H}}_{\bar{\boldsymbol{A}}}$ with the unit sphere plus stereographic projection), the hyperplanes spanned by the origin and the intersections of all possible pairs of spheres are precisely those of $\boldsymbol{\mathcal{SH}}(\boldsymbol{A})$. This is why, under this representation, sweeps correspond to straight rays emanating from the origin.

Lemma 3.6.1. *Let $\boldsymbol{A} = (\boldsymbol{a}_1, \dots, \boldsymbol{a}_n) \in \mathbb{R}^{d\times[n]}$ be a point configuration; let $\boldsymbol{\mathcal{H}}_{\bar{\boldsymbol{A}}}$ be the hyperplane arrangement in $\mathbb{R}^{d+1}$ composed of the linear hyperplanes $\boldsymbol{H}_i = \left\{\boldsymbol{x} \in \mathbb{R}^{d+1} \,\middle|\, \langle \boldsymbol{x}, \bar{\boldsymbol{a}}_i\rangle = 0\right\}$ (oriented towards $\bar{\boldsymbol{a}}_i$) for $\boldsymbol{a}_i \in \boldsymbol{A}$, where $\bar{\boldsymbol{a}} = (\boldsymbol{a}, 1)$; and let $\boldsymbol{Z}(\bar{\boldsymbol{A}}) = \sum_{i=1}^{n}[-\bar{\boldsymbol{a}}_i, \bar{\boldsymbol{a}}_i]$ be the associated zonotope.*

There is a bijection between:

(i) pseudo-sweeps of $\boldsymbol{A}$,

(ii) cellular strings of $\boldsymbol{\mathcal{H}}_{\bar{\boldsymbol{A}}}$ *with respect to the all-positive tope* $+_n$*, and*

(iii) h-monotone cellular strings of $\boldsymbol{Z}(\bar{\boldsymbol{A}})$ *(h-coherent subdivisions of* $h(\boldsymbol{Z}(\bar{\boldsymbol{A}}))$*);*

and if moreover $\boldsymbol{A}$ *does not have repeated points, then there is a bijection between:*

(i) pseudo-sweep permutations of $\boldsymbol{A}$*,*

(ii) minimal galleries of $\boldsymbol{\mathcal{H}}_{\bar{\boldsymbol{A}}}$ *from the tope* $+_n$ *to its opposite* $-_n$*, and*

(iii) h-monotone paths of $\boldsymbol{Z}(\bar{\boldsymbol{A}})$*.*

Proof. The proof amounts simply to translate between definitions (the definition of cellular strings induced by a projection was given in Section 3.2.3). We omit the details and only give some indications.

To a sequence of affine functionals $\gamma_r(\boldsymbol{x}) = \langle \boldsymbol{u}_r, \boldsymbol{x}\rangle - c_r$ for $1 \le r \le m$ such that for each point $\boldsymbol{a}_i \in \boldsymbol{A}$ there is an r with $\gamma_r(\boldsymbol{a}_i) = 0$, $\gamma_s(\boldsymbol{a}_i) > 0$ for all $s < r$, and $\gamma_s(\boldsymbol{a}_i) < 0$ for all $r < s$; we can associate

(i) the ordered partition $I_1, \dots, I_m$ of $[n]$ given by $I_r = \{i \mid \gamma_r(\boldsymbol{a}_i) = 0\}$,

(ii) the sequence of non-tope covectors $X^1, \dots, X^m$ obtained by considering the sign of evaluating γ_r on each of the points of $\boldsymbol{A}$, and

(iii) the sequence $\boldsymbol{F}_1, \dots, \boldsymbol{F}_m$ of faces of $\boldsymbol{Z}(\bar{\boldsymbol{A}})$, where $\boldsymbol{F}_r$ is the face of $\boldsymbol{Z}(\bar{\boldsymbol{A}})$ minimized by the linear functional $\ell_r : \mathbb{R}^{d+1} \to \mathbb{R}$ given by $(\boldsymbol{x}, x_{d+1}) \mapsto \langle \boldsymbol{u}_r, \boldsymbol{x}\rangle - c_r x_{d+1}$.

One can easily check that the conditions imposed on $\gamma_1, \dots, \gamma_m$ imply that these sequences are a pseudo-sweep of $\boldsymbol{A}$, a cellular string of $\boldsymbol{\mathcal{H}}_{\bar{\boldsymbol{A}}}$ with respect to the all-positive tope $+_n$, and a h-monotone cellular string of $\boldsymbol{Z}(\bar{\boldsymbol{A}})$, respectively. And conversely, for any pseudo-sweep or cellular string of $\boldsymbol{\mathcal{H}}_{\bar{\boldsymbol{A}}}$ or $\boldsymbol{Z}(\bar{\boldsymbol{A}})$, one can find such a sequence of affine functionals. This is direct for pseudo-sweeps and cellular strings of $\boldsymbol{\mathcal{H}}_{\bar{\boldsymbol{A}}}$. For cellular strings $\boldsymbol{F}_1, \dots, \boldsymbol{F}_m$ of $\boldsymbol{Z}(\bar{\boldsymbol{A}})$, we associate to each face $\boldsymbol{F}_r$ an affine map γ_r obtained by restricting the linear functional minimized by $\boldsymbol{F}_r$ in $\boldsymbol{Z}(\bar{\boldsymbol{A}})$ to the hyperplane $x_{d+1} = 1$.

The map that associates the partition $I_1, \dots, I_m$ to the sequence $X^1, \dots, X^m$ with $(X^r)_i = 0$ if $i \in I_r$, $(X^r)_i = -$ if $i \in I_s$ with $s < r$ and $(X^r)_i = +$ if $i \in I_s$ with $s > r$, is hence a bijection between pseudo-sweeps and cellular strings of $\boldsymbol{\mathcal{H}}_{\bar{\boldsymbol{A}}}$. And similarly the map that sends a cellular string $X^1, \dots, X^m$ of $\boldsymbol{\mathcal{H}}_{\bar{\boldsymbol{A}}}$ to the cellular string $\boldsymbol{F}_1, \dots, \boldsymbol{F}_m$ of $\boldsymbol{Z}(\bar{\boldsymbol{A}})$ given by

$$\boldsymbol{F}_r = \sum_{(X^r)_i = +} \{-\bar{\boldsymbol{a}}_i\} + \sum_{(X^r)_i = -} \{\bar{\boldsymbol{a}}_i\} + \sum_{(X^r)_i = 0} [-\bar{\boldsymbol{a}}_i, \bar{\boldsymbol{a}}_i]$$

is also a bijection.

The second part of the statement arises from the observation that these bijections are order-preserving. ☐

In particular, we can define pseudo-sweeps of a realizable oriented matroid in terms of its cellular strings. We extend this definition to abstract oriented matroids.

Definition 3.6.2. A *pseudo-sweep* of an acyclic oriented matroid $\mathcal{M}$ is an ordered partition $(I_1, \ldots, I_m)$ arising from a cellular string $(X^1, \ldots, X^m)$ of $\mathcal{M}$ via $I_i = S(X^i \circ +_n, X^i \circ -_n)$, that is, I_i is the set of zeros of X^i.

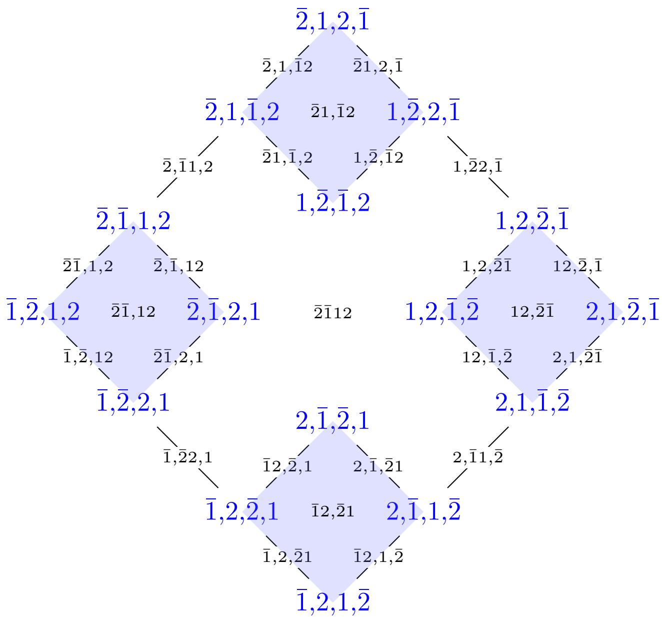

Figure 3.12: The pseudo-sweeps of the point configuration $\boldsymbol{B}_2$. Without the trivial sweep, they index a non-pure cellular complex that retracts to the boundary of the sweep polytope $\boldsymbol{SP}(\boldsymbol{B}_2)$ from Figure 3.4, a 1-sphere.

Remark 3.6.3. If $\boldsymbol{A}'$ is a (full-dimensional) admissible projective transformation of $\boldsymbol{A}$, then any sweep of $\boldsymbol{A}'$ gives rise to a pseudo-sweep of $\boldsymbol{A}$. Indeed, under an admissible projective transformation a pencil of parallel hyperplanes is mapped into a pencil of hyperplanes containing a codimension 2 flat that does not intersect $\operatorname{conv}(\boldsymbol{A})$. The k-sets defined by these hyperplanes clearly give rise to a pseudo-sweep. However, not all pseudo-sweeps arise this way. For example, if $\{\boldsymbol{a}_1, \ldots, \boldsymbol{a}_6\}$ are the vertices of a regular hexagon in cyclic order, then $[1, 2, 3, 6, 5, 4]$ is a pseudo-sweep permutation that is not a sweep of any of its projective transformations. (Because in every realization the vector $\boldsymbol{a}_6 - \boldsymbol{a}_3$ is a positive linear combination of the vectors $\boldsymbol{a}_1 - \boldsymbol{a}_2$ and $\boldsymbol{a}_5 - \boldsymbol{a}_4$.)

Remark 3.6.4 (Pseudo-sweeps and shellings). One of Stanley's motivations for studying sweep permutations in [Sta15] is that they are in correspondence with Bruggesser-Mani line-shelling orders of polytopes [BM71]. For a convex polytope $\boldsymbol{P}$ and a line $\boldsymbol{L}$ through its interior, this is the order in which the facets of $\boldsymbol{P}$ become visible to a point following $\boldsymbol{L}$ from the interior of $\boldsymbol{P}$ to infinity, plus the order in which the remaining facets lose visibility when the point returns from the opposite side to the interior of $\boldsymbol{P}$ along $\boldsymbol{L}$. Now, let $\boldsymbol{P}^\circ$ be the polar of $\boldsymbol{P}$ with respect to an interior point $\boldsymbol{p}$ of $\boldsymbol{P}$, and let $\boldsymbol{L}$ be a line through $\boldsymbol{p}$.

(Here, we are considering the usual projective polarity, as in [Mat02, Sec. 5.1], but after a translation by $-\boldsymbol{p}$.) Since $\boldsymbol{L}$ contains $\boldsymbol{p}$, which is mapped to the hyperplane at infinity by polarity, the set of points in $\boldsymbol{L}$ corresponds to a family of parallel affine hyperplanes orthogonal to a common direction. The shelling order given by $\boldsymbol{L}$ coincides with the sweep permutation of the vertices of $\boldsymbol{P}^\circ$ with respect to this direction. Thus, sweep permutations of a point configuration in convex position are in bijection with line shelling orders of the polar polyhedron for lines that go through the center of polarity (here, the origin, which is the image of the hyperplane at infinity).

Actually, not only sweeps, but all pseudo-sweeps, give rise to shelling orders. And this is true in the more general level of oriented matroids. Indeed, every pseudo-sweep of $\mathcal{M}$ induces a shelling order of the (Edmonds-Mandel) face lattice of the tope $+_n$ [EM82, Sec. 3.VI], see also [BLS$^+$99, Sec. 4.3]. (To the best of our knowledge, it is still an open problem whether the opposite of this lattice, called the Las Vergnas face lattice, is shellable.) Pseudo-sweep shellings have been recently rediscovered by Heaton and Samper in the special case of matroid polytopes under the name of *broken line shellings* [HS20].

3.6.2 The poset of pseudo-sweeps and the generalized Baues problem

Just like sweeps, pseudo-sweeps can be naturally ordered by refinement. We denote by $\widetilde{\Pi}(\mathcal{M}, T)$ the poset of pseudo-sweeps of $\mathcal{M}$. Topological properties of this poset have been studied in the context of a special case of the *generalized Baues problem* (GBP), that we presented in Section 1.3.4. We recall that by the topology of a poset X we mean the topology of its *order complex* $\Delta(X)$: the simplicial complex whose simplices are the chains of X (see [Bjö95] or [BLS$^+$99, Sec. 4.7]).

Billera, Kapranov and Sturmfels [BKS94b, Thm. 2.3] showed that the strong version of the GBP holds for monotone paths of polytopes. This implies that, in the realizable case, the poset of sweeps of a point configuration is a deformation retract of the poset of pseudo-sweeps. For the case of zonotopes, Björner [Bjö92, Thm. 2] gave an alternative combinatorial proof for the weak version of the GBP (in the sense of [Rei99, Q. 2.2]) that extends to oriented matroids. Namely, he proved that the poset of pseudo-sweeps of an oriented matroid is homotopy equivalent to a sphere (once the trivial sweep $([n])$ is removed). A further generalization to shellable CW-spheres, for an appropriate definition of cellular strings induced by shellings, was proven in [AER00].

Theorem 3.6.5 ([Bjö92, Thm. 2])**.** *The poset of pseudo-sweeps of an oriented matroid $\mathcal{M}$ of rank r with respect to a tope T without the trivial sweep has the homotopy type of an $(r-2)$-sphere.*

Note that, by Proposition 3.3.9, for oriented matroids that admit a sweep oriented matroid (in the sense that they are the little oriented matroid of some sweep oriented matroid) the poset of sweeps is an explicit $(r-2)$-sphere embedded in the poset of pseudo-sweeps. We will show that it is in fact a deformation retract; thus proving the strong GBP for cellular strings of little oriented matroids. In the realizable case, this holds by [BKS94b, Thm. 2.3]. In the more general case, Björner also remarks that he expects the poset of pseudo-sweeps to retract to a subcomplex homeomorphic to a $(r-2)$-sphere [Bjö92, below Thm. 2], but does not provide a candidate subcomplex.

Theorem 3.6.6. *Let $\mathcal{M}^{\mathsf{lit}}$ be the little oriented matroid of a sweep oriented matroid $\mathcal{M}^{\mathsf{sw}}$. Then the poset of sweeps of $\mathcal{M}^{\mathsf{sw}}$ is a strong deformation retract of the poset of pseudo-sweeps of $\mathcal{M}^{\mathsf{lit}}$; and the poset of non-trivial sweeps is a strong deformation retract of the poset of non-trivial pseudo-sweeps.*

The proof of Theorem 3.6.6 needs some auxiliary results concerning (combinatorial) homotopy theorems. We refer to [Bjö95] for a very good introduction to the topic. First, we present a result that allows us to weaken the statement to prove, as a consequence of the fact that the *homotopy extension property* holds for order complexes of subposets (c.f. [Hat02, Ch. 0]). Then we recall three results on the homotopy type of posets: the Carrier Lemma, Quillen's Fiber Theorem and Babson's Lemma (the last two being corollaries of the first one). Next, inspired by [AER00], we use the function that returns the first part of an ordered partition to show the contractibility of some subsets of pseudo-sweeps and sweeps, thanks to Babson's Lemma. Finally, we combine all these results to prove that the inclusion induces a homotopy equivalence.

The first result that we need shows that it suffices to prove a weaker statement, namely that the inclusion is a homotopy equivalence. A *CW pair* of a cell complex (such as a simplicial complex) is a pair (X, A) consisting of a cell complex X and a subcomplex A. In particular, if S is a subposet of P, then $(\Delta(P), \Delta(S))$ is a CW pair.

Lemma 3.6.7 ([Hat02, Prop. 0.16 and Cor. 0.20])**.** *If (X, A) is a CW pair and the inclusion $A \hookrightarrow X$ is a homotopy equivalence, then A is a strong deformation retract of X.*

We will use the following version of the Carrier Lemma, from [Bjö95]. For a simplicial complex Δ and a space T, let $C : \Delta \to 2^T$ be an order-preserving map ($C(\sigma) \subseteq C(\tau)$ for all $\sigma \subseteq \tau$). A mapping $f : \|\Delta\| \to T$ is *carried* by C if $f(\|\sigma\|) \subseteq C(\sigma)$ for all $\sigma \in \Delta$, where $\|\cdot\|$ denotes the associated geometric realization of the simplicial complex.

Lemma 3.6.8 (Carrier Lemma [Bjö95, Lem. 10.1])**.** *Let $C : \Delta \to 2^T$ be an order-preserving map such that $C(\sigma)$ is contractible for all $\sigma \in \Delta$. If $f, g : \|\Delta\| \to T$ are both carried by C, then f and g are homotopy equivalent, $f \sim g$.*

We will also need Quillen's Fiber Theorem [Qui78]. For a poset Q and $x \in Q$, let $Q_{\geq x} = \{y \in Q \mid y \geq x\}$. For the claim about the carrier, see the proof in [Bjö95, Thm. 10.5].

Theorem 3.6.9 (Quillen's Fiber Theorem [Qui78])**.** *Let $f : P \to Q$ be an order-preserving map of posets. If $f^{-1}(Q_{\geq x})$ is contractible for all $x \in Q$, then f induces a homotopy equivalence between $\Delta(P)$ and $\Delta(Q)$ whose homotopy inverse is carried by $C(\sigma) = f^{-1}(Q_{\geq \min \sigma})$.*

For this variant of Quillen's Fiber Theorem, known as Babson's Lemma [Bab94, Lem. 1 in Sec. 0.4.3], see also [SZ93, Lem. 3.2].

Lemma 3.6.10 (Babson's Lemma [Bab94])**.** *If an order-preserving map of posets $f : P \to Q$ fulfills*

(i) $f^{-1}(x)$ is contractible for all $x \in Q$, and

(ii) $f^{-1}(x) \cap P_{\geq y}$ is contractible for all $x \in Q$ and $y \in P$ with $f(y) \leq x$,

then f induces a homotopy equivalence between $\Delta(P)$ and $\Delta(Q)$.

Moreover, we will need the following lemmas certifying the contractibility of certain subsets of pseudo-sweeps and sweeps. If $F \subseteq [n]$ is the zero-set of a non-negative covector Z of $\mathcal{M}^{\mathsf{lit}}$, we denote by $\overline{\Pi}(\mathcal{M}^{\mathsf{sw}})_{\subseteq F}$ the sets of sweeps $(I_1, \ldots, I_m)$ with $I_1 \subseteq F$. Similarly, we denote by $\widetilde{\Pi}(\mathcal{M}^{\mathsf{lit}}, +_n)_{\subseteq F}$ the sets of pseudo-sweeps $(I_1, \ldots, I_m)$ with $I_1 \subseteq F$.

Lemma 3.6.11. *Let $F \subseteq [n]$ be the zero-set of a non-negative covector Z of $\mathcal{M}^{\mathsf{lit}}$, then $\widetilde{\Pi}(\mathcal{M}^{\mathsf{lit}}, +_n)_{\subseteq F}$ is contractible.*

Proof. The proof of [AER00, Lem. 5.5] can be adapted to prove that $\widetilde{\Pi}(\mathcal{M}^{\mathsf{lit}}, +_n)_{\subseteq F}$ is contractible. First, we note that with the same proof we can make a slightly stronger statement. Namely, they define a map $f : \omega(P, \mathcal{O}, a) \to D(P, \mathcal{O}, a)$, between certain posets $\omega(P, \mathcal{O}, a)$ and $D(P, \mathcal{O}, a)$ that we describe below, and show that it induces a homotopy equivalence. However, the exact same proof also shows that $f : \omega(P, \mathcal{O}, a) \cap f^{-1}(I) \to I$ induces a homotopy equivalence for any order ideal (lower set) I of $D(P, \mathcal{O}, a)$.

To match their notations, we call P the poset opposite to the big face lattice of $\mathcal{M}^{\mathsf{lit}}$ (the atoms of P are the topes of $\mathcal{M}^{\mathsf{lit}}$ and its 1-skeleton is the tope graph) and $\mathcal{O}$ the orientation of the tope graph that goes from $-_n$ to $+_n$. For a tope a, the poset $\omega(P, \mathcal{O}, a)$ is the poset of partial cellular strings ending at a (i.e. sequences of non-tope covectors $(X^1, \ldots, X^m)$ such that $X^1 \circ -_n = -_n$, $X^m \circ +_n = a$, and $X^i \circ +_n = X^{i+1} \circ -_n$ for all i). Therefore taking $a = a_{max} = +_n$ we have that $\omega(P, \mathcal{O}, a_{max}) = \omega(P, \mathcal{O})$ is exactly the poset of cellular strings of $\mathcal{M}^{\mathsf{lit}}$ with respect to $-_n$, which is in bijection with $\widetilde{\Pi}(\mathcal{M}^{\mathsf{lit}}, +_n)$. However, their partial order is the opposite of our refinement order and the cellular strings have to be read in reverse order. The poset $D(P, \mathcal{O}, a)$ is the poset of the non-tope covectors X such that $X \circ +_n = a$. Therefore, $D(P, \mathcal{O}, a_{max})$ corresponds to the half-interval $[\mathbf{0}, +_n)$ in the face lattice of $\mathcal{M}^{\mathsf{lit}}$.

If we take I the lower set of $D(P, \mathcal{O}, a_{max})$ corresponding to the interval $[Z, +_n)$, their function $f : \omega(P, \mathcal{O}, a_{max}) \cap f^{-1}(I) \to I$ corresponds to the function that sends the pseudo-sweep $(I_1, \ldots, I_m) \in \widetilde{\Pi}(\mathcal{M}^{\mathsf{lit}}, +_n)_{\subseteq F}$ to the non-negative covector $Y \in [Z, +_n)$ with zero-set I_1. Hence it induces a homotopy equivalence from $\widetilde{\Pi}(\mathcal{M}^{\mathsf{lit}}, +_n)_{\subseteq F}$ to $[Z, +_n)$, which has a contractible order poset because it has a unique minimal element. $\square$

We wish to prove the same when restricted to sweeps. For this, we use an auxiliary result from [BCK18]. Let $\mathcal{M} \subseteq \{+, -, 0\}^E$ be the set of covectors of an oriented matroid on E. Then, each element $e \in E$ defines two *halfspaces* $\{X \in \mathcal{M} \mid X_e = +\}$ and $\{X \in \mathcal{M} \mid X_e = -\}$, and a *hyperplane* $\{X \in \mathcal{M} \mid X_e = 0\}$.

Lemma 3.6.12. *Let $\mathcal{M}$ be the set of covectors of an oriented matroid. Then, any non-empty intersection of one or more halfspaces and hyperplanes, seen as a subposet of the face lattice, is contractible.*

Proof. This is a consequence of [BCK18, Prop. 15]. Indeed, an intersection of halfspaces and hyperplanes is a COM, because it satisfies Face symmetry and Strong elimination, see [BCK18, Def. 1]. $\square$

Lemma 3.6.13. *Let $F \subseteq [n]$ be the zero-set of a non-negative covector Z of $\mathcal{M}^{\mathsf{lit}}$, then $\overline{\Pi}(\mathcal{M}^{\mathsf{sw}})_{\subseteq F}$ is contractible.*

Proof. Inspired by the proof of [AER00, Lem. 5.5], we apply Babson's Lemma 3.6.10 with the function f from the subposet of sweeps $\overline{\Pi}(\mathcal{M}^{\mathsf{sw}})_{\subseteq F}$ to the half-open interval of the face lattice $[Z, +_n)$ that sends a sweep $(I_1, \dots, I_m)$ to the non-negative covector with zero-set I_1.

Let Y be a covector in $[Z, +_n)$, with zero-set $G \subseteq F$.

(i) $f^{-1}(Y)$ is the set of sweeps whose first part is G. It is not empty because Y must be of the form $\tilde{Y}^1$ for a covector $\tilde{Y} \in \mathcal{M}^{\mathsf{sw}}$ (in the sense of Definition 3.4.2), and such $\tilde{Y}$ corresponds to a sweep with first part G. Moreover, $f^{-1}(Y)$ is the intersection of halfspaces $\left\{X \in \mathcal{M}^{\mathsf{sw}} \,\middle|\, X_{(i,j)} = +\right\}$ for all $i \in G$, $j \notin G$ and $i < j$, and $\left\{X \in \mathcal{M}^{\mathsf{sw}} \,\middle|\, X_{(i,j)} = -\right\}$ for all $i \in G$, $j \notin G$ and $i > j$. By Lemma 3.6.12 it is contractible.

(ii) Let $J = (J_1, \dots, J_r)$ be a sweep in $\overline{\Pi}(\mathcal{M}^{\mathsf{sw}})_{\subseteq F}$ such that $f(J) \leq Y$, i.e. $G \subseteq J_1$. The intersection $f^{-1}(Y) \cap (\overline{\Pi}(\mathcal{M}^{\mathsf{sw}})_{\subseteq F})_{\geq J}$ is the set of sweeps that refine J and whose first part is G. As for $f^{-1}(Y)$, this set is an intersection of halfspaces. It is not empty because it contains the sweep corresponding to $J \circ \tilde{Y}$. Hence it is contractible.

It follows from Babson's Lemma that $\overline{\Pi}(\mathcal{M}^{\mathsf{sw}})_{\subseteq F}$ is homotopy equivalent to $[Z, +_n)$, which has a contractible order poset because it has a unique minimal element. $\square$

Proof of Theorem 3.6.6. To simplify the exposition, we denote by $P = \widetilde{\Pi}(\mathcal{M}^{\mathsf{lit}}, +_n)$ the poset of pseudo-sweeps of $\mathcal{M}^{\mathsf{lit}}$ with respect to $+_n$, by $S = \overline{\Pi}(\mathcal{M}^{\mathsf{sw}})$ the poset of sweeps of $\mathcal{M}^{\mathsf{sw}}$, and by $Q = [\mathbf{0}, +_n)$ the half-open interval between $\mathbf{0}$ and $+_n$ in the face lattice of $\mathcal{M}^{\mathsf{lit}}$ (this is its Edmonds-Mandel lattice without the top element).

By Lemma 3.6.7 it suffices to show that the inclusion map $\iota : S \hookrightarrow P$ induces a homotopy equivalence. As in the proof of Lemmas 3.6.11 and 3.6.13, let $f : P \to Q$ be the map that sends a pseudo-sweep $(I_1, \dots, I_m)$ to the non-negative covector with zero-set I_1.

$$\begin{tikzcd} S = \overline{\Pi}(\mathcal{M}^{\mathsf{sw}}) \arrow[r, hook, "\iota"] & P = \widetilde{\Pi}(\mathcal{M}^{\mathsf{lit}}, +_n) \arrow[d, "f"] \\ & Q = [\mathbf{0}, +_n) \arrow[ul, "g"] \end{tikzcd}$$

For any covector $Z \in Q$ with zero-set F, we have that $(f \circ \iota)^{-1}(Q_{\geq Z}) = \overline{\Pi}(\mathcal{M}^{\mathsf{sw}})_{\subseteq F}$, which is contractible by Lemma 3.6.13.

We conclude by Quillen's Theorem 3.6.9 that $f \circ \iota : S \to Q$ induces a homotopy equivalence with a homotopy inverse $g : Q \to S$ carried by $C(\sigma) = (f \circ \iota)^{-1}(Q_{\geq \min \sigma})$.

We will show that $g \circ f : P \to S$ is a homotopy inverse of the inclusion map $\iota : S \hookrightarrow P$. We trivially have that $g \circ f \circ \iota \sim \mathrm{id}_S$ from the fact that $(f \circ \iota)$ and g are homotopy inverses.

It remains to show that $\iota \circ g \circ f \sim \mathrm{id}_P$. Now, for σ in the order complex of P, let $C'(\sigma) = \left\| f^{-1}(Q_{\geq \min f(\sigma)}) \right\|$. Note that $f^{-1}(Q_{\geq \min f(\sigma)})$ is of the form $\widetilde{\Pi}(\mathcal{M}^{\mathsf{lit}}, +_n)_{\subseteq F}$ where F is the first part of the smallest ordered partition in σ. It is therefore contractible by Lemma 3.6.11. We claim that id_p and $\iota \circ g \circ f$ are both carried by C', and thus that they must be homotopy equivalent by Lemma 3.6.8. Indeed, id_P is trivially carried by C'; and so is $\iota \circ g \circ f$ because g is carried by C.

The same proof works if we restrict to non-trivial sweeps in S and P. □

3.7 Allowable graphs of permutations and sweep acycloids

In this section we present an alternative generalization of allowable sequences to high dimensions that is closer to the original formulation, in terms of moves between permutations. As we will see, the resulting objects naturally have the structure of acycloids, and we recover sweep oriented matroids as a special case.

3.7.1 Allowable graphs of permutations

In this setting it is useful to see a permutation $\sigma \in \mathfrak{S}_n$ as the word $[\sigma(1), \ldots, \sigma(n)]$ on the alphabet $[n]$. A *substring* of σ is then a contiguous sequence of characters, of the form $[\sigma(j), \sigma(j+1), \ldots, \sigma(k)]$ for certain $1 \leq j < k \leq n$. Such a substring is said to be *increasing* if $\sigma(j) < \sigma(j+1) < \ldots < \sigma(k)$.

Definition 3.7.1. Let $\Pi \subseteq \mathfrak{S}_n$ be a set of permutations, and $\sigma, \sigma' \in \Pi$. We define an *allowable sequence* in Π from σ to σ' as a sequence of permutations of Π: $\sigma = \sigma_0, \ldots, \sigma_l = \sigma'$ such that

(M1) for each $1 \leq k \leq l$ the *move* from σ_{k-1} to σ_k consists of reversing a set m_k of one or more disjoint substrings of σ_{k-1};

(M2) each pair i, j is reversed at most once along the path. In other words, there is at most one move m_k such that i and j are in the same substring of m_k.

A move is *simple* if it consists of a single substring of two elements; and an allowable sequence is *simple* if all its moves are.

For example, $(1,3,2,6,5,4) \xrightarrow{[3,2],[6,5,4]} (1,2,3,4,5,6)$ and $(6,5,4,3,1,2) \xrightarrow{[1,2]} (6,5,4,3,2,1)$ are valid moves, the second being moreover simple. The sequence

$$(1,2,3,4,5) \xrightarrow{[1,2,3]} (3,2,1,4,5) \xrightarrow{[1,4]} (3,2,4,1,5) \xrightarrow{[2,4],[1,5]} (3,4,2,5,1)$$

is an allowable sequence from $(1,2,3,4,5)$ to $(3,4,2,5,1)$ in $\mathfrak{S}_5$; whereas

$$(1,2,3,4,5) \xrightarrow{[1,2,3]} (3,2,1,4,5) \xrightarrow{[1,4]} (3,2,4,1,5) \xrightarrow{[3,2,4],[1,5]} (4,2,3,5,1)$$

is not an allowable sequence in $\mathfrak{S}_5$, because the pair $\{2,3\}$ is reversed twice. In fact, in an allowable sequence from the identity permutation, only increasing substrings can be reversed. Note that if there is a move m from σ to γ, then from γ to σ there is the *reverse move* $\overline{m}$ whose substrings are $\overline{s} = [s_k, \ldots, s_0]$ for each substring $s = [s_0, \ldots, s_k]$ of m. This way, every allowable sequence can be reversed.

Another way to describe allowable sequences is by looking at the set of pairs that are reversed at each move. For a permutation σ, we denote by $\mathrm{inv}(\sigma)$ its set of inversions; that is, the set of pairs $(\sigma(i), \sigma(j)) \in \binom{[n]}{2}$ such that $i < j$ and $\sigma(i) > \sigma(j)$. We denote by $\triangle$ the symmetric difference operation on sets.

Definition 3.7.2. If there is a move m from a permutation σ to a permutation γ, we define the *set of inversions* of the move m by $\mathrm{inv}_m = \mathrm{inv}(\sigma) \triangle \mathrm{inv}(\gamma)$.

For example, for the move $(1,3,2,6,5,4) \xrightarrow{[3,2],[6,5,4]} (1,2,3,4,5,6)$ we obtain the set of inversions $\{(2,3),(4,5),(4,6),(5,6)\}$.

The conditions defining allowable sequences become:

(M1') if (a,b) or (b,a) is in inv_{m_k} and (b,c) or (c,b) is in inv_{m_k}, then (a,c) or (c,a) is in inv_{m_k};

(M2') the inversion sets inv_{m_k} are pairwise disjoint.

Note also that $\mathrm{inv}_m = \mathrm{inv}_{\overline{m}}$.

Remark 3.7.3. An *allowable sequence* in the sense of Goodman and Pollack in [GP80a, GP82, GP84, GP93] is exactly what we call an allowable sequence from $\mathrm{id} = (1,2,\ldots,n)$ to $\overline{\mathrm{id}} = (n, n-1, \ldots, 1)$ in $\mathfrak{S}_n$.

We need to introduce another concept before our main definition.

Definition 3.7.4. A set of permutations $\Pi \subseteq \mathfrak{S}_n$ is *symmetric* if $\overline{\sigma} \in \Pi$ for all $\sigma \in \Pi$, where $\overline{\sigma}$ is the *reverse* of σ, defined by $\sigma(t) = \overline{\sigma}(n-t+1)$ for all $t \in [n]$.

Definition 3.7.5. Consider a set of permutations $\Pi \subseteq \mathfrak{S}_n$ and a set $\mathcal{L}$ of moves such that:

(P1) Π is symmetric,

(P2) for any $\sigma, \sigma' \in \Pi$, there is an allowable sequence from σ to σ' whose moves belong to $\mathcal{L}$,

(P3) for $m, s \in \mathcal{L}$, either $\mathrm{inv}_m = \mathrm{inv}_s$ or $\mathrm{inv}_m \cap \mathrm{inv}_s = \emptyset$.

The graph with vertex set Π and whose edges are the pairs of permutations differing by a move in $\mathcal{L}$ is an *allowable graph of permutations*.

An allowable graph of permutations is *simple* if $\mathcal{L}$ consists only of simple moves.

Lemma 3.7.6. *The graph is completely determined by Π and does not depend on $\mathcal{L}$. More precisely, $\sigma, \sigma' \in \Pi$ form an edge if and only if there is no $\sigma'' \in \Pi \setminus \{\sigma\}$ such that $\mathrm{inv}(\sigma) \triangle \mathrm{inv}(\sigma'') \subsetneq \mathrm{inv}(\sigma) \triangle \mathrm{inv}(\sigma')$.*

Proof. Suppose that $\sigma, \sigma' \in \Pi$ form an edge. It means that there is a move m in $\mathcal{L}$ with inversion set $\mathrm{inv}(\sigma) \triangle \mathrm{inv}(\sigma')$. Suppose that $\sigma'' \in \mathcal{L}$ satisfies $\mathrm{inv}(\sigma) \triangle \mathrm{inv}(\sigma'') \subseteq \mathrm{inv}(\sigma) \triangle \mathrm{inv}(\sigma')$. For any move m' in $\mathcal{L}$ along an allowable sequence from σ to σ'' we have $\mathrm{inv}_{m'} \subseteq \mathrm{inv}(\sigma) \triangle \mathrm{inv}(\sigma'')$, thus $\mathrm{inv}_{m'} \cap \mathrm{inv}_m \neq \emptyset$. We deduce from Condition (P3) of Definition 3.7.5 that $\mathrm{inv}_{m'} = \mathrm{inv}_m$, thus $\mathrm{inv}(\sigma) \triangle \mathrm{inv}(\sigma'') = \mathrm{inv}(\sigma) \triangle \mathrm{inv}(\sigma')$.

Reciprocally, suppose that $\sigma, \sigma' \in \Pi$ do not form an edge and let $\sigma'' \in \Pi \setminus \{\sigma\}$ be the neighbor of σ on an allowable sequence from σ to σ'. By Condition (P3) of Definition 3.7.5, we have $\mathrm{inv}(\sigma) \triangle \mathrm{inv}(\sigma'') \subseteq \mathrm{inv}(\sigma) \triangle \mathrm{inv}(\sigma')$, as if there was a pair in $\mathrm{inv}(\sigma) \triangle \mathrm{inv}(\sigma'') \setminus \mathrm{inv}(\sigma) \triangle \mathrm{inv}(\sigma')$, then it would be reversed twice in the allowable sequence: first between σ and σ'' and later between σ'' and σ'. Moreover, $\sigma' \neq \sigma''$ because σ and σ'' form an edge, and thus $\mathrm{inv}(\sigma) \triangle \mathrm{inv}(\sigma'') \neq \mathrm{inv}(\sigma) \triangle \mathrm{inv}(\sigma')$. □

We will therefore usually identify Π with the corresponding allowable graph, and directly call Π an *allowable graph of permutations*.

Remark 3.7.7. The set of moves can be recovered from the graph by gathering all moves between adjacent permutations in the graph.

Remark 3.7.8. If Π forms an allowable graph of permutations and $\omega \in \mathfrak{S}_n$, then $\omega \circ \Pi = \{\omega \circ \sigma \,|\, \sigma \in \Pi\}$ is still an allowable graph of permutations. Sometimes it is convenient to suppose that the identity permutation id belongs to Π, as Goodman and Pollack did, which can always be obtained by multiplying by an ω that is the inverse of a permutation in Π.

Remark 3.7.9. Note that in the case of a simple allowable graph of permutations Condition (P3) of Definition 3.7.5 is redundant. However, the example of Figure 3.13 shows that it is necessary in the general case and this is why we needed to fix a set of moves in Definition 3.7.5.

In this example, a valid set of moves $\mathcal{L}$ would necessarily contain all the moves represented with the arrows (and their reverse), which are all the singletons $\{[i,j]\}$ for $(i,j) \in \binom{[n]}{2}$. However, in order to satisfy Condition (P2) of Definition 3.7.5, $\mathcal{L}$ also has to contain the move $\{[1,2],[3,4]\}$ represented by the dashed segment joining permutations $(3,4,5,2,1)$ and $(4,3,5,1,2)$, since there is no other allowable sequence between these two permutations. Indeed, we can see that the edges adjacent to $(3,4,5,2,1)$ are labeled $[2,5]$ and $[4,5]$ but those pairs should not be reversed on an allowable sequence to $(4,3,5,1,2)$. Thus, both conditions (P3) and (P2) of Definition 3.7.5 cannot be satisfied simultaneously.

We need to have both conditions in order to have the structure of acycloids, as stated in Theorem 3.7.12.

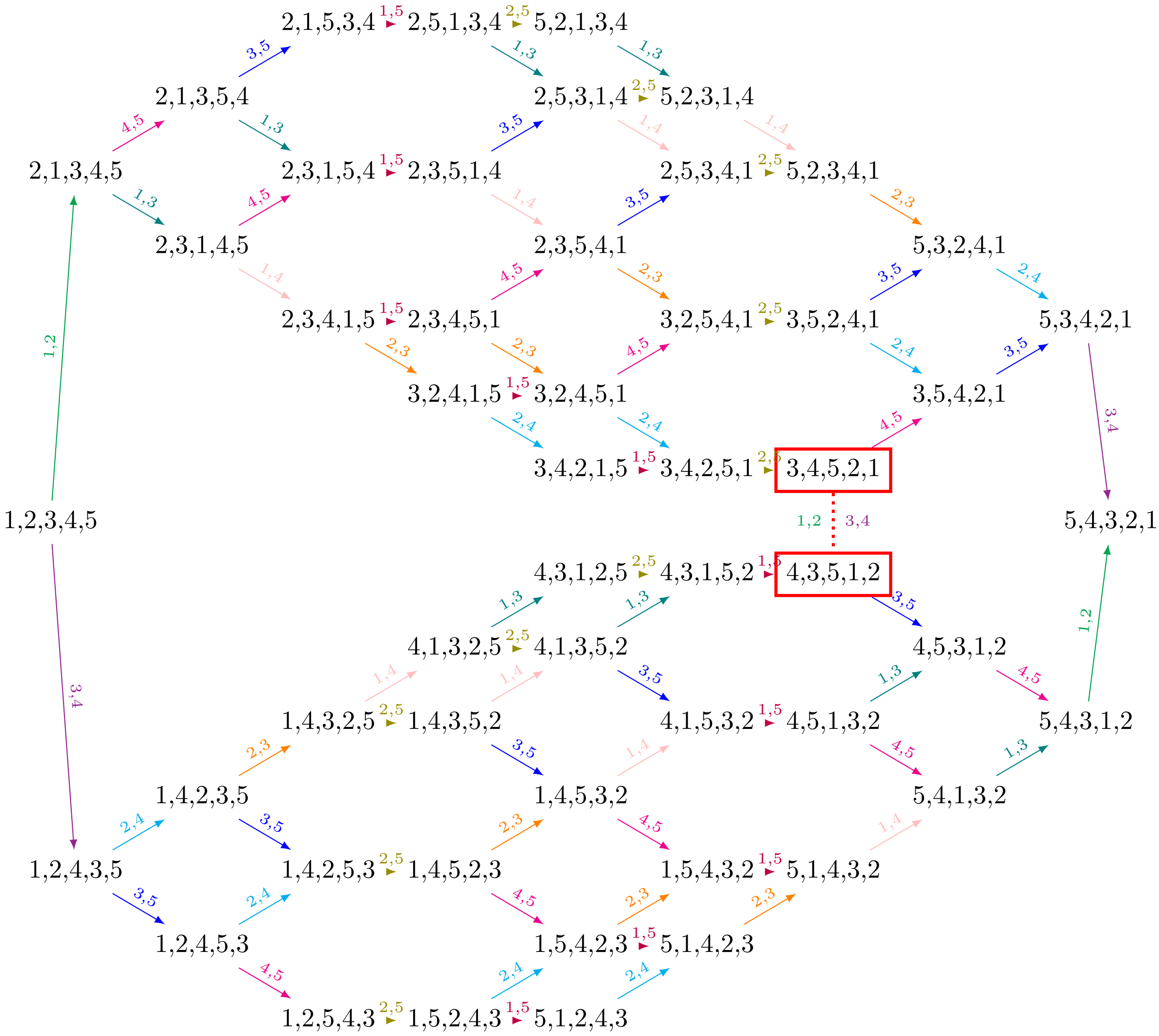

Figure 3.13: Example of a set of permutations that do not satisfy the definition of allowable graph of permutations. Neither graphs with or without the dashed segment are partial cubes.

3.7.2 Sweep acycloids

Acycloids are combinatorial objects widely studied in connection with the characterization of tope sets of oriented matroids, c.f. [Han90, FH93]. They are equivalent to *antipodal partial cubes* (see [KM20]), a concept well-studied in metric graph theory. A graph is a *partial cube* if it is (isomorphic to) an isometric subgraph of a hypercube graph, and it is *antipodal* (also called *symmetric even* [BK88]) if for every vertex v there exists exactly one vertex $\tilde{v}$, called the antipode of v, such that the distance from v to $\tilde{v}$ is larger than the distance from v to any neighbor of $\tilde{v}$.

Following [Han90], we introduce *acycloids* in terms of its topes, which are subsets of sign-vectors. We use the same notation for the notions of reorientation, support and parallelism classes of oriented matroids from Section 3.3.1, which carry on verbatim to arbitrary subsets of sign vectors.

Definition 3.7.10. A collection of sign-vectors $\mathcal{T} \subseteq \{+,-,0\}^E$ is the set of topes of an *acycloid* if and only if it satisfies the following axioms[4]:

(T1) $X, Y \in \mathcal{T}$ implies $\underline{X} = \underline{Y}$ (this set is called the *support* of the acycloid),

(T2) $X \in \mathcal{T}$ implies $-X \in \mathcal{T}$,

(T3) if $X \neq Y \in \mathcal{T}$ then there exists $f \in S(X,Y)$ such that ${}_{-\overline{\overline{f}}}X \in \mathcal{T}$.

These three axioms are satisfied by the topes of an oriented matroid but they are not sufficient; there are examples of acycloids that are not oriented matroids, see [Han93, Sec. 7].

To describe the link between allowable graphs of permutations and acycloids, we associate a sign-vector X^σ in $\{+,-\}^{\binom{[n]}{2}}$ to each permutation $\sigma \in \mathfrak{S}_n$ via the map (3.4). For simplicity, we will sometimes implicitly identify permutations and sign-vectors when it is clear from the context. For a set of permutations $\Pi \subseteq \mathfrak{S}_n$, we denote $\mathcal{T}_\Pi = \{X^\sigma \mid \sigma \in \Pi\} \subseteq \{+,-\}^{\binom{[n]}{2}}$.

Lemma 3.7.11. *Let $\Pi \subseteq \mathfrak{S}_n$ form an allowable graph of permutations, and let $\mathcal{T}_\Pi \subseteq \{+,-\}^{\binom{[n]}{2}}$ be the set of sign-vectors associated to its permutations. Then the inversion sets of the moves in $\mathcal{L}$ coincide with the parallelism classes of $\mathcal{T}_\Pi$.*

Proof. First, the fact that Π is symmetric and the existence of a valid path between σ and $\overline{\sigma}$ for any $\sigma \in \Pi$ implies that any pair $\{i,j\}$ is in the inversion set of at least one move in $\mathcal{L}$, which is necessarily unique by the disjointness condition (P3) of Definition 3.7.5 . Hence, the inversion sets of the moves in $\mathcal{L}$ define equivalence classes on the pairs $\binom{[n]}{2}$. It is straightforward to check that these coincide with the parallelism classes of $\mathcal{T}_\Pi$. $\square$

[4]Recall that the parallelism class $\overline{\overline{f}}$ of f is the set of elements $e \in E$ such that $X_f = X_e$ for all covectors X or $X_f = -X_e$ for all covectors X. The reorientation ${}_{-F}X$ is the signed vector Z such that $Z_f = -X_f$ for all $f \in F$ and $Z_f = X_f$ otherwise. The separation set $S(X,Y)$ of covectors X, Y are the elements $e \in E$ such that $(X_e, Y_e) \in \{(+,-),(-,+)\}$.

Theorem 3.7.12. *Let $\Pi \subseteq \mathfrak{S}_n$ form an allowable graph of permutations. Then $\mathcal{T}_\Pi \subset \{+,-,0\}^{\binom{[n]}{2}}$ is the set of topes of an acycloid.*

Proof. The support of all the covectors is $\binom{[n]}{2}$, and we have symmetry by definition. Hence, it suffices to verify that $\mathcal{T}_\Pi$ satisfies the reorientation property (T3) from Definition 3.7.10. Let $X, Y \in \mathcal{T}_\Pi$ and $\sigma, \gamma \in \Pi$ be the associated permutations. Let $\sigma = \gamma_0, \dots, \gamma_l = \gamma$ be an allowable sequence from σ to γ. $S(X,Y)$ corresponds to the pairs reversed along this path. Let Z be the sign-vector associated to γ_1 by the map (3.4). Then Z is in $\mathcal{T}_\Pi$ and $Z =_{-\,\mathrm{inv}_m} X$ where m is the move from σ to γ_1. Lemma 3.7.11 shows that inv_m is the parallelism class of any pair $\{i,j\}$ reversed by m. □

We can characterize which acycloids arise from allowable graphs of permutations. We do it in a slightly more general context.

Definition 3.7.13. A *sweep acycloid* is an acycloid on the ground set $\binom{[n]}{2}$ such that

(i) its topes fulfill the transitivity condition from Lemma 3.3.8; namely for every covector X and every choice of $1 \leq i < j < k \leq n$, the triple $(X_{(i,j)}, X_{(j,k)}, X_{(i,k)})$ is orthogonal to the sign vector $(+,+,-)$, and

(ii) its parallelism classes verify the transitivity condition (M1') (after Definition 3.7.2); namely, if $\overline{\overline{(i,j)}}$ or $\overline{\overline{(j,i)}}$ coincides with $\overline{\overline{(j,k)}}$ or $\overline{\overline{(k,j)}}$, then it also coincides with $\overline{\overline{(i,k)}}$ or $\overline{\overline{(k,i)}}$.

As we show in Theorem 3.7.15 below, sweep acycloids are essentially equivalent to allowable graphs of permutations. The only nuance is that sweep acycloids might have some elements outside its support, which under the map (3.4) would give rise to some partitions that are not permutations. In this case, there would be pairs of elements that belong to the same part in all the partitions. However, up to merging non-singleton parts and relabeling, one can suppose that these maximal ordered partitions are permutations. We recover then an allowable graph of permutations.

These operations of merging and relabeling do not affect the tope-graphs.

Lemma 3.7.14. *Let $\mathcal{T} \subseteq \{+,-,0\}^{\binom{[n]}{2}}$ be a sweep acycloid with support $S \subseteq \binom{[n]}{2}$. For $1 \leq i < j \leq n$, if $(i,j) \notin S$, then the restriction of $\mathcal{T}$ to $\binom{[n]\setminus\{j\}}{2}$ is a sweep acycloid with isomorphic tope-graph.*

Proof. That this restriction is a sweep acycloid is straigthforward from the definition. Moreover, from the characterization in Lemma 3.3.8 one sees that for $X \in \mathcal{T}$ and $k \neq i, j$, the values of X on the pairs (i,k) (resp. (k,i)) and (j,k) (resp. (k,j)) determine each other uniquely (the sign depending on the relative order of i, j, k), because $X_{(i,j)} = 0$. Therefore, there is a bijection between topes (resp. parallelism classes) of $\mathcal{T}$ and topes (resp. parallelism classes) of the restriction. □

If $\mathcal{T}$ is the tope set of a sweep acycloid, we denote by $\Pi_\mathcal{T} = \{I_X \mid X \in \mathcal{T}\}$ the set of associated ordered partitions.

Theorem 3.7.15. *If $\Pi \subseteq \mathfrak{S}_n$ forms an allowable graph of permutations, then $\mathcal{T}_\Pi$ is the set of topes of a sweep acycloid. Conversely, if $\mathcal{T}$ is the tope set of a sweep acycloid of full support $\binom{[n]}{2}$, then $\Pi_\mathcal{T}$ forms an allowable graph of permutations.*

Proof. The first claim follows directly from Theorem 3.7.12. Indeed, the topes of the form X^σ for a permutation $\sigma \in \mathfrak{S}_n$ fulfill the transitivity condition from Lemma 3.3.8 by construction. Moreover, the parallelism classes of $\mathcal{T}_\Pi$ are the moves of Π by Lemma 3.7.11, and they fulfill condition (M1') (after Definition 3.7.2) by definition.

For the second claim, note first that $\Pi_\mathcal{T}$ is clearly symmetric by 3.7.10. Following Lemma 3.7.11, we set $\mathcal{L}$ to be the moves whose inversion sets are parallelism classes of the topes. By construction, two distinct moves in this family are either disjoint, or they are reverse to each other and have the same set of inversions.

Finally, let $\sigma_X, \sigma_Y \in \Pi_\mathcal{T}$ be the permutations associated to the topes $X, Y \in \mathcal{T}$. We will prove that they are joined by an allowable sequence by induction on the cardinality of the symmetric difference of their inversion sets. By the reorientation property (T3) of Definition 3.7.10, there is an element $f \in S(X,Y)$ such that $Z = {}_{-\overline{\overline{f}}}\, X \in \mathcal{T}$. The parallelism class $\overline{\overline{f}}$ corresponds to a move $m \in \mathcal{L}$ such that $\mathrm{inv}_m \subseteq \mathrm{inv}_{\sigma_X} \triangle \mathrm{inv}_{\sigma_Y}$. Hence, Z is associated to a permutation σ_Z such that $\mathrm{inv}_{\sigma_Z} \triangle \mathrm{inv}_{\sigma_Y} = (\mathrm{inv}_{\sigma_X} \triangle \mathrm{inv}_{\sigma_Y}) \setminus \mathrm{inv}_m$. By induction there is an allowable sequence $\sigma_Z \to \cdots \to \sigma_Y$ with labels in $\mathcal{L}$. Note that m is not a label of this path because its inversion set is disjoint from $\mathrm{inv}_{\sigma_Z} \triangle \mathrm{inv}_{\sigma_Y}$. Then, $\sigma_X \xrightarrow{m} \sigma_Z \to \cdots \to \sigma_Y$ is an allowable sequence from σ_X to σ_Y. □

3.7.3 Sweeps and potential sweeps of sweep acycloids

With Handa's notation from [Han93], a *face* of an acycloid $\mathcal{T} \subseteq \{+,-,0\}^E$ is a sign-vector $X \in \{+,-,0\}^E$ such that $X \circ T \in \mathcal{T}$ for all $T \in \mathcal{T}$; and a *coboundary* of $\mathcal{T}$ is a sign-vector $X \in \{+,-,0\}^E$ that conforms to a tope (which means that there is a tope that refines it) and such that, for every $T \in \mathcal{T}$ with $X \circ T = T$ we have $X \circ (-T) \in \mathcal{T}$. In the language of partial cubes, faces correspond to gated subgraphs, and coboundaries are antipodal subgraphs. In an acycloid, every gated subgraph is antipodal, which shows that every face is a coboundary (see [KM20] for definitions and details). In general, the converse is not true. However, if $\mathcal{T}$ is the set of topes of an oriented matroid, then faces and coboundaries coincide, and correspond to the covectors of the oriented matroid.

Augmented with a top element, the set of faces of an acycloid forms a lattice, the *big face lattice* of the acycloid [Han93]. Face lattices of acycloids lack many nice properties of those of oriented matroids. In particular, they are not always graded.

We can translate these concepts to sweeps. To this end, define the *composition* $I \circ J$ of two ordered partitions $I = (I_1, \dots, I_l)$ and $J = (J_1, \dots, J_{l'})$ of $[n]$ as

$$I \circ J = (I_{1,1}, \dots, I_{1,r_1}, \dots, I_{l,1}, I_{l,r_l}),$$

where for any $k \in \{1, \dots, l\}$, $(I_{k,1}, \dots, I_{k,r_k})$ is the sequence $(I_k \cap J_1, I_k \cap J_2, \dots, I_k \cap J_{l'})$ where the empty parts are removed. That is, the ordered partition of the elements of I_k induced by J.

Definition 3.7.16. Let $\Pi \subseteq \mathfrak{S}_n$ be an allowable graph of permutations.

- A *sweep* of Π is an ordered partition I such that $I \circ \sigma \in \Pi$ for all $\sigma \in \Pi$.
- A *potential sweep* of Π is an ordered partition I of $[n]$ refined by some permutation in Π and such that any sweep permutation $\sigma \in \Pi$ that refines I satisfies $I \circ \overline{\sigma} \in \Pi$.

Lemma 3.7.17. *Let $\Pi \subseteq \mathfrak{S}_n$ form an allowable graph of permutations and let $\mathcal{T}_\Pi$ be its associated sweep acycloid. Then the sweeps of Π are in bijection with the faces of $\mathcal{T}_\Pi$ and the potential sweeps of Π are in bijection with the coboundaries of $\mathcal{T}_\Pi$.*

Proof. We prove first the equivalence between potential sweeps and coboundaries. It is clear that X^I is a coboundary of $\mathcal{T}_\Pi$ for any potential sweep I of Π. Indeed, if σ refines I, it implies that X^I conforms to X^σ, i.e. $X^I \circ X^\sigma = X^\sigma$. Moreover, $I \circ \overline{\sigma} \in \Pi$ implies that $X^I \circ (-X^\sigma) = X^I \circ X^{\overline{\sigma}} = X^{I \circ \overline{\sigma}}$ is in $\mathcal{T}_\Pi$.

For the converse statement, let Y be a coboundary of $\mathcal{T}_\Pi$. We need to show that it is of the form X^I for an ordered partition I of $[n]$. Then it is clear from the definitions that I is a potential sweep of Π. Suppose that there are $1 \leq i < j < k \leq n$ such that $(Y_{(i,j)}, Y_{(j,k)}, Y_{(i,k)})$ is one of the forbidden patterns in Lemma 3.3.8. Let $\sigma \in \Pi$ be a sweep permutation such that $Z := Y \circ X^\sigma = X^\sigma$. We denote $\tilde{\sigma}$ the permutation in Π such that $\tilde{Z} := Y \circ (-X^\sigma) = X^{\tilde{\sigma}}$. The fact that Z and $\tilde{Z}$ satisfy the transitivity condition implies that the forbidden pattern of Y must be one of the last six ones (with two zeroes). We consider the case $(Y_{(i,j)}, Y_{(j,k)}, Y_{(i,k)}) = (0, 0, -)$, the other ones are similar. Then we must have $\{(Z_{(i,j)}, Z_{(j,k)}, Z_{(i,k)}), (\tilde{Z}_{(i,j)}, \tilde{Z}_{(j,k)}, \tilde{Z}_{(i,k)})\} = \{(+, -, -), (-, +, -)\}$, i.e. the elements i, j, k are ordered k, i, j and j, k, i in σ and $\tilde{\sigma}$. As a consequence of condition 3.7.1, in any allowable sequence in Π from σ to $\tilde{\sigma}$, there must be a permutation where the elements i, j, k are ordered k, j, i. Such τ satisfies $Y \circ X^\tau = X^\tau$. Indeed, any pair (k, l) with $Y_{(k,l)} \neq 0$ satisfies $Z_{(k,l)} = \tilde{Z}_{(k,l)}$, thus it cannot be reversed in an allowable sequence from σ to $\tilde{\sigma}$. But then the covector $Y \circ (-X^\tau)$ should belong to $\mathcal{T}_\Pi$ while it has the forbidden pattern $(+, +, -)$. We conclude that any coboundary satisfies the transitivity condition from Lemma 3.3.8.

To finish, it is clear that any sweep I of Π gives a covector $X^I \in \{+, -, 0\}^{\binom{[n]}{2}}$ such that for any $\sigma \in \Pi$, $X^I \circ X^\sigma = X^{I \circ \sigma} \in \mathcal{T}_\Pi$, thus X^I is a face of $\mathcal{T}_\Pi$. For the converse, note that any face Y of $\mathcal{T}_\Pi$ is a coboundary, and hence it must be of the form X^I associated to a potential sweep I. The condition of being a face shows that this potential sweep is indeed a sweep. $\square$

Note in particular that the *poset of sweeps* of an allowable graph of permutations, augmented with a top element, is always a lattice, as it is isomorphic to the big face lattice of an acycloid.

3.7.4 Sweep oriented matroids from sweep acycloids and allowable graphs of permutations

The set of topes of an oriented matroid is always an acycloid, but the converse statement is not true. However, the conditions in the definition of sweep acycloid guarantee that, whenever they correspond to an oriented matroid, it is a sweep oriented matroid.

Note that, for this, the transitivity condition 3.7.1 on the parallelism classes of sweep acycloids is necessary. Indeed, $(+,+,+), (-,-,-), (-,+,+), (+,-,-)$ satisfy the conditions of Lemma 3.3.8 (they are orthogonal to $(+,+,-)$) and they are the topes of an oriented matroid, but not a sweep oriented matroid. This gives an acycloid whose topes fulfill the transitivity condition from Lemma 3.3.8 and that arises from an oriented matroid, but that is not a sweep oriented matroid. However, thanks to Lemma 3.7.17, we know that the conditions on topes and subtopes in the definition of sweep acycloids extend to the whole set of covectors.

Corollary 3.7.18. *The set of topes of a sweep oriented matroid is a sweep acycloid. Conversely, if a sweep acycloid is the set of topes of an oriented matroid, then it is a sweep oriented matroid.*

The following hierarchy summarizes our current knowledge:

Theorem 3.7.19.

$$\Big\{\textit{Posets of sweeps of point configurations}\Big\}$$
$$\subsetneq$$
$$\Big\{\textit{Posets of sweeps of sweep oriented matroids}\Big\}$$
$$\subseteq$$
$$\Big\{\textit{Posets of sweeps of sweep acycloids}\Big\}$$

Goodman and Pollack's unrealizable pentagon proves that the first inclusion is strict. For the second inclusion, it is known that there are acycloids that are not oriented matroids, but we do not know of any example that has the additional structure given by the transitivity condition from Lemma 3.3.8.

Corollary 3.7.18 allows us to use characterizations of acycloids arising from oriented matroids to characterize which allowable graphs of permutations arise from sweep oriented matroids. We know three families of such characterizations, summarized in [KM20, Cor. 7.2]. In the language of permutations, da Silva's characterization [dS95, Thm. 4.1] concerns sweeps and potential sweeps. Handa's characterization is stated in terms of contractions. If Π is an allowable graph of permutations, and $m \in \mathcal{L}$ is one of its moves, the *elementary contraction* Π/m is obtained by taking all permutations $\gamma \in \Pi$ that are separated from another permutation of Π by m, and replacing the substring m by its minimal element. One obtains this way a new set of permutations on the ground set $[n] \setminus m \cup \{\min(m)\}$. For a collection of moves $M = \{m_1, \ldots, m_l\}$, the *contraction* Π/M, is defined inductively by $\Pi/M = (((\Pi/m_1)/m_2)\cdots)/m_l$. The characterization by Knauer and Marc [KM20, Cor. 7.2] is in terms of excluded partial cube minors. This operation goes outside the scope of allowable graphs of permutations. We will hence not present its details and refer the reader to the source [KM20].

Corollary 3.7.20. *Let Π form an allowable graph of permutations. The following conditions are equivalent:*

(i) Π arises from a sweep oriented matroid,

(ii) every potential sweep of Π is a sweep,

(iii) all its contractions are allowable graphs of permutations,

(iv) the graph is in $\mathcal{F}(\mathcal{Q}^-)$ in the sense of [KM20].

These characterizations might be useful to answer the question whether all sweep acycloids are sweep oriented matroids. We have not been able to construct any counterexample, but we do not have any evidence on why the properties defining sweep acycloids should force these conditions to be satisfied.

Question 3.7.21. Is every sweep acycloid an oriented matroid?

3.8 Further directions

Elementary homotopies between sweep oriented matroids

In [Fel04, FW01] it is proven that if an allowable sequence has two consecutive moves with disjoint support, then these can be merged into a single move and the result is still an allowable sequence; and that conversely, if a move consists of more than one disjoint substrings, these can be split into two disjoint moves. These operations induce an equivalence relation among sweep oriented matroids of rank 2 whose equivalence classes are in correspondence with the associated little oriented matroids.

Extending this result to higher rank is closely related to some of the open questions indicated in the chapter. First of all, the higher analogue of the operation of merging would consist in collapsing some flats of a sweep oriented matroid to get a flat whose rank is lower than the one expected by (3.5). The reverse operation would break a flat with unexpected low rank into pieces fulfilling (3.5). Understanding this procedure would provide a method to prove Conjecture 3.5.4.

Even if the operations were well described, it is not clear that one could find a connectivity result analogous to that by Felsner and Weil in rank 2 [FW01]. Note that, even if Theorem 3.6.6 goes in this direction, as it shows that all sweep oriented matroids are homotopy equivalent in the complex of pseudo-sweeps, it is not clear that there is a way to do this where all the intermediate steps are also sweep oriented matroids.

Are all sweep acycloids oriented matroids?

Another natural problem that is left open is Question 3.7.21, which asks whether every sweep acycloid is an oriented matroid. The answer would be very interesting in either direction. If it is affirmative, then the two categories of sweep acycloids and sweep oriented matroids would collapse into a single concept. This would make allowable graphs of permutations a useful alternative characterization of sweep oriented matroids. If, on the contrary, the answer is negative, then it would be interesting to understand the gap between the two categories.

We do not have any good reason to conjecture that every sweep acycloid is an oriented matroid, beyond the fact that we could not find any counter-example. This does not tell much, because the naive approaches to computationally generate all allowable graphs of permutations of a certain size fail badly very soon because of the rapid growth of these objects.

Allowable graphs in Coxeter groups

We already saw the hyperoctahedral group B_n naturally appear before. First, in Section 3.2.2, because the permutahedron of type B is the sweep polytope of the crosspolytope. Then also in Example 3.4.5 to explain the supersolvability of the associated matroid. In fact, the definition of allowable graph extends naturally to any Coxeter group, specially in the simple case; namely, a *simple allowable graph of Coxeter permutations* is a symmetric set Π of elements of the Coxeter group, in which for every pair of elements $w, w' \in \Pi$ there is a path from w to w' following a reduced decomposition of $w^{-1}w'$. For the non-simple case one has to partition the generators into a collection of disjoint subsets to define the allowable moves.

Higher sweep oriented matroids and permutahedra

As we saw in Section 3.5.1, sweep oriented matroids are closely related to the first Dilworth truncation. What about higher truncations? In the realizable case, instead of studying the intersection of the lines spanned by the points of $\boldsymbol{A}$ with a hyperplane (at infinity), we would study the intersection of a flat F of codimension k (playing the role of hyperplane at infinity) with every flat spanned by $k+1$ points of $\boldsymbol{A}$. In [Sta15, Thm. 8], Stanley states (in the polar formulation) that for a sufficiently generic choice of the flat, this gives rise to an arrangement whose lattice of flats is the kth Dilworth truncation of the original arrangement. Let's call this operation the *kth Dilworth truncation* of $\boldsymbol{A}$ with respect to F. Doing the kth Dilworth truncation of an standard $(n-1)$-simplex gives rise to "higher" analogues of braid arrangements, which are the normal fans of the *kth higher n-permutahedra*. However, in comparison with the $k=1$ case, there is no $\mathfrak{S}_n$-invariant subspace that gives a canonical choice for F. Indeed, different choices for F can give rise to different combinatorial types of hyperplane arrangements and zonotopes, even if the flats are sufficiently generic in the sense of Stanley. See Figure 3.14 for some

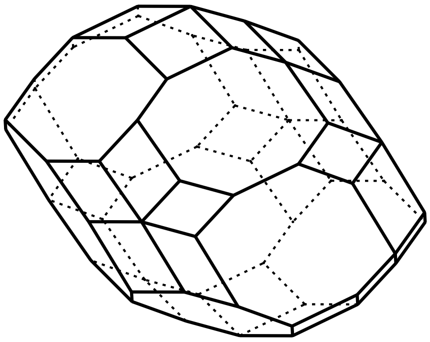

(a) A generic 2nd higher 5-permutahedron.

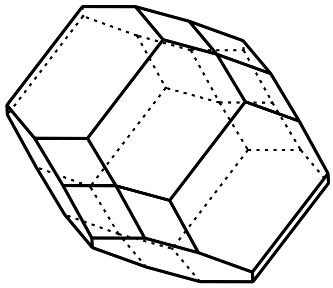

(b) A degenerate 2nd higher 5-permutahedron.

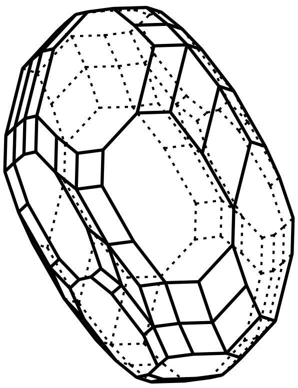

(c) A generic 3rd higher 6-permutahedron.

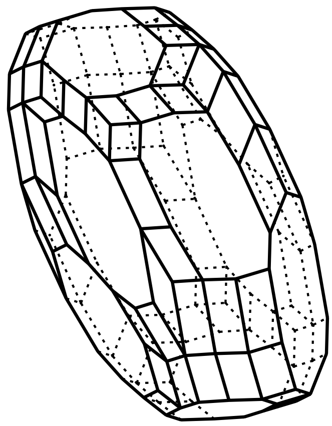

(d) Another generic 3rd higher 6-permutahedron.

Figure 3.14: The first row shows a generic and a degenerate 2nd higher 5-permutahedra. The second row depicts two combinatorially different generic 3rd higher 6-permutahedra.

examples. Nevertheless, every zonotope associated to a kth Dilworth truncation of a point configuration still arises as the projection of some kth higher permutahedron.

Which matroids are little oriented matroids?

In Section 3.4.3 we proved that not every oriented matroid is a little oriented matroid. This begs the question of which are the oriented matroids that are sweepable, in the sense that they can be extended to a big oriented matroid. Or, at least, to find sufficient conditions. For example, we know that realizable oriented matroids are sweepable, and also all oriented matroids of rank 3, by Theorem 3.4.11.

As shown in [Hoc16], Euclidean oriented matroids (see [BLS$^+$99, Section 10.5]) always admit topological sweepings (see Section 3.1). Is there a relation between being Euclidean and being sweepable? Our example of non-sweepable oriented matroid in Section 3.4.3 is based on a well-known example of non-Euclidean oriented matroid.

Chapter 4

Geometric realizations of the s-weak order and its quotients

This chapter includes joint work with Rafael S. González D'León, Alejandro H. Morales, Daniel Tamayo Jiménez and Martha Yip which gave rise to the preprint *Realizing the s-permutahedron via flow polytopes* [GDMP+23], and recent joint work with Vincent Pilaud which gave rise to the preprint *Geometric realizations of the* s*-weak order and its lattice quotients* [PP24]. We also include a few new results and sketch lines of research that are currently developed with the same collaborators plus Matias von Bell and Yannic Vargas.

Ceballos and Pons introduced the s-weak order on s-decreasing trees, for any weak composition s. They proved that it has a semidistributive lattice structure and that the s-Tamari lattice can be recovered from it as a lattice quotient. They further conjectured that the s-weak order can be realized as the 1-skeleton of a polytopal subdivision of a polytope, and that the s-associahedron can be recovered from it by removing facets.

We answer the first conjecture in the case where s is a strict composition by providing three geometric realizations of the s-permutahedron. The first one is the dual graph of a triangulation of a flow polytope of high dimension. Along the way, we prove a few new results about the dual graph of DKK triangulations of flow polytopes in general. The second realization of the s-permutahedron, obtained using the Cayley trick, is the dual graph of a fine mixed subdivision of a sum of cubes that has the conjectured dimension. The third one, obtained using tropical geometry, is the 1-skeleton of a polytopal complex for which we can provide explicit coordinates of the vertices and whose support is a permutahedron as conjectured.

We give some elements on the study of all quotients of the s-weak order and related geometric realizations. In particular, this allows us to answer Ceballos and Pons second conjecture.

4.1 Introduction

The starting point of this work is a conjecture of Ceballos and Pons ([CP20, Conjecture 1] and [CP23, Conjecture 3.1.2], also Conjecture 4.1.1 below) stating that a certain combinatorial complex on s-*decreasing trees* can be geometrically realized as a polytopal subdivision of a polytope. The family of s-decreasing trees is parameterized by *weak compositions* $s = (s_1, \dots, s_n)$ where s_i are non-negative integers for $i = 1, 2, \dots, n$. Ceballos and Pons [CP20, CP22] showed that for every s, the set of s-decreasing trees admits a lattice structure called the s-*weak order*. In the special case when $s = (1, \dots, 1)$, the set of s-decreasing trees is in bijection with the set of permutations of $[n]$, and the s-weak order is the classical (right) weak order on the permutations of $[n]$.

It turns out that when s is a (strict) *composition*, that is $s_i > 0$ for all i, the properties of the s-weak order and the s-permutahedron can also be described in terms of *Stirling* s-*permutations*. These are multipermutations of $[n]$ avoiding the pattern 121 (a number j somewhere in between two occurrences i with $i < j$) and with s_i occurrences of i for each $i \in [n]$. These multipermutations generalize the family of permutations (the case when $s = (1, \dots, 1)$) and the family of Stirling permutations (the case when $s = (2, \dots, 2)$) initially introduced by Gessel and Stanley in [GS78b]. A further generalization of Stirling permutations (to the case when $s = (m, \dots, m)$) was studied by Park in [Par94c, Par94b, Par94a]. Further study of combinatorial formulas and statistics on Stirling s-permutations such as descents, ascents and plateaux have been carried out by many other authors (see for example [Bón09, JKP11, KP11]). We refer the reader to Gessel's note in [Ges20] which includes a list of articles on the family of Stirling s-permutations.

Figure 4.1 shows the Hasse diagram of the s-weak order for the case $s = (1, 2, 1)$. The vertices are indexed by s-decreasing trees and Stirling s-permutations. From this figure the reader can already appreciate how the s-permutahedron may be geometrically realizable. Ceballos and Pons posed the following conjecture on realizations of Perm_s, that they could prove for the cases $n \leq 4$ ([CP23, Section 3.3]).

Conjecture 4.1.1 ([CP20, Conjecture 1])**.** *Let* s *be a weak composition. The* s*-permutahedron* Perm_s *can be realized as a polyhedral subdivision of a polytope which is combinatorially isomorphic to the zonotope* $\sum_{1 \leq i < j \leq n} s_j [\boldsymbol{e}_i, \boldsymbol{e}_j]$

In the same way that the weak order on permutations restricts to the lattice on Catalan objects introduced by Tamari in [Tam62] (as implied by a classical bijection of Stanley [Sta12, Section 1.5]), Ceballos and Pons show in [CP22, Theorem 2.2] that the s-weak order restricts to the s-*Tamari lattice*. They also show that when s is a (strict) composition the s-Tamari lattice is a lattice quotient of the s-weak order. The s-Tamari lattice was first introduced by Préville–Ratelle and Viennot [PRV17] as the ν-*Tamari lattice* on grid paths weakly above the path $\nu = NE^{s_n} \dots NE^{s_1}$ (see [CP20, Theorem 3.5] for the isomorphism between the ν-Tamari and the s-Tamari lattices). It is a further generalization of the m-Tamari lattice, recovered with $s = (m, \dots, m)$, which was introduced by Bergeron and Préville–Ratelle in [BPR12] to study the Frobenius characteristic of the

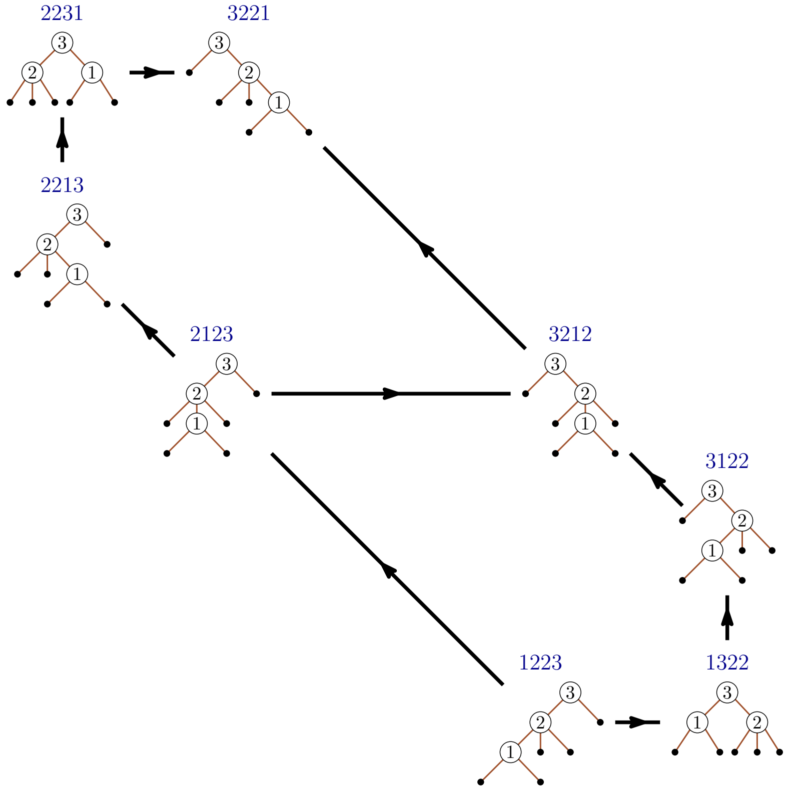

Figure 4.1: Hasse diagram of the s-weak order (1-skeleton of the s-permutahedron) for the case s $= (1, 2, 1)$. The vertices are indexed by s-decreasing trees and Stirling s-permutations.

space of higher diagonal coinvariant spaces in representation theory. Ceballos, Padrol and Sarmiento provided a geometric realization of the ν-Tamari lattice as the 1-skeleton of a polytopal complex called the *ν-associahedron* [CPS19].

Inspired by the fact that certain realizations of the associahedron can be obtained by removing facets from the standard permutahedron (as we saw in Section 1.4.6), Ceballos and Pons conjectured that similar geometric relations hold between the s-associahedron and the s-permutahedron when s is a composition. They could prove the following conjecture for $n \leq 4$ ([CP23, Section 3.3]). See Figure 4.2 for an example.

Conjecture 4.1.2 ([CP20, Conjecture 2])**.** *Let* s *be a strict composition. There exists a geometric realization of the* s*-permutahedron such that the* s*-associahedron can be obtained from it by removing certain facets.*

4.1.1 Geometric realizations of the s-permutahedron

Our main goal is to provide solutions to Conjecture 4.1.1 in the case when s is a strict composition (see Theorem 4.1.3). We will use techniques similar to those that were previ-

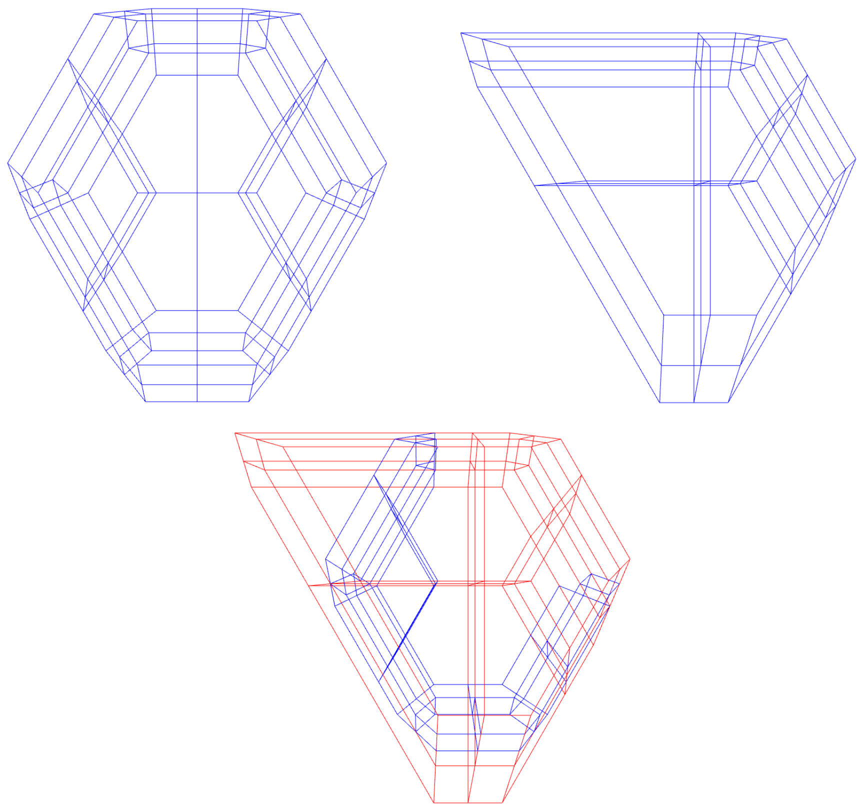

Figure 4.2: Realizations of the s-permutahedron (left), of the s-associahedron (right), and the superposition of both (below), for $s = (1, 2, 2, 2)$. Figure from [CP20].

ously employed for realizing the s-associahedron. Ceballos, Padrol and Sarmiento [CPS19] realized the Hasse diagram of the s-Tamari lattice as the graph dual to a triangulation of a subpolytope of a product of simplices called $\mathcal{U}_{I,\overline{J}}$ and as the graph dual to a fine mixed subdivision of a generalized permutahedron. They could dualize these subdivisions to obtain the s-associahedron as a subdivision of the usual associahedron induced by an arrangement of tropical hyperplanes. Another realization of the s-Tamari lattice was given by von Bell, González D'León, Mayorga Cetina and Yip [BGMY23] via flow polytopes. This construction is related to the Ceballos-Padrol-Sarmiento one since von Bell and Yip [BY23] showed that the polytopes $\mathcal{U}_{I,\overline{J}}$ are integrally equivalent to flow polytopes.

A flow polytope $\boldsymbol{\mathcal{F}}_G$ is the set of valid flows on a directed acyclic graph G. Geometric information about this polytope can be recovered from combinatorial information of the graph, for example computing the volume or constructing certain triangulations. In the recent literature there has been an increased interest in developing techniques in this direction, see for example [CKM17, JK19, MM15, MM19, MMS19]. In particular, Danilov, Karzanov and Koshevoy [DKK12] described a method for obtaining regular unimodular triangulations for $\boldsymbol{\mathcal{F}}_G$ by placing a structure on G called a *framing* (see Section 4.2.2). Von

Bell et al. [BGMY23] used the method of Danilov, Karzanov and Koshevoy to show that the flow polytope of the s-*caracol graph* Car(s) (see the left side of Figure 4.3) has a DKK triangulation whose dual graph is the s-Tamari lattice.

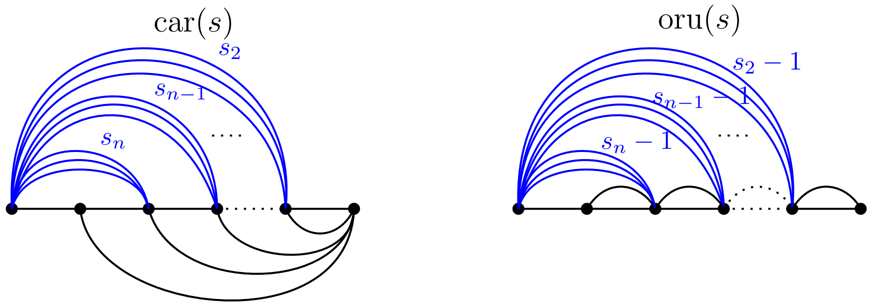

Figure 4.3: The s-caracol and s-oruga graphs.

In a similar vein, we introduce the graph Oru(s) which we call the s-*oruga graph* (see Definition 4.4.1 and the right side of Figure 4.3). Its associated flow polytope possesses a DKK triangulation which allows us to answer Conjecture 4.1.1 as follows.

Theorem 4.1.3 (Geometric realizations). *Let* $\mathrm{s} = (s_1, \ldots, s_n)$ *be a composition. The face poset of the (combinatorial)* s*-permutahedron* $Perm_{\mathrm{s}}$ *is isomorphic to*

1. **(Theorem 4.4.15)** *The dual of the poset of internal faces of a DKK triangulation of the flow polytope* $\mathcal{F}_{\mathrm{Oru(s)}}$ *of dimension* $\sum_{i=1}^{n} s_i$*.*

2. **(Theorem 4.4.22)** *The dual of the poset of internal faces of a mixed subdivision of a sum of cubes in* $\mathbb{R}^n$*.*

3. **(Theorem 4.4.30)** *The poset of bounded faces of a polyhedral complex induced by an arrangement of tropical hypersurfaces in* $\mathbb{R}^n$*. The support of the polyhedral complex is combinatorially equivalent to the* $(n-1)$*-dimensional permutahedron.*

We are able to provide explicit coordinates for the third realization. $3d$-examples of this realization are available on this webpage[1] and code can be found on this webpage[2].

Structure of this chapter

We first provide in Section 4.2 some background on flow polytopes and their Danilov-Karzanov-Koshevoy (DKK) triangulations, which allow for a nice interplay between cells of a triangulation and combinatorial objects. Sections 4.2.3 and 4.2.4 contain new results

[1]https://sites.google.com/view/danieltamayo22/gallery-of-s-permutahedra
[2]https://cocalc.com/ahmorales/s-permutahedron-flows/demo-realizations

about the structure of the dual graphs of these triangulations. In particular, Theorem 4.2.22 provides a geometric decomposition of DKK triangulations that reflects a Baldoni-Vergne-Lidskii formula on volumes of flow polytopes.

In Section 4.3 we present the combinatorial structures that are at the heart of this chapter: the s-weak order and the s-permutahedron. In Section 4.3.1, we first give the initial definitions of Ceballos and Pons ([CP20],[CP22]) in terms of s-decreasing trees. In Section 4.3.2 we restrict to the case where s is a (strict) composition and translate the definitions of the s-weak order and the s-permutahedron to the language of Stirling s-permutations. Indeed, this is the setting we use for our geometric realizations.

Section 4.4 is the main section of this chapter. In Section 4.4.1 we introduce the s-oruga graph Oru(s) and present our first geometric realization of the s-permutahedron as the dual of a DKK triangulation of the flow polytope $\mathcal{F}_{\mathrm{Oru(s)}}$. In Section 4.4.2 we show how the Cayley trick gives us a second geometric realization of the s-permutahedron as the dual of a fine mixed subdivision of a sum of cubes. In Section 4.4.3 we dualize the previous construction and realize the s-permutahedron as the collection of bounded faces of an arrangement of tropical hypersurfaces. This third realization provides a complete answer to Ceballos and Pons conjecture in the case where s is a composition.

In Section 4.5 we give some context about lattice quotients of the s-weak order and their realizations as quotientopes via shards and shard polytopes. We sketch how these constructions can be adapted to the lattice quotients of the s-weak order. This allows us to give a new answer to Conjecture 4.1.1 which also works when s is a weak composition, and to answer Conjecture 4.1.2. We also give some elements on another way to obtain geometric realizations of a specific family of quotients of the s-weak order, via flow polytopes and a graph operation on the s-oruga graph.

4.2 Background on subdivisions of flow polytopes

4.2.1 Flow polytopes

Let $G = (V, E)$ be a loopless connected oriented multigraph on vertices $V = \{v_0, \ldots, v_n\}$ with each edge on vertices (v_i, v_j) oriented from v_i to v_j if $i < j$ and such that v_0 (respectively v_n) is the only source (respectively sink) of G. Since we allow multiple edges between pairs of vertices, we will sometimes abuse notations and write $e = (v_i, v_j)$ to mean that the edge e has vertices (v_i, v_j) (but then we could have $f = (v_i, v_j)$ and yet $e \neq f$). In what follows we will always assume that these conditions are fulfilled (see for example Figures 4.3 or 4.5). A vertex is an *inner vertex* if it is not a source nor a sink. For any vertex v_i we denote by In_i its set of incoming edges and by Out_i its set of outgoing edges. We also denote $\mathrm{indeg}_G(v_i) := |In_i|$ and $\mathrm{outdeg}_G(v_i) := |Out_i|$.

A *netflow* for G is a vector $\boldsymbol{a} = (a_0, a_1 \ldots, a_{n-1}, -\sum_{i=0}^{n-1} a_i)$ such that $a_i \in \mathbb{Z}_{\geq 0}$ for all $i \in \{0, \ldots, n-1\}$. A *flow* of G with netflow $\boldsymbol{a}$ is a vector $(f_e)_{e \in E} \in (\mathbb{R}_{\geq 0})^E$ such that: $\sum_{e \in In_i} f_e + a_i = \sum_{e \in Out_i} f_e$ for all $i \in [0, n]$. A flow $(f_e)_{e \in E}$ of G is called an *integer flow* if all f_e are integers. We denote by $\boldsymbol{\mathcal{F}}_G^{\mathbb{Z}}(\boldsymbol{a})$ the set of integer flows of G with netflow $\boldsymbol{a}$.

The *flow polytope* of G is

$$\boldsymbol{\mathcal{F}}_G(\boldsymbol{a}) = \Big\{(f_e)_{e\in E} \text{ flow of } G \text{ with netflow } \boldsymbol{a}\Big\} \subseteq \mathbb{R}^E.$$

When the netflow is not specified, *i.e.* when we write $\boldsymbol{\mathcal{F}}_G$, it is assumed to be $\boldsymbol{a} = (1, 0, \ldots, 0, -1)$. In this case, $\boldsymbol{\mathcal{F}}_G$ is a polytope of dimension $|E| - |V| + 1$, and the vertices of $\boldsymbol{\mathcal{F}}_G$ correspond exactly to indicator vectors of the routes of G ([GS78a, Corollary 3.1]). A *route* of G is a path from v_0 to v_n *i.e.* a sequence of edges $(e_0, \ldots, e_l)$ such that $e_i = (v_{k_i}, v_{k_{i+1}})$ with $0 = k_0 < k_1 < k_2 < \ldots < k_l < n = k_{l+1}$. The corresponding indicator vector is the vector in $\mathbb{R}^E$ with coordinates 1 at edges e_i and 0 on all other edges.

See Figure 4.4 for an example of flow polytope of dimension 3.

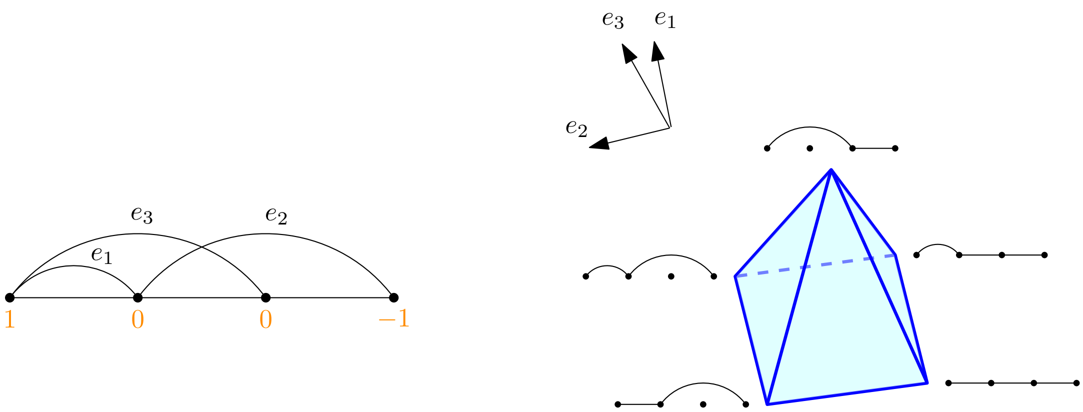

Figure 4.4: A graph G with netflow $(1, 0, 0, -1)$ (left) and its flow polytope $\boldsymbol{\mathcal{F}}_G$ embedded in the space of edges e_1, e_2, e_3 of G (right). Each vertex of the flow polytope is labeled by the route of G it corresponds to. Figure adapted from [TJ23, Figure 5.4].

4.2.2 Danilov-Karzanov-Koshevoy triangulations

Flow polytopes admit several nice subdivisions that can be understood via combinatorial properties of the graph G, in particular the triangulations defined by Danilov, Karzanov and Koshevoy in [DKK12] in the case of the netflow $\boldsymbol{a} = (1, 0, \ldots, 0, -1)$. These triangulations will be our main tool for obtaining geometric realizations of s-permutahedra.

Let P be a route of G that contains vertices v_i and v_j. We denote by Pv_i the prefix of P that ends at v_i, v_iP the suffix of P that starts at v_i and v_iPv_j the subroute of P that starts at v_i and ends at v_j.

A *framing* $\preceq$ of G is a choice of total orders $\preceq_{In_i}$ and $\preceq_{Out_i}$ on the sets of incoming and outgoing edges for each inner vertex v_i. This induces a total order on the set of partial routes from v_0 to v_i (respectively from v_i to v_n) by taking $Pv_i \preceq Qv_i$ if $e_P \preceq_{In_j} e_Q$ where v_j is the first vertex after which the two partial routes coincide, and e_P, e_Q are the edges of

P and Q that end at v_j (respectively $v_iP \preceq v_iQ$ if $e_P \preceq_{Out_j} e_Q$ where v_j is the last vertex before which the two partial routes coincide, and e_P, e_Q are the edges of P and Q that start at v_j). When G is endowed with such a framing $\preceq$, we say that G is *framed*. See Figure 4.5 for an example. From now on, we will always draw the framed graphs in such a way that the framing is obtained by reading the incoming or outgoing edges of a vertex from top to bottom.

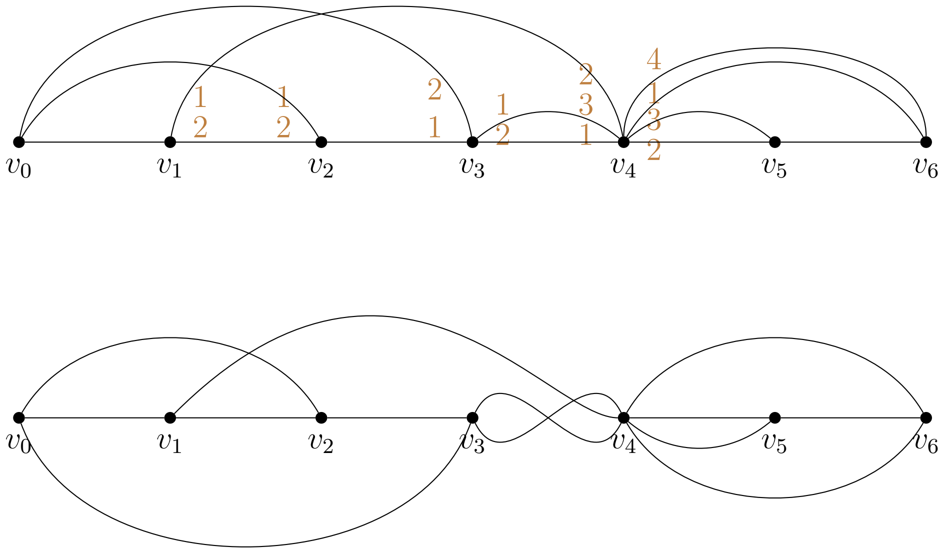

Figure 4.5: Example of a framed graph. On the top figure the framing is depicted with numbers in brown that indicate the ordering. The bottom figure represents the same framed graph, the framing is obtained by reading the incoming and outgoing edges of a vertex from top to bottom. This is the convention we will use in the rest of the figures.

Let P and Q be routes of G with a common subroute between inner vertices v_i and v_j (possibly with $v_i = v_j$). We say that P and Q are *in conflict* at $[v_i, v_j]$ if the initial parts Pv_i and Qv_i are ordered differently than the final parts v_jP, v_jQ. Otherwise we say that P and Q are *coherent* at $[v_i, v_j]$. We say that P and Q are *coherent* if they are coherent at each common inner subroute. See Figure 4.6 for an example of routes in conflict, and Figure 4.8 for an example of coherent routes. Note that with our convention of drawing, a conflict at a subroute corresponds visually to a crossing at this subroute.

The relation on routes being coherent is reflexive and symmetric and we can consider sets of mutually coherent routes which are called the *cliques* of $(G, \preceq)$. We denote by *Cliques*$(G, \preceq)$ the set of cliques of $(G, \preceq)$, and *MaxCliques*$(G, \preceq)$ the subset of cliques that are maximal under inclusion. For a set of routes C, let Δ_C be the convex hull of the vertices

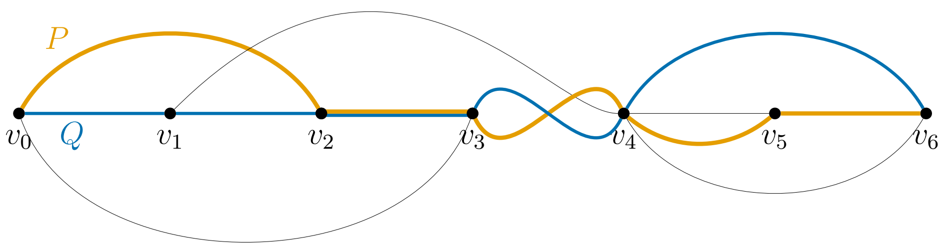

Figure 4.6: The routes P (in bold orange) and Q (in blue) are in conflicts at subroutes $[v_2, v_3]$ and $[v_4, v_4]$.

of the flow polytope $\boldsymbol{\mathcal{F}}_G$ corresponding to the elements in C:

$$\Delta_C := \operatorname{conv}\left(\left\{ \sum_{f \text{ edge of } P} \boldsymbol{e}_f \,\middle|\, P \in C \right\}\right) \subset \mathbb{R}^E.$$

Theorem 4.2.1 ([DKK12, Theorem 1 & 2])**.** *The simplices $\{\Delta_C \,|\, C \in \mathit{MaxCliques}(G, \preceq)\}$ are the maximal cells of a regular triangulation of $\boldsymbol{\mathcal{F}}_G$.*

Proof. We do not repeat here the proof of [DKK12, Theorem 1 & 2]. The formulation there is in terms of the cone $\mathcal{F}_+$ of flows with any netflow $\boldsymbol{a} = (\lambda, 0, \ldots, 0, -\lambda)$, for $\lambda \in \mathbb{R}_+$. To obtain the theorem in our formulation for the flow polytope $\boldsymbol{\mathcal{F}}_G$, we only need to intersect this cone with the affine hyperplane corresponding to taking $\lambda = 1$. $\square$

The triangulation obtained this way is the *DKK triangulation* of $\boldsymbol{\mathcal{F}}_G$ with respect to the framing $\preceq$ and we denote it by $\boldsymbol{\mathit{Triang}}_{DKK}(G, \preceq)$.

Figure 4.7 depicts the DKK triangulation of the flow polytope from Figure 4.4. One can see that in this graph G, only two routes are in conflict.

4.2.3 Dual graphs of DKK triangulations

We are interested in studying the graph dual to the DKK triangulation. Such graph has one vertex for each maximal clique $C \in \text{MaxCliques}(G, \preceq)$ and an edge between maximal cliques C and C' if the corresponding simplices Δ_C and $\Delta_{C'}$ of $\textbf{Triang}_{DKK}(G, \preceq)$ share a common facet, which is equivalent to say that C and C' differ in exactly one route $P \in C$ and $Q \in C'$.

We first introduce the following new notions.

Definition 4.2.2. Let P and Q be a pair of non-coherent routes of $(G, \preceq)$ that are in conflict at subroutes $[x_1, y_1]$, $\ldots$, $[x_k, y_k]$, where $x_1 \le y_1 < x_2 \le y_2 \ldots < x_k \le y_k$ and

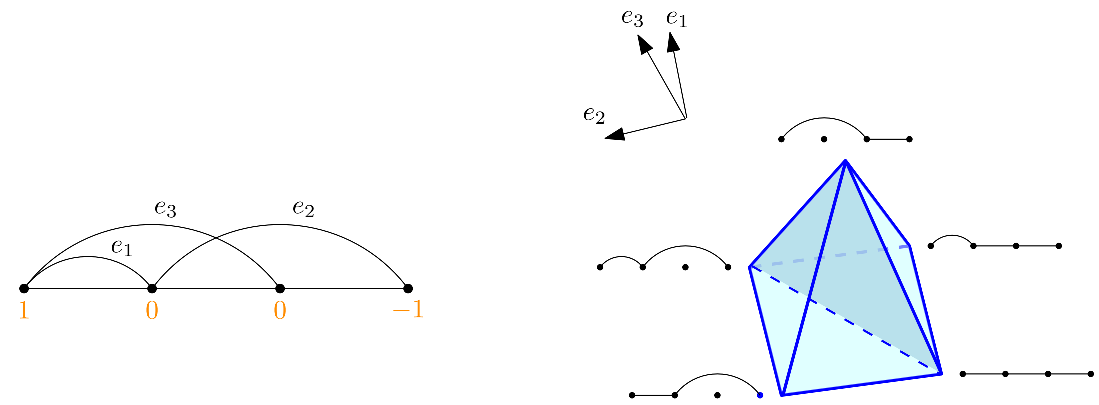

Figure 4.7: A graph G with framing from top to bottom (left) and the corresponding DKK triangulation of its flow polytope $\boldsymbol{\mathcal{F}}_G$ embedded in the space of edges e_1, e_2, e_3 of G (right). Figure adapted from [TJ23, Figure 5.4].

the subroutes $[x_i, y_i]$ are as long as possible. We define the route P' as the alternated concatenation of subroutes Px_1, x_1Qx_2, x_2Px_3, $\ldots$, that we denote $Px_1Qx_2Px_3\ldots$ and Q' the concatenation $Qx_1Px_2Qx_3\ldots$. We call P' and Q' the *resolvents* of P and Q.

It is clear that $P + Q = P' + Q'$ (where $P + Q$ denotes the union of edges in P and edges in Q) and P' and Q' are coherent.

Figure 4.8 depicts the resolvents P' and Q' of routes P and Q from Figure 4.6.

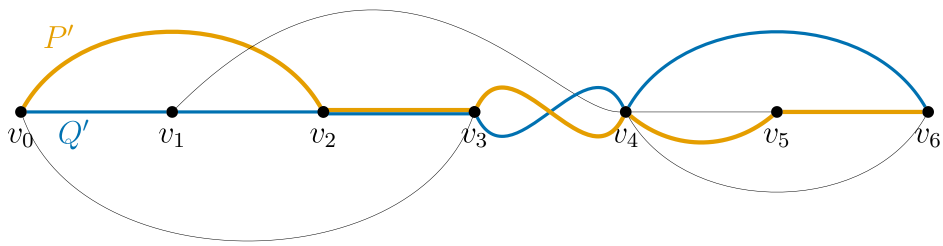

Figure 4.8: P' (in bold orange) and Q' (in blue) are the resolvents of P and Q from Figure 4.6.

Definition 4.2.3. We say that there is a *minimal conflict* between two routes P and Q of $(G, \preceq)$ if the following conditions are satisfied:

- P and Q are in conflict at exactly one subroute $[v_i, v_j]$,
- the edges of P and Q that end at v_i are adjacent for the total order $\preceq_{In_i}$,

- the edges of P and Q that start at v_j are adjacent for the total order $\preceq_{Out_j}$.

See Figure 4.9 for an example of minimal conflict.

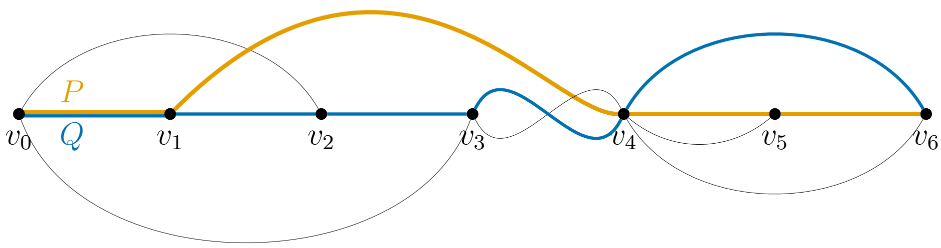

Figure 4.9: P (in bold orange) and Q (in blue) are in minimal conflict at $[v_4, v_4]$.

Lemma 4.2.4. *Let C and C' be maximal cliques in MaxCliques$(G, \preceq)$ that differ in exactly one route $P \in C$ and $Q \in C'$. Then there is a minimal conflict between P and Q.*

Proof. P and Q are not coherent, since otherwise $C \cup C'$ would be a clique that strictly contains C and this contradicts the maximality of C. In order to prove that P and Q are in minimal conflict, we show that if it were not the case we could add two distinct routes R and R' to $C \cap C'$ that are not coherent with both P and Q (hence they are not contained in $C \cap C'$), and such that $(C \cap C') \cup \{R, R'\}$ is a clique. This would contradict the maximality of C, since all maximal cliques have the same cardinality.

Assume that P and Q are in conflict at $k > 1$ subroutes $[x_1, y_1], \ldots, [x_k, y_k]$ with $x_1 \leq y_1 < \ldots < x_k \leq y_k$ and the subroutes $[x_i, y_i]$ are as long as possible. In a similar way that we defined the resolvents, we set

$$R := \begin{cases} Px_1Qx_2 \ldots Qx_kQ & \text{if } k \text{ is even,} \\ Px_1Qx_2 \ldots Px_kP & \text{if } k \text{ is odd,} \end{cases}$$

$$R' := \begin{cases} Px_1Px_2Qx_3 \ldots Px_kQ & \text{if } k \text{ is even,} \\ Px_1Px_2Qx_3 \ldots Qx_kP & \text{if } k \text{ is odd.} \end{cases}$$

(The idea is that we almost resolve all conflicts except the last one in R and the first one in R'.) Then, R is in conflict with P at $[x_k, y_k]$ if k is even or with Q at $[x_k, y_k]$ if k is odd, and R' is in conflict with Q at $[x_1, y_1]$. It is clear that R and R' are coherent. Let us show by contradiction that $(C \cap C') \cup \{R, R'\}$ is a clique. Let T be a route in $C \cap C'$ and assume that it is not coherent with R (the arguments would be very similar for R'). We show that this implies that T is in conflict with either P or Q, which is a contradiction with $T \in C \cap C'$. Let $[a, b]$ be a subroute where T and R are in conflict. We denote by

$i, j \in [0, k-1]$ the indices such that $x_i < a \leq x_{i+1}$ (or $x_{k-1} < a \leq v_n$ if $i = k-1$) and $x_j \leq b < x_{j+1}$ (or $x_{k-1} \leq b < v_n$ if $j = k-1$), where the ordering on the vertices of G is given by the ordering of their labels, and we set $x_0 := v_0$. In what follows, we assume that i is even, which means that when the route T arrives on a, it first follows edges of P. The case of odd i can be obtained by reversing the roles of P and Q.

Case 1: If j is even, we have that the incoming edge of a in R, as well as the outgoing edge of b in R, belong to P. Since T and R are in conflict at $[a, b]$, we obtain that Ta and Pa are ordered differently than bT and bP. Thus T and P must be in conflict at some common subroute between a and b.

Case 2: If j is odd (in particular $b \geq x_{i+1}$), we distinguish the following two cases.

Case 2.1: If Ta and Pa are ordered differently than $y_{i+1}Q$ and $y_{i+1}P$ (which are ordered similarly as $y_{i+1}T$ and $y_{i+1}P$), then T is in conflict with P at $[a, y_{i+1}]$.

Case 2.2: If Ta and Pa are ordered similarly than $y_{i+1}Q$ and $y_{i+1}P$, then these are ordered differently than bT and bQ (since T and R are in conflict at $[a, b]$ and the outgoing edge of b in R belongs to Q). Moreover, since P and Q have a conflict at $[x_{i+1}, y_{i+1}]$, we have that $y_{i+1}Q$ and $y_{i+1}P$ are ordered differently than Qx_{i+1} and Px_{i+1}, which are ordered similarly as Qx_{i+1} and Tx_{i+1}. We conclude that Tx_{i+1} and Qx_{i+1} are ordered differently than bT and bQ, thus T and Q must be in conflict at some common route between x_{i+1} and b.

Hence, we have proved by contradiction that P and Q are in conflict at exactly one subroute, which can be denoted by $[v_i, v_j]$. Now, we want to show that the edges of P and Q that end at v_i are adjacent for the total order $\preceq_{In_i}$, and the edges of P and Q that start at v_j, which we denote by e_P and e_Q, are adjacent for the total order $\preceq_{Out_j}$. Assume that it is not the case, for example that there is an edge f such that $e_Q \prec_{Out_j} f \prec_{Out_j} e_P$ (the reasoning with incoming edges of v_i is the same).

We build a subpath S of G from v_j to v_n as follows. We start with $f_1 := f$. Note that any route that contains f_1 has a conflict either with P or with Q, thus f_1 cannot be contained in any route of $C \cap C'$. After choosing an edge f_k, we look at its endpoint v_{i_k}. If $i_k = n$ we stop and define S as the concatenation of edges $f_1, \ldots, f_k$. Otherwise, we look if there is a route in $C \cap C'$ that passes through v_{i_k}. If it is not the case, we choose f_{k+1} to be any outgoing edge of v_{i_k} and we continue the process. Otherwise, we consider all routes of $C \cap C'$ that pass through v_{i_k} and we order them according to the ordering induced by $\preceq_{In_{i_k}}$ on their prefixes and the ordering induced by $\preceq_{Out_{i_k}}$ on their suffixes (these two orderings are compatible since these routes are coherent). The edge f_k is not contained in any of these routes (since otherwise we would have stopped the process before). The position of f_k in $\preceq_{In_{i_k}}$ gives a way to insert it between two routes R_1 and R_2 of $C \cap C'$ that pass through v_{i_k} and are adjacent for the previously described ordering. Then, we define S to be the concatenation of edges $f_1, \ldots, f_k$ and the suffix $v_{i_k}R_1$.

Then, we set $R := Pv_jS$ and $R' := Qv_jS$. It is clear that R and Q are in conflict at $[v_i, v_j]$ and R' and P are in conflict at $[v_i, v_j]$. To finish the argument by contradiction, we need to justify that $(C \cap C') \cup \{R, R'\}$ is a clique. Let T be a route in $C \cap C'$ that shares a common subroute $[a, b]$ with R. (The reasoning can be easily adapted to R'). Recall that T cannot contain any edge f_k. If $a, b < v_j$, then T and R are coherent at $[a, b]$ since T and

P are. If $a, b > v_j$, then T and R are coherent at $[a, b]$ since T and R_1 are. The last case is $a \leq v_j$ and $b = v_j$. Then either $Ta \preceq Pa \preceq Qa$ and $v_jT \preceq v_jQ \preceq v_jR$ (since T and Q are coherent at $[a, b]$), or $Pa \preceq Qa \preceq Ta$ and $v_jR \preceq v_jP \preceq v_jT$ (since T and P are coherent at $[a, b]$). The case $Pa \prec Ta \prec Qa$ cannot occur without creating a conflict with P or Q. In all cases T and R are coherent at $[a, b]$.

This finishes the proof by contradiction that e_P and e_Q are adjacent for $\preceq_{Out_j}$.

□

Now, we describe a way to orient the graph dual to the triangulation $\textbf{Triang}_{DKK}(G, \preceq)$.

Definition 4.2.5. We define the *oriented graph dual to* $\textbf{Triang}_{DKK}(G, \preceq)$ to be the oriented graph with set of vertices $\mathrm{MaxCliques}(G, \preceq)$ and an edge from C to C' if C and C' are maximal cliques of $(G, \preceq)$ that differ in exactly one route $P \in C$ and $Q \in C'$ such that P and Q are in minimal conflict at $[v_i, v_j]$ and $Pv_i \preceq Qv_i$ (thus $v_jQ \preceq v_jP$).

In fact, this oriented graph is the Hasse diagram of a poset on $\mathrm{MaxCliques}(G, \preceq)$ which is currently studied by von Bell and Ceballos ([BC2X], in preparation).

On the example of Figure 4.7, the oriented graph dual to $\textbf{Triang}_{DKK}(G, \preceq)$ consists of one edge from the clique corresponding to the maximal simplex in the back to the clique corresponding to the maximal simplex in the front.

See also Figures 4.22, 4.14 and 4.15 for examples of oriented graphs dual to DKK triangulations.

4.2.4 Baldoni-Vergne-Lidskii formulas and an associated geometric decomposition

One of the nice features of flow polytopes is that there are formulas to express their volume in terms of the number of integer points in other flow polytopes: the celebrated Baldoni-Vergne-Lidskii formulas (Theorem 4.2.8). In this subsection we provide background on these formulas and give a new geometric interpretation in terms of a coarsening of the DKK triangulation. Our presentation relies on the articles [MM19] and [KMS21].

Volume formulas

The *normalized volume* $\mathrm{vol}_{\mathrm{norm}}(\boldsymbol{P})$ of a d-dimensional polytope $\boldsymbol{P} \subset \mathbb{R}^N$ is the evaluation on $\boldsymbol{P}$ of the volume form $\mathrm{vol}_{\mathrm{norm}}(\cdot)$ that assigns a volume of 1 to any *unimodular simplex* of the lattice $\mathbb{Z}^N \cap \mathrm{aff}(\boldsymbol{P})$, that is to say a lattice simplex with vertices $\boldsymbol{p}_0, \ldots, \boldsymbol{p}_d \in \mathrm{aff}(\boldsymbol{P})$ such that the vectors $\boldsymbol{p}_1 - \boldsymbol{p}_0, \ldots, \boldsymbol{p}_d - \boldsymbol{p}_0$ form a basis of the lattice $\mathbb{Z}^N \cap \mathrm{aff}(\boldsymbol{P})$. If $\boldsymbol{P}$ admits a *unimodular triangulation*, i.e. a triangulation all of whose maximal cells are unimodular simplices, then the number of maximal cells in this triangulation gives the normalized volume of $\boldsymbol{P}$. Moreover, if $\boldsymbol{P}$ is full-dimensional ($d = N$), then $\mathrm{vol}_{\mathrm{norm}}(P) = d!\,\mathrm{vol}_{\mathrm{Eucl}}(P)$. We will justify in Lemma 4.2.18 that DKK triangulations are unimodular.

We say that two polytopes $\boldsymbol{P} \subset \mathbb{R}^N$ and $\boldsymbol{Q} \subset \mathbb{R}^M$ with integer coordinates are *integrally equivalent* if there is an affine transformation $\phi : \mathbb{R}^N \to \mathbb{R}^M$ that induces a bijection between $\mathbb{Z}^N \cap \operatorname{aff}(\boldsymbol{P})$ and $\mathbb{Z}^M \cap \operatorname{aff}(\boldsymbol{Q})$. Note that integrally equivalent polytopes are combinatorially equivalent and they have the same normalized volume.

Let G be a graph on vertices $\{v_0, \dots, v_n\}$ with netflow $\boldsymbol{a}$. We denote by $K_G(\boldsymbol{a}) := |\boldsymbol{\mathcal{F}}_G^{\mathbb{Z}}(\boldsymbol{a})|$ the number of integer points in the flow polytope $\boldsymbol{\mathcal{F}}_G(\boldsymbol{a})$. It is equal to the number of ways to write $\boldsymbol{a}$ as a nonnegative integral combination of the vectors $\boldsymbol{e}_i - \boldsymbol{e}_j$ for edges (i, j) in G, which is called the *generalized Kostant partition function*. The classical Kostant partition function, which was introduced in relation to representation theory, is recovered when G is a complete graph.

Formulas relating the normalized volume of the flow polytope $\boldsymbol{\mathcal{F}}_G(\boldsymbol{a})$ to generalized Kostant partition functions were first found by Lidskii in [Lid84] for the case where G is a complete graph, and then generalized to any graph G by Baldoni and Vergne in [BV08, Theorem 38] with an analytic proof relying on residue computations. Then, Mészáros and Morales ([MM19]) and Kapoor, Mészáros and Setiabrata ([KMS21]) provided geometric proofs of these formulas, based on a recursive procedure to subdivide flow polytopes discovered by Postnikov and Stanley (unpublished: [Pos14], [Sta00]). Mészáros, Morales and Striker ([MMS19, Section 7]) showed that the DKK triangulations could also be recovered with this Postnikov-Stanley procedure and that this leads to the following explicit bijection between the maximal cliques of $(G, \preceq)$ and the integer flows on G with the specific netflow $\boldsymbol{d} = (0, d_1, \dots, d_{n-1}, -\sum_i d_i)$ where $d_i = \operatorname{indeg}_G(v_i) - 1$.

We define the function

$$\Omega_{G,\preceq} : \begin{cases} \operatorname{MaxCliques}(G, \preceq) & \to \boldsymbol{\mathcal{F}}_G^{\mathbb{Z}}(\boldsymbol{d}) \\ C & \mapsto (n_C(e) - 1)_{e \in E(G)} \end{cases},$$

where $n_C(e)$ is the number of times the edge $e = (v_i, v_j)$ appears in the set of prefixes $\{Pv_j \mid P \in C\}$ of the maximal clique C.

Theorem 4.2.6 ([MMS19, Theorem 7.8])**.** *Given a framed graph $(G, \preceq)$, the map $\Omega_{G,\preceq}$ is a bijection between maximal cliques in MaxCliques$(G, \preceq)$ and integer flows in $\boldsymbol{\mathcal{F}}_G^{\mathbb{Z}}(\boldsymbol{d})$.*

As a corollary, we recover the following special case of the Baldoni-Vergne-Lidskii formulas.

Corollary 4.2.7 ([Sta00] and [BV08, Thm. 38])**.** *For a graph G on $\{v_0, \dots, v_n\}$ with netflow $\boldsymbol{d} = (0, d_1, \dots, d_{n-1}, -\sum_i d_i)$ where $d_i = \operatorname{indeg}(v_i) - 1$, we have that*

$$\operatorname{vol}_{\text{norm}} \boldsymbol{\mathcal{F}}_G = \left| \boldsymbol{\mathcal{F}}_G^{\mathbb{Z}}(\boldsymbol{d}) \right| = K_G(\boldsymbol{d}).$$

This special case allows us to reformulate the Lidskii-Baldoni-Vergne formulas, initially stated as integer point enumerations, as volume formulas, which can be proved by enumerating the number of maximal cells in a unimodular triangulation.

Let $m \in \mathbb{N}$. A *weak composition* of m of length l is a tuple $\boldsymbol{j} = (j_1, \ldots, j_l)$ such that $j_i \in \mathbb{N}$ for all $i \in [l]$ and $\sum_{i=1}^{l} j_i = m$. The *dominance order* between weak compositions is defined by $(j_1, \ldots, j_l) \geq (j'_1, \ldots, j'_l)$ if $\sum_{t=1}^{k} j_t \geq \sum_{t=1}^{k} j'_t$ for all $k \in [l]$. For $n, k \in \mathbb{N}_{>0}$ we denote by $\left(\!\binom{n}{k}\!\right)$ the binomial coefficient $\left(\!\binom{n}{k}\!\right) := \binom{n+k-1}{k} = \frac{(n+k-1)\times\ldots\times n}{k!}$. We also set the conventions $\left(\!\binom{0}{0}\!\right) := 1$ and $\left(\!\binom{0}{k}\!\right) := 0$ if $k > 0$.

Theorem 4.2.8 (Reformulation of a Lidskii-Baldoni-Vergne formula, [BV08, Thm. 38])**.** *Let H be a connected directed multigraph on vertices $\{v_0, \ldots, v_n, v_{n+1}\}$ with each edge (v_i, v_j) oriented from v_i to v_j if $i < j$ and such that v_0 (respectively v_{n+1}) is the only source (respectively sink) of H. For any $i \in [n]$ we denote by c_i the number of source-edges (v_0, v_i) and $o_i := \mathrm{outdeg}_H(v_i) - 1$. We denote by $m := |E(H)| - \sum_{i=1}^{n+1} c_i$ the number of non-source edges of H. Then*

$$\mathrm{vol}_{\mathrm{norm}}(\boldsymbol{\mathcal{F}}_H) = \sum_{\substack{\boldsymbol{j} \text{ weak composition of } m-n \text{ of length } n \\ \text{s.t. } \boldsymbol{j} \geq (o_1, \ldots, o_n)}} \left(\!\binom{c_1}{j_1}\!\right) \cdots \left(\!\binom{c_n}{j_n}\!\right) K_H((0, j_1 - o_1, \ldots, j_n - o_n, 0)). \tag{4.1}$$

We will present the proof provided in [KMS21, Equation (1.3)], with slight adaptations that will allow us to interpret Equation 4.1 with a geometric decomposition of $\boldsymbol{\mathcal{F}}_H$. The equivalence of notations is the following. We denote by G the restriction of H to vertices $\{v_1, \ldots, v_{n+1}\}$. Then our graph H corresponds to their graph $G(\boldsymbol{c})$ ([KMS21, Definition 3.1]). It follows from Corollary 4.2.7 that $\mathrm{vol}_{\mathrm{norm}}(\boldsymbol{\mathcal{F}}_H) = K_G(\boldsymbol{a})$, with $a_i = c_i + \mathrm{indeg}_G(v_i) - 1$ for all $i \in [n]$.

Bipartite noncrossing trees

We present the combinatorial structure of bipartite noncrossing trees, which is helpful to describe certain decompositions of flow polytopes.

Let L and R be disjoint sets that have linear orders $\preceq_L$ and $\preceq_R$. We label their elements by $l_1, \ldots, l_{|L|}$ and $r_1, \ldots, r_{|R|}$ such that $l_1 \preceq_L \ldots \preceq_L l_{|L|}$ and $r_1 \preceq_R \ldots \preceq_R r_{|R|}$. We say that a bipartite tree T on the partition of vertices (L, R) is *noncrossing* if it has no pair of edges $(l_a, r_d), (l_b, r_c)$ such that $l_a \prec_L l_b$ and $r_c \prec_R r_d$. See Figure 4.10 for an example. The number of edges in such a tree is $|L| + |R| - 1$. We denote by *NCTrees*$(\preceq_L, \preceq_R)$ the set of bipartite noncrossing trees on (L, R) with linear orders $\preceq_L, \preceq_R$.

For two integers $m, k \in \mathbb{N}$, we denote by $\left(\!\binom{[m]}{k}\!\right)$ the collection of multisets of $[m]$ of size k. This collection has cardinality $\left(\!\binom{m}{k}\!\right)$. The *Gale order* on $\left(\!\binom{[m]}{k}\!\right)$ is given by $A \leq B$ if $a_i \leq b_i$ for all $i \in [k]$, where $a_1, \ldots, a_k$ (respectively $b_1, \ldots, b_k$) are the elements of A (respectively B) ordered increasingly (see [Gal68]). We denote this partial order on $\left(\!\binom{[m]}{k}\!\right)$ by *Gale*(k, m). Figure 4.11 depicts the Hasse diagram of *Gale*(k, m) for $k = 2$ and $m = 3$.

Proposition 4.2.9. *If $|L|, |R| \geq 1$, then NCTrees$(\preceq_L, \preceq_R)$ is in bijection with $\left(\!\binom{[|L|]}{|R|-1}\!\right)$.*

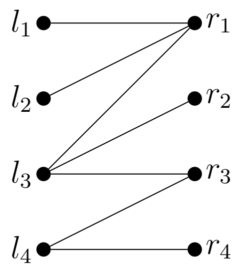

Figure 4.10: Example of a noncrossing bipartite tree, which is associated to the multiset $\{3, 3, 4\}$ of $[4]$.

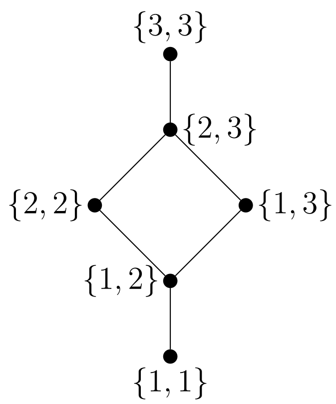

Figure 4.11: Hasse diagram of the poset $Gale(2, 3)$.

Proof. Let $T \in \mathrm{NCTrees}(\preceq_L, \preceq_R)$. For $i \in [|R| - 1]$, we denote by a_i the greatest index $j \in [|L|]$ such that $(l_j, r_i) \in E(T)$. We define $\phi(T)$ to be the multiset $\{a_1, \ldots, a_{|R|-1}\}$.

Conversely, let $B = \{b_1, \ldots, b_{|R|-1}\}$ be a multisubset of $|L|$, where the b_i's are ordered increasingly for $\preceq_L$. We define $\psi(B)$ to be the bipartite graph on vertices (L, R) with edges $\{(l_k, r_i) \,|\, i \in [|R|] \text{ and } b_{i-1} \leq k \leq b_i\}$, where we set $b_0 := 1$ and $b_{|R|} := |L|$. Then it is easy to see that $\psi(B)$ is a bipartite noncrossing tree on (L, R) with linear orders $\preceq_L$, $\preceq_R$.

Moreover, $\psi \circ \phi(T) = T$ and $\phi \circ \psi(B) = B$, so we indeed have a bijection. See Figure 4.10 for an example of this bijection. $\square$

Corollary 4.2.10. $|NCTrees(\preceq_L, \preceq_R)| = \begin{cases} \left(\!\binom{|L|}{|R|-1}\!\right) & \text{if } |L|, |R| \geq 1, \\ 1 & \text{if } |L| = 0 \text{ or } |R| = 0. \end{cases}$

Moreover, the bijection allows us to endow $\mathrm{NCTrees}(\preceq_L, \preceq_R)$ with the order relation $\leq$ coming from the Gale order $Gale(|R| - 1, |L|)$.

Proposition 4.2.11. *Let $T, T' \in NCtrees(\preceq_L, \preceq_R)$.*

They form a cover relation $T \leq T'$ of the Gale order if and only if there are $j \in [|L| - 1]$ and $i \in [|R| - 1]$ such that:

- $(l_j, r_{i+1}) \in E(T)$ *and* $(l_{j+1}, r_i) \in E(T')$,
- $E(T) \setminus \{(l_j, r_{i+1})\} = E(T') \setminus \{(l_{j+1}, r_i)\}$.

Proof. Let $A = \{a_1, \dots, a_{|R|-1}\}$ and $B = \{b_1, \dots, b_{|R|-1}\}$ (ordered increasingly) be the two elements of the Gale order $Gale(|R|-1, |L|)$ such that $A = \phi(T)$ and $B = \phi(T')$ (for the function ϕ defined in the proof of Proposition 4.2.9). It is clear from the definition of the Gale order that there is a cover relation $A \leq B$ exactly if there is $i \in [|R|-1]$ such that $b_i = a_i + 1$ and $b_k = a_k$ for all $k \in [|R|-1] \setminus \{i\}$. We set $j = a_i$. Then it follows from the definition of ψ that $(l_j, r_{i+1}) \in E(T)$ (because $j = a_i$), $(l_{j+1}, r_i) \in T'$ (because $j + 1 = a_i + 1 = b_i$) and all other edges are common to T and T'.

Conversely, it is direct to show that if these conditions are satisfied, then $\phi(T) \leq \phi(T')$ is a cover relation in the Gale order $Gale(|R|-1, |L|)$ (they only differ on the elements $a_i = j$ in $A = \phi(T)$ and $b_i = j + 1$ in $B = \phi(T')$). $\square$

Compounded reductions

We explain how a graph-operation, indexed by a set of bipartite noncrossing trees, translates into a geometric decomposition of the flow polytope of the graph.

Let G be a connected directed multigraph on vertices $\{v_0, \dots, v_n, v_{n+1}\}$ with each edge (v_i, v_j) oriented from v_i to v_j if $i < j$ and such that v_0 (respectively v_{n+1}) is the only source (respectively sink) of G.

Let $i \in [n]$. We consider In'_i a submultiset of the incoming edges of inner vertex v_i. If $In'_i \neq In_i$ we add to it the element v_i. We endow this set, as well as the set of outgoing edges Out_i, with linear orders $\preceq_{In'_i}$ and $\preceq_{Out_i}$. This is a benign difference with [KMS21, p.3], where v_i is always the last element of the order $\preceq_{In'_i}$.

Let $T \in \mathrm{NCTrees}(\preceq_{In'_i}, \preceq_{Out_i})$ with set of edges $E(T) \subseteq In'_i \times Out_i$. For two edges $e = (v_h, v_i) \in In'_i \setminus \{v_i\}$ and $f = (v_i, v_j) \in Out_i$, we denote by $e + f$ the pair of vertices (v_h, v_j) labeled by the path in G made of edges e and f. We call *basic reduction* of G at vertex v_i with respect to T, and denote by $G_T^{(i)}$, the graph obtained from G by removing all edges in $In'_i \setminus \{v_i\} \cup Out_i$ and adding (or putting back) the multiset of edges

$$\begin{cases} \{e + f \mid e \in In'_i \setminus \{v_i\},\ (e, f) \in E(T)\} \cup \{f \mid (v_i, f) \in E(T)\} & \text{if } v_i \in In'_i, \\ \{e + f \mid e \in In'_i,\ (e, f) \in E(T)\} \cup \{(v_i, v_{n+1})\} & \text{if } v_i \notin In'_i. \end{cases}$$

Note that in this graph, the only incoming edges of v_i are the edges in $In_i \setminus In'_i$. Moreover, $G_T^{(i)}$ has the same total number of edges than G.

See Figure 4.12 for an example.

Recall that the polytope $\boldsymbol{\mathcal{F}}_G$ lives in $\mathbb{R}^{E(G)}$. We denote by $(\boldsymbol{e}_f)_{f \in E(G)}$ the canonical basis of $\mathbb{R}^{E(G)}$ and define the linear transformation $\phi : \mathbb{R}^{E(G_T^{(i)})} \to \mathbb{R}^{E(G)}$ such that the

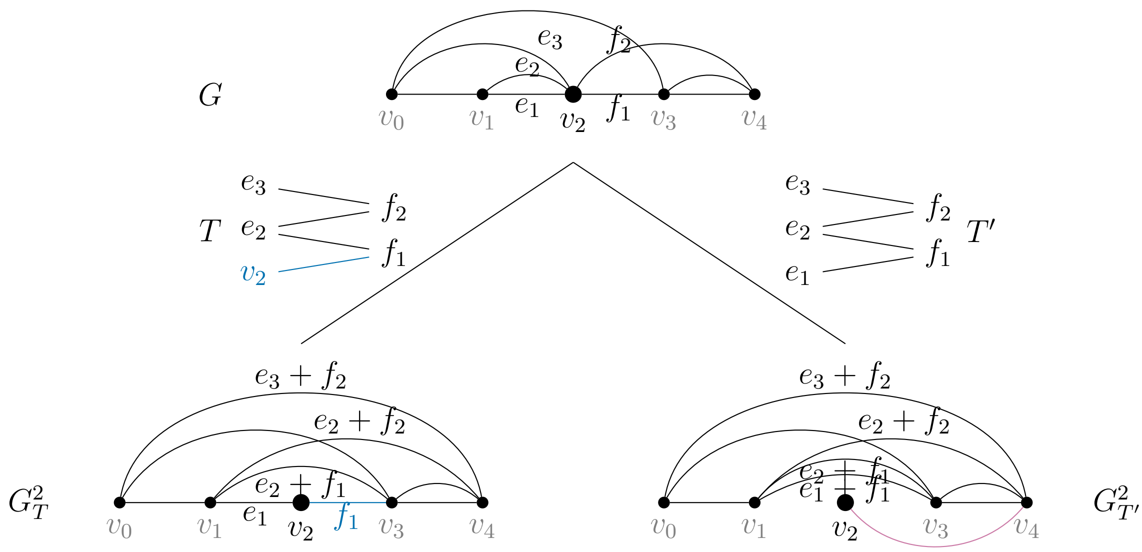

Figure 4.12: Two basic reductions G^2_T (bottom left) and $G^2_{T'}$ (bottom right) of a graph G (top) at vertex v_2 with respect to two noncrossing trees T and T' with different left sets (respectively $In'_2 = \{e_3, e_2, v_2\}$ and $In'_2 = \{e_3, e_2, e_1\}$).

image of a basis vector $\boldsymbol{e}_f$ for $f \in E(G^{(i)}_T)$ is

$$\phi(\boldsymbol{e}_f) = \begin{cases} \boldsymbol{e}_f & \text{if } f \text{ is an edge in } E(G), \\ \boldsymbol{e}_{f_1} + \boldsymbol{e}_{f_2} & \text{if } f \text{ is the sum } f_1 + f_2 \text{ of edges } f_1, f_2 \in E(G), \\ 0 & \text{if } In'_i = In_i \text{ and } f = (v_i, v_{n+1}). \end{cases}$$

Then, the polytopes $\mathcal{F}_{G^{(i)}_T}$ and $\phi(\mathcal{F}_{G^{(i)}_T})$ are integrally equivalent. Indeed, it is clear that the routes of $G^{(i)}_T$ (whose indicator vectors are the integer points of $\mathcal{F}_{G^{(i)}_T}$) are in bijection with the routes of G whose indicator vectors are in $\phi(\mathcal{F}_{G^{(i)}_T})$.

In the remainder of this work we will abuse notations and identify $\mathcal{F}_{G^{(i)}_T}$ with its image $\phi(\mathcal{F}_{G^{(i)}_T})$ in $\mathbb{R}^{E(G)}$.

Lemma 4.2.12 (Compounded reduction lemma, [KMS21, Lemma 2.1], [MM19, Lemma 3.4])**.** *Let G be a connected directed multigraph on vertices $\{v_0, \dots, v_{n+1}\}$. Let $i \in [n]$, In'_i a submultiset of In_i with v_i adjoined if $In'_i \neq In_i$, and let $\preceq_{In'_i}$, $\preceq_{Out_i}$ be linear orders on In'_i and Out_i. Then:*

$$\mathcal{F}_G = \bigcup_{T \in NCTrees(\preceq_{In'_i}, \preceq_{Out_i})} \mathcal{F}_{G^{(i)}_T}. \tag{4.2}$$

Moreover, the flow polytopes $\left\{ \mathcal{F}_{G^{(i)}_T} \middle| T \in NCTrees(\preceq_{In'_i}, \preceq_{Out_i}) \right\}$ are interior disjoint and they have the same dimension as $\mathcal{F}_G$.

We refer to replacing G by $\left\{G_T^{(i)} \,\middle|\, T \in \mathrm{NCTrees}(\preceq_{In'_i}, \preceq_{Out_i})\right\}$ as in Lemma 4.2.12 as a *compounded reduction*. The qualifying adjective *compounded* refers to the fact that this operation can be obtained by repeated application of basic Postnikov-Stanley reduction, as explained in [MM19, Section 3].

Figure 4.13 displays two compounded reductions: one on the top graph H at vertex v_3 (there is only one noncrossing bipartite tree) that gives the middle graph, and one on the middle graph at vertex v_2, that gives the three bottom graphs.

Note that it is not clear that this decomposition forms a valid subdivision of $\boldsymbol{\mathcal{F}}_G$, because a priori there could be a face $\boldsymbol{F}$ of a certain $\boldsymbol{\mathcal{F}}_{G_T^{(i)}}$ and a face $\boldsymbol{F}'$ of another $\boldsymbol{\mathcal{F}}_{G_{T'}^{(i)}}$ such that the intersection $\boldsymbol{F} \cap \boldsymbol{F}'$ is not a common face of $\boldsymbol{F}$ and $\boldsymbol{F}'$ and Definition 1.1.8 is not satisfied. This is why we will call this decomposition a *dissection* of $\boldsymbol{\mathcal{F}}_G$.

As explained in [KMS21, Lemma 2.1] and [MM19, Lemma 3.4], we can encode a series of reductions in a *compounded reduction tree* rooted at the original graph and such that the children of a node N are the graphs $\left\{N_T^{(i)} \,\middle|\, T \in \mathrm{NCTrees}(\preceq_{In'_i}, \preceq_{Out_i})\right\}$ for certain choices of inner vertex v_i of N, subset In'_i and orders $\preceq_{In'_i}$ and $\preceq_{Out_i}$.

A Lidskii-type decomposition

Now we consider a graph H as in Theorem 4.2.8 and we endow it with a framing $\preceq^H$ such that for any $i \in [n]$, all c_i source-edges (v_0, v_i) of H are consecutive in the order $\preceq^H_{In_i}$. We define the specific compounded reduction tree $R_{H,\preceq^H}$ as follows.

Its root is the framed graph $(H, \preceq^H)$ (depth 0). For a node $(N, \preceq^N)$ at depth $k \in [0, n-2]$, its children are the framed graphs $\left\{(N_T^{(i)}, \preceq^{N_T^{(i)}}) \,\middle|\, T \in \mathrm{NCTrees}(\preceq^N_{In'_i}, \preceq^N_{Out_i})\right\}$ obtained from Lemma 4.2.12 where

- $i = n - k$,
- In'_i is the set of non-source incoming edges of v_i potentially adjoined with the vertex v_i:

$$In'_i := \begin{cases} \{e = (v_h, v_i) \,|\, h \in [i-1],\ e \in E(H)\} \cup \{v_i\} & \text{if } c_i > 0, \\ \{e = (v_h, v_i) \,|\, h \in [i-1],\ e \in E(H)\} & \text{if } c_i = 0, \end{cases}$$

- the orders $\preceq^N_{In'_i}$ and $\preceq^N_{Out_i}$ are given by $\preceq^N$: if $c_i > 0$, a non-source incoming edge e satisfies $e \prec^N_{In'_i} v_i$ (resp. $e \succ^N_{In'_i} v_i$) if $e \prec^N_{In_i} f$ (resp. $e \succ^N_{In_i} f$) for any source-edge f adjacent to v_i,
- for any $T \in \mathrm{NCTrees}(\preceq^N_{In'_i}, \preceq^N_{Out_i})$, we endow the graph $N' := N_T^{(i)}$ with a framing $\preceq^{N'}$ inherited from $\preceq^N$ as follows. For a vertex v_h with $h \in [i-1]$, its set of outgoing edges Out_h in N' contains more edges than in N. If e_0, $e_1 + f_1$, $e_2 + f_2$ are outgoing edges of v_h in N', with e_0 outgoing edge of v_h in N, e_1 and e_2 edges of N on vertices (v_h, v_i) and f_1, f_2 outgoing edges of v_i in N such that $(e_1, f_1), (e_2, f_2) \in E(T)$, then we set $e_0 \prec^{N'}_{Out_h} e_1 + f_1$ (resp. $e_0 \succ^{N'}_{Out_h} e_1 + f_1$) if $e_0 \prec^N_{Out_h} e_1$ (resp. $e_0 \succ^N_{Out_h} e_1$) and $e_1 + f_1 \preceq^{N'}_{Out_h} e_2 + f_2$ if $e_1 \prec^N_{Out_h} e_2$ or $e_1 = e_2$ and $f_1 \preceq^N_{Out_i} f_2$.

Note that with this construction, a node N at depth k satisfies that for all $i \in [n-k, n]$ the only outgoing edges of v_i in N are sink-edges on vertices (v_i, v_{n+1}), labeled by a path of edges in the original graph H. Moreover, the choice of noncrossing trees with respect to orders induced by $\preceq^H$ implies that the paths labeling these outgoing edges of v_i in N are mutually distinct and coherent with respect to the framing $\preceq^H$ (where we extend trivially the notion of being coherent to paths starting at v_i instead of v_0).

In particular, a leaf of the compounded reduction tree is a framed graph $(L, \preceq^L)$ on vertices $\{v_0, \dots, v_{n+1}\}$ such that for all $i \in [n]$, the incoming edges at vertex v_i are the c_i source-edges (v_0, v_i) that were already in H, and there are a certain number $j_i + 1$ of outgoing edges that are all sink-edges, with $j_i = 0$ if $c_i = 0$. (Such a graph is denoted by $G[\boldsymbol{j} + \mathbf{1}](\boldsymbol{c})$ in [KMS21, Theorem 3.4, Lemma 3.7].) We say that such a leaf is of *type* $\boldsymbol{j} = (j_1, \dots, j_n)$. Geometrically, the corresponding flow polytope $\boldsymbol{\mathcal{F}}_L$ is the join of products of simplices $\triangle_{c_i - 1} \times \triangle_{j_i}$ for all $i \in [n]$ such that $c_i > 0$.

Example 4.2.13. Figure 4.13 depicts a framed graph $(H, \preceq^H)$ (the framing is obtained by reading the edges from top to bottom) and its compounded reduction tree $R_{H,\preceq^H}$. Each edge of the reduction tree from a parent N at depth k to a child N' at depth $k+1$ is labeled by the bipartite noncrossing tree T such that $N' = N_T^{(3-k)}$. The types $\boldsymbol{j}$ of the leaves of the compounded reduction tree are indicated at the bottom.

The following two results can be seen as refinements of [KMS21, Lemma 3.7] since they unveil the geometric structure of the pieces $\boldsymbol{\mathcal{F}}_L$, in relation with the DKK triangulation $\mathbf{Triang}_{DKK}(H, \preceq^H)$.

Lemma 4.2.14. *The dissection*

$$\boldsymbol{\mathcal{F}}_H = \bigcup_{L \text{ is a leaf of } R_{H,\preceq^H}} \boldsymbol{\mathcal{F}}_L$$

coarsens the triangulation $\mathbf{Triang}_{DKK}(H, \preceq^H)$ *of* $\boldsymbol{\mathcal{F}}_H$.

Moreover, the number of maximal simplices of $\mathbf{Triang}_{DKK}(H, \preceq^H)$ *contained in* $\boldsymbol{\mathcal{F}}_L$ *for a leaf* L *of type* $\boldsymbol{j}$ *is* $\left(\!\binom{c_1}{j_1}\!\right) \cdots \left(\!\binom{c_n}{j_n}\!\right)$.

Proof. Let L be a leaf of $R_{H,\preceq^H}$ of type $\boldsymbol{j}$. We define another compounded reduction tree R_L as follows. Its root is the graph L with the framing $\preceq^L$ induced by $\preceq^H$ along $R_{H,\preceq^H}$. For a node $(N, \preceq^N)$ at depth $k \in [0, n-1]$, either its child is again $(N, \preceq^N)$ if $c_i = 0$ or its children are the $\left(\!\binom{c_i}{j_i}\!\right)$ framed graphs $\left\{ (N_T^{(i)}, \preceq^{N_T^{(i)}}) \,\middle|\, T \in \mathrm{NCTrees}(\preceq^N_{In'_i}, \preceq^N_{Out_i}) \right\}$ obtained from Lemma 4.2.12 where

- $i = n - k$,
- In'_i is the set of c_i source-edges (v_0, v_i),
- the order $\preceq^N_{In'_i}$ is the initial order $\preceq^H_{In'_i}$ on the c_i source-edges of H,
- the order $\preceq^N_{Out_i}$ is the order $\preceq^L_{Out_i}$ on the $j_i + 1$ sink-edges (v_i, v_{n+1}) of L, which is inherited from the order $\preceq^H$ on paths of H that go from v_i to v_{n+1}.

It is clear that this compounded reduction tree R_L has $\left(\!\binom{c_1}{j_1}\!\right) \cdots \left(\!\binom{c_n}{j_n}\!\right)$ leaves, indexed by $\mathrm{NCTrees}(\preceq^H_{In'_1}, \preceq^L_{Out_1}) \times \ldots \times \mathrm{NCTrees}(\preceq^H_{In'_n}, \preceq^L_{Out_n})$. The compounded reduction lemma

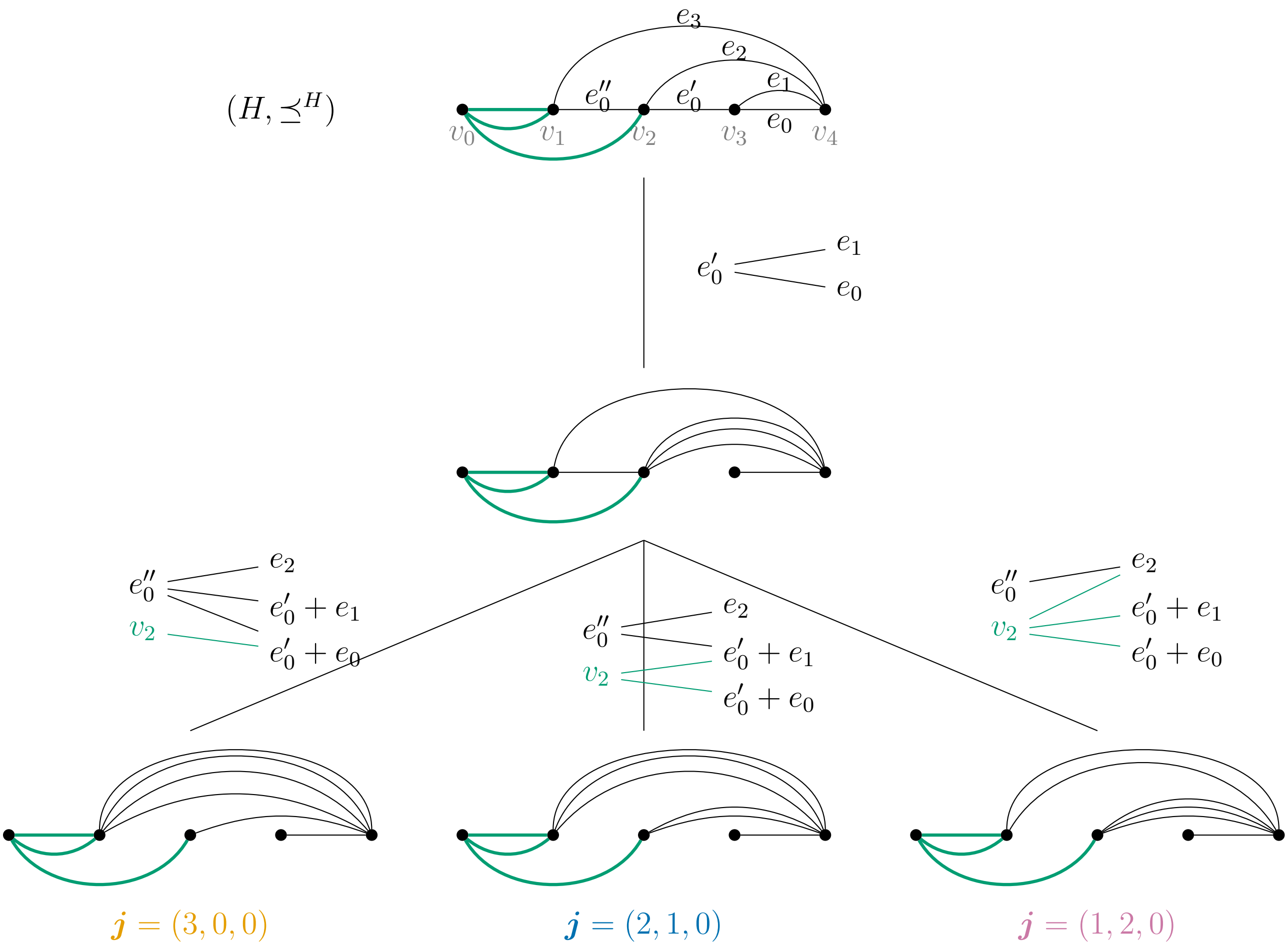

Figure 4.13: Reduction tree $R_{H,\preceq^H}$ of the graph $(H, \preceq^H)$ depicted at the top. See Example 4.2.13.

(4.2.12) implies that

$$\boldsymbol{\mathcal{F}}_L = \bigcup_{L' \text{ is a leaf of } R_L} \boldsymbol{\mathcal{F}}_{L'}.$$

Let us show that the $\boldsymbol{\mathcal{F}}_{L'}$ are maximal simplices of $\mathbf{Triang}_{DKK}(H, \preceq^H)$.

By construction, a leaf L' of R_L has one sink-edge (v_i, v_{n+1}) for all $i \in [n]$ and $|E(H)|-n$ edges (v_0, v_{n+1}), which are labeled by routes that are mutually distinct and coherent with respect to the framing $\preceq^H$. Hence, these labels provide a maximal clique C of $(H, \preceq^H)$ and (up to compositions of integral equivalences as mentioned before Lemma 4.2.12) $\boldsymbol{\mathcal{F}}_{L'}$ is exactly the simplex Δ_C of $\mathbf{Triang}_{DKK}(H, \preceq^H)$.

Conversely, from a maximal clique C of $(H, \preceq^H)$, the following procedure explains how to go from H to a leaf L of $R_{H,\preceq^H}$ and then from L to a leaf L' of R_L whose labels on edges (v_0, v_{n+1}) are exactly the routes in C. We start at the root of $R_{H,\preceq^H}$ and follow a downward path of $R_{H,\preceq^H}$. If we are at an internal node N of depth $k \in [0, n-1]$, we build the bipartite graph T on vertices (In'_i, Out_i) with edges (e, f) for $e \in In'_i \setminus \{v_i\}$, $f \in Out_i$ such that there is at least one route in C that ends with the path $e + f$ and edges (v_i, f) for $f \in Out_i$ such that there is at least one route in C consisting of a source-edge (v_0, v_i) followed by the path f. The fact that C is a clique implies that T is noncrossing, and the fact that C is maximal implies that T is a tree. Hence, we choose $N_T^{(i)}$ for the next node on our path. When we arrive at a leaf L of $R_{H,\preceq^H}$ we follow a similar procedure on R_L until arriving at a leaf L'. □

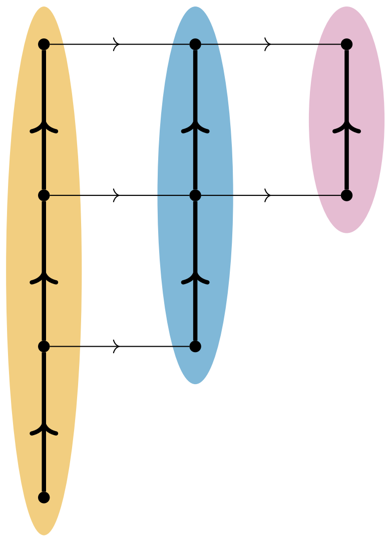

Figure 4.14: Oriented graph dual to the DKK triangulation of the framed graph $(H, \preceq^H)$ depicted on top of Figure 4.13. The bold and colored parts correspond to the three pieces of the Lidskii-type decomposition.

Example 4.2.15. Figure 4.14 shows the oriented graph dual to the DKK triangulation of the framed graph $(H, \preceq^H)$ represented on Figure 4.13. The bold and colored parts correspond to the three pieces of the dissection showcased in Lemma 4.2.14. The colors as well as the respective positions (left, middle, right) indicate the correspondence with the leaves of the compounded reduction tree of Figure 4.13.

Before concluding the proof of Theorem 4.2.8, we specify how the maximal simplices of $\textbf{Triang}_{DKK}(H, \preceq^H)$ are arranged inside a piece $\boldsymbol{\mathcal{F}}_L$.

Theorem 4.2.16. *Let L be a leaf of $R_{H,\preceq^H}$ of type $\boldsymbol{j}$. Then, the oriented graph dual to the restriction of $\textbf{Triang}_{DKK}(H, \preceq^H)$ to $\boldsymbol{\mathcal{F}}_L$ is isomorphic to the Hasse diagram of the product of Gale orders $Gale(j_1, c_1) \times \ldots \times Gale(j_n, c_n)$.*

Proof. The proof of Lemma 4.2.14 gives a bijection between the maximal simplices of $\textbf{Triang}_{DKK}(H, \preceq^H)$ that are in $\boldsymbol{\mathcal{F}}_L$ and the product of sets of noncrossing trees $\mathrm{NCTrees}(\preceq^H_{In'_1}, \preceq^L_{Out_1}) \times \ldots \times \mathrm{NCTrees}(\preceq^H_{In'_n}, \preceq^L_{Out_n})$. Let us show that this bijection induces a directed graph isomorphism between the oriented graph dual to the restriction of

$\textbf{Triang}_{DKK}(H, \preceq^H)$ to $\boldsymbol{\mathcal{F}}_L$ and the Hasse diagram of the product of Gale orders $Gale(j_1, c_1) \times \ldots \times Gale(j_n, c_n)$ on $\mathrm{NCTrees}(\preceq^H_{In'_1}, \preceq^L_{Out_1}) \times \ldots \times \mathrm{NCTrees}(\preceq^H_{In'_n}, \preceq^L_{Out_n})$. (We explained in Section 4.2.4 how to endow each set $\mathrm{NCTrees}(\preceq^H_{In'_k}, \preceq^L_{Out_k})$ with the Gale order structure $Gale(j_k, c_k)$.)

Let C_1, C_2 be maximal cliques of $(H, \preceq^H)$ such that the associated simplices Δ_{C_1} and Δ_{C_2} are contained in $\boldsymbol{\mathcal{F}}_L$. This implies that for both C_1 and C_2, for all $i \in [n]$ the set of suffixes that follow a source-edge (v_0, v_i) is equal to the set of paths that label sink-edges (v_i, v_{n+1}) in the leaf L.

Assume that there is an edge from C_1 to C_2 in the oriented graph dual to $\textbf{Triang}_{DKK}(H, \preceq^H)$. It follows from Lemma 4.2.4 that P and Q are in minimal conflict at a subroute $[v_i, v_j]$. Then the incoming edges of v_i in P and Q, that we denote e_P and e_Q, are source-edges (v_0, v_i). Indeed, if for example P started with a source-edge (v_0, v_{i_0}) with $i_0 < i$, then the suffix $v_{i_0}P$ would not be contained in the set of suffixes of Q that follow a source-edge (v_0, v_{i_0}) and this would contradict the fact that Δ_{C_1} and Δ_{C_2} are in $\boldsymbol{\mathcal{F}}_L$.

Then we look at how the cliques C_1 and C_2 are obtained as leaves of the compounded reduction tree R_L introduced in the proof of Lemma 4.2.14, or in other words what are their associated element of $\mathrm{NCTrees}(\preceq^H_{In'_1}, \preceq^L_{Out_1}) \times \ldots \times \mathrm{NCTrees}(\preceq^H_{In'_n}, \preceq^L_{Out_n})$. It is clear that we need to choose the same tree from $\mathrm{NCTrees}(\preceq^H_{In'_k}, \preceq^L_{Out_k})$ for all $k \in [n] \setminus \{i\}$. We denote by T_1 (resp. T_2) the element of $\mathrm{NCTrees}(\preceq^H_{In'_i}, \preceq^L_{Out_i})$ chosen to obtain C_1 (resp. C_2). Then, all edges of T_1 and T_2 are the same except the edges $(e_P, v_iP) \in T_1$ and $(e_Q, v_iQ) \in T_2$. Moreover, the fact that P and Q are in minimal conflict implies that e_P and e_Q are adjacent in the ordering $\preceq^H_{In_i}$ (with $e_P \preceq^H_{In_i} e_Q$ since we assumed that the edge of the dual graph of the DKK triangulation is oriented from C_1 to C_2) and v_iP and v_iQ are adjacent in the ordering $\preceq^L_{Out_i}$ (with $v_iQ \preceq^L_{Out_i} v_iP$ since P and Q are in conflict). It follows from Proposition 4.2.11 that T_1 and T_2 form a cover relation $T_1 \leq T_2$ of the Gale order $Gale(j_i, c_i)$. Thus, they give an edge of the Hasse diagram of the product $Gale(j_1, c_1) \times \ldots \times Gale(j_n, c_n)$.

Conversely, there is an edge in this Hasse diagram between two families of trees $(T_1^1, \ldots, T_1^n), (T_2^1, \ldots, T_2^n) \in \mathrm{NCTrees}(\preceq^H_{In'_1}, \preceq^L_{Out_1}) \times \ldots \times \mathrm{NCTrees}(\preceq^H_{In'_n}, \preceq^L_{Out_n})$ if there is $i \in [n]$ such that $T_1^k = T_2^k$ for all $k \in [n] \setminus \{i\}$ and $T_1^i \leq T_2^i$ is a cover relation in $Gale(j_i, c_i)$. This implies that the corresponding cliques C_1 and C_2 have the same elements except two routes that are in minimal conflict. □

Example 4.2.17. One can see an example of Theorem 4.2.16 on Figure 4.14. For all three leaves of the compounded reduction tree of Figure 4.13 only the poset $Gale(j_1, c_1)$ is not reduced to a singleton, and it is always linear since $j_1 = 1$.

See also Figures 4.15 and 4.23.

The next result is well-known in the literature even though it is not proven in Danilov-Karzanov-Koshevoy article [DKK12]. We state it here because it is necessary to justify that the normalized volume of the flow polytope $\boldsymbol{\mathcal{F}}_H$ is the number of maximal simplices in its DKK triangulation.

Lemma 4.2.18. *The triangulation* $\textbf{Triang}_{DKK}(H, \preceq^H)$ *is unimodular.*

Proof. Along the proof of Lemma 4.2.14 we have seen that the maximal simplices of $\mathbf{Triang}_{DKK}(H, \preceq^H)$ are integrally equivalent to flow polytopes $\boldsymbol{\mathcal{F}}_{L'}$ where L' is a graph whose only routes are sink-to-source edges (v_0, v_{n+1}). It is clear that such a flow polytope, seen in $\mathbb{R}^{E(L')}$, is a unimodular simplex, and this property is preserved under integral equivalence. □

Finally, the number of leaves of the reduction tree $R_{H,\preceq^H}$ is given by the following two lemmas, which finish the proof of Theorem 4.2.8.

Lemma 4.2.19 ([MM19, Lemma 4.5])**.** *If a tuple $\boldsymbol{j} = (j_1, \ldots, j_n)$ is the type of a leaf in $R_{H,\preceq^H}$, then it is a weak composition of $m - n$ that is greater than $(o_1, \ldots, o_n)$ for the dominance order. Moreover, $j_i = 0$ for all $i \in [n]$ such that $c_i = 0$.*

Lemma 4.2.20 ([MM19, Lemma 4.1])**.** *Let $\boldsymbol{j} = (j_1, \ldots, j_n)$ be a weak composition of $m - n$ that is greater than $(o_1, \ldots, o_n)$ for the dominance order. Then the number of leaves of $R_{H,\preceq^H}$ of type $\boldsymbol{j}$ is $K_H((0, j_1 - o_1, \ldots, j_n - o_n, 0))$.*

Example 4.2.21. One can again see an example of Lemma 4.2.19 and Lemma 4.2.20 on Figure 4.13. Indeed, the three types $(3, 0, 0), (2, 1, 0), (1, 2, 0)$ are weak compositions $\boldsymbol{j}$ of $6 - 3 = 3$ that are greater than $(o_1, o_2, o_3) = (1, 1, 1)$ and such that $j_3 = 0$ (since $c_3 = 0$). Moreover, one can see that for such $\boldsymbol{j}$ there is only one flow for H with netflow $(0, j_1 - o_1, j_2 - o_2, j_3 - o_3, 0)$, which passes only through the horizontal edges e_0'', e_0' and e_0. Indeed, the other edges of H are source or sink edges and they cannot receive a positive flow since the first and last values of the netflow are 0.

We sum up our refinement of Theorem 4.2.8 in the following theorem.

Theorem 4.2.22. *Let $(H, \preceq)$ be a framed graph such that for any $i \in [n]$, all source-edges (v_0, v_i) of H are consecutive in the order $\preceq_{In_i}$.*

For any $i \in [n+1]$ we denote by c_i the number of source-edges (v_0, v_i) and for $i \in [n]$, $o_i := \mathrm{outdeg}_H(v_i) - 1$. We denote by $m := |E(H)| - \sum_{i=1}^{n+1} c_i$ the number of non-source edges of H. Then there is a dissection of $\boldsymbol{\mathcal{F}}_H$ that coarsens $\mathbf{Triang}_{DKK}(H, \preceq)$ into pieces such that:

- *each piece has a certain type $\boldsymbol{j} = (j_1, \ldots, j_n)$ which is a weak composition of $m - n$ that is greater than $(o_1, \ldots, o_n)$ for the dominance order and satisfies $j_i = 0$ for all $i \in [n]$ such that $c_i = 0$,*
- *for each type $\boldsymbol{j}$ there are $K_H((0, j_1 - o_1, \ldots, j_n - o_n, 0))$ pieces of the dissection of type $\boldsymbol{j}$,*
- *the oriented graph dual to the restriction of $\mathbf{Triang}_{DKK}(H, \preceq^H)$ to any piece of type $\boldsymbol{j}$ is isomorphic to the Hasse diagram of the product of Gale orders $\mathrm{Gale}(j_1, c_1) \times \ldots \times \mathrm{Gale}(j_n, c_n)$.*

We call such dissection $\boldsymbol{\mathcal{F}}_H$ the *Lidskii-type decomposition* of $\mathbf{Triang}_{DKK}(H, \preceq)$.

Remark 4.2.23. A remarkable property of the Lidskii-type decomposition is that the structure of its pieces do not depend on the framing $\preceq$. This means that for a given graph H, all framings that satisfy the property that source-edges are adjacent will induce an oriented graph dual to their DKK triangulation that decomposes into the same pieces. However, the way how these pieces are related to each other varies with the framing.

An example of this property can be seen on Figure 4.15, to be compared with Figure 4.14.

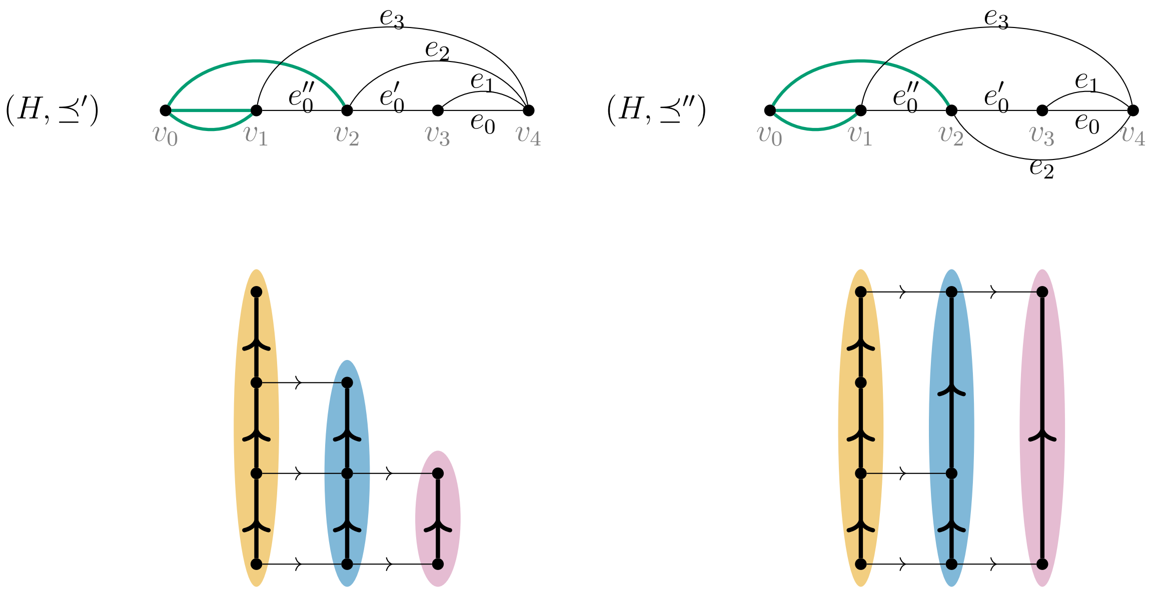

Figure 4.15: Top: Graph H from Figure 4.13 with two other framings $\preceq$ and $\preceq''$. Bottom: The oriented graphs dual to the corresponding DKK triangulations, with coloured pieces of the Lidskii decomposition.

We finish this section with two natural conjectures on the Lidskii-type decomposition of $\mathbf{Triang}_{DKK}(H, \preceq)$.

Conjecture 4.2.24. *The Lidskii-type decomposition of* $\boldsymbol{Triang}_{DKK}(H, \preceq)$ *is a valid subdivision of* $\boldsymbol{\mathcal{F}}_H$.

Conjecture 4.2.25. *The pieces of the Lidskii-type decomposition of* $\boldsymbol{Triang}_{DKK}(H, \preceq)$ *give intervals of the poset structure on MaxCliques*$(H, \preceq)$ *defined by von Bell and Ceballos ([BC2X], in preparation).*

4.3 Combinatorics of the s-weak order and the s-permutahedron

The structures of the s-weak order and the s-permutahedron were first defined by Ceballos and Pons in terms of s-decreasing trees, which allows them to deal with any weak composition s. We remind their main definitions in Section 4.3.1 but the objects that we will use in the rest of the chapter are the Stirling s-permutations (Section 4.3.2), which are defined only when s is a strict composition.

4.3.1 s-decreasing trees

Let $s = (s_1, \ldots, s_n)$ be a weak composition. An *s-decreasing tree* T is a planar rooted tree on n internal vertices (called nodes), labeled by $[n]$, such that the node labeled a has $s_a + 1$ children and any descendant b of a satisfies $b < a$. We denote by $T_0^a, \ldots, T_{s_a}^a$ the subtrees of node a from left to right. See examples on Figures 4.16 and 4.1.

We denote by $\mathcal{T}_s$ the set of all s-decreasing trees. It is known (see for example [CGD19, Section 5.1] and Corollary 4.4.4) that the number of s-decreasing trees is given by

$$|\mathcal{T}_s| = (1 + s_n)(1 + s_n + s_{n-1}) \cdots (1 + s_n + s_{n-1} + \cdots + s_2), \tag{4.3}$$

which can be viewed as a generalization of the factorial numbers since this formula reduces to $n!$ in the case $s = (1, \ldots, 1)$.

It can be seen in this formula that the value of s_1 is inconsequential for determining the combinatorial properties of $\mathcal{T}_s$ (indeed, all the children of the node 1 are leaves), so without loss of generality we can assume that $s_1 = 1$ throughout this thesis.

Let T be an s-decreasing tree. We denote by $\mathrm{inv}(T)$ the multiset of *tree-inversions* of T formed by pairs (c, a) with multiplicity (also called cardinality)

$$\#_T(c, a) = \begin{cases} 0, & \text{if } a \text{ is left of } c, \\ i, & \text{if } a \in T_i^c, \\ s_c, & \text{if } a \text{ is right of } c, \end{cases}$$

for all $1 \leq a < c \leq n$.

In [CP20, Definition 2.5] Ceballos and Pons introduced the *s-weak order* $\trianglelefteq$ on $\mathcal{T}_s$ and showed in [CP22, Theorem 1.21] that it has the structure of a lattice. For s-decreasing trees R and T we define $R \trianglelefteq T$ if $\mathrm{inv}(R) \subseteq \mathrm{inv}(T)$.

Figure 4.1 depicts the Hasse diagram of the s-weak order for $s = (1, 2, 1)$.

To understand the cover relations in the s-weak order we define the notion of ascents and transitivity.

An *ascent* on an s-decreasing tree T is a pair (a, c) satisfying

1. $a \in T_i^c$ for some $0 \leq i < s_c$,
2. if $a < b < c$ and $a \in T_i^b$, then $i = s_b$,
3. if $s_a > 0$, then $T_{s_a}^a$ consists of only one leaf.

Visually, there is an ascent (a, c) if the rightmost child of a is a leaf (unless $s_a = 0$) that is followed by a cavern of c.

Similarly, a *descent* of T is a pair (a, c) such that $a \in T_i^c$ for some $0 < i \leq s_c$, if $a < b < c$ and $a \in T_j^b$ then $j = 0$, and if $s_a > 0$ then T_0^a consists of only one leaf. The notions of ascents and descents on s-decreasing trees generalize the same concepts from classical permutations, see Lemma 4.3.4.

A multiset of inversions I is *transitive* if for all $a < b < c$, either $\#_I(b,a) = 0$ or $\#_I(c,a) \geq \#_I(c,b)$. This property is satisfied by all multisets of tree-inversions ([CP22, Definition 1.5 and Lemma 1.6]). The *transitive closure* of a multiset set of inversion I can be defined as the smallest multiset of inversion I' that contains I and that is transitive (see also [CP22, Definition 1.14 and Lemma 1.16] for an equivalent definition).

If T is an s-decreasing tree that has an ascent (a,c), the s-*tree rotation* of T along the ascent (a,c) is the s-decreasing tree T' whose mulitset of tree-inversions is the transitive closure of the multiset of inversions obtained from $\mathrm{inv}(T)$ after increasing $\#_T(c,a)$ by 1.

Lemma 4.3.1 ([CP22, Theorem 1.32])**.** *There is a cover relation $T \trianglelefteq T'$ in the* s*-weak order exactly if T' is an* s*-tree rotation of T along a certain ascent (a,c) of T.*

Example 4.3.2. Let $\mathrm{s} = (1,1,2,1,3,1,2)$ and consider the s-decreasing tree T shown on the left of Figure 4.16. Its set of ascents is $\{(3,7),(2,5),(4,5),(5,7),(1,6)\}$ and its set of descents is $\{(2,7),(4,5),(1,7)\}$. The pair $(7,5)$ has multiplicity $\#_T(7,5) = 1$.

The rotation of T along the ascent $(5,7)$ yields the tree T' represented on the right of Figure 4.16. In T', the pair $(7,5)$ has multiplicity $\#_{T'}(7,5) = 2$. The multiplicity of the pair $(7,4)$ is also augmented by one from T to T'.

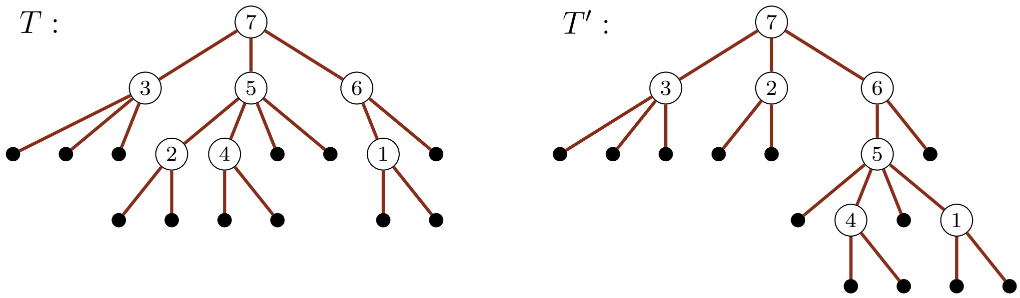

Figure 4.16: Two examples of s-decreasing trees, for $\mathrm{s} = (1,1,2,1,3,1,2)$. There is an s-tree rotation along the ascent $(5,7)$ between T and T'.

If A is a subset of ascents of T, we denote by $T + A$ the s-decreasing tree whose inversion set is the transitive closure of $\mathrm{inv}(T) + A$ (where this notation means that we add 1 to the multiplicities $\#_T(c,a)$ for all ascents $(a,c) \in A$).

Definition 4.3.3 (Definition 4.1 [CP20])**.** The (combinatorial) s-*permutahedron*, denoted Perm_s, is the combinatorial complex with faces (T,A) where T is an s-decreasing tree and A is a subset of ascents of T.

In the s-permutahedron, the face (T,A) is contained in (T',A') if and only if $[T, T+A] \subseteq [T', T'+A']$ as intervals in the s-weak order. In particular, the vertices of Perm_s are the s-decreasing trees and the edges correspond to s-tree rotations. The dimension of a face (T,A) is the cardinality of A.

On the example of Figure 4.1, we can see two pentagonal 2-dimensional faces of the $(1,2,1)$-permutahedron. These faces are obtained with the tree T that is the minimum element of the face, and the set $A = \{(1,2),(1,3)\}$.

4.3.2 Stirling s-permutations

We now explain how the s-weak order can be defined on Stirling s-permutations when s is a composition, i.e. it has no zero entries. This condition is necessary for us to build the s-oruga graph and use the flow polytope technology.

In the remainder of this section we assume that $\mathrm{s} = (s_1, \ldots, s_n)$ is a composition. A *Stirling* s-*permutation* is a word with s_i occurrences of the letter i for $i \in [n]$ that avoids the pattern 121, which means that there is never a letter j in between two occurrences of i with $i < j$. We denote by $\mathcal{W}_{\mathrm{s}}$ the set of all Stirling s-permutations.

The set of Stirling s-permutations is in bijection with the set of s-decreasing trees. This bijection is obtained by reading nodes along the infix order traversal of the caverns (spaces between consecutive siblings) of an s-decreasing tree (see Figure 4.17). Reversely, from a Stirling s-permutation w, we can build an s-decreasing tree $T(w)$ recursively by first placing the node with maximal label a in w and the $s_a + 1$ branches below it. The s_a occurrences of a split the word w into $s_a + 1$ subwords $u_1, \ldots, u_{s_a+1}$. The subtree T_i^a is a leaf if the subword u_i is empty, otherwise it is obtained by applying the recursive procedure to u_i. Note that this bijection induces a correspondence between the prefixes of a Stirling s-permutation w and the leaves of its corresponding tree $T(w)$.

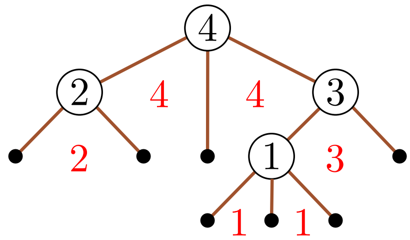

Figure 4.17: A $(2, 1, 1, 2)$-decreasing tree with vertices labeled via in-order. The corresponding Stirling s-permutation is $w = 244113$.

Analogous to the case of classical permutations, the cover relations in the s-weak order can be described in terms of transpositions of substrings in Stirling s-permutations.

Let w be a Stirling s-permutation. For $a \in [n]$, we define the *a-block B_a* of w to be the shortest substring of w containing all s_a occurrences of a. In Example 4.3.6, we see that the 5-block of $w = 33725455716$ is $B_5 = 5455$. Note that an a-block of w necessarily starts and ends with a by minimality, and contains only letters in $[a]$ because w is 121-avoiding. Furthermore for $a < c$, w contains the consecutive substring ac if and only if it is of the form $w = u_1 B_a c u_2$, where u_1 and u_2 denote consecutive substrings of w.

Let w be a Stirling s-permutation. A pair (a, c) with $1 \leq a < c \leq n$ is called an *ascent* of w if ac is a consecutive substring of w. It is a *descent* of w if ca is a consecutive substring of w. If w is of the form $w = u_1 B_a c u_2$ and $a < c$, the *transposition* of w along the ascent (a, c) is the Stirling s-permutation $u_1 c B_a u_2$. We denote by $\mathrm{inv}(w)$ the multiset of inversions formed by pairs (c, a) with multiplicity $\#_w(c, a) \in [0, s_c]$ the number of occurrences of c that precede the a-block in w. As in the case of tree-rotations, if A is a subset of ascents of w, we denote by $w + A$ the Stirling s-permutation whose inversion set is the transitive closure of $\mathrm{inv}(w) + A$. We have the following correspondence between concepts on the family of s-decreasing trees and on the family of Stirling s-permutations, whose proof follows easily from the definitions.

Lemma 4.3.4. *Let w be a Stirling* s*-permutation and $T(w)$ its corresponding* s*-decreasing tree. Let $1 \leq a < c \leq n$.*

(a) The pair (a, c) is an ascent of $T(w)$ if and only if it is an ascent of w.

(b) The pair (a, c) is a descent of $T(w)$ if and only if it is a descent of w.

(c) $\#_{T(w)}(c, a) = \#_w(c, a)$.

Moreover, suppose (a, c) is an ascent of $T = T(w)$ so that w is of the form $w = u_1 B_a c u_2$. Then T' is the s*-tree rotation of T along (a, c) if and only if $T' = T(w')$ where $w' = u_1 c B_a u_2$.*

Corollary 4.3.5. *Let w and w' be Stirling* s*-permutations. Then w' covers w in the* s*-weak order if and only if w' is the transposition of w along an ascent.*

Example 4.3.6. Let $s = (1, 1, 2, 1, 3, 1, 2)$ and consider the s-permutation $w = 33725455716$. The transposition of w along the ascent $(5, 7)$ switches the 5-block of w with the 7 that immediately follows it and yields $w' = 33727545516$. The corresponding s-decreasing tree $T = T(w)$ is shown on the left of Figure 4.16. The rotation of T along the ascent $(5, 7)$ yields $T' = T(w')$.

Remark 4.3.7. If s is a composition, the s-permutahedron Perm_s of Definition 4.3.3 can be alternatively defined as the combinatorial complex with faces (w, A) where w is a Stirling s-permutation and A is a subset of ascents of w.

4.4 Geometric realizations of the s-permutahedron

4.4.1 The flow polytope realization

We introduce the s-oruga graphs along with a fixed framing, and apply the combinatorial method of Danilov, Karzanov and Koshevoy to obtain a triangulation of the associated flow polytope. Combining previous results, we will have bijections between s-decreasing trees $\mathcal{T}_s$, Stirling s-permutations $\mathcal{W}_s$, integer $\boldsymbol{d}$-flows on $\mathrm{Oru(s)}$, and maximal cliques in the framed graph $(\mathrm{Oru(s)}, \preceq)$, represented in the following diagram:

$$\begin{tikzcd}
\mathcal{T}_s \arrow[r, leftrightarrow, "\text{Sec } 4.3.2"] \arrow[rr, leftrightarrow, bend right, "\text{Rem } 4.4.5"'] & \mathcal{W}_s \arrow[r, leftrightarrow, "\text{Prop } 4.4.3"] \arrow[rr, leftrightarrow, bend right, "\text{Lem } 4.4.6"'] & \mathcal{F}_G^{\mathbb{Z}}(\boldsymbol{d}) \arrow[r, leftrightarrow, "\text{Thm } 4.2.6"] & \mathrm{MaxCliques}(\mathrm{Oru(s)}, \preceq)
\end{tikzcd}$$

The s-oruga graph and a DKK triangulation of its flow polytope

Definition 4.4.1. Let $s = (s_1, \ldots, s_n)$ be a composition, and for convenience of notation we also set $s_{n+1} = 2$. The framed graph $(\mathrm{Oru}(s), \preceq)$ consists of vertices $\{v_{-1}, v_0, \ldots, v_n\}$ and

- for $i \in [n+1]$, there are $s_i - 1$ *source-edges* (v_{-1}, v_{n+1-i}) labeled $e^i_1, \ldots, e^i_{s_i-1}$,
- for $i \in [n]$, there are two edges $(v_{n+1-i-1}, v_{n+1-i})$ called *bump* and *dip* labeled e^i_0 and $e^i_{s_i}$,
- the incoming edges of v_{n+1-i} are ordered $e^i_j \prec_{In_{n+1-i}} e^i_k$ for $0 \leq j < k \leq s_i$,
- the outgoing edges of v_{n+1-i} are ordered $e^{i-1}_0 \prec_{Out_{n+1-i}} e^{i-1}_{s_{i-1}}$.

We call Oru(s) the s-*oruga graph*. We will also denote by Oru_n the induced subgraph of Oru(s) with vertices $\{v_0, \ldots, v_n\}$ and call this the *oruga graph* of length n (it does not depend on s).

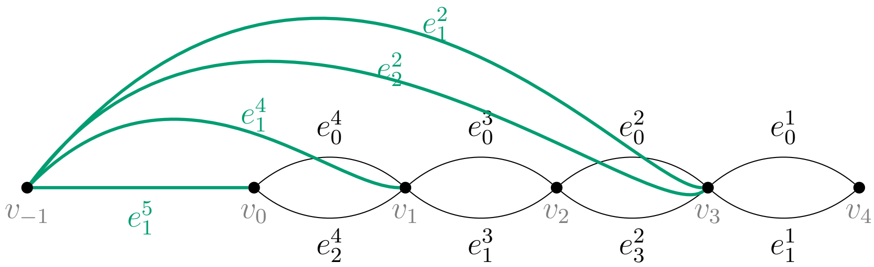

Figure 4.18: The s-oruga graph Oru(s) for $s = (1, 3, 1, 2)$ with edge labels. The framing is obtained by reading the ingoing or outgoing edges of a vertex from top to bottom. The source-edges are depicted in bold green.

Figure 4.18 shows an example of this construction. We always draw the graph Oru(s) in such a way that the framing of the incoming and outgoing edges at each inner vertex is ordered from "top to bottom". Note that the corresponding flow polytope $\mathcal{F}_{\mathrm{Oru}(s)}$ has dimension $|\,s\,| := \sum_{i=1}^n s_i$.

The routes of Oru(s) will play a key role, thus we will describe them as $\mathrm{R}(k, t, \delta)$ intuitively as follows. Every route of Oru(s) starts from v_{-1}, lands in a vertex v_{n+1-k} via a source-edge labeled e^k_t and then follows $k - 1$ edges that are either bumps or dips denoted by a 01-vector δ.

Formally, for $k \in [n+1]$, $t \in [s_k - 1]$, and $\delta = (\delta_{k-1}, \ldots, \delta_1) \in \{0, 1\}^{k-1}$, we denote by $\mathrm{R}(k, t, \delta)$ the sequence of edges $(e^k_{t_k}, e^{k-1}_{t_{k-1}}, \ldots, e^1_{t_1})$ where

- $t_k = t$,
- for all $j \in [k-1]$, $t_j = \delta_j s_j$.

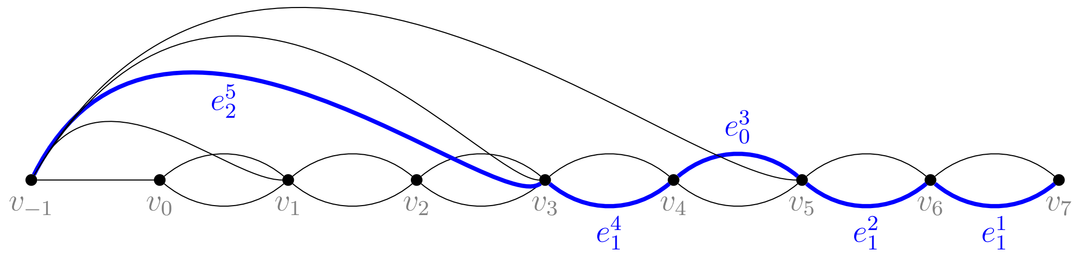

Figure 4.19: The s-oruga graph Oru(s) for s $=$ $(1, 1, 2, 1, 3, 1, 2)$. The route $\mathrm{R}(5, 2, (1, 0, 1, 1))$ is depicted in bold blue and its edge labels are indicated.

Remark 4.4.2. Although the graph Oru(s) starts with vertex v_{-1} instead of v_0 all the technology of Section 4.2.1 can be applied to it. To see this, we can either simply relabel the vertices with $[0, n+1]$, or contract the edge e_1^{n+1} (between v_{-1} and v_0) to obtain a graph $\widehat{\mathrm{Oru}(\mathrm{s})}$ whose flow polytope is integrally equivalent to $\boldsymbol{\mathcal{F}}_{\mathrm{Oru(s)}}$ (see the left part of Figure 4.23). In both cases the resulting graph has flows and routes directly in bijection with the flows and routes of Oru(s).

Proposition 4.4.3. *Let* s *be a composition and let* $\boldsymbol{d} = (0, 0, s_n, s_{n-1}, \dots, s_2, -\sum_{i=2}^{n} s_i)$. *The set of Stirling* s*-permutations is in bijection with the set of integer* $\boldsymbol{d}$*-flows of* Oru(s).

Proof. First, we notice that an integer flow $(f_e)_e$ on Oru(s) with netflow $\boldsymbol{d}$ necessarily has zero flow on every source-edge, so $(f_e)_e$ is characterized by the fact that the total flow on each pair of bump and dip edges satisfies $f_{e_0^i} + f_{e_{s_i}^i} = s_n + \cdots + s_{i+1}$ for all $i \in [n-1]$. Thus to describe an integer $\boldsymbol{d}$-flow on Oru(s), it is enough to determine the flow on the bump edges e_0^i for all $i \in [n-1]$. Given a Stirling s-permutation w, let $f_{e_0^i}$ be the number of letters strictly greater than i that occur before the i-block B_i in w. This implies $0 \leq f_{e_0^i} \leq s_n + \cdots + s_{i+1}$, and thus defines an integer $\boldsymbol{d}$-flow on Oru(s).

Conversely, any Stirling s-permutation can be built iteratively by an insertion algorithm associated to a choice of integers $f_{e_0^i} \in [0, s_n + \cdots + s_{i+1}]$ for $i \in [n-1]$ in the following way. Start with a block of s_n consecutive copies of n (step $i = 0$). At step i for $i \in [n-1]$, there are $s_n + \cdots + s_{n-i+1} + 1$ possible positions for the next insertion. We insert a block of s_{n-i} consecutive copies of $(n-i)$ in the $(f_{e_0^{n-i}})$-th position. This creates a 121-avoiding permutation of the word $1^{s_1} 2^{s_2} \cdots n^{s_n}$. $\square$

See Figure 4.20 for an example illustrating the insertion algorithm described in the proof of Proposition 4.4.3.

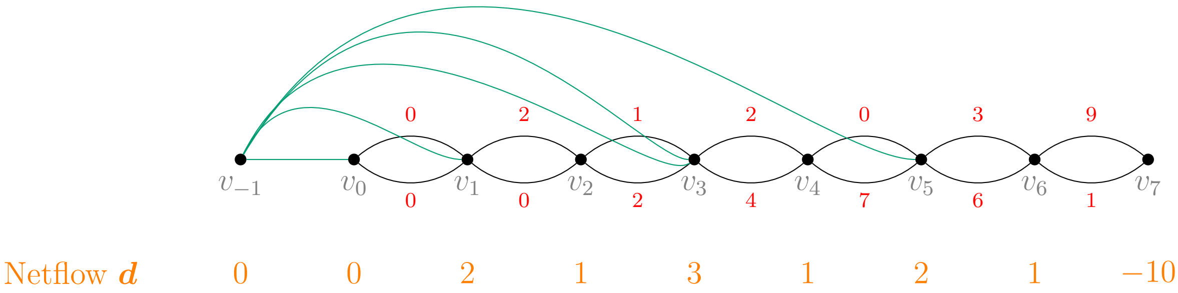

Step i	Flow on edge e_0^{n-i}	Construction of w
0	0	7 7
1	2	7 7 6
2	1	7 5 5 5 7 6
3	2	7 5 4 5 5 7 6
4	0	3 3 7 5 4 5 5 7 6
5	3	3 3 7 2 5 4 5 5 7 6
6	9	3 3 7 2 5 4 5 5 7 1 6

Figure 4.20: An integer $\boldsymbol{d}$-flow of $\mathrm{Oru}((1,1,2,1,3,1,2))$ (the flow on the non-source edges is shown in red) and the steps of the insertion algorithm of Proposition 4.4.3 that output the corresponding Stirling s-permutation $w = 33725455716$.

By Corollary 4.2.7, since the normalized volume of the flow polytope $\mathcal{F}_{\mathrm{Oru(s)}}$ is the number of integer $\boldsymbol{d}$-flows on Oru(s), then we obtain the following as a corollary.

Corollary 4.4.4. *Given a composition* s*, then*

$$\mathrm{vol}_{\mathrm{norm}}\, \boldsymbol{\mathcal{F}}_{\mathrm{Oru(s)}} = |\mathcal{T}_{\mathrm{s}}| = |\mathcal{W}_{\mathrm{s}}| = \prod_{i=1}^{n-1} \left(1 + s_{n-i+1} + s_{n-i+2} + \cdots + s_n\right).$$

Proof. We only need to justify that the right hand side of this formula is the number of $\boldsymbol{d}$-flows on Oru(s). We have seen that a $\boldsymbol{d}$-flow on Oru(s) is determined by its values $f_{e_0^i} \in [0, s_n + \cdots + s_{i+1}]$ for $i \in [n-1]$. □

Remark 4.4.5. We can also give an explicit correspondence between s-decreasing trees and integer $\boldsymbol{d}$-flows of Oru(s). Note that this correspondence holds in the more general setting where s is a weak composition and we consider integer $\boldsymbol{d}$-flows on the oruga graph Oru_n since the source-edges do not play any role.

Given an integer $\boldsymbol{d}$-flow $(f_e)_e$ of Oru(s) (note again that it is enough to know the values $f_{e_0^i}$ for $i \in [n-1]$ to determine the entire integer flow), we build an s-decreasing tree inductively as follows. Start with the tree given by the node n and $s_n + 1$ leaves. At step i for $i \in [n-1]$, we have a partial s-decreasing tree with labeled nodes n to $n+1-i$, and $1 + \sum_{k=n+1-i}^{n} s_k$ leaves that we momentarily label from 0 to $\sum_{k=n+1-i}^{n} s_k$ along the counterclockwise traversal of the partial tree. Attach the next node $n-i$, with $s_{n-i}+1$ pending leaves, to the leaf of the partial tree labeled $f_{e_0^{n-i}}$. This procedure produces decreasing trees with the correct number of children at each node. Hence, after the n-th step we obtain an s-decreasing tree. Reciprocally, any s-decreasing tree can be built iteratively in this way, so it is associated to a choice of integers $f_{e_0^i} \in [0, \sum_{k=n+1-i}^{n} s_k]$ for all $i \in [n-1]$. The interested reader can verify that this procedure applied to the flow in the example of Figure 4.20 produces the tree T on the left of Figure 4.16.

We can now explicitly describe the DKK maximal cliques of coherent routes of Oru(s) via Stirling s-permutations. This is an important construction for the results which follow.

Let s be a composition, and u a (possibly empty) prefix of a Stirling s-permutation. For all $a \in [n]$, we denote by t_a (or $t_a(u)$ if u is not clear from the context) the number of occurrences of a in u, and we denote by c the smallest value in $[n]$ such that $0 < t_c < s_c$. If there is no such value, we set $c = n+1$ and $t_{n+1} = 1$. The definition of c implies that for all $a < c$, either $t_a = 0$ or $t_a = s_a$. Then we define $\mathrm{R}[u]$ to be the route $(e^c_{t_c},\, e^{c-1}_{t_{c-1}},\, \dots,\, e^1_{t_1})$. For example, for the prefix $u = 3372545$ of $w = 33725455716$ in the example of Figure 4.20 we have that $c = 5$, $t_5 = 2, t_4 = 1, t_3 = 2, t_2 = 1, t_1 = 0$ so $\mathrm{R}[u] = (e^5_2,\, e^4_1, e^3_2, e^2_1, e^1_0) = \mathrm{R}(5, 2, (1, 1, 1, 0))$.

Let w be a Stirling s-permutation. For $i \in [|\,\mathrm{s}\,|]$, we denote by w_i the i-th letter of w, and for $i \in [0, |\,\mathrm{s}\,|]$ we denote by $w_{[i]}$ the prefix of w of length i, with $w_{[0]} := \emptyset$. Let Δ_w be the set of routes $\{\mathrm{R}[w_{[i]}] \,|\, i \in [0, |\,\mathrm{s}\,|]\}$ and identify it with the simplex whose vertices are the indicator vectors of these routes.

Note that each maximal clique always contains the routes $\mathrm{R}[w_{[0]}] = (e^{n+1}_1, e^n_0, \dots, e^1_0) = \mathrm{R}(n+1, 1, (0)^n)$ and $\mathrm{R}[w_{[|\,\mathrm{s}\,|]}] = (e^{n+1}_1, e^n_{s_n}, \dots, e^1_{s_1}) = \mathrm{R}(n+1, 1, (1)^n)$. See Figure 4.21 for the example of Δ_w corresponding to the Stirling $(1, 2, 1)$-permutation $w = 3221$.

Lemma 4.4.6. *The maximal simplices of* $\boldsymbol{Triang}_{DKK}(\mathrm{Oru(s)}, \preceq)$ *are exactly the simplices* Δ_w *where* w *ranges over all Stirling* s*-permutations.*

Proof. Recall that by Theorem 4.2.1 the maximal simplices of $\mathbf{Triang}_{DKK}(\mathrm{Oru(s)}, \preceq)$ are the simplices Δ_C, where C is a maximal clique of coherent routes of $(\mathrm{Oru(s)}, \preceq)$.

Let w be a Stirling s-permutation. We will check that Δ_w is a clique of coherent routes of $(\mathrm{Oru(s)}, \preceq)$. Let $1 \le i < i' \le [|\,\mathrm{s}\,|]$ index two routes $\mathrm{R}[w_{[i]}]$ and $\mathrm{R}[w_{[i']}]$ in Δ_w. Since $i < i'$, we have that $t_a(w_{[i]}) \le t_a(w_{[i']})$ for all $a \in [n]$. Thus, for any vertex v_{n+1-a} that appears in both routes $\mathrm{R}[w_{[i]}]$ and $\mathrm{R}[w_{[i']}]$, we have that the incoming (respectively outgoing) edge of $\mathrm{R}[w_{[i]}]$ precedes the incoming (respectively outgoing) edge of $\mathrm{R}[w_{[i']}]$ for the order $\preceq$. Hence, the routes $\mathrm{R}[w_{[i]}]$ and $\mathrm{R}[w_{[i']}]$ are coherent, and Δ_w is a clique for the coherence relation. Moreover, since Δ_w has $|\,\mathrm{s}\,| + 1 = \dim(\boldsymbol{\mathcal{F}}_{\mathrm{Oru(s)}}) + 1$ elements, it is a maximal clique, and corresponds to a maximal simplex in the DKK triangulation of $\boldsymbol{\mathcal{F}}_{\mathrm{Oru(s)}}$.

$\mathrm{R}[w_{[0]}] =$ 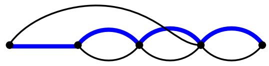

$\mathrm{R}[w_{[1]}] =$ 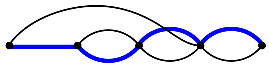

$\mathrm{R}[w_{[2]}] =$ 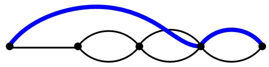

$\mathrm{R}[w_{[3]}] =$ 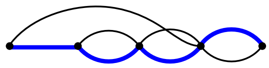

$\mathrm{R}[w_{[4]}] =$ 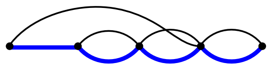

Figure 4.21: The maximal clique $\Delta_w = \{\mathrm{R}[w_{[0]}], \dots, \mathrm{R}[w_{[|\,\mathrm{s}\,|]}]\}$ corresponding to the Stirling $(1,2,1)$-permutation $w = 3221$.

Now, suppose that w' is a Stirling s-permutation distinct from w. We need to check that $\Delta_w \neq \Delta_{w'}$. Suppose that the minimal index $i \in [|\,\mathrm{s}\,| - 1]$ such that $w_i \neq w'_i$ satisfies $w_i < w'_i$. Then $\mathrm{R}[w'_{[i]}]$ cannot belong to Δ_w. Indeed, if we denote a the value of w_i, we have that $e^a_{t_a(w_{[i]})-1}$ is an edge of the route $\mathrm{R}[w'_{[i]}]$ but for any $j > i$, $t_a(w_{[j]}) \geq t_a(w_{[i]})$, so the route $\mathrm{R}[w_{[j]}]$ does not contain this edge. Thus, the map $w \mapsto \Delta_w$ is an injection from Stirling s-permutations to maximal simplices of $\textbf{Triang}_{DKK}(\mathrm{Oru}(\mathrm{s}), \preceq)$.

Then, it follows from the bijection between s-decreasing trees and maximal simplices of $\textbf{Triang}_{DKK}(\mathrm{Oru}(\mathrm{s}), \preceq)$ (Remark 4.4.5) and the bijection between s-decreasing trees and Stirling s-permutations (Section 4.3.2) that this injection is a bijection. □

The Hasse diagram of the s-weak order

We show that the oriented graph dual to the triangulation $\textbf{Triang}_{DKK}(\mathrm{Oru}(\mathrm{s}), \preceq)$ coincides with the Hasse diagram of the s-weak order.

Theorem 4.4.7. *Let $s = (s_1, \dots, s_n)$ be a composition. Let w and w' be two Stirling* s*-permutations. There is a cover relation between $w \leq w'$ in the* s*-weak order if and only if there is an edge from Δ_w to $\Delta_{w'}$ in the oriented graph dual to $\textbf{Triang}_{DKK}(\mathrm{Oru}(\mathrm{s}), \preceq)$.*

Figure 4.22 shows the graph dual to the DKK triangulation of $\mathcal{F}_{\mathrm{Oru}(\mathrm{s})}$ for $s = (1,2,1)$, which corresponds to the (unoriented) Hasse diagram of the $(1,2,1)$-weak order. Note that in this Figure we are omitting the routes $\mathrm{R}[w_{[0]}]$ and $\mathrm{R}[w_{[|\,\mathrm{s}\,|]}]$ since both appear in Δ_w for every $w \in \mathcal{W}_{(1,2,1)}$.

Proof. Suppose that w' is obtained from w by a transposition along the ascent (a, c). We show that the vertices of Δ_w and $\Delta_{w'}$ differ only in one element, and that the corresponding edge in the oriented graph dual to $\textbf{Triang}_{DKK}(\mathrm{Oru}(\mathrm{s}), \preceq)$ is oriented from Δ_w to $\Delta_{w'}$. It follows from Corollary 4.3.5 that $w = u_1 B_a c u_2$ and $w' = u_1 c B_a u_2$, where B_a is the a-block of w. We denote by $\ell(u)$ the length of a word u. For all $i \in [0, \ell(u_1)]$ and

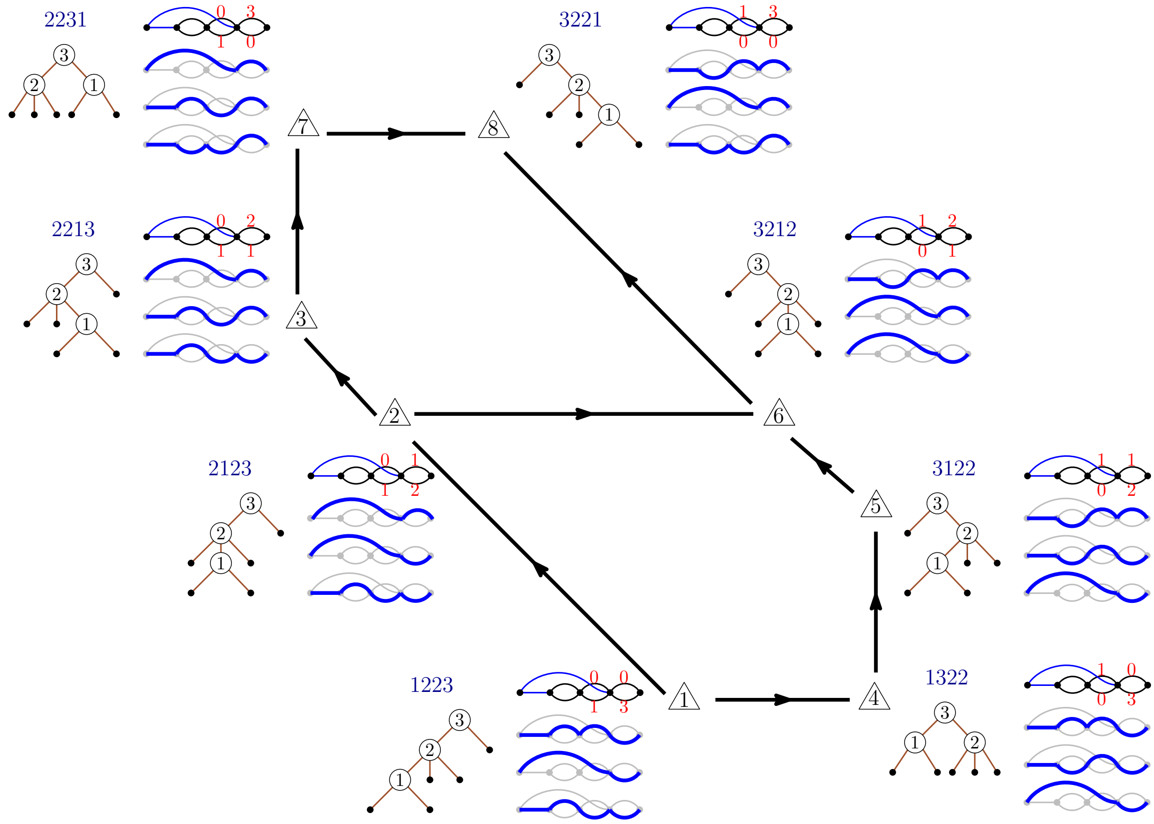

Figure 4.22: The s-permutahedron for the case $\mathrm{s} = (1, 2, 1)$. The vertices are indexed by the following combinatorial objects: s-decreasing trees, Stirling s-permutations, maximal cliques of routes (omitting $\mathrm{R}[w_{[0]}]$ and $\mathrm{R}[w_{[|\,\mathrm{s}\,|]}]$), and integer $\boldsymbol{d}$-flows for $\boldsymbol{d} = (0, 0, 1, 2, -3)$ (in red on the topmost graph, omitting the edges on which the integer $\boldsymbol{d}$-flows are always 0). They correspond to simplices or maximal mixed cells in our first and second realizations. The edges are oriented so that we recover the Hasse diagram of the s-weak order, or the oriented graph dual to the DKK triangulation.

$i \in [\ell(u_1) + \ell(B_a) + 1, |\,\mathrm{s}\,|]$, the routes $\mathrm{R}[w_{[i]}]$ and $\mathrm{R}[w'_{[i]}]$ are equal since $w_{[i]}$ and $w'_{[i]}$ have the same letters. For all $i \in [\ell(u_1) + 1, \ell(u_1) + \ell(B_a) - 1]$, the routes $\mathrm{R}[w_{[i]}]$ and $\mathrm{R}[w'_{[i+1]}]$ are equal as well. Indeed, for such i we have that $t_b(w_{[i]}) = t_b(w'_{[i+1]})$ for all $b \in [n] \setminus \{c\}$ and since $0 < t_a(w_{[i]}) < s_a$ (because we are reading the substring B_a) with $a < c$, the value of $t_c(w_{[i]})$ (respectively $t_c(w'_{[i+1]})$) does not play a role in the route $\mathrm{R}[w_{[i]}]$ (respectively $\mathrm{R}[w'_{[i+1]}]$). Hence, the vertices of Δ_w and $\Delta_{w'}$ differ only in one element: $\mathrm{R}[u] \in \Delta_w$ corresponding to the prefix $u = u_1 B_a$ of w and $\mathrm{R}[u'] \in \Delta_{w'}$ corresponding to the prefix $u' = u_1 c$ of w'. This means that the corresponding simplices in the DKK triangulation of $\boldsymbol{\mathcal{F}}_{\mathrm{Oru(s)}}$ share a common facet. Moreover, for the prefixes u and u' we have that $t_d(u) = t_d(u')$ for all $d \in [a + 1, c - 1] \cup [c + 1, n]$, $t_c(u) = t_c(u') - 1$, $t_a(u) = 0$ and $t_a(u') = s_a$. Thus, we see that the routes $\mathrm{R}[u]$ and $\mathrm{R}[u']$ are in minimal conflict at $[v_{n+1-c}, v_{n-a}]$ and the incoming edge of v_{n+1-c} in $\mathrm{R}[u]$ (which is $e^c_{t_c(u)}$) comes before the incoming edge of v_{n+1-c} in $\mathrm{R}[u']$ (which is $e^c_{t_c(u')}$) in the order $\preceq_{In_{n+1-c}}$ given by the framing on Oru(s). This means that the oriented edge of the graph dual to $\mathbf{Triang}_{DKK}(\mathrm{Oru(s)}, \preceq)$ is oriented from Δ_w to $\Delta_{w'}$.

Reciprocally, suppose that the vertices of Δ_w and $\Delta_{w'}$ differ only in one element. We denote u_1 the longest common prefix of w and w'. We denote $a := w_{\ell(u_1)+1}$, $c := w'_{\ell(u_1)+1}$ and suppose that $a < c$. Let B_a be the a-block of w. Then:

- The substring u_1 contains no occurrence of a, because otherwise there would be a subword aca in w', which contradicts the 121-pattern avoidance.
- The route $\mathrm{R}[w_{[\ell(u_1)+\ell(B_a)]}]$, corresponding to the prefix u_1B_a of w, is in Δ_w but not in $\Delta_{w'}$.
- The route $\mathrm{R}[w'_{[\ell(u_1)+1]}]$, corresponding to the prefix u_1c of w', is in $\Delta_{w'}$ but not in Δ_w.

Thus, the only possibility that Δ_w and $\Delta_{w'}$ differ only on these elements is that $w = u_1B_acu_2$ and $w' = u_1cB_au_2$, where u_2 is their longest common suffix. This means that there is an s-tree rotation along the ascent (a, c) between w and w'. □

In this situation, we will say that the common facet of Δ_w and $\Delta_{w'}$ is associated to the transposition of w along (a, c). Note that such facets are exactly the interior facets (codimension-1 simplices) of $\mathbf{Triang}_{DKK}(\mathrm{Oru(s)}, \preceq)$.

Higher faces of the s-permutahedron

We show that the faces of the s-permutahedron other than vertices and edges are also encoded in the triangulation $\mathbf{Triang}_{DKK}(\mathrm{Oru(s)}, \preceq)$, after proving several technical results.

We say that a simplex of $\mathbf{Triang}_{DKK}(\mathrm{Oru(s)}, \preceq)$ is *interior* if it is not contained in the boundary of the polytope $\boldsymbol{\mathcal{F}}_{\mathrm{Oru(s)}}$. Otherwise it is in the boundary of $\mathbf{Triang}_{DKK}(\mathrm{Oru(s)}, \preceq)$.

Lemma 4.4.8. *Let w be a Stirling s-permutation. Let $\mathrm{R} = \mathrm{R}(k, t, \delta)$ be a route of Oru(s). Then, R is a vertex of Δ_w if and only if the multiset of inversions of w satisfies the following inequalities:*

1. $\#_w(k, i) \geq t$ *for all* $1 \leq i < k$ *such that* $\delta_i = 0$,
2. $\#_w(k, i) \leq t$ *for all* $1 \leq i < k$ *such that* $\delta_i = 1$,
3. $\#_w(j, i) = 0$ *for all* $1 \leq i < j < k$ *such that* $(\delta_i, \delta_j) = (1, 0)$,
4. $\#_w(j, i) = s_j$ *for all* $1 \leq i < j < k$ *such that* $(\delta_i, \delta_j) = (0, 1)$.

We say that the route R *implies* these inequalities on inversion sets.

Proof. Suppose that R is a vertex of Δ_w. It means that $\mathrm{R} = \mathrm{R}[w_{[r]}]$ for a certain $r \in [0, |\,\mathrm{s}\,|]$ and it conveys information on the prefix $u = w_{[r]}$. More precisely, t is the number of occurrences of k in u, and for all $1 \leq i < k$, the number of occurrences of i in u is either 0 if $\delta_i = 0$ or s_i if $\delta_i = 1$. This gives the announced inequalities on the inversion set of w.

Reciprocally, suppose that the inversion set of w satisfies these inequalities. Then there is a prefix $u = w_{[r]}$ of w that contains no occurrence of i for i such that $\delta_i = 0$, all s_i occurrences of i for i such that $\delta_i = 1$, and exactly t occurrences of k. Then this prefix is exactly the one associated to the route $\mathrm{R}[u] = \mathrm{R}(k, t, \delta) = \mathrm{R}$. $\square$

Let w be a Stirling s-permutation, A a subset of ascents of w, and $1 \leq a < c \leq n$ such that $\#_w(c, a) < s_c$. We say that the pair (a, c) is *A-dependent* in w if there is a sequence $a \leq b_1 < \ldots < b_k < b_{k+1} = c$ such that:

(i) b_1 is the greatest letter strictly smaller than c such that the a-block is contained in the b_1-block,
(ii) for all $i \in [k-1]$, the b_i-block is directly followed by the b_{i+1}-block,
(iii) the b_k-block is directly followed by an occurrence of c,
(iv) $(b_i, b_{i+1}) \in A$ for all $i \in [k]$.

Note that in particular, every ascent (a, c) in A is A-dependent taking $k = 1$, $b_1 = a$ and $b_2 = c$.

For example for the Stirling s-permutation $w = 33725455716$ and $A = \{(2, 5), (5, 7), (1, 6)\}$ there is an A-dependency between 2 and 7 given by the sequence $b_1 = 2$, $b_2 = 5$ and $b_3 = 7$ but there is no A-dependency between 2 and 6 since the second occurrence of 7 does not form a block and it is followed by 1.

Proposition 4.4.9. *Let w be a Stirling s-permutation, A a subset of its ascents. Then for all $1 \leq a < c \leq n$ we have that*

$$\#_{w+A}(c, a) = \begin{cases} \#_w(c, a) + 1 & \text{if } (a, c) \text{ is } A\text{-dependent in } w \\ \#_w(c, a) & \text{otherwise.} \end{cases}$$

Example 4.4.10. If $w = 33725455716$ and $A = \{(2, 5), (5, 7), (1, 6)\}$, then the resulting Stirling s-permutation is $w + A = 33775245561$ and the pairs whose inversion number has been increased by 1 are $(2, 5), (2, 7), (4, 7), (5, 7)$ and $(1, 6)$.

Proof. Let be I the multiset of inversions defined by

$$\#_I(c, a) := \begin{cases} \#_w(c, a) + 1 & \text{if } (a, c) \text{ is } A\text{-dependent in } w \\ \#_w(c, a) & \text{otherwise.} \end{cases}$$

Note that if (a, c) is A-dependent and $d > c$ this implies that $\#_I(d, c) = \#_I(d, a)$. Indeed, in this case either both (a, d) and (c, d) are A-dependent or both are not.

We will prove that $I = \mathrm{inv}(w + A)$ by showing that I is the smallest transitive multiset of inversions that contains $\mathrm{inv}(w) + A$. We recall that by transitivity of I we mean that if $a < b < c$, then $\#_I(b, a) = 0$ or $\#_I(c, a) \geq \#_I(c, b)$.

First, it is clear that I contains $\mathrm{inv}(w) + A$ since every pair in A is A-dependent.

Let us show that any transitive multiset of inversions I' that contains $\mathrm{inv}(w) + A$ necessarily contains I. Note that for such I' we have $\#_{I'}(c, a) \geq \#_w(c, a)$ for all pairs (a, c). Let (a, c) be A-dependent with an associated sequence $a \leq b_1 < \ldots < b_k < b_{k+1} = c$ and we proceed by induction on k.

If $k = 1$, we have that:

- either $b_1 = a$ and (a,c) is in A, and directly $\#_{I'}(c,a) \geq \#_w(c,a)+1$,
- or $a < b_1 < c$, which in this case $\#_{I'}(b_1,a) \geq \#_w(b_1,a) > 0$ since the a-block is contained in the b_1-block in w. We get that

$$\#_{I'}(c,a) \geq \#_{I'}(c,b_1) \geq \#_w(c,b_1)+1 = \#_w(c,a)+1 \tag{4.4}$$

  where the first inequality comes from transitivity, the second from the previous case since $(b_1,c) \in A$ and the last equality again because the (a,b_1) are A-dependent.

Suppose that $k > 1$. Then the induction hypothesis implies that $\#_{I'}(b_k,a) \geq \#_w(b_k,a)+1 > 0$. Just like in equation (4.4), applying transitivity to $a < b_k < c$ and using that $(b_k,c) \in A$ and (a,b_k) is A-dependent (so there cannot be any occurrance of c between a and b_k) gives us the inequalities $\#_{I'}(c,a) \geq \#_{I'}(c,b_k) \geq \#_w(c,b_k)+1 = \#_w(c,a)+1$.

Finally, we check that I is indeed transitive. Let $1 \leq a < b < c \leq n$ and $\#_I(b,a) > 0$. We need to check that $\#_I(c,a) \geq \#_I(c,b)$.

Case 1: if $\#_w(b,a) = 0$, then (a,b) is A-dependent and $\#_I(c,a) = \#_I(c,b)$.

Case 2: Suppose that $\#_w(b,a) > 0$.

Case 2.1: If $\#_I(c,b) = \#_w(c,b)$, due to the inclusion $\mathrm{inv}(w) \subset I$ and the transitivity of $\mathrm{inv}(w)$ we have that $\#_I(c,a) \geq \#_w(c,a) \geq \#_w(c,b) = \#_I(c,b)$.

Case 2.2: Suppose that $\#_I(c,b) = \#_w(c,b)+1$ *i.e.* (b,c) is A-dependent. If $\#_w(c,a) \geq \#_w(c,b)+1$, we have $\#_I(c,a) \geq \#_w(c,a) \geq \#_w(c,b)+1 = \#_I(c,b)$. Otherwise, we have $\#_w(c,a) = \#_w(c,b) =: i$. It follows from the assumption $\#_w(b,a) > 0$ that the a-block appears in w between the first occurrence of b and the i-th occurrence of c. This implies that (a,c) is also A-dependent, with a corresponding sequence that is included in the one giving the the A-dependency of (b,c). The two A-dependencies together with the transitivity of w for $a < b < c$ imply that $\#_I(c,a) = \#_w(c,a)+1 \geq \#_w(c,b)+1 = \#_I(c,b)$. □

Let (w,A) be a face of Perm_s. We define $\Delta_{(w,A)}$ to be the following intersection of facets of Δ_w:

$$\Delta_{(w,A)} := \bigcap_{(a,c)\in A} \{\Delta_w \cap \Delta_{w'} \mid w' \text{ is the transposition of } w \text{ along } (a,c)\}, \tag{4.5}$$

and $\Delta_{(w,A)} := \Delta_w$ if $A = \emptyset$.

Note that the $|A|$ routes that are in Δ_w and not in $\Delta_{(w,A)}$ correspond to the prefixes of w that end at an ascent in A.

Lemma 4.4.11. *Let (w,A) be a face of Perm$_s$ and w' a Stirling s-permutation. We denote by $[w, w+A]$ the interval of the s-weak order defined by w and $w+A$.*

Then, $\Delta_{(w,A)} \subseteq \Delta_{w'}$ if and only if $w' \in [w, w+A]$.

Proof. Recall that the inversion set of $w+A$ is described in Proposition 4.4.9 and that $w' \in [w, w+A]$ if and only if its inversion set satisfies that for all $1 \leq a < c \leq n$, $\#_w(c,a) \leq \#_{w'}(c,a) \leq \#_{w+A}(c,a)$. We show that these inequalities are exactly the ones implied by the union of routes that give vertices of $\Delta_{(w,A)}$, in the sense of Lemma 4.4.8.

Let (a,c) be a pair with $\#_w(c,a) = t$.

We have to show these three inequalities:

1. There is a route R in $\Delta_{(w,A)}$ such that $R \in \Delta_{w'}$ implies the inequality $\#_{w'}(c,a) \geq t$. We can take the route that corresponds to the first prefix of w containing the t-th occurrence of c that does not end at an ascent in A. Such a prefix cannot contain any a since $a < c$.

2. There is a route R in $\Delta_{(w,A)}$ such that $\#_{w'}(c,a) \leq t$ for all w' with $R \in \Delta_{w'}$ if and only if $\#_{w+A}(c,a) = t$, that is, the pair (a,c) is not A-dependent. Indeed, this inequality is only implied by routes that contain the edges e^c_t and $e^a_{s_a}$. Such routes in Δ_w correspond to prefixes in w that contain the a-block and the t-th occurrence of c and that do not end inside a b-block for any $b < c$. The pair (a,c) is A-dependent exactly when all such prefixes end at a descent in A, so the corresponding routes are removed in $\Delta_{(w,A)}$.

3. If $t+1 < s_c$ and $\#_{w+A}(c,a) = t+1$, i.e. (a,c) is an A-dependent pair, there is a route R in $\Delta_{(w,A)}$ such that $R \in \Delta_{w'}$ implies $\#_{w'}(c,a) \leq t+1$. Indeed, we can take the route that corresponds to the prefix of w that ends at the $(t+1)$-th occurrence of c. Since $t+1 < s_c$, c appears afterwards so this prefix does not end at an ascent. (Note that if $t+1 = s_c$ there is no need to check that $\#_{w'}(c,a) \leq s_c$). □

Lemma 4.4.11 leads to the following alternative characterization of $\Delta_{(w,A)}$.

Corollary 4.4.12. $\Delta_{(w,A)} = \bigcap_{w' \in [w, w+A]} \Delta_{w'}$.

Lemma 4.4.13. *If C is a clique of routes of $(\mathrm{Oru(s)}, \preceq)$ that contains $\mathrm{R}(n+1, 1, (0)^n), \mathrm{R}(n+1, 1, (1)^n)$ and at least one route that starts with e for each source-edge e that is not (v_{-1}, v_0), then Δ_C is in the interior of $\textbf{Triang}_{DKK}(\mathrm{Oru(s)}, \preceq)$.*

Proof. Suppose that Δ_C is a boundary simplex of $\textbf{Triang}_{DKK}(\mathrm{Oru(s)}, \preceq)$. Then it is contained in a facet that is in the boundary of $\textbf{Triang}_{DKK}(\mathrm{Oru(s)}, \preceq)$. This facet corresponds to a clique of the form $\Delta_w \setminus R$, where w is a Stirling s-permutation and R is a route of Δ_w that does not correspond to an ascent nor a descent of w. Hence, either $R \in \{\mathrm{R}(n+1, 1, (0)^n), \mathrm{R}(n+1, 1, (1)^n)\}$, or R corresponds to a prefix $w_{[i]}$ such that $w_i = w_{i+1}$. In this case, suppose that w_i is the t-th occurrence of c in w. Then R is the only route of Δ_w that starts with the edge e^c_t. In any case, since $C \subseteq \Delta_w \setminus R$, it does not satisfy the condition of the lemma. □

Corollary 4.4.14. *Let w be a Stirling* s*-permutation and A a subset of its ascents. Then $\Delta_{(w,A)}$ is an interior simplex of $\textbf{Triang}_{DKK}(\mathrm{Oru(s)}, \preceq)$.*

Proof. It is sufficient to show that $\Delta_{(w,A)}$ contains $\mathrm{R}(n+1, 1, (0)^n), \mathrm{R}(n+1, 1, (1)^n)$ and at least one route that starts with e for each source-edge e that is not (v_{-1}, v_0).

First, it is clear that $\mathrm{R}(n+1, 1, (0)^n)$ and $\mathrm{R}(n+1, 1, (1)^n)$ are in $\Delta_{(w,A)}$ since they do not correspond to ascents in w.

Let $c \in [n]$ and $t \in [s_c - 1]$. Then the prefix of w that ends with the t-th occurrence of c corresponds to a route R that contains the edge source-edge e^c_t. Moreover, there cannot be an ascent of w after this prefix since there are still occurrences of c afterwards. Thus the route R is not removed from Δ_w to $\Delta_{(w,A)}$. □

Theorem 4.4.15. *The map* $(w, A) \mapsto \Delta_{(w,A)}$ *induces a poset isomorphism between the face poset of the* s*-permutahedron* $\mathrm{Perm}_{\mathrm{s}}$ *and the set of interior simplices of the triangulation* $\boldsymbol{Triang}_{DKK}(\mathrm{Oru}(\mathrm{s}), \preceq)$ *ordered by reverse inclusion.*

Proof. The fact that all $\Delta_{(w,A)}$ are interior simplices of $\mathbf{Triang}_{DKK}(\mathrm{Oru}(\mathrm{s}), \preceq)$ is stated in Corollary 4.4.14. The injectivity follows from Lemma 4.4.11.

Let us show the surjectivity. Let F be an interior simplex of $\mathbf{Triang}_{DKK}(\mathrm{Oru}(\mathrm{s}), \preceq)$. Let w be a Stirling s-permutation that is minimal for the s-weak order with respect to the condition that $F \subseteq \Delta_w$. Then, F is an intersection of facets of Δ_w. These facets correspond to certain transpositions involving w. We denote by A the set of ascents corresponding to these transpositions. The minimality of w implies that all elements in A are ascents (and not descents) of w. Thus, $F = \Delta_{(w,A)}$, and the choice of w was unique.

Finally, let w, w' be Stirling s-permutations and A, A' subsets of their respective ascents. Lemma 4.4.11 implies that $[w, w + A] \subseteq [w', w' + A']$ if and only if $\Delta_{(w',A')} \subseteq \Delta_{(w,A)}$, which proves that the map is a poset isomorphism. □

In a similar way that the minimal elements of the face poset of $\mathrm{Perm}_{\mathrm{s}}$ have a characterization as the maximal cliques of $\mathbf{Triang}_{DKK}(\mathrm{Oru}(\mathrm{s}), \preceq)$, the maximal elements of the face poset also have an explicit characterization in terms of cliques.

Corollary 4.4.16. *A simplex* Δ_C *of* $\boldsymbol{Triang}_{DKK}(\mathrm{Oru}(\mathrm{s}), \preceq)$ *corresponds with a maximal interior face of* $\mathrm{Perm}_{\mathrm{s}}$ *if and only if* C *is a clique of size* $|\,\mathrm{s}\,| - n + 2$ *that satisfies the following:*

- $\mathrm{R}[w_{[0]}]$ *and* $\mathrm{R}[w_{[|\,\mathrm{s}\,|]}]$ *are in* C*, and*
- *each source-edge of* $\mathrm{Oru}(\mathrm{s})$ *that is different from* (v_{-1}, v_0) *is contained in exactly one route in* C*.*

Proof. We first note that for each $i \in [n]$, the graph $\mathrm{Oru}(\mathrm{s})$ has $s_i - 1$ source-edges, so $\mathrm{Oru}(\mathrm{s})$ indeed has $\sum_{i=1}^{n}(s_i - 1) = |\,\mathrm{s}\,| - n$ source-edges that are not (v_{-1}, v_0). By Lemma 4.4.13, a clique C with the above stated properties corresponds with a maximal interior face of $\mathrm{Perm}_{\mathrm{s}}$.

Conversely, let (w, A) be a maximal face of $\mathrm{Perm}_{\mathrm{s}}$. We will check that $C = \Delta_{(w,A)}$ satisfies the specified properties. Let $N \subset [0, |\,\mathrm{s}\,|]$ denote the set of non-ascent positions in w, so that $C = \cup_{j \in N} \mathrm{R}[w_{[j]}]$.

Observe that since w is 121-avoiding, if it has $n-1$ ascents, then the ascents are of the form (i, c_i) where $i < c_i$ for each $i \in [n-1]$. Moreover, for each $i \in [n-1]$, it is the s_i-th occurrence of i in w which produces an ascent pair in w. Therefore, the set $N \backslash \{0, |\,\mathrm{s}\,|\}$ indexes the first $s_i - 1$ occurrences of i in w.

Now suppose $j \in N \backslash \{0, |\,\mathrm{s}\,|\}$ is a non-ascent position of w so that $\mathrm{R}[w_{[j]}] \in C$. We denote a the letter w_j. If w_j is the k-th occurrence of a in w for some $k \in [s_a - 1]$, then the route $\mathrm{R}[w_{[j]}]$ contains the proper source-edge e_k^a. Lastly, since $|N \backslash \{0, |\,\mathrm{s}\,|\}| = |\,\mathrm{s}\,| - n$, then C has the desired properties. □

Lidskii-type decompositions of the s-weak order

In this section, we apply Theorem 4.2.22 to provide a Lidskii-type decomposition of the s-weak order.

In fact, we propose two Lidskii-type decompositions, depending on whether we consider the graph $\mathrm{Oru}(\mathrm{s})$ or the graph $\widehat{\mathrm{Oru}(\mathrm{s})}$ where the edge (v_{-1}, v_0) is contracted (See Remark 4.4.2 and the left part of Figure 4.23).

Lemma 4.4.17. *Let* $\mathrm{s} = (s_1, \dots, s_n)$ *be a composition. Then the* s*-weak order can be partitioned into subposets such that:*

- *each subposet has a certain type* $\boldsymbol{j} = (j_1, \dots, j_n)$ *which is a weak composition of* n *that is greater than* $(1, \dots, 1)$ *for the dominance order and satisfies* $j_i = 0$ *for all* $i \in [2, n]$ *such that* $s_{n+2-i} = 1$*,*
- *for each type* $\boldsymbol{j}$ *there are* $\prod_{k=1}^{n}(j_1 + \cdots + j_k - k + 1)$ *pieces of the dissection of type* $\boldsymbol{j}$*,*
- *a subposet of type* $\boldsymbol{j}$ *is isomorphic to the Hasse diagram of the product of Gale orders* $Gale(j_1, 1) \times Gale(j_2, s_n - 1) \times \ldots \times Gale(j_n, s_2 - 1)$*.*

Proof. This is a direct application of Theorem 4.2.22 on $\mathrm{Oru}(\mathrm{s})$, whose vertices can be relabeled $v_0, \dots, v_{n+1}$ in order to match the notations of the theorem. Then we have that for all $i \in [n]$, $c_i = s_{n+2-i} - 1$ and $o_i = 1$ (with the convention $s_{n+1} = 2$). We only need to justify why $K_{\mathrm{Oru}(\mathrm{s})}((0, j_1 - 1, \dots, j_n - 1, 0)) = \prod_{k=1}^{n}(j_1 + \cdots + j_k - k + 1)$. An integer flow on $\mathrm{Oru}(\mathrm{s})$ with netflow $(0, j_1 - 1, \dots, j_n - 1, 0)$ has a value 0 on all source edges and sink edges. Therefore it is uniquely determined by its values $f_{e_0^k}$ on edges e_0^i for all $k \in [n]$ (then the value on edge $e_{s_k}^k$ is determined). For all $k \in [n]$, $f_{e_0^k}$ can take any integer value in $[0, \sum_{i=1}^{n+1-k}(j_i - 1)]$. Hence

$$K_{\mathrm{Oru}(\mathrm{s})}((0, j_1 - 1, \dots, j_n - 1, 0)) = |\boldsymbol{\mathcal{F}}_{G\mathrm{s}}^{\mathbb{Z}}((0, j_1 - 1, \dots, j_n - 1, 0))| = \prod_{k=1}^{n}(j_1 + \cdots + j_k - k + 1).$$

□

Lemma 4.4.18. *Let* $\mathrm{s} = (s_1, \dots, s_n)$ *be a composition. Then the* s*-weak order can be partitioned into subposets such that:*

- *each subposet has a certain type* $\boldsymbol{j} = (j_1, \dots, j_{n-1})$ *which is a weak composition of* $n - 1$ *that is greater than* $(1, \dots, 1)$ *for the dominance order and satisfies* $j_i = 0$ *for all* $i \in [2, n - 1]$ *such that* $s_{n+1-i} = 1$*,*
- *for each type* $\boldsymbol{j}$ *there are* $\prod_{k=1}^{n-1}(j_1 + \cdots + j_k - k + 1)$ *pieces of the dissection of type* $\boldsymbol{j}$*,*
- *a subposet of type* $\boldsymbol{j}$ *is isomorphic to the Hasse diagram of the product of Gale orders* $Gale(j_1, s_n + 1) \times Gale(j_2, s_{n-1} - 1) \ldots \times Gale(j_n, s_2 - 1)$*.*

Proof. This time, we apply Theorem 4.2.22 to $\widehat{\mathrm{Oru}(\mathrm{s})}$, whose vertices are $v_0, \dots, v_n$. In this case we have that $c_1 = s_n + 1$ and for all $i \in [2, n-1]$, $c_i = s_{n+1-i} - 1$ and for all $i \in [n-1]$, $o_i = 1$. The justification that $K_{\widehat{\mathrm{Oru}(\mathrm{s})}}((0, j_1 - 1, \dots, j_{n-1} - 1, 0)) = \prod_{k=1}^{n-1}(j_1 + \cdots + j_k - k + 1)$ the same as in the previous lemma. □

Corollary 4.4.19. *For a composition $s = (s_1, \ldots, s_n)$, the number of elements of the* s*-weak order decomposes as*

$$\prod_{i=1}^{n-1}\left(1 + \sum_{r=n-i+1}^{n} s_r\right) = \sum_{\substack{\boldsymbol{j} \text{ weak composition of } n \\ \text{of length } n \\ \text{s.t. } \boldsymbol{j} \geq (1,\ldots,1)}} \left(\!\!\binom{1}{j_1}\!\!\right) \prod_{k=2}^{n} \left(\!\!\binom{s_{n+2-k} - 1}{j_k}\!\!\right) \prod_{k=1}^{n} \binom{\sum_{i=1}^{n+1-k} j_i - k + 1}{} \tag{4.6}$$

$$= \sum_{\substack{\boldsymbol{j} \text{ weak composition of } n-1 \\ \text{of length } n-1 \\ \text{s.t. } \boldsymbol{j} \geq (1,\ldots,1)}} \left(\!\!\binom{s_n + 1}{j_1}\!\!\right) \prod_{k=2}^{n-1} \left(\!\!\binom{s_{n+1-k} - 1}{j_k}\!\!\right) \prod_{k=1}^{n-1} \left(\sum_{i=1}^{n-k} j_i - k + 1\right). \tag{4.7}$$

Example 4.4.20. Figure 4.23 shows the Lidskii-type decompositions of the $(1, 3, 2)$-weak order from Lemma 4.4.17 (top) and Lemma 4.4.18 (bottom). For the first one (top) there are:

- six pieces of type $(3, 0, 0)$, which are singletons (represented in pink at the vertices of the big hexagon),
- four pieces of type $(2, 1, 0)$, which are singletons (represented in yellow on the side edges of the big hexagon),
- two pieces of type $(1, 2, 0)$, which are singletons (represented in green inside the big hexagon),
- two pieces of type $(2, 0, 1)$, which are chains of size 2 (represented in violet at the top and bottom),
- one piece of type $(1, 1, 1)$, which is a chain of size 2 (represented in blue in the centre).

For the second one (bottom), there are:

- two pieces of type $(2, 0)$, which are the Hasse diagrams of *Gale*$(2, 3)$ (represented in pink on the sides),
- one piece of type $(1, 1)$, which is the product of *Gale*$(1, 3)$ and *Gale*$(1, 2)$ where each is a chain of respective sizes 3 and 2 (represented in blue in the centre).

Remark 4.4.21. In [GDMP+23, Corollary 6.2], we also present the following enumerative formula, which comes Lidskii-Baldoni-Vergne formula that we did not present here because it does not seem to translate into a geometric decomposition of the DKK triangulation of the flow polytope.

$$\prod_{i=1}^{n-1}\left(1 + \sum_{r=n-i+1}^{n} s_r\right) = \sum_{\substack{\boldsymbol{j} \text{ weak composition of } n-1 \\ \text{of length } n-1 \\ \text{s.t. } \boldsymbol{j} \geq (1,\ldots,1)}} \prod_{k=1}^{n-1} \binom{s_{n+1-k} + 1}{j_k} \prod_{k=1}^{n-1} \left(\sum_{i=1}^{n-k} j_i - k + 1\right). \tag{4.8}$$

Moreover, in this article we present a purely combinatorial proofs of the enumerative formula 4.7 (Equation 4.6 can be recovered in a similar way), that provides good evi-

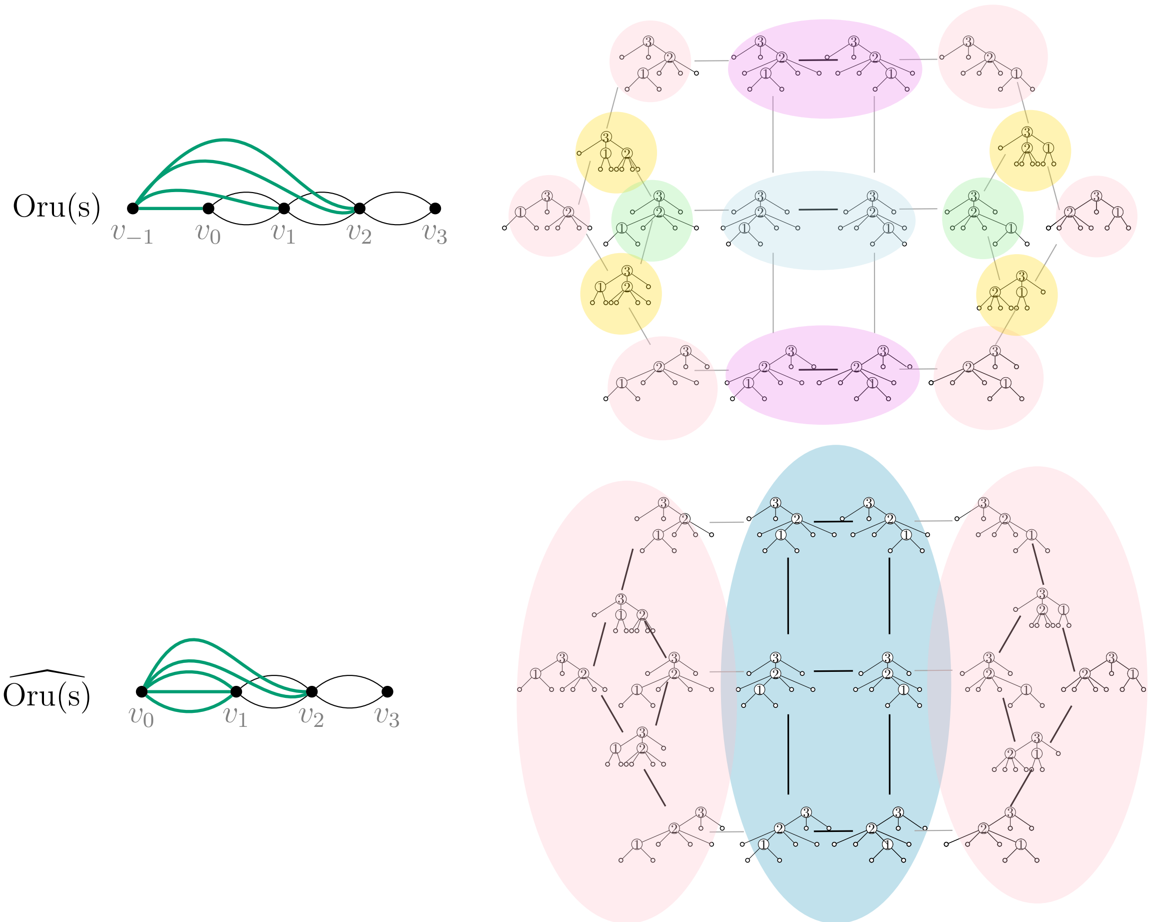

Figure 4.23: The framed graphs Oru(s) and $\widehat{\mathrm{Oru(s)}}$ and the associated Lidskii-type decompositions of the s-weak order for $s = (1, 3, 2)$. See Example 4.4.20.

dence that the pieces of the Lidskii-type decompositions are *intervals* of the s-weak order (particular case of Conjecture 4.2.25).

4.4.2 The sum of cubes realization

The Cayley trick, that we presented in Section 1.1.4, allows us to give another geometric realization of the s-permutahedron, as a fine mixed subdivision of a n-dimensional polytope (or even as a $(n-1)$-dimensional one). The Cayley trick was applied to flow polytopes by Mészáros and Morales in [MM19, Section 7]. We slightly adapt their work for our special case of the flow polytope $\boldsymbol{\mathcal{F}}_{\mathrm{Oru(s)}}$.

To apply the Cayley trick to our triangulation $\mathbf{Triang}_{DKK}(\mathrm{Oru(s)}, \preceq)$ of the flow polytope $\boldsymbol{\mathcal{F}}_{\mathrm{Oru(s)}}$, we need to describe it as the Cayley embedding of some lower-dimensional polytopes. Recall that $\boldsymbol{\mathcal{F}}_{\mathrm{Oru(s)}}$ lives in the space of edges of the graph Oru(s). We parameterize this space as $\mathbb{R}^p \times \mathbb{R}^{2n}$, where $p = 1+\sum_{i=1}^n (s_i - 1)$ and $\mathbb{R}^p$ corresponds to the space of source-edges and $\mathbb{R}^{2n}$ to the space of bumps and dips (edges of Oru_n, see Definition 4.4.1). Moreover, for all $i \in [n]$ and for any point in $\boldsymbol{\mathcal{F}}_{\mathrm{Oru(s)}}$, (i.e. a flow of Oru(s)), we have that the sum of its coordinates along edges e_0^i and $e_{s_i}^i$ is determined by the coordinates along the source-edges e_t^k for $k \in [i+1, n+1]$, $t \in [s_k - 1]$. Thus, $\boldsymbol{\mathcal{F}}_{\mathrm{Oru(s)}}$ is affinely equivalent to its projection on the space $\mathbb{R}^p \times \mathbb{R}^n$ where $\mathbb{R}^n$ corresponds to the space of edges e_0^i for $i \in [n]$.

With this parameterization, the indicator vector of the route of Oru(s) denoted $\mathrm{R}(k, t, \delta)$ (as in the discussion after Definition 4.4.1) with $k \in [n+1]$, $t \in [s_k - 1]$ and $\delta \in \{0, 1\}^{k-1}$ is:

$$e_t^k \times \sum_{i \in [k-1],\, \delta_i = 0} e_0^i.$$

Thus, if we denote by $\square_{k-1}$ these $(k-1)$-dimensional cubes with vertices $\{0,1\}^{k-1} \times 0^{n-k+1}$ embedded in $\mathbb{R}^n$, we see that $\boldsymbol{\mathcal{F}}_{\mathrm{Oru(s)}}$ is the Cayley embedding of $\square_n$ and $\square_{k-1}$ repeated $s_k - 1$ times for $k \in [n]$.

We denote by ***Subdiv***$_\square$(s) the fine mixed subdivision of the Minkowski sum of cubes $\square_n + \sum_{i=1}^n (s_i - 1)\square_{i-1} \subseteq \mathbb{R}^n$ obtained by intersecting the triangulation $\mathbf{Triang}_{DKK}(\mathrm{Oru(s)}, \preceq)$ (projected onto $\mathbb{R}^p \times \mathbb{R}^n$) with the subspace $\left\{\frac{1}{p}\right\}^p \times \mathbb{R}^n$.

The following theorem follows directly from the Cayley trick (Proposition 1.1.15), and the isomorphism between the face poset of $\mathrm{Perm_s}$ and the interior simplices of the DKK triangulation given in Theorem 4.4.15.

Theorem 4.4.22. *The face poset of the s-permutahedron* $\mathrm{Perm_s}$ *is isomorphic to the set of interior cells of* ***Subdiv***$_\square$(s) *ordered by reverse inclusion.*

In particular, the s-decreasing trees are in bijection with the maximal cells of **Subdiv**$_\square$(s).

Remark 4.4.23. We can use a different parameterization of the space where $\boldsymbol{\mathcal{F}}_{\mathrm{Oru(s)}}$ lives by considering the cube $\square_n$ as the Cayley embedding of two cubes $\square_{n-1}$, or equivalently by intersecting $\mathbb{R}^n$ with the hyperplane $x_n = \frac{1}{2}$. This allows us to lower the dimension and obtain a fine mixed subdivision of the Minkowski sum of cubes $(s_n+1)\square_{n-1} + \sum_{i=1}^{n-1}(s_i - 1)\square_{i-1}$. This is also what we would directly obtain if we considered the graph $\widehat{\mathrm{Oru(s)}}$, where the edge (v_{-1}, v_0) of Oru(s) is contracted (see Remark 4.4.2). We use this representation for the figures.

Figure 4.24a shows the mixed cell corresponding to the Stirling $(1,2,1)$-permutation $w = 3221$, obtained from the clique Δ_w with the Cayley trick. Figure 4.24b shows the entire mixed subdivision for the case $s = (1, 2, 1)$. Both figures are represented in the coordinate system (e_0^2, e_0^1).

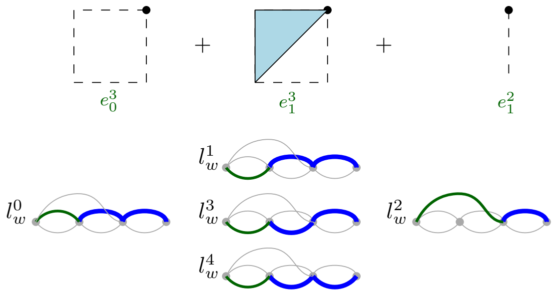

(a)

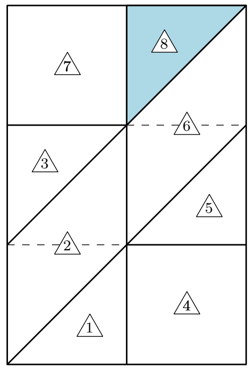

(b)

Figure 4.24: (a) Summands of the Minkowski cell corresponding to $w = 3221$ together with their corresponding routes in the clique Δ_w. (b) Mixed subdivision of $2\square_2 + \square_1$ corresponding dually to the $(1, 2, 1)$-permutahedron. The cells are numbered according to Figure 4.22. The highlighted cell in blue corresponds to $w = 3221$ as obtained in Figure 4.24a.

4.4.3 The tropical realization

In the two realizations that we provided in Sections 4.4.1 and 4.4.2, the s-decreasing trees index the maximal cells of a polytopal complex. However, Conjecture 4.1.1 asks for a polytopal complex where the s-decreasing trees index the vertices.

In this Section, we explain how tropical dualization and its interplay with the Cayley trick, that we presented in Section 1.2.2, allow us to obtain such a polytopal realization and fully answer the conjecture for strict compositions.

Before applying Theorem 1.2.10 to our mixed subdivision $\textbf{Subdiv}_\square(\mathrm{s})$, we explain how to obtain admissible lifting functions.

DKK admissible lifting functions

Danilov, Karzanov and Koshevoy provided explicit constructions of admissible lifting functions for the DKK triangulation of a flow polytope ([DKK12, Lemma 2 & 3]) that we can adapt to our particular graph Oru(s). Note that since their definition of regular subdivisions is in terms of upper faces (linearity areas of a concave function) we change the sign from their w to our ℓ. We slightly refine their results, using the notion of resolvents that we introduced in Definition 4.2.2.

Lemma 4.4.24 (adaptation of [DKK12, Lemma 2])**.** *Let $(G, \preceq)$ be a framed graph. A function ℓ from the routes of G to $\mathbb{R}$ is an admissible lifting function of $\textbf{Triang}_{DKK}(G, \preceq)$ if and only if:*

For any two non-coherent routes P and Q with resolvents P' and Q' we have:

$$\ell(P) + \ell(Q) > \ell(P') + \ell(Q'). \tag{4.9}$$

Proof. The original statement of [DKK12, Lemma 2] is that a weaker version of this condition, where P' and Q' are not necessarily the resolvents but can be any two routes that satisfy $P + Q = P' + Q'$, is sufficient. Let us show (with the same ideas as their proof) that it is also necessary and that we can even choose P', Q' to be the resolvents of P and Q. Suppose that ℓ is an admissible lifting function of $\mathbf{Triang}_{DKK}(G, \preceq)$ and let P, Q be two non-coherent routes of $(G, \preceq)$ with resolvents P', Q'. Since they form a clique, P' and Q' are the vertices of an edge of the DKK triangulation of $\boldsymbol{\mathcal{F}}_G$. The point $F = \frac{1}{2}(P + Q) = \frac{1}{2}(P' + Q')$ belongs to this edge. Since this edge as to be lifted to a lower face of the lift of the flow polytope $\boldsymbol{\mathcal{F}}_G$ given by the lifting function ℓ, which is admissible for $\mathbf{Triang}_{DKK}(G, \preceq)$, we necessarily have $\ell(P') + \ell(Q') < \ell(P) + \ell(Q)$. □

This statement can be made slightly stronger by restricting condition 4.9 to minimal conflicts.

Lemma 4.4.25. *Let $(G, \preceq)$ be a framed graph. A function ℓ from the routes of G to $\mathbb{R}$ is an admissible lifting function of $\boldsymbol{Triang}_{DKK}(G, \preceq)$ if and only if:*

For any minimal conflict between two routes P and Q with resolvents P' and Q', we have

$$\ell(P) + \ell(Q) > \ell(P') + \ell(Q'). \tag{4.10}$$

Proof. Let ℓ be a function from the routes of G to $\mathbb{R}$ such that for any minimal conflict between two routes P and Q with resolvents P' and Q', we have $\ell(P)+\ell(Q) > \ell(P')+\ell(Q')$. It follows from Lemma 4.4.24 that we only need to show that for any two non-coherent routes P and Q, there exist routes P' and Q' such that $P+Q = P'+Q'$ and $\ell(P)+\ell(Q) > \ell(P') + \ell(Q')$.

First, suppose that P and Q are conflicting at exactly one subroute $[v_i, v_j]$. We can build partial routes $R_1 = Pv_i, R_2, \dots, R_k = Qv_i$ that end at v_i and such that $R_1 \prec R_2 \prec \dots \prec R_k$, their ending edges are adjacent in $\preceq_{In_i}$ and they are not in conflict. This can be done by building these partial routes from right to left: the ending edge is determined and we can choose the other ones as we want but if we arrive at a vertex common to a previously built partial route we choose the same edges as in this partial route. Similarly we can build partial routes $S_1 = v_jQ, S_2, \dots, S_t = v_jP$ that start at v_j and such that $S_1 \prec S_2 \prec \dots \prec S_t$, their starting edges are adjacent in $\preceq_{Out_j}$ and they are not in conflict. Then for any $x \in [k-1]$, $y \in [t-1]$ the routes $R_xv_iPv_jS_{y+1}$ and $R_{x+1}v_iPv_jS_y$ are in minimal conflict, with resolvents $R_xv_iPv_jS_y$ and $R_{x+1}v_iPv_jS_{y+1}$. Hence the condition on ℓ implies the following inequality:

$$\ell(R_xv_iPv_jS_{y+1}) + \ell(R_{x+1}v_iPv_jS_y) > \ell(R_xv_iPv_jS_y) + \ell(R_{x+1}v_iPv_jS_{y+1}). \tag{$W_{x,y}$}$$

When we sum all these inequalities for all $x \in [k-1]$, $y \in [t-1]$ we see that all terms of the form $\ell(R_xv_iPv_jS_y)$ are cancelled out by pairs, except for $(x, y) \in \{(1, 1), (k, t), (1, t), (k, 1)\}$.

We end up with:

$$\ell(R_1 v_i P v_j S_t) + \ell(R_k v_i P v_j S_1) > \ell(R_1 v_i P v_j S_1) + \ell(R_k v_i P v_j S_t),$$

which is exactly $\ell(P) + \ell(Q) > \ell(P') + \ell(Q')$, where P' and Q' are the resolvents of P, Q.

Now, we can finish the proof by induction on the number of conflicts. Suppose that ℓ satisfies that for any pair of non-coherent routes P and Q with at most n conflicts their resolvents P', Q' satisfy $\ell(P) + \ell(Q) > \ell(P') + \ell(Q')$. Let P and Q be non-coherent routes with $n+1$ conflicts at subroutes $[x_1, y_1], \ldots, [x_{n+1}, y_{n+1}]$. Since the routes P and Px_1Q have n conflicts and their resolvents are $Px_1P' = P'$ and Px_1Q', the induction hypothesis gives us:

$$\ell(P) + \ell(Px_1Q) > \ell(P') + \ell(Px_1Q').$$

Similarly we have:

$$\ell(Q) + \ell(Qx_1P) > \ell(Qx_1P') + \ell(Q').$$

Moreover, the routes P and Qx_1P' only have one conflict and their resolvents are P' and Qx_1P, so we have

$$\ell(P) + \ell(Qx_1P') > \ell(P') + \ell(Qx_1P),$$

and similarly:

$$\ell(Q) + \ell(Px_1Q') > \ell(Px_1Q) + \ell(Q').$$

When we sum up these four inequalities, some terms cancel out and we recover:

$$\ell(P) + \ell(Q) > \ell(P') + \ell(Q'). \qquad \square$$

Recall that the routes of $\mathrm{Oru}(\mathrm{s})$ are denoted $\mathrm{R}(k, t, \delta)$ as in the discussion after Definition 4.4.1. Adapting [DKK12, Lem 3] to our context gives us the following lemma.

Lemma 4.4.26. *Let* s *be a composition and $\varepsilon > 0$ a sufficiently small real number. Consider ℓ_ε to be the function that associates to a route $\mathrm{R} = \mathrm{R}(k, t_k, \delta)$ of $\mathrm{Oru}(\mathrm{s})$ the quantity*

$$\ell_\varepsilon(\mathrm{R}) = -\sum_{k \geq c > a \geq 1} \varepsilon^{c-a}(t_c + \delta_a)^2, \tag{4.11}$$

where $t_c = \begin{cases} 0 & \text{if } \delta_c = 0, \\ s_c & \text{if } \delta_c = 1, \end{cases}$ *for all* $c \in [k-1]$.

Then ℓ_ε is an admissible lifting function for $\textbf{Triang}_{DKK}(\mathrm{Oru}(\mathrm{s}), \preceq)$.

Proposition 4.4.27. *In Lemma 4.4.26, it is enough to take $\varepsilon < \frac{1}{n(1+\sum_{j=2}^{n}(2s_j+1))}$.*

Proof. Let $P = \mathrm{R}(k, t, \delta)$ and $Q = \mathrm{R}(k', t', \delta')$ be two routes of $\mathrm{Oru}(\mathrm{s})$ that are in minimal conflict at a common route $[v_{n+1-y}, v_{n-x}]$. We can suppose that $Pv_{n+1-y} \prec Qv_{n+1-y}$. Note that this implies that $\delta_x = 1$ and $\delta'_x = 0$. We deal separately with the three following cases (which are the only possible ones for a minimal conflict) and compute the quantity $H := \ell_\varepsilon(P) + \ell_\varepsilon(Q) - \ell_\varepsilon(P') - \ell_\varepsilon(Q')$.

Case 1: $k = k' = y$**,** $t \in [s_y - 2]$**,** $t' = t + 1$**.**

In the computation of $\ell_\varepsilon(P) + \ell_\varepsilon(Q) - \ell_\varepsilon(P') - \ell_\varepsilon(Q')$, we see that all pairs (a, c) in formula 4.11 cancel out either with $\ell_\varepsilon(P) - \ell_\varepsilon(Q')$ or $\ell_\varepsilon(Q) - \ell_\varepsilon(P')$, except for $(a, c) = (x, y)$. Thus we have:

$$\begin{aligned} H &= \ell_\varepsilon(P) + \ell_\varepsilon(Q) - \ell_\varepsilon(P') - \ell_\varepsilon(Q') \\ &= -\varepsilon^{y-x}\Big((t+1)^2 + ((t+1)+0)^2 - (t+0)^2 - ((t+1)+1)^2\Big) \\ &= 2\ \varepsilon^{y-x} > 0. \end{aligned}$$

Case 2: $k > k' = y$**,** $\delta_y = 0$**,** $t' = 1$**.**

Here the pairs that do not cancel out are all pairs (a, c) for $k \geq c \geq y$ and $x \geq a$. Then we have:

$$\begin{aligned} H &= -\sum_{x \geq a} \varepsilon^{y-a}\Big(\delta_a^2 + (1 + \delta'_a)^2 - {\delta'_a}^2 - (1 + \delta_a)^2\Big) - \sum_{k \geq c > y,\ x \geq a} \varepsilon^{c-a}\Big((t_c + \delta_a)^2 - (t_c + \delta'_a)^2\Big) \\ &= 2\ \varepsilon^{y-x} - 2\ \sum_{x > a} \varepsilon^{y-a}(\delta'_a - \delta_a) - \sum_{k \geq c > y,\ x \geq a} \varepsilon^{c-a}\Big(2\ t_c(\delta_a - \delta'_a) + \delta_a^2 - {\delta'_a}^2\Big) \\ &\geq 2\ \varepsilon^{y-x} - 2\ \sum_{x > a} \varepsilon^{y-a} - \sum_{k \geq c > y,\ x \geq a} \varepsilon^{c-a}(2s_c + 1) \\ &\geq 2\ \varepsilon^{y-x} - 2\ \varepsilon^{y-x+1}\Big(x - 1 + x \sum_{k \geq c > y} (2s_c + 1)\Big) \\ &\geq 2\ \varepsilon^{y-x}\Big(1 - \varepsilon\Big(y - 2 + (y-1) \sum_{k \geq c > y} (2s_c + 1)\Big)\Big) \end{aligned}$$

Then, we see that if $\varepsilon < \frac{1}{n(1 + \sum_{j=2}^{n}(2s_j + 1))}$, then for any $y \in [2, n]$ we have

$$1 - \varepsilon\Big(y - 2 + (y-1) \sum_{k \geq c > y} (2s_c + 1)\Big) > 0,$$

thus $H > 0$.

Case 3: $k' > k = y$**,** $t = s_y - 1, \delta'_y = 1$**.** Here again, the pairs that do not cancel out are all pairs (a, c) for $k \geq c \geq y$ and $x \geq a$ and we have:

$$\begin{aligned} H = &- \sum_{x \geq a} \varepsilon^{y-a}\Big((s_y - 1 + \delta_a)^2 + (s_y + \delta'_a)^2 - (s_y - 1 + \delta'_a)^2 - (s_y + \delta_a)^2\Big) \\ &- \sum_{k \geq c > y,\ x \geq a} \varepsilon^{c-a}\Big((t'_c + \delta'_a)^2 - (t'_c + \delta_a)^2\Big) \\ = &\ 2\ \varepsilon^{y-x} + 2 \sum_{x > a} \varepsilon^{y-a}(\delta'_a - \delta_a) - \sum_{k \geq c > y,\ x \geq a} \varepsilon^{c-a}\Big(2\ t'_c(\delta'_a - \delta_a) + {\delta'_a}^2 - \delta_a^2\Big), \end{aligned}$$

and the rest of the computations are very similar to the Case 2. □

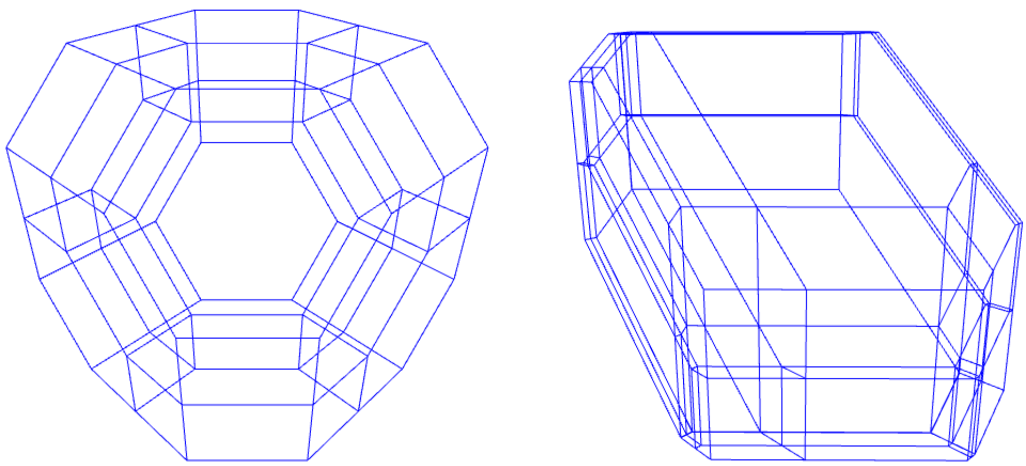

Figure 4.25: The $(1,1,1,2)$-permutahedron (left) and the $(1,2,2,2)$-permutahedron (right) via their tropical realization.

Coordinates for the s-permutahedron

For the remainder of this section s is assumed to be a composition and ℓ an admissible lifting function for $\mathbf{Triang}_{DKK}(\mathrm{Oru}(\mathrm{s}), \preceq)$.

Since we defined in Section 4.4.2 the mixed subdivision $\mathbf{Subdiv}_\square(\mathrm{s})$ from the regular triangulation $\mathbf{Triang}_{DKK}(\mathrm{Oru}(\mathrm{s}), \preceq)$ via the Cayley trick, the following theorem directly follows from Theorem 1.2.10.

Theorem 4.4.28. *The tropical dual of the mixed subdivision* $\mathbf{Subdiv}_\square(\mathrm{s})$ *is the polyhedral complex of cells induced by the arrangement of tropical hypersurfaces*

$$\mathcal{H}_\mathrm{s}(\ell) := \left\{ \mathcal{T}(F_t^k) \mid k \in [2, n+1],\ t \in [s_k - 1] \right\},$$

where $F_t^k(\boldsymbol{x}) = \bigoplus \ell(\mathrm{R}(k,t,\delta)) \odot \boldsymbol{x}^\delta = \min\left\{ \ell(\mathrm{R}(k,t,\delta)) + \sum_{i\in[k-1]} \delta_i x_i \mid \delta \in \{0,1\}^{k-1} \right\}.$

Definition 4.4.29. We denote by $\boldsymbol{Perm}_\mathrm{s}(\ell)$ the polyhedral complex of bounded cells induced by the arrangement $\mathcal{H}_\mathrm{s}(\ell)$.

Theorem 4.4.30. *The face poset of the geometric polyhedral complex* $\boldsymbol{Perm}_\mathrm{s}(\ell)$ *is isomorphic to the face poset of the combinatorial* s*-permutahedron* Perm_s.

Proof. We showed in Theorem 4.4.22 that the face poset of Perm_s is anti-isomorphic to the face poset of interior cells of the mixed subdivision $\mathbf{Subdiv}_\square(\mathrm{s})$. It then follows from Lemma 1.2.9 and Theorem 4.4.28 that this poset is isomorphic to the poset of bounded cells of $\mathcal{H}_\mathrm{s}(\ell)$, which is the face poset of $\mathbf{Perm}_\mathrm{s}(\ell)$. □

Figure 4.25 shows some examples of such realizations of the s-permutahedron.

Moreover, we can describe the explicit coordinates of the vertices of $\mathbf{Perm}_{\mathrm{s}}(\ell)$. For a Stirling s-permutation w, $a \in [n]$ and $t \in [s_a]$, we denote $i(a^t)$ the length of the prefix of w that precedes the t-th occurrence of a. As explained in the argument leading to Lemma 4.4.6, this prefix is associated to the route $\mathrm{R}[w_{[i(a^t)]}]$ in the clique Δ_w.

Theorem 4.4.31. *The vertices of $\boldsymbol{Perm}_{\mathrm{s}}(\ell)$ are in bijection with Stirling* s*-permutations. Moreover, the vertex $\boldsymbol{v}(w) = (\boldsymbol{v}(w)_a)_{a\in[n]}$ associated to a Stirling* s*-permutation w has coordinates*

$$\boldsymbol{v}(w)_a = \sum_{t=1}^{s_a} \big(\ell(\mathrm{R}[w_{[i(a^t)]}]) - \ell(\mathrm{R}[w_{[i(a^t)+1]}])\big)\,. \tag{4.12}$$

Proof. The bijection between vertices of $\mathbf{Perm}_{\mathrm{s}}(\ell)$ and Stirling s-permutations is a direct consequence of Theorem 4.4.30.

Let w be a Stirling s-permutation. It is associated via Theorem 4.4.28 to the intersection of all regions of the form

$$\Big\{\boldsymbol{x} \in \mathbb{R}^n \;\Big|\; \ell(\mathrm{R}(c,t,\delta)) + \sum_{a\in[c-1]} \delta_a x_a = \min_{\theta\in\{0,1\}^{c-1}} \{\ell(\mathrm{R}(c,t,\theta)) + \sum_{a\in[c-1]} \theta_a x_a\}\Big\}, \tag{4.13}$$

where $\mathrm{R}(c,t,\delta)$ is a route in the clique Δ_w. It follows from the previous remark that this intersection is a single point, that we denote $\boldsymbol{v}$. We show that $\boldsymbol{v}$ necessarily has the coordinates given by the theorem. Let $a \in [n]$. Both routes $\mathrm{R}[w_{[i(a^1)]}]$ and $\mathrm{R}[w_{[i(a^{s_a})+1]}]$ are of the form $\mathrm{R}(c,t,\delta)$ and $\mathrm{R}(c,t,\delta')$ respectively, where c is the smallest letter such that the a-block is contained in the c-block in w, and t denotes the number of occurrences of c that precedes the a-block. If the a-block is contained in no other block we set $c = n+1$ and $t = 1$. The indicator vectors δ and δ' satisfy that $\delta' - \delta$ is the indicator vector of the letters $b \le a$ such that the b-block is contained in the a-block in w. The fact that both routes belong to Δ_w implies that $\ell(\mathrm{R}[w_{[i(a^1)]}]) + \sum_{b\in[c-1]} \delta_b v_b = \ell(\mathrm{R}[w_{[i(a^{s_a})+1]}]) + \sum_{b\in[c-1]} \delta'_b v_b$, thus

$$\sum_{\substack{b\in[a] \text{ s.t.}\\ b\text{-block} \subseteq a\text{-block}}} v_b = \ell(\mathrm{R}[w_{[i(a^1)]}]) - \ell(\mathrm{R}[w_{[i(a^{s_a})+1]}]).$$

Then, we obtain Equation 4.12 by induction on a. Indeed, if the equation is true for all $b < a$, then all terms in $\sum_{\substack{b\in[a-1] \text{ s.t.}\\ b\text{-block} \subset a\text{-block}}} v_b$ cancel by pairs except the terms that correspond to a prefix ending at or just before an occurrence of a in w, which are of the form $-\ell(\mathrm{R}[w_{[i(a^r)]}])$ for $r \in [2, s_a]$ or $\ell(\mathrm{R}[w_{[i(a^r)+1]}])$ for $r \in [s_a - 1]$. $\square$

Corollary 4.4.32. *The* s*-permutahedron $\boldsymbol{Perm}_{\mathrm{s}}(\ell)$ is contained in the hyperplane*

$$\left\{\boldsymbol{x} \in \mathbb{R}^n \;\middle|\; \sum_{i=1}^{n} x_i = \ell(\mathrm{R}(n+1,1,(0)^n) - \ell(\mathrm{R}(n+1,1,(1)^n))\right\}. \tag{4.14}$$

Theorem 4.4.33. *Let $1 \leq a < c \leq n$. Let w and w' be Stirling* s*-permutations of the form $u_1 B_a c u_2$ and $u_1 c B_a u_2$ respectively, where B_a is the a-block of w and w'.*

Then the edge of $\boldsymbol{Perm}_{\mathrm{s}}(\ell)$ corresponding to the transposition between w and w' is:

$$\boldsymbol{v}(w') - \boldsymbol{v}(w) = (\ell(\mathrm{R}[u_1 c]) + \ell(\mathrm{R}[u_1 B_a]) - \ell(\mathrm{R}[u_1]) - \ell(\mathrm{R}[u_1 B_a c]))\,(\boldsymbol{e}_a - \boldsymbol{e}_c), \tag{4.15}$$

where $(\boldsymbol{e}_i)_{i\in[n]}$ is the canonical basis of $\mathbb{R}^n$.

Proof. We denote $t := \#_w(c,a) + 1$, so that the transposition from w to w' exchanges the a-block with the t-th occurrence of c. We use the expression of the explicit coordinates given in Theorem 4.4.31 to compute $\boldsymbol{v}(w') - \boldsymbol{v}(w)$. The only routes that do not cancel out are the ones corresponding to prefixes u_1, $u_1 c$, $u_1 B_a$ and $u_1 B_a c$, which gives the same route as $u_1 c B_a$. Indeed, a prefix contained in u_1 is common to w and w' ; a prefix that ends inside the a-block does not give information on c, so the corresponding route will be common to w and w', and a prefix that ends inside u_2 does not give information on the relative order of the a-block and letter c, so the corresponding route will also be common to w and w'. Hence:

$$\begin{aligned}
\boldsymbol{v}(w') - \boldsymbol{v}(w) &= (\boldsymbol{v}(w')_a - \boldsymbol{v}(w)_a)\,\boldsymbol{e}_a + (\boldsymbol{v}(w')_c - \boldsymbol{v}(w)_c)\,\boldsymbol{e}_c \\
&= \big(\ell(\mathrm{R}[w'_{[i(a^1)]}]) - \ell(\mathrm{R}[w'_{[i(a^{s_a})+1]}]) - \ell(\mathrm{R}[w_{[i(a^1)]}]) + \ell(\mathrm{R}[w_{[i(a^{s_a})+1]}])\big)\,\boldsymbol{e}_a \\
&\quad + \big(\ell(\mathrm{R}[w'_{[i(c^t)]}]) - \ell(\mathrm{R}[w'_{[i(c^t)+1]}]) - \ell(\mathrm{R}[w_{[i(c^t)]}]) + \ell(\mathrm{R}[w_{[i(c^t)+1]}])\big)\,\boldsymbol{e}_c \\
&= (\ell(\mathrm{R}[u_1 c]) - \ell(\mathrm{R}[u_1 c B_a]) - \ell(\mathrm{R}[u_1]) + \ell(\mathrm{R}[u_1 B_a]))\,\boldsymbol{e}_a \\
&\quad + (\ell(\mathrm{R}[u_1]) - \ell(\mathrm{R}[u_1 c]) - \ell(\mathrm{R}[u_1 B_a]) + \ell(\mathrm{R}[u_1 B_a c]))\,\boldsymbol{e}_c \\
&= (\ell(\mathrm{R}[u_1 c]) + \ell(\mathrm{R}[u_1 B_a]) - \ell(\mathrm{R}[u_1]) - \ell(\mathrm{R}[u_1 B_a c]))\,(\boldsymbol{e}_a - \boldsymbol{e}_c).
\end{aligned}$$

It follows from Lemma 4.4.25 that we have

$$\ell(\mathrm{R}[u_1 c]) + \ell(\mathrm{R}[u_1 B_a]) - \ell(\mathrm{R}[u_1]) - \ell(\mathrm{R}[u_1 B_a c]) > 0,$$

since $P := \mathrm{R}[u_1 B_a]$ and $Q := \mathrm{R}[u_1 c]$ are in minimal conflict at $[v_{n+1-c}, v_{n+1-a}]$ and $P' := \mathrm{R}[u_1]$ and $Q' := \mathrm{R}[u_1 B_a c]$ are their resolvents. □

Lemma 4.4.34. *For any strictly decreasing sequence of real numbers $\kappa_1 > \ldots > \kappa_n$, if we orient the edges of $\boldsymbol{Perm}_{\mathrm{s}}(\ell)$ according to the direction $\sum_{i=1}^n \kappa_i \boldsymbol{e}_i$ we recover the Hasse diagram of the* s*-weak order.*

Proof. This is a direct consequence of Theorem 4.4.33 and the remark at the end of its proof. □

Lemma 4.4.35. *The support supp$(\boldsymbol{Perm}_{\mathrm{s}}(\ell))$, i.e. the union of faces of $\boldsymbol{Perm}_{\mathrm{s}}(\ell)$, is a polytope combinatorially isomorphic to the $(n-1)$-dimensional permutahedron. More precisely it has:*

1. *vertices $\boldsymbol{v}(w^\sigma)$ for all permutation σ of $[n]$ where w^σ is the Stirling* s*-permutation*

$$w^\sigma = \underbrace{\sigma(1)\ldots\sigma(1)}_{s_{\sigma(1)}\text{ times}}\ldots\underbrace{\sigma(n)\ldots\sigma(n)}_{s_{\sigma(n)}\text{ times}},$$

2. *facet defining inequalities*

$$\langle \delta, \boldsymbol{x} \rangle \geq \ell(\mathrm{R}(n+1, 1, (0)^n)) - \ell(\mathrm{R}(n+1, 1, \delta)), \tag{4.16}$$

$$\langle \mathbf{1} - \delta, \boldsymbol{x} \rangle \leq \ell(\mathrm{R}(n+1, 1, \delta)) - \ell(\mathrm{R}(n+1, 1, (1)^n)), \tag{4.17}$$

for all $\delta \in \{0,1\}^n$.

Proof. 1. Let σ be a permutation of $[n]$. we consider the linear functional $f(x) = \sum_{a \in [n]} \sigma(a) x_a$. Among the vertices of $\mathbf{Perm}_{\mathrm{s}}(\ell)$, f is maximized on $\boldsymbol{v}(w^\sigma)$. Indeed, let w' be a Stirling s-permutation.

- If w' contains an ascent (a, c) such that $\sigma(a) > \sigma(c)$, then f is increasing along the edge of direction $\boldsymbol{e}_a - \boldsymbol{e}_c$ corresponding to the transposition of w' along the ascent (a, c).
- If w' contains a descent (c', a') such that $\sigma(a') < \sigma(c')$, then f is increasing along the edge of direction $\boldsymbol{e}_{c'} - \boldsymbol{e}_{a'}$ corresponding to the transposition of w' along the descent (c', a').
- If w' is in neither of the above cases, than necessarily $w' = w^\sigma$.

This shows that the vertices of $\mathrm{supp}(\mathbf{Perm}_{\mathrm{s}}(\ell))$ have the same normal cones as the $(n-1)$-permutahedron (embedded in $\mathbb{R}^n$), hence its normal fan is the braid fan.

2. It follows from the fact that all cliques Δ_w contain the routes $\mathrm{R}(n+1, 1, (0)^n)$ and $\mathrm{R}(n+1, 1, (1)^n)$ (see the remark before Lemma 4.4.6) that all vertices of $\mathbf{Perm}_{\mathrm{s}}(\ell)$ are contained in the region

$$\Big\{ \boldsymbol{x} \in \mathbb{R}^n \;\Big|\; \ell(\mathrm{R}(n+1, 1, (0)^n)) = \ell(\mathrm{R}(n+1, 1, (1)^n)) + \sum_{a \in [n]} x_a$$
$$= \min_{\theta \in \{0,1\}^n} \{ \ell(\mathrm{R}(n+1, 1, \theta)) + \sum_{a \in [n]} \theta_a x_a \} \Big\}.$$

This region is exactly defined by intersecting the half-spaces defined by 4.16 and 4.17.

Moreover, let $\delta \in \{0,1\}^n$ and $I := \{ i \in [n] \mid \delta_i = 1 \}$. The equality in 4.16 and 4.17 is achieved exactly on vertices $\boldsymbol{v}(w^\sigma)$ where $\{\sigma(1), \ldots, \sigma(|I|)\} = I$. Hence, these inequalities define the facets of $\mathrm{supp}(\mathbf{Perm}_{\mathrm{s}}(\ell))$.

□

Remark 4.4.36. With similar arguments we can see that the restriction of the s-weak order to a face of $\mathrm{supp}(\mathbf{Perm}_{\mathrm{s}}(\ell))$, associated to an ordered partition, will correspond to a product of s′-weak orders, one for each part of the ordered partition.

Note that Lemma 4.4.35 finishes to answer Conjecture 4.1.1 in the case where s is a composition, because then the zonotope $\sum_{1 \leq i < j \leq n} s_j [\boldsymbol{e}_i, \boldsymbol{e}_j]$ is combinatorially isomorphic to the $(n-1)$-dimensional permutahedron.

In the case where ℓ is given by Lemma 4.4.26, we can even go a bit further.

Proposition 4.4.37. *Let $\varepsilon > 0$ be a small enough real number so that ℓ_ε is an admissible lifting function for $\boldsymbol{Triang}_{DKK}(\mathrm{Oru}(\mathrm{s}), \preceq)$.*

Then the support $\mathrm{supp}(\boldsymbol{Perm}_{\mathrm{s}}(\ell_\varepsilon))$ is a translation of the zonotope $2\sum_{1\leq a<c\leq n} s_c\, \varepsilon^{c-a}[\boldsymbol{e}_a, \boldsymbol{e}_c]$.

Proof. It follows from Lemma 4.4.35 that the edges of $\mathrm{supp}(\mathbf{Perm}_{\mathrm{s}}(\ell_\varepsilon))$ are of the form $[\boldsymbol{v}(w^\sigma), \boldsymbol{v}(w^{\sigma'})]$, where σ and σ' are permutations of $[n]$ related by a transposition along an ascent (a, c). When we plug the expression 4.11 of ℓ_ε into the formula 4.15, where the letter c is replaced by s_c occurrences of c, we see that the only terms that do not cancel out are those involving the pair (a, c):

$$\begin{aligned}\boldsymbol{v}(w^{\sigma'}) - \boldsymbol{v}(w^\sigma) &= -\varepsilon^{c-a}\Big((0+1)^2 + (s_c+0)^2 - (0+0)^2 - (s_c+1)^2\Big)(\boldsymbol{e}_a - \boldsymbol{e}_c)\\ &= 2\; s_c\; \varepsilon^{c-a}(\boldsymbol{e}_a - \boldsymbol{e}_c).\end{aligned}$$

Hence all edges of the same direction have the same length, and since $\mathrm{supp}(\mathbf{Perm}_{\mathrm{s}}(\ell_\varepsilon))$ is combinatorially equivalent to a permutahedron, it follows that it is a zonotope. $\square$

4.5 Perspectives on geometric realizations of the quotients of the s-weak order

In this section, we sketch briefly the directions that we worked on recently, which deal with Ceballos and Pons second conjecture and more generally with geometric realizations for lattice quotients of the s-weak order.

We first provide some background about lattice quotients, and some elements related to lattice quotients of the weak order.

4.5.1 Background on lattice quotients of the weak order

Let $(X, \preceq)$ be a lattice.

A *join irreducible* element in X is an element that covers exactly one other element of X.

A *canonical join representation* of an element $y \in X$ is a way to write $y = \bigvee J$ that is irredundant (there is no $J' \subsetneq J$ such that $y = \bigvee J'$) and minimal (for any other $J' \subseteq X$ such that $y = \bigvee J'$, we have that for any element $x \in J$ there is $x' \in J'$ such that $x \preceq x'$). Such a J is an antichain of join irreducible elements.

A *lattice congruence* on the lattice X is an equivalence relation $\equiv$ on X which respects $\vee$ and $\wedge$: for any $x_1, x_2, y_1, y_2 \in X$ such that $x_1 \equiv x_2$ and $y_1 \equiv y_2$ we have $x_1 \vee y_1 \equiv x_2 \vee y_2$ and $x_1 \wedge y_1 \equiv x_2 \wedge y_2$.

The *lattice quotient* of X by $\equiv$ is then the lattice $X/\equiv$ whose elements are the equivalence classes of $\equiv$ with the order $A \preceq B$ if and only if there are $a \in A$, $b \in B$ such that $a \preceq b$.

A lattice X is *semidistributive* if for any $x, y, z \in X$, $x \vee y = x \vee z$ implies $x \vee (y \wedge z) = (x \vee y) \wedge (x \vee z)$ and $x \wedge y = x \wedge z$ implies $x \wedge (y \vee z) = (x \wedge y) \vee (x \wedge z)$.

A semidistributive lattice X has the following special properties:

- Any $y \in X$ admits a *canonical join representation* with join irreducible elements.
- To describe a lattice quotient it is sufficient to know which of the join irreducible elements are *contracted* (i.e. they are not the minimal element in their equivalence class).

Figure 4.26 depicts the sylvester congruence on the weak order on $\mathfrak{S}_4$, whose corresponding lattice quotient is the Tamari lattice.

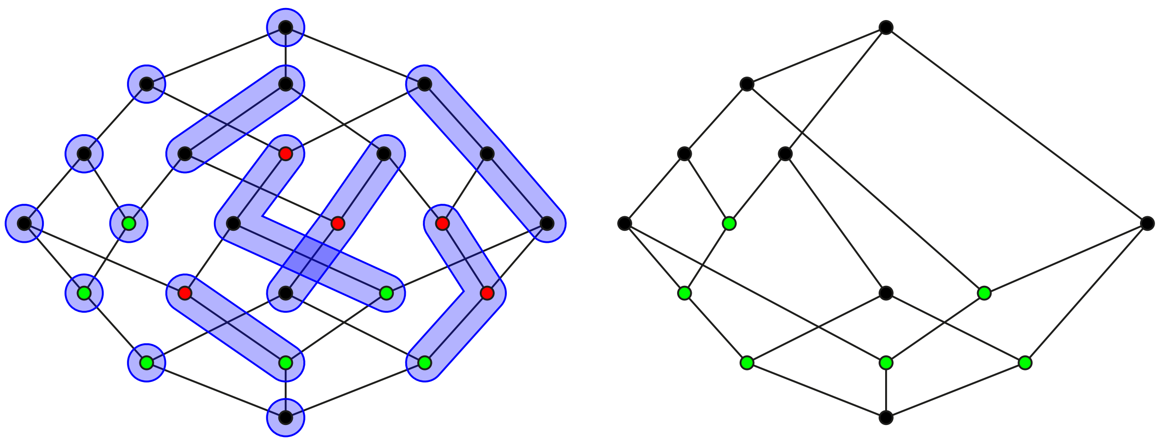

Figure 4.26: Example of lattice quotient: from the weak order (left) to the Tamari lattice (right). The join irreducible elements of the weak order are colored in red if they are contracted by the sylvester congruence or in green if they are preserved. Figure from Vincent Pilaud.

Lattice quotients of the weak order on $\mathfrak{S}_n$ were extensively studied by Nathan Reading in [Rea05, Rea04, Rea15]. In [Rea05], he proves that for any lattice congruence $\equiv$ of the weak order, the operation of gluing together the cones of the braid fan that belong to the same congruence class still defines a complete fan, called the *quotient fan* of $\equiv$, whose dual graph gives the Hasse diagram of the lattice quotient $\mathfrak{S}_n/\equiv$. He provides a way to build the quotient fan of $\equiv$ by associating to each join irreducible element α of the weak order an $(n-1)$-dimensional cone $S(\alpha)$, called the *shard* of α. The quotient fan of $\equiv$ is then obtained by taking the union of all shards $S(\alpha)$ for the join irreducible elements α that are not contracted by the congruence $\equiv$. In [Rea15], Reading gives a handy combinatorial model for the join irreducible elements of the weak order in terms of *arcs*, such that the canonical join representations correspond to *non-crossing arc diagrams*. See examples on the left of Figure 4.27.

Pilaud and Santos ([PS19]) showed that the quotient fan of $\equiv$ is the normal fan of a polytope, called a *quotientope*. Padrol, Pilaud and Ritter ([PPR23]) provided a simpler realization of quotientopes as Minkowski sums of elementary polytopes $\boldsymbol{SP}(\alpha)$, called the *shard polytopes*. See examples on the right of Figure 4.27.

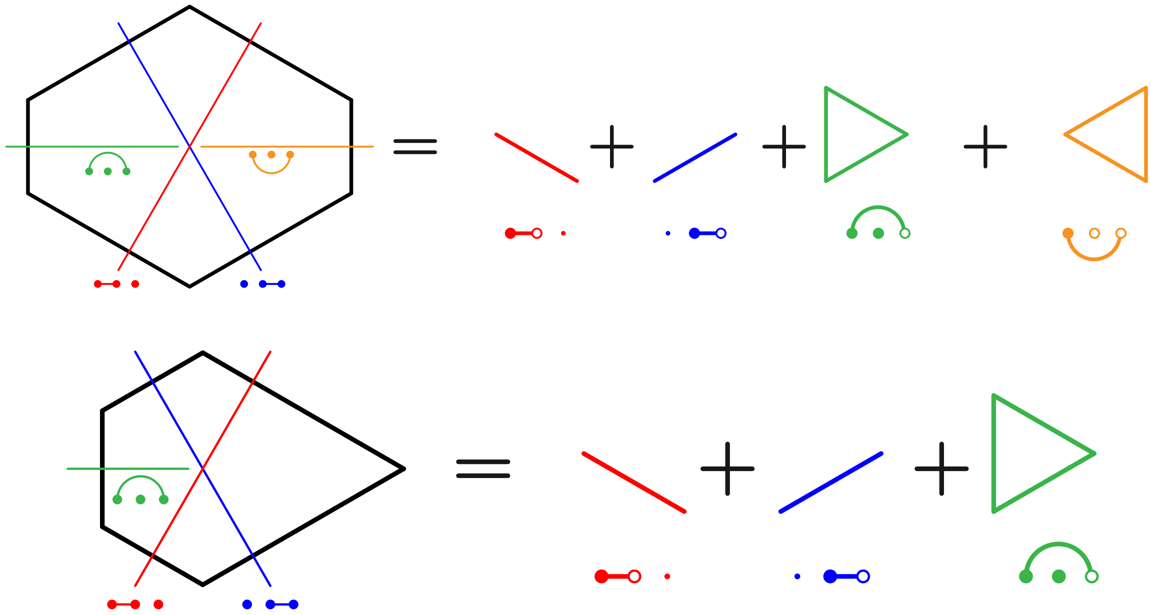

Figure 4.27: Quotient fans of the trivial (above) and sylvester (below) congruences on the weak order on $\mathfrak{S}_3$ and the corresponding Minkowski sums of shard polytopes. Each shard and shard polytope is indexed by the arc of the join irreducible of the weak order it corresponds to. Figures from Vincent Pilaud.

Among all lattice congruences of the weak order, a special family was identified by Pilaud and Pons [PP18] under the name *permutrees*, which interpolates the weak order, the Tamari lattice, the boolean lattice, and contains all the Cambrian lattices ([Rea06]). These congruences are obtained by choosing which join irreducible elements of rank 2 are contracted or not. They are indexed by a parameter $\delta \in \{⦶, Ⓨ, ⓐ, ⊗\}^{n-2}$ and can be described as a poset on combinatorial objects called *δ-permutrees*. Their Hasse diagram can be realized as the edge-graph of polytopes called *δ-permutreehedra*, which have the special property that they are the only quotientopes that can be obtained from the standard permutahedron by removing facets ([PP18, CPS21]).

4.5.2 Towards realizations of the s-quotientoplexes via s-shardoplexes

In [PP24], with Vincent Pilaud we recently generalized these constructions for the s-weak order, which is also a semidistributive lattice ([CP22, Proposition 1.37]).

We define s-arcs and s-shards to model the join-irreducible elements of the s-weak order. The union of all s-shards does not define a fan anymore, but a polyhedral complex that covers $\mathbb{R}^n$ with set of vertices V, and that we call the *s-foam*. See Figure 4.28 for an example with $s = (1, 2, 1)$, where the polyhedral complex has two vertices $\{v_1, v_2\}$ (in gray).

Then, we associate to each s-arc α a collection of polytopes $\{\boldsymbol{Sh}(\alpha)_v\}_{v\in V}$ where each

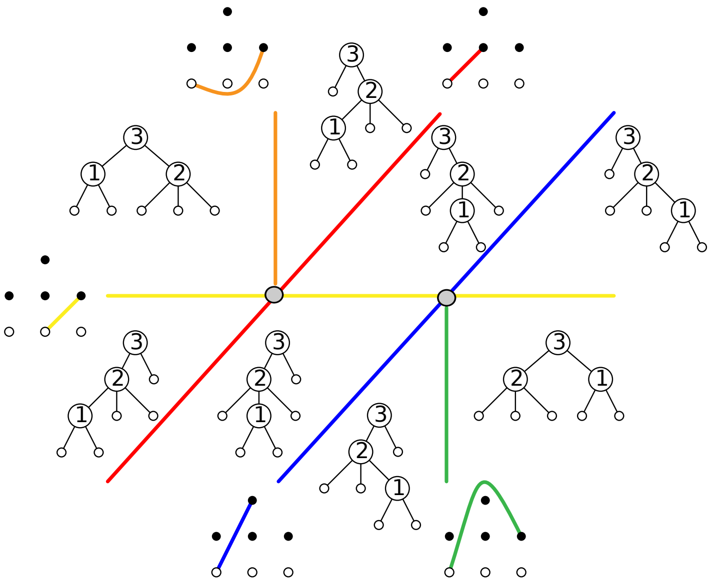

Figure 4.28: $(1,2,1)$-foam. The shards are indexed by their corresponding $(1,2,1)$-arc. The 2-cells are indexed by the $(1,2,1)$-decreasing trees. Figure from Vincent Pilaud.

$\boldsymbol{Sh}(\alpha)_v$ is a shard polytope or a face of it. These polytopes form a polytopal complex that we call the *α-shardoplex*.

Let $\equiv$ be a lattice congruence of the s-weak order, $L_\equiv$ the corresponding lattice quotient and $A_\equiv$ the set of join-irreducible elements of the s-weak order that are not contracted by $\equiv$. Then we have that:

- the graph dual to the polyhedral complex defined by the s-shards $S(\alpha)$ for $\alpha \in A_\equiv$ (called the *quotient foam*) gives the Hasse diagram of $L_\equiv$,
- the polytopes $\{\sum_{\alpha\in A_\equiv} \boldsymbol{Sh}(\alpha)_v\}_{v\in V}$ are the maximal cells of a polytopal complex of dimension $n-1$ whose graph gives the Hasse diagram of $L_\equiv$ and whose support is a quotientope. We call this polytopal complex the *s-quotientoplex*.

See Figure 4.29 for the continuation of the example with $s = (1,2,1)$ from Figure 4.28.

Note that this gives a new answer to Conjecture 4.1.1, that works also when s is a weak composition (when it has zero entries). Moreover, when s is a composition, the s-Tamari lattice is a lattice quotient of the s-weak order ([CP22, Theorem 2.20]), so we obtain a realization of the s-associahedron that can be obtained from a realization of the s-permutahedron, as asked in Conjecture 4.1.2. Indeed, we have a continuous deformation of the s-permutahedron into the s-associahedron by taking the polytopal complexes $\{\sum_{\alpha\in A} \boldsymbol{Sh}(\alpha)_v\}_{v\in V} + \lambda\{\sum_{\beta\in B} \boldsymbol{Sh}(\beta)_v\}_{v\in V}$ where A is the set of join irreducible that are not contracted by the s-sylvester congruence and B the set of join irreducible that are contracted by the s-sylvester congruence, for λ varying from 1 to 0. The correspondence with the dual polyhedral complex shows that some codimension 1-faces disappear at the end.

Moreover, the representation of the join irreducible elements with s-arcs gives a natural

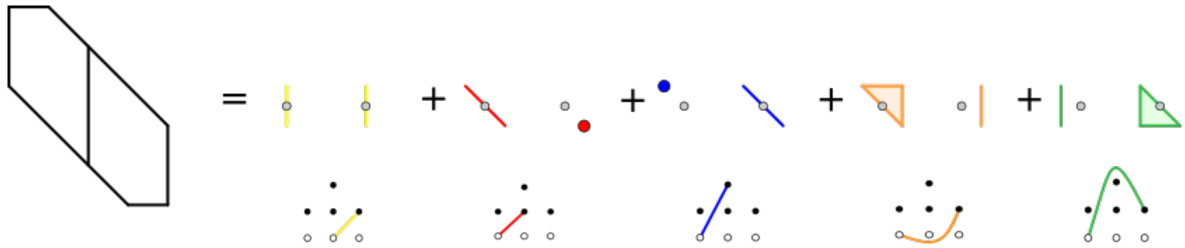

Figure 4.29: The $(1,2,1)$-permutahedron obtained as the $(1,2,1)$-quotientoplex. Each summand of the Minkowski sum of α-shardoplexes $\{\boldsymbol{Sh}(\alpha)_{v_1}, \boldsymbol{Sh}(\alpha)_{v_2}\}$ is labeled by the $(1,2,1)$-arc corresponding to the join irreducible element α of the $(1,2,1)$-weak order and colored according to the shards on Figure 4.28.

way to extend the permutree congruences to a family of lattice congruences of the s-weak order. The corresponding lattice quotients can be modeled by lattices on (s, δ)*-permutrees* for any $\delta \in \{⦶, ⦸, ⦹, \otimes\}^{n-2}$.

4.5.3 Towards realizations of the (s,δ)-permutreehedra via flow polytopes and M-moves on the s-oruga graph

With Matias von Bell, Rafael S. González D'León, Alejandro H. Morales, Daniel Tamayo Jiménez, Yannic Vargas and Martha Yip, we are working on several research directions that arise from our collaboration on realizing the s-permutahedron via triangulations of flow polytopes. We define a graph operation, called the M-move, that can be applied to some edges of the s-oruga graph to recover the s-caracol graph, which allows to realize the s-Tamari order ([BGMY23]).

Conjecture 4.5.1. *By applying the M-move to all possible subsets of non-source and non-sink edges of the* s*-oruga graph, we can recover exactly the* (s,δ)*-permutree lattices for all* $\delta \in \{⦶, ⦸, ⦹, \otimes\}^{n-2}$.

The case $\mathrm{s} = (1, ..., 1)$ of Conjecture 4.5.1, where we recover the classical weak order and the permutrees, is already written down in Daniel Tamayo Jiménez's PhD thesis [TJ23, Theorem 7.3.5 and Corollary 7.3.7].

We are also studying the M-move operation on framed graphs in more generality. In particular, von Bell and Ceballos have a way to associate a lattice structure on the set of maximal cliques of any framed graph ([BC2X], in preparation). It seems that applying the M-move always corresponds to taking a lattice quotient.

Other directions of research are: to study the combinatorial structures induced by the DKK triangulation of the s-oruga graph endowed with other framings, to find analogues of the s-oruga graph for other Coxeter types.

Bibliography

[ADHV19] Omer Angel, Duncan Dauvergne, Alexander E. Holroyd, and Bálint Virág. The local limit of random sorting networks. *Ann. Inst. Henri Poincaré Probab. Stat.*, 55(1):412–440, 2019. 74

[AER00] Christos A. Athanasiadis, Paul H. Edelman, and Victor Reiner. Monotone paths on polytopes. *Math. Z.*, 235(2):315–334, 2000. 77, 113, 114, 115, 116

[AG86] Noga Alon and Ervin Győri. The number of small semispaces of a finite set of points in the plane. *J. Combin. Theory Ser. A*, 41(1):154–157, 1986. 75

[AHRV07] Omer Angel, Alexander E. Holroyd, Dan Romik, and Bálint Virág. Random sorting networks. *Adv. Math.*, 215(2):839–868, 2007. 74

[Alo86] Noga Alon. The number of polytopes, configurations and real matroids. *Mathematika*, 33(1):62–71, 1986. 56

[AP17] Karim A. Adiprasito and Arnau Padrol. The universality theorem for neighborly polytopes. *Combinatorica*, 37(2):129–136, 2017. 27

[AS01] Christos A. Athanasiadis and Francisco Santos. Monotone paths on zonotopes and oriented matroids. *Canad. J. Math.*, 53(6):1121–1140, 2001. 77

[Ath99] Christos A. Athanasiadis. The largest intersection lattice of a discriminantal arrangement. *Beiträge Algebra Geom.*, 40(2):283–289, 1999. 57

[AW03] Artur Andrzejak and Emo Welzl. In between k-sets, j-facets, and i-faces: (i, j)-partitions. *Discrete Comput. Geom.*, 29(1):105–131, 2003. 76, 84

[Bab94] Eric K. Babson. *A combinatorial flag space*. PhD thesis, Massachusetts Institute of Technology, 1994. 114, 115

[Bau80] H. J. Baues. Geometry of loop spaces and the cobar construction. *Mem. Amer. Math. Soc.*, 25(230):ix+171, 1980. 47

[BB05] Anders Björner and Francesco Brenti. *Combinatorics of Coxeter groups*, volume 231 of *Graduate Texts in Mathematics*. Springer, New York, 2005. 81

[BC2X] Matias von Bell and Cesar Ceballos. Framing lattices and flow polytopes. In preparation, 202X. 143, 155, 187

[BCK18] Hans-Jürgen Bandelt, Victor Chepoi, and Kolja Knauer. COMs: complexes of oriented matroids. *J. Combin. Theory Ser. A*, 156:195–237, 2018. 115, 116

[BDLLS22] Alexander E Black, Jesús A De Loera, Niklas Lütjeharms, and Raman Sanyal. The polyhedral geometry of pivot rules and monotone paths. Preprint, `arXiv:2201.05134`, 2022. 76

[BEZ90] Anders Björner, Paul H. Edelman, and Günter M. Ziegler. Hyperplane arrangements with a lattice of regions. *Discrete Comput. Geom.*, 5(3):263–288, 1990. 88

[BGMY23] Matias von Bell, Rafael González D'León, Francisco Mayorga Cetina, and Martha Yip. A unifying framework for the ν-tamari lattice and principal order ideals in Young's lattice. *Combinatorica*, 2023. 134, 135, 187

[BGR92] Edward A. Bender, Zhicheng Gao, and L. Bruce Richmond. Submaps of maps. I. General 0-1 laws. *J. Combin. Theory Ser. B*, 55(1):104–117, 1992. 55

[Bjö84] Anders Björner. Posets, regular CW complexes and Bruhat order. *European J. Combin.*, 5(1):7–16, 1984. 94

[Bjö92] Anders Björner. Essential chains and homotopy type of posets. *Proc. Amer. Math. Soc.*, 116(4):1179–1181, 1992. 76, 77, 79, 113, 114

[Bjö95] Anders Björner. Topological methods. In *Handbook of combinatorics, Vol. 1, 2*, pages 1819–1872. Elsevier Sci. B. V., Amsterdam, 1995. 46, 94, 113, 114

[BK88] Abraham Berman and Anton Kotzig. Cross-cloning and antipodal graphs. *Discrete Math.*, 69(2):107–114, 1988. 121

[BKS94a] L. J. Billera, M. M. Kapranov, and B. Sturmfels. Cellular strings on polytopes. *Proc. Amer. Math. Soc.*, 122(2):549–555, 1994. 47

[BKS94b] Louis J. Billera, Mikhail M. Kapranov, and Bernd Sturmfels. Cellular strings on polytopes. *Proc. Amer. Math. Soc.*, 122(2):549–555, 1994. 75, 77, 113, 114

[BLS+99] Anders Björner, Michel Las Vergnas, Bernd Sturmfels, Neil White, and Günter M. Ziegler. *Oriented matroids*, volume 46 of *Encyclopedia of Mathematics and its Applications*. Cambridge University Press, Cambridge, second edition, 1999. 46, 74, 76, 78, 79, 81, 87, 88, 89, 90, 92, 93, 94, 100, 104, 105, 107, 113, 129

[BM71] Heinz Bruggesser and Peter Mani. Shellable decompositions of cells and spheres. *Math. Scand.*, 29(2):197–205, 1971. 74, 112

[Bón09] Miklós Bóna. Real zeros and normal distribution for statistics on Stirling permutations defined by Gessel and Stanley. *SIAM J. Discrete Math.*, 23(1):401–406, 2008/09. 132

[Bon06] Joseph E. Bonin. Extending a matroid by a cocircuit. *Discrete Math.*, 306(8-9):812–819, 2006. 76, 103

[Bor87] Karl-Heinz Borgwardt. *The simplex method*, volume 1 of *Algorithms and Combinatorics: Study and Research Texts*. Springer-Verlag, Berlin, 1987. A probabilistic analysis. 46

[BPR12] François Bergeron and Louis-François Préville-Ratelle. Higher trivariate diagonal harmonics via generalized Tamari posets. *J. Comb.*, 3(3):317–341, 2012. 132

[Bry75] Tom Brylawski. Modular constructions for combinatorial geometries. *Trans. Amer. Math. Soc.*, 203:1–44, 1975. 76, 100

[Bry86] Thomas Brylawski. Constructions. In *Theory of matroids*, volume 26 of *Encyclopedia Math. Appl.*, pages 127–223. Cambridge Univ. Press, Cambridge, 1986. 76, 106

[BS92] Louis J. Billera and Bernd Sturmfels. Fiber polytopes. *Annals of Mathematics*, pages 527–549, 1992. 44, 45, 47, 51, 75, 77, 85

[BV08] Welleda Baldoni and Michèle Vergne. Kostant partitions functions and flow polytopes. *Transform. Groups*, 13(3-4):447–469, 2008. 144, 145

[BW88] Edward A. Bender and Nicholas C. Wormald. The number of rooted convex polyhedra. *Canad. Math. Bull.*, 31(1):99–102, 1988. 55

[BY23] Matias von Bell and Martha Yip. On the subdivision algebra for the polytope $U_{I,J}$. *Ann. Comb.*, 2023. 134

[CGD19] Cesar Ceballos and Rafael S. González D'León. Signature Catalan combinatorics. *J. Comb.*, 10(4):725–773, 2019. 156

[CKM17] Sylvie Corteel, Jang Soo Kim, and Karola Mészáros. Flow polytopes with catalan volumes. *Comptes Rendus Mathematique*, 355(3):248–259, 2017. 134

[CLL$^+$23] Federico Castillo, Jean-Philippe Labbé, Julia Liebert, Arnau Padrol, Eva Philippe, and Christian Schilling. An effective solution to convex 1-body n-representability. *Annales Henri Poincaré*, 24(7):2241–2321, February 2023. 20, 76

[CM93] Raul Cordovil and Maria Leonor Moreira. A homotopy theorem on oriented matroids. *Discrete Math.*, 111(1-3):131–136, 1993. Graph theory and combinatorics (Marseille-Luminy, 1990). 77

[CP20] Cesar Ceballos and Viviane Pons. The s-weak order and s-permutahedra. *Sém. Lothar. Combin.*, 82B:Art. 76, 12, 2020. 132, 133, 134, 136, 156, 157

[CP22] Cesar Ceballos and Viviane Pons. The s-weak order and s-permutahedra i: combinatorics and lattice structure, 2022. 132, 136, 156, 157, 185, 186

[CP23] Cesar Ceballos and Viviane Pons. The s-weak order and s-permutahedra ii: The combinatorial complex of pure intervals, 2023. 132, 133

[CPS19] Cesar Ceballos, Arnau Padrol, and Camilo Sarmiento. Geometry of ν-Tamari lattices in types A and B. *Trans. Amer. Math. Soc.*, 371(4):2575–2622, 2019. 133, 134

[CPS21] Cesar Ceballos, Arnau Padrol, and Camilo Sarmiento. Removahedral congruences versus permutree congruences. *Electron. J. Combin.*, 28(4):p.4–8, 2021. 185

[CZ12] Cesar Ceballos and Günter M. Ziegler. *Realizing the Associahedron: Mysteries and Questions*, page 119–127. Springer Basel, 2012. 54

[Dau19] Duncan Dauvergne. The archimedean limit of random sorting networks. Preprint, arXiv:1802.08934, 2019. 74

[dBCvKO08] Mark de Berg, Otfried Cheong, Marc van Kreveld, and Mark Overmars. *Computational geometry*. Springer-Verlag, Berlin, third edition, 2008. Algorithms and applications. 74

[Del72] Pierre Deligne. Les immeubles des groupes de tresses généralisés. *Invent. Math.*, 17:273–302, 1972. 77

[Dey93] Tamal Krishna Dey. On counting triangulations in d dimensions. *Computational Geometry*, 3(6):315–325, 1993. 71

[Dil44] Robert P. Dilworth. Dependence relations in a semi-modular lattice. *Duke Math. J.*, 11:575–587, 1944. 76, 106

[DKK12] Vladimir I. Danilov, Alexander V. Karzanov, and Gleb A. Koshevoy. Coherent fans in the space of flows in framed graphs. In *FPSAC 2012*, DMTCS Proc., pages 481–490. 2012. 134, 137, 139, 153, 175, 176, 177

[DRS10] Jesús A. De Loera, Jörg Rambau, and Francisco Santos. *Triangulations: Structures for Algorithms and Applications*, volume 25 of *Algorithms and Computation in Mathematics*. Springer Verlag, 2010. 23, 32, 42, 44, 52, 56, 57, 58, 62, 65, 67, 71

[dS95] Ilda P. F. da Silva. Axioms for maximal vectors of an oriented matroid: a combinatorial characterization of the regions determined by an arrangement of pseudohyperplanes. *European J. Combin.*, 16(2):125–145, 1995. 77, 125

[DS04] Mike Develin and Bernd Sturmfels. Tropical convexity. *Documenta Mathematica*, 9:1–27, 2004. 40

[Ede00] Paul H. Edelman. Ordering points by linear functionals. *European J. Combin.*, 21(1):145–152, 2000. Combinatorics of polytopes. 75, 76, 78, 79, 105, 108

[EG87] Paul Edelman and Curtis Greene. Balanced tableaux. *Adv. in Math.*, 63(1):42–99, 1987. 74

[EG89] Herbert Edelsbrunner and Leonidas J Guibas. Topologically sweeping an arrangement. *Journal of Computer and System Sciences*, 38(1):165–194, 1989. 78

[EJLM21] Rob Edman, Pakawut Jiradilok, Gaku Liu, and Thomas McConville. Zonotopes whose cellular strings are all coherent. *European Journal of Combinatorics*, 96:103352, 2021. 77

[EM82] Jack Edmonds and Arnaldo Mandel. *Topology of oriented matroids, Ph.D. Thesis of A. Mandel*. PhD thesis, University of Waterloo, 1982. 113

[EOS86] Herbert Edelsbrunner, Joseph O'Rourke, and Raimund Seidel. Constructing arrangements of lines and hyperplanes with applications. *SIAM Journal on Computing*, 15(2):341–363, 1986. 78

[EVW97] Herbert Edelsbrunner, Pavel Valtr, and Emo Welzl. Cutting dense point sets in half. *Discrete Comput. Geom.*, 17(3):243–255, 1997. 76, 84

[Fel04] Stefan Felsner. *Geometric graphs and arrangements*. Advanced Lectures in Mathematics. Friedr. Vieweg & Sohn, Wiesbaden, 2004. Some chapters from combinatorial geometry. 75, 78, 104, 126

[FF02] Lukas Finschi and Komei Fukuda. Generation of oriented matroids—a graph theoretical approach. *Discrete Comput. Geom.*, 27(1):117–136, 2002. Geometric combinatorics (San Francisco, CA/Davis, CA, 2000). 88

[FH93] Komei Fukuda and Keiichi Handa. Antipodal graphs and oriented matroids. *Discrete Math.*, 111(1-3):245–256, 1993. Graph theory and combinatorics (Marseille-Luminy, 1990). 77, 121

[FR15] Alex Fink and Felipe Rincón. Stiefel tropical linear spaces. *Journal of Combinatorial Theory, Series A*, 135:291–331, 2015. 40

[FW01] Stefan Felsner and Helmut Weil. Sweeps, arrangements and signotopes. *Discrete Appl. Math.*, 109(1-2):67–94, 2001. 14th European Workshop on Computational Geometry CG'98 (Barcelona). 78, 104, 126

[FZ01] Stefan Felsner and Günter M. Ziegler. Zonotopes associated with higher Bruhat orders. *Discrete Math.*, 241(1-3):301–312, 2001. Selected papers in honor of Helge Tverberg. 78

[Gal68] David Gale. Optimal assignments in an ordered set: An application of matroid theory. *J. Combinatorial Theory*, 4:176–180, 1968. 145

[GDMP+23] Rafael S. González D'León, Alejandro H. Morales, Eva Philippe, Daniel Tamayo Jiménez, and Martha Yip. Realizing the s-permutahedron via flow polytopes. Preprint, arXiv:2307.03474, 2023. 20, 40, 131, 172

[Ges20] Ira M Gessel. A note on stirling permutations. *arXiv preprint arXiv:2005.04133*, 2020. 132

[GKZ94] Israel M. Gel'fand, Mikhail M. Kapranov, and Andrei V. Zelevinsky. *Discriminants, resultants, and multidimensional determinants*. Mathematics: Theory & Applications. Birkhäuser Boston, Inc., Boston, MA, 1994. 32, 42

[GP80a] Jacob E. Goodman and Richard Pollack. On the combinatorial classification of nondegenerate configurations in the plane. *J. Combin. Theory Ser. A*, 29(2):220–235, 1980. 74, 99, 118

[GP80b] Jacob E. Goodman and Richard Pollack. Proof of Grünbaum's conjecture on the stretchability of certain arrangements of pseudolines. *Journal of Combinatorial Theory, Series A*, 29(3):385 – 390, 1980. 74, 75

[GP82] Jacob E. Goodman and Richard Pollack. A theorem of ordered duality. *Geom. Dedicata*, 12(1):63–74, 1982. 74, 118

[GP84] Jacob E. Goodman and Richard Pollack. Semispaces of configurations, cell complexes of arrangements. *J. Combin. Theory Ser. A*, 37(3):257–293, 1984. 74, 118

[GP86] Jacob E. Goodman and Richard Pollack. Upper bounds for configurations and polytopes in R^d. *Discrete Comput. Geom.*, 1(3):219–227, 1986. 55

[GP93] Jacob E. Goodman and Richard Pollack. Allowable sequences and order types in discrete and computational geometry. In *New trends in discrete and computational geometry*, volume 10 of *Algorithms Combin.*, pages 103–134. Springer, Berlin, 1993. 74, 75, 78, 79, 118

[GP16] Bernd Gonska and Arnau Padrol. Neighborly inscribed polytopes and Delaunay triangulations. *Adv. Geom.*, 16(3):349–360, 2016. 56, 65, 67, 69

[GR63] G Th Guilbaud and Pierre Rosenstiehl. Analyse algébrique d'un scrutin. *Mathématiques et Sciences humaines*, 4:9–33, 1963. 49

[Grü03] Branko Grünbaum. *Convex polytopes*, volume 221 of *Graduate Texts in Mathematics*. Springer-Verlag, New York, second edition, 2003. Prepared and with a preface by Volker Kaibel, Victor Klee and Günter M. Ziegler. 55

[GS55] Saul Gass and Thomas Saaty. The computational algorithm for the parametric objective function. *Naval Res. Logist. Quart.*, 2:39–45, 1955. 46

[GS78a] Giorgio Gallo and Claudio Sodini. Extreme points and adjacency relationship in the flow polytope. *Calcolo*, 15(3):277–288, 1978. 137

[GS78b] Ira Gessel and Richard P. Stanley. Stirling polynomials. *J. Combinatorial Theory Ser. A*, 24(1):24–33, 1978. 132

[GS93] Peter Gritzmann and Bernd Sturmfels. Minkowski addition of polytopes: computational complexity and applications to Gröbner bases. *SIAM J. Discrete Math.*, 6(2):246–269, 1993. 75, 83

[GS21] Antonio González and Francisco Santos. Associahedra minimize f-vectors of secondary polytopes of planar point sets. *arXiv*, arXiv:2110.00544, 2021. 64

[Han90] Keiichi Handa. A characterization of oriented matroids in terms of topes. *European J. Combin.*, 11(1):41–45, 1990. 77, 121

[Han93] Keiichi Handa. Topes of oriented matroids and related structures. *Publ. Res. Inst. Math. Sci.*, 29(2):235–266, 1993. 77, 121, 123

[Hat02] Allen Hatcher. *Algebraic topology*. Cambridge University Press, Cambridge, 2002. 114

[HM18] Udo Hoffmann and Keno Merckx. A universality theorem for allowable sequences with applications. Preprint, `arXiv:1801.05992`, 2018. 75, 100

[Hoc16] Winfried Hochstättler. Topological sweeping in oriented matroids. Technical report `https://www.fernuni-hagen.de/MATHEMATIK/DMO/pubs/feu-dmo042-16.pdf`, 2016. 78, 129

[HRS00] Birkett Huber, Jörg Rambau, and Francisco. Santos. The cayley trick, lifting subdivisions and the bohne-dress theorem on zonotopal tilings. *J. Eur. Math. Soc.*, 2:179–198, 2000. 32, 33

[HS20] Alexander Heaton and Jose Alejandro Samper. Dual matroid polytopes and internal activity of independence complexes. Preprint, `arXiv:2005.04252`, 2020. 113

[JK19] Jihyeug Jang and Jang Soo Kim. Volumes of flow polytopes related to caracol graphs. *arXiv preprint arXiv:1911.10703*, 2019. 134

[JKP11] Svante Janson, Markus Kuba, and Alois Panholzer. Generalized Stirling permutations, families of increasing trees and urn models. *J. Combin. Theory Ser. A*, 118(1):94–114, 2011. 132

[Jos17] Michael Joswig. The cayley trick for tropical hypersurfaces with a view toward ricardian economics. *Homological and Computational Methods in Commutative Algebra*, pages 107–128, 2017. 37

[Jos21] Michael Joswig. *Essentials of tropical combinatorics*, volume 219. American Mathematical Society, 2021. 37, 38, 40

[Kal88] Gil Kalai. Many triangulated spheres. *Discrete Comput. Geom.*, 3(1):1–14, 1988. 56

[KM20] Kolja Knauer and Tilen Marc. On Tope Graphs of Complexes of Oriented Matroids. *Discrete Comput. Geom.*, 63(2):377–417, 2020. 77, 121, 123, 125, 126

[KMS21] Kabir Kapoor, Karola Mészáros, and Linus Setiabrata. Counting integer points of flow polytopes. *Discrete Comput. Geom.*, 66(2):723–736, 2021. 143, 144, 145, 147, 148, 149, 150

[KN86] Joseph P. S. Kung and Hien Q. Nguyen. Weak maps. In *Theory of matroids*, volume 26 of *Encyclopedia Math. Appl.*, pages 254–271. Cambridge Univ. Press, Cambridge, 1986. 108

[Knu98] Donald E. Knuth. *The art of computer programming. Vol. 3*. Addison-Wesley, Reading, MA, 1998. Sorting and searching, Second edition. 74

[KP11] Markus Kuba and Alois Panholzer. Analysis of statistics for generalized Stirling permutations. *Combin. Probab. Comput.*, 20(6):875–910, 2011. 132

[KVY23] Andrey Kupavskii, Aleksei Volostnov, and Yury Yarovikov. Minimum number of partial triangulations. *European Journal of Combinatorics*, 108:103636, 2023. 64

[Lee89] Carl W Lee. The associahedron and triangulations of the n-gon. *European Journal of Combinatorics*, 10(6):551–560, 1989. 54

[Lid84] Boris Viktorovich Lidskii. Kostant function of the root system an. *Functional Analysis and Its Applications*, 18(1):65–67, 1984. 144

[Liu20] Gaku Liu. A counterexample to the extension space conjecture for realizable oriented matroids. *J. Lond. Math. Soc. (2)*, 101(1):175–193, 2020. 47

[Lod04] Jean-Louis Loday. Realization of the stasheff polytope. *Archiv der Mathematik*, 3(889X/04):030267–12, 2004. 54

[LVWW04] László Lovász, Katalin Vesztergombi, Uli Wagner, and Emo Welzl. Convex quadrilaterals and k-sets. In *Towards a theory of geometric graphs*, volume 342 of *Contemp. Math.*, pages 139–148. Amer. Math. Soc., Providence, RI, 2004. 75

[Mas77] John H. Mason. Matroids as the study of geometrical configurations. In *Higher combinatorics (Proc. NATO Advanced Study Inst., Berlin, 1976)*, volume 31 of *NATO Adv. Study Inst. Ser., Ser. C: Math. Phys. Sci.*, pages 133–176. Reidel, Dordrecht-Boston, Mass., 1977. 106

[Mat02] Jiří Matoušek. *Lectures on discrete geometry*, volume 212 of *Graduate Texts in Mathematics*. Springer-Verlag, New York, 2002. 109, 113

[McM70] Peter McMullen. The maximum numbers of faces of a convex polytope. *Mathematika*, 17:179–184, 1970. 56, 63

[McM03] Peter McMullen. Fibre tilings. *Mathematika*, 50(1-2):1–33 (2005), 2003. 87

[MG06] Jiří Matoušek and Bernd Gärtner. *Understanding and Using Linear Programming (Universitext)*. Springer-Verlag, Berlin, Heidelberg, 2006. 74

[MHPS12] F. Müller-Hoissen, J.M. Pallo, and J. Stasheff, editors. *Associahedra, Tamari Lattices and Related Structures: Tamari Memorial Festschrift*. Progress in Mathematics. Springer Basel, 2012. 53

[MM15] Karola Mészáros and Alejandro H. Morales. Flow polytopes of signed graphs and the Kostant partition function. *Int. Math. Res. Not. IMRN*, (3):830–871, 2015. 134

[MM19] Karola Mészáros and Alejandro H. Morales. Volumes and Ehrhart polynomials of flow polytopes. *Math. Z.*, 293(3-4):1369–1401, 2019. 134, 143, 144, 148, 149, 154, 173

[MMS19] Karola Mészáros, Alejandro H. Morales, and Jessica Striker. On flow polytopes, order polytopes, and certain faces of the alternating sign matrix polytope. *Discrete Comput. Geom.*, 62(1):128–163, 2019. 134, 144

[Mnë88] Nicolai E. Mnëv. The universality theorems on the classification problem of configuration varieties and convex polytopes varieties. In *Topology and geometry—Rohlin Seminar*, volume 1346 of *Lecture Notes in Math.*, pages 527–543. Springer, Berlin, 1988. 27, 75

[MS89] Yuri I. Manin and Vadim V. Schechtman. Arrangements of hyperplanes, higher braid groups and higher Bruhat orders. In *Algebraic number theory*, volume 17 of *Adv. Stud. Pure Math.*, pages 289–308. Academic Press, Boston, MA, 1989. 78

[MSP21] Leonardo Martínez-Sandoval and Arnau Padrol. The convex dimension of hypergraphs and the hypersimplicial Van Kampen-Flores theorem. *J. Combin. Theory Ser. B*, 149:23 – 51, 2021. 84

[MW71] Peter McMullen and David W. Walkup. A generalized lower-bound conjecture for simplicial polytopes. *Mathematika*, 18(2):264–273, 1971. 62

[NSW16] Eran Nevo, Francisco Santos, and Stedman Wilson. Many triangulated odd-dimensional spheres. *Math. Ann.*, 364(3-4):737–762, 2016. 56

[OS22] Jorge Alberto Olarte and Francisco Santos. Hypersimplicial subdivisions. *Selecta Mathematica*, 28(1):4, 2022. 47

[Pad13] Arnau Padrol. Many neighborly polytopes and oriented matroids. *Discrete Comput. Geom.*, 50(4):865–902, 2013. 56, 57, 65, 67, 68, 69, 70

[Par94a] SeungKyung Park. Inverse descents of r-multipermutations. *Discrete Math.*, 132(1-3):215–229, 1994. 132

[Par94b] SeungKyung Park. P-partitions and q-Stirling numbers. *J. Combin. Theory Ser. A*, 68(1):33–52, 1994. 132

[Par94c] SeungKyung Park. The r-multipermutations. *J. Combin. Theory Ser. A*, 67(1):44–71, 1994. 132

[Per82] Raoul Perrin. Sur le problème des aspects. *Bull. Soc. Math. France*, 10:103–127, 1882. 74

[Pos09] Alexander Postnikov. Permutohedra, associahedra, and beyond. *Int. Math. Res. Not. IMRN*, 2009(6):1026–1106, 2009. 84

[Pos14] Alexander Postnikov. *Personal communication*, 2010; 2014. 144

[PP18] Vincent Pilaud and Viviane Pons. Permutrees. *Algebraic Combinatorics 1*, (2):173–224, 2018. 185

[PP23] Arnau Padrol and Eva Philippe. Sweeps, polytopes, oriented matroids, and allowable graphs of permutations. *Combinatorica*, pages 1–61, 2023. 19, 73

[PP24] Eva Philippe and Vincent Pilaud. Geometric realizations of the s-weak order and its lattice quotients. Preprint, arXiv:2405.02092, 2024. 21, 131, 185

[PPR23] Arnau Padrol, Vincent Pilaud, and Julian Ritter. Shard polytopes. *International Mathematics Research Notices*, 2023(9):7686–7796, 2023. 184

[PPS23] Arnau Padrol, Eva Philippe, and Francisco Santos. Many regular triangulations and many polytopes. *Mathematische Annalen*, pages 1–19, 2023. 19, 55

[PRV17] Louis-François Préville-Ratelle and Xavier Viennot. The enumeration of generalized Tamari intervals. *Trans. Amer. Math. Soc.*, 369(7):5219–5239, 2017. 132

[PS19] Vincent Pilaud and Francisco Santos. Quotientopes. *Bulletin of the London Mathematical Society*, 51(3):406–420, 2019. 184

[PSZ23] Vincent Pilaud, Francisco Santos, and Günter M Ziegler. Celebrating loday's associahedron. *Archiv der Mathematik*, 121(5):559–601, 2023. 53

[Qui78] Daniel Quillen. Homotopy properties of the poset of nontrivial p-subgroups of a group. *Adv. in Math.*, 28(2):101–128, 1978. 114

[R94] Victor Reiner and Günter M. . Coxeter-associahedra. *Mathematika*, 41(2):364–393, 1994. 47, 81

[Ram97] Jörg Rambau. Triangulations of cyclic polytopes and higher Bruhat orders. *Mathematika*, 44(1):162–194, 1997. 58

[Rea04] Nathan Reading. Lattice congruences of the weak order. *Order*, 21(4):315–344, 2004. 184

[Rea05] Nathan Reading. Lattice congruences, fans and hopf algebras. *Journal of Combinatorial Theory, Series A*, 110(2):237–273, 2005. 184

[Rea06] N. Reading. Cambrian lattices. *Advances in Mathematics 205*, (2):313–353, 2006. 185

[Rea15] Nathan Reading. Noncrossing arc diagrams and canonical join representations. *SIAM Journal on Discrete Mathematics*, 29(2):736–750, 2015. 184

[Rei99] Victor Reiner. The generalized Baues problem. In *New perspectives in algebraic combinatorics (Berkeley, CA, 1996–97)*, volume 38 of *Math. Sci. Res. Inst. Publ.*, pages 293–336. Cambridge Univ. Press, Cambridge, 1999. 46, 77, 113

[RG93] Jürgen Richter-Gebert. Oriented matroids with few mutations. *Discrete Comput. Geom.*, 10(3):251–269, 1993. 104

[RG96] Jürgen Richter-Gebert. *Realization Spaces of Polytopes*, volume 1643 of *Lecture Notes in Mathematics*. Springer, Berlin, 1996. 27

[RR13] Victor Reiner and Yuval Roichman. Diameter of graphs of reduced words and galleries. *Trans. Amer. Math. Soc.*, 365(5):2779–2802, 2013. 77

[RS00] Jörg Rambau and Francisco Santos. The generalized Baues problem for cyclic polytopes. I. *European J. Combin.*, 21(1):65–83, 2000. 58

[RW82] L. Bruce Richmond and Nicholas C. Wormald. The asymptotic number of convex polyhedra. *Trans. Amer. Math. Soc.*, 273(2):721–735, 1982. 55

[RZ96] J. Rambau and G. M. Ziegler. Projections of polytopes and the generalized Baues conjecture. *Discrete Comput. Geom.*, 16(3):215–237, 1996. 47

[Sal87] Mario Salvetti. Topology of the complement of real hyperplanes in $\mathbf{C}^N$. *Invent. Math.*, 88(3):603–618, 1987. 77

[San05] Francisco Santos. The Cayley trick and triangulations of products of simplices. In *Integer points in polyhedra—geometry, number theory, algebra, optimization*, volume 374 of *Contemp. Math.*, pages 151–177. Amer. Math. Soc., Providence, RI, 2005. 32

[San06] Francisco Santos. Geometric bistellar flips: the setting, the context and a construction. In *International Congress of Mathematicians. Vol. III*, pages 931–962. Eur. Math. Soc., Zürich, 2006. 47

[Sch11] Pieter Hendrik Schoute. Analytic treatment of the polytopes regularly derived from the regular polytopes, verhandelingen der koninklijke akademie van wetenschappen te amsterdam. *Eerste Sectie*, 11:1–87, 1911. 50

[SH91] Jack Snoeyink and John Hershberger. Sweeping arrangements of curves. In *Discrete and computational geometry (New Brunswick, NJ, 1989/1990)*, volume 6 of *DIMACS Ser. Discrete Math. Theoret. Comput. Sci.*, pages 309–349. Amer. Math. Soc., Providence, RI, 1991. 104

[She82] Ido Shemer. Neighborly polytopes. *Israel J. Math.*, 43(4):291–314, 1982. 56

[Sta63] James D. Stasheff. Homotopy associativity of h-spaces, I & II. *Trans. Amer. Math. Soc*, 108:313–327, 1963. 53

[Sta71] Richard P. Stanley. Modular elements of geometric lattices. *Algebra Universalis*, 1:214–217, 1971. 76, 100

[Sta72] Richard P. Stanley. Supersolvable lattices. *Algebra Universalis*, 2:197–217, 1972. 97

[Sta84] Richard P. Stanley. On the number of reduced decompositions of elements of Coxeter groups. *European J. Combin.*, 5(4):359–372, 1984. 74

[Sta00] Richard P. Stanley. Acyclic flow polytopes and kostant's partition function. *Conference transparencies*, 2000. 144

[Sta12] Richard P. Stanley. *Enumerative combinatorics. Volume 1*, volume 49 of *Cambridge Studies in Advanced Mathematics*. Cambridge University Press, Cambridge, second edition, 2012. 132

[Sta15] Richard P. Stanley. Valid orderings of real hyperplane arrangements. *Discrete Comput. Geom.*, 53(4):951–964, 2015. 75, 76, 78, 79, 105, 108, 112, 127

[Stu94] Bernd Sturmfels. On the Newton polytope of the resultant. *J. Algebraic Combin.*, 3(2):207–236, 1994. 32, 37

[SZ93] Bernd Sturmfels and Günter M. Ziegler. Extension spaces of oriented matroids. *Discrete Comput. Geom.*, 10(1):23–45, 1993. 114

[Tam51] Dov Tamari. *Monoides préordonnés et chaînes de Malcev*. PhD thesis, Univeristé Paris Sorbonne, 1951. 53

[Tam62] Dov Tamari. The algebra of bracketings and their enumeration. *Nieuw Arch. Wisk. (3)*, 10:131–146, 1962. 132

[Tit69] Jacques Tits. Le problème des mots dans les groupes de Coxeter. In *Symposia Mathematica (INDAM, Rome, 1967/68), Vol. 1*, pages 175–185. Academic Press, London, 1969. 77

[TJ23] Daniel Tamayo Jiménez. *Combinatorics of permutreehedra and geometry of s-permutahedra*. PhD thesis, Univeristé Paris-Saclay, 2023. 137, 140, 187

[Ung82] Peter Ungar. $2N$ noncollinear points determine at least $2N$ directions. *J. Combin. Theory Ser. A*, 33(3):343–347, 1982. 75

[Wel86] Emo Welzl. More on k-sets of finite sets in the plane. *Discrete Comput. Geom.*, 1(1):95–100, 1986. 75

[Whi86] Neil White, editor. *Theory of matroids*, volume 26 of *Encyclopedia of Mathematics and its Applications*. Cambridge University Press, Cambridge, 1986. 105

[Zie93] Günter M. Ziegler. Higher Bruhat orders and cyclic hyperplane arrangements. *Topology*, 32(2):259–279, 1993. 78

[Zie95] Günter M. Ziegler. *Lectures on Polytopes*, volume 152 of *Graduate texts in Mathematics*. Springer-Verlag, New York, 1995. 23, 26, 27, 30, 31, 44, 50, 51, 62, 63, 64, 74, 87, 91, 109